

**The Nature, Distribution and Significance of Organic
Carbon within Structurally Intact Soils Contrasting in
Total SOC Content.**

Katie Elizabeth Smith

September 2010

Thesis submitted for the degree of
Doctor of Philosophy
School of Biological & Environmental Sciences
The University of Stirling

Acknowledgments

Thanks to my supervisors, Donald Davison, Ian Grieve, Richard Whalley and Clare Wilson for all their guidance and support over the years, I've always felt truly fortunate to have a fantastic team of supervisors continuously looking out for me.

Thanks for all the technical support I've received while at the University of Stirling, Rothamsted Research and SUERC. Special thanks to: George MacLeod for the manufacture of soil thin-sections and SEM-EDS advice; Jean Devonshire, for hours of SEM-EDS training, cups of coffee and lovely chats; Tony Fallick and Terry Donnelly for their support and LA-IRMS training; Kate Howie and Rodger White for statistical advice. There are so many people to thank at Rothamsted for being readily available to help at a moments notice: Chris Watts, Andy Gregory, Colin Webster, Andy MacDonald, Nigel Bird, Andy Whitmore and Darren McCabe.

Thanks to all the PhD students of SBES who have supported me over the years particularly my office mates of 3a124a.

Thanks to Roxy, for the mind numbing DVD's and tolerating a housemate who was always disappearing either for work or for "work".

Special thanks to Charlie, for the whisky, laughter and encouragement. Your support has meant so much to me.

Thanks to Mum, Dad, Kevin and Elsa for all your encouragement over the years; I could not have achieved this without your support.

This thesis is dedicated to my Mum and Dad, who bravely taught me how to “plod on” and enjoy life through the toughest of times.

Declaration of Authenticity

I certify that this dissertation is my original work, gathered and utilised especially to fulfil the requirements of this research degree and has not been previously submitted to any other University for the degree of Doctor in Philosophy. All external sources of information are duly referenced and acknowledged.

Signed: Katie Elizabeth Smith

Date: 12 September 2010

Abstract

Soil structure influences many chemical, biological and physical processes and it is well established that organic carbon acts as a soil binding agent. However, the precise location of organic matter and carbon in relation to structural features within intact samples is unknown. The sensitivity of organic carbon to decomposition is dependent not only upon its intrinsic chemical recalcitrance, but also its location within the soil structure. Soil structure provides organic carbon with chemical and physical protection, the extent of which varies between structural units. Furthermore soil structure is transient, and is sensitive to both environmental changes and physical disturbance, therefore it is difficult to determine and quantify the impact of this dynamic entity upon the storage of organic carbon.

To date the majority of research that has advanced our understanding of the role soil structure plays in the storage of organic carbon, has relied upon some form of fractionation technique to separate aggregates from the bulk soil. However this approach has its disadvantages as much of the soil structure is destroyed; clearly when studying the impact of soil structure upon organic carbon-storage it is advantageous to implement any method that minimises disturbance to the soil structure.

This study entails removing intact soil samples (through the use of kubiena tins) from long-term agricultural experimental fields at Rothamsted Research, (Hertfordshire, UK) with the aim of comparing and evaluating the location of organic matter and its associated organic carbon, in soils with contrasting organic carbon contents and a well documented land-use history. Thin sections will be analysed by integrating conventional micromorphology, image analysis and sub-microscopy combined with microscale chemical analysis scanning electron microscopy-energy dispersive spectroscopy (SEM-EDS). In doing so a new alternative method for analysing the distribution of organic matter and organic carbon is proposed.

It was found that agricultural soils, which are the same in all aspects except total-OC content, differ in total organic matter, water release characteristics, aggregate stability and pore size distribution; therefore these differences could be attributed to the relationship between OC and soil structure. The water release curve, aggregate stability and pore size distribution also differed between soils with similar OC-contents but from different land-uses.

The analysis of organic matter within intact soil samples provided evidence for the redistribution of organic matter as it is decomposed within the soil structure, for instance, less decomposed organ and tissue forms were located in or near to soil pores while more decomposed amorphous forms were located within the soil matrix. Since the same pattern of redistribution was observed in both agricultural and grassland soil this is likely to be directed by soil macro and micro fauna. It is

concluded that since the location of different forms of organic matter is consistent across all soil, organic matter location is not responsible for creating differences in aggregate stability between treatments. Instead the results indicate that the amount and strength of organic carbon bonds and its hydrophobic properties are responsible.

Micromorphology results demonstrated an absence of defined aggregation between treatments. Despite the difficulties in the interpretation of aggregation, the results contradict theories of aggregation, which state that aggregates are formed around “fresh” organic matter and it is argued that OM will undergo substantial decomposition before it acts as core for aggregation.

Initial SEM-EDS analysis, has shown that in the soil matrix adjacent to organic matter (plant/organ) fragments there is a heightened concentration of C, indicating that these fragments are acting as a source of organic carbon. Interestingly BC, which represent one of the most recalcitrant C forms is also acting as a source of C, although these initial results suggest to a lesser extent than more labile C-sources. This source of organic carbon could stimulate microbial activity thereby enhancing soil structural stability. Alternatively, the release of liable carbon into soil pores may represent one route by which labile carbon enters sub-soil horizons.

Contents

Abstract	i
Contents	iii
List of Figures	vii
List of Tables	xiv
Table of Abbreviations and Definitions	xv
Chapter 1: The Nature, Distribution and Significance of Organic Carbon in Soils	
1.1 Introduction	1
1.2 Carbon Compounds in Soil Organic-Matter	6
1.3 An Introduction to Soil Structure	10
1.4 The Importance of Soil Structure for Soil Functionality	11
1.4.1 Soil Porosity	12
1.4.2 Soil Aggregation	13
1.5 Modelling the Turnover of Aggregates	15
1.6 The Spatial Distribution of Soil Biota	19
1.7 The Spatial Distribution of Soil Biota: Soil Fauna as Ecosystem Engineers	20
1.7.1 The Spatial Distribution of Soil Biota: Interactions between Soil Biota and Ecosystem Engineers	21
1.8 Land Management, it's consequences for SOC-content and Soil Structure	23
1.9 Soil Texture and Mineralogy	27
1.10 Conclusion	29
Chapter 2: Research Framework	
2.1 Methodological Considerations for Investigating Soil Organic Carbon	30
2.1.1 Soil Depth	30
2.1.2 Carbon Amount versus Carbon Concentration	31
2.1.3 Seasonal variability	31
2.2 Research Questions	31
2.2.1 The Relationship between Soil Structure and Soil Organic Carbon	31
2.2.2 Soil Carbon Content and Land Use	32
2.2.3 The Redistribution of Old versus New Carbon Inputs	33
2.3 Summary and Research Structure	33
Chapter 3: Field Sites and Methodology	36
3.1 Field Descriptions	36
3.1.1 Broadbalk Winter-Wheat and Broadbalk Wilderness	36
3.1.2 Sampling Protocol	40
3.1.3 Hoosfield Continuous Maize	43
3.2 Chemical Analysis	44
3.2.1 Soil pH	44
3.2.2 Loss-on-Ignition	44
3.2.3 Laser Ablation and Isotope-Ratio Mass Spectrometry (LA-IRMS)	45
3.3 Physical Analysis	47
3.3.1 Bulk Density	47

3.3.2 Aggregate Water Stability	47
3.3.3 Water-Retention-Characteristics	49
3.4 Microscopy and Sub-Microscopy with Elemental Analysis	51
3.4.1 Micromorphology	51
3.4.2 Summary of Thin-Section Analysis	51
3.4.3 Thin-Section Production	52
3.4.4 Micromorphology Description	52
3.4.5 Procedure for Sub-Sampling within Thin-Sections	53
3.4.6 Procedure for Sub-Sampling within Hoosfield Thin-Sections	55
3.4.7 The Classification of Organic Matter	55
3.4.8 Image Analysis	59
3.4.9 Some Considerations for the Classification of Organic Matter	60
3.4.10 Protocol for SEM-EDS	61
3.4.11 Alternative SEM-EDS System	62
3.5 Statistical Analysis	64

Chapter 4: The Structural Characteristics of Broadbalk Soils Contrasting in Total Organic Carbon Content.

Chapter 4: The Structural Characteristics of Broadbalk Soils Contrasting in Total Organic Carbon Content.	65
4.1 Specific Objectives and Hypotheses	65
4.2 General Chemical and Physical Attributes of Broadbalk Winter-Wheat and Broadbalk Wilderness	67
4.3 Aggregate Water Stability	69
4.4 Water Release Characteristics	70
4.5 Micromorphology Descriptions	72
4.5.1 Coarse fine Mineral Material	72
4.5.2 Soil Structure	72
4.6 Image Analysis: Porosity at 12.5x	76
4.6.1 Porosity by Treatment and Pore Shape	76
4.6.2 Image Analysis: Pore Frequency by Treatment and Shape	78
4.6.3 Image Analysis: Porosity at 40x	79
4.6.4 Image Analysis: Pore Frequency by Treatment and Shape	81
4.7 Image Analysis: Comparison of Porosity Characteristics between 12.5x and 40x	82
4.8 Image Analysis: Pore Size Distribution	83
4.8.1 Image Analysis: Pore Size Distribution at 12.5x	83
4.8.2 Image Analysis: Pore Size Distribution at 40x	85
4.8.3 Image Analysis: Comparison of Pore Size Distribution at 12.5x and 40x.	87
4.9 Summary of Results	88
4.9.1 Bulk Analysis	88
4.9.2 Aggregate Water Stability	88
4.9.3 Water Release	89
4.9.4 Describing Soil Structure	89
4.9.5 Image Analysis of Soil Porosity	90
4.9.6 Image Analysis: Pore Size Distribution	90

Chapter 5: The Distribution and Significance of Organic Matter and Organic Carbon, in Broadbalk Soils	92
5.1 Specific Objectives and Hypotheses	92
5.2 Total Organic Matter	94
5.3 Micromorphology: Pedofeatures	95
5.4 Image Analysis: Total Organic Matter at 40x	97
5.4.1 Image Analysis: Organic Matter by Form and Decomposition	98
5.4.2 The Location of Organic Matter in Relation to Soil Pores	102
5.5 The Distribution of Elemental Carbon	103
5.5.1 Elemental O:C Ratios of Features Analysed at 5 keV	103
5.5.2 The Concentration of Carbon Associated with Features Analysed at 5 keV.	105
5.5.3 The Elemental Signature of Features	107
5.5.4 Elemental Maps, at 5 keV	113
5.5.5 Elemental Signatures obtained by Phase Analysis	114
5.5.6 Comparison of Point and Mapping Analysis at 5 keV	114
5.5.7 Elemental Mapping at 15 keV	118
5.5.8 Elemental Signatures Obtained by Phase Analysis at 15 keV	120
5.5.9 Comparison of Elemental Mapping at 5 and 15 keV	120
5.6 Introduction and Methodology, to Investigate C-Distribution within an Intact Soil Structure	123
5.6.1 A Theoretical Model of the Change in Carbon Distribution away from Organic Matter and Black Carbon Particles.	125
5.6.2 Elemental Transects of Broadbalk Soils	127
5.7 Summary of Results	136
5.6.1 Total Organic Matter	136
5.6.2 Micromorphology Results	136
5.6.3 Image Analysis of Organic Matter	136
5.6.4 The Location of Organic Matter	137
5.6.5 SEM-EDS: Point Analysis at 5 keV	137
5.6.6 SEM-EDS: Mapping	138
5.6.7 SEM-EDS Comparison of Mapping at 5 keV and 15 keV	138
5.6.8 Elemental Transects: Methods and Theoretical Model for Changes in C-Concentration	138
5.6.9 Elemental Transects: Initial Results	139
Chapter 6: Discussion, The Structural Characteristics of Broadbalk Soils Contrasting in Total Organic-Carbon Content	140
6.1 Describing the Structural Characteristics of Broadbalk Soils	140
6.2 Structural Characteristics Determined by Bulk Analysis	142
6.3 Quantifying Porosity within Structurally Intact Soil	142
6.3.1 Quantifying Porosity within Structurally Intact Soil: Pore Size Distribution	147
6.3.2 Quantifying Porosity within Structurally Intact Soil: Differences with Scale	148
6.4 Water Release Characteristics	149
6.5 The Occurrence and Nature of in and Between Soils Contrasting in Total Organic Carbon Content.	149
6.5.1 Describing Organic Inclusions Within Intact Samples	150

6.5.2 The Nature and Quantification of Organic Matter within Intact Samples	151
6.5.3 The Location of Organic Matter within Intact Samples	152
6.6 Identifying Features within Intact Samples using SEM-EDS	154
6.6.1 Elemental Analysis of Features at 5 keV	154
6.6.2 Elemental Analysis of Features at 15 keV	156
6.7 The Change in C-Concentration within an Intact Soil Structure	159
Chapter 7: The Processes Controlling OC-Storage and the Wider Significance of the Research Findings	161
7.1 Exploring the Processes Controlling OC-Storage	161
7.2 The Redistribution of OM and Soil Structural Development	163
7.3 The Role of Black Carbon within the Soil Structure	165
7.4 Organic Matter and Soil Structure as an Indication of Soil Quality	167
7.5 Recommendations for the Identification and Mapping of Features within Thin-Sections	167
7.6 Reviewing the Classification of Organic Matter	168
7.7 Recommendations for Further Study	169
7.8 Summary	171
Bibliography	172
Appendix 1: Summary Table of Micromorphology Results for Broadbalk Samples	186
Appendix 2 Summary Table of Micromorphology Results for Hoosfield Continuous Maize Samples	187
Appendix 3: The Redistribution of Organic Carbon as it is Retained within the Soil Structure.	188
3.1 Aims and Objectives	188
3.2 Slide Quality and Micromorphology	189
3.3 Results from Hoosfield Continuous Maize	190
3.4 Short Term δ -13C Experiment	192
3.4.1 Design of Short Term δ -13C Experiment	192
3.4.2 Modification to the Impregnation Method	194

Figures

Figure 1.1: The main components of the natural carbon cycle showing, carbon storage (Pg C) and fluxes (Pg C/Yr). Thick arrows denote current important fluxes to ensure balance of CO₂ exchange including gross primary production and respiration by the land biosphere and physical air-sea exchange. Thin lines denote smaller additionally natural fluxes, with dashed lines representing fluxes of CaCO₃ CO₂ from these fluxes are balanced on longer-term scales. Also shown is river export (0.8 Pg C/yr) comprising the export of dissolved organic carbon (DOC) (0.4 Pg C/yr) and dissolved inorganic carbon (DIC) from the weathering of CaCO₃ (0.4 Pg C/yr). Once reaching the ocean DOC is respired and released into the atmosphere while only one half of DIC is returned to the atmosphere the remaining is incorporated into deep sea sediments and forms carbonate rocks. Vulcanism is responsible for 0.02-0.05 Pg C/yr (Williams et al., 1992; Brickle, 1994). **2**

Figure 1.2: The extent to which environmental factors alter C-storage remains ambiguous. Major C-inputs include litter and Rhizodeposition. Major C-losses are dominated by the gaseous release of CO₂. While minor losses include the release of methane (CH₄), dissolved organic carbon (DOC), dissolved inorganic carbon (DIC) and particulate organic carbon (POC). Adapted from Davidson & Janssens, 2006. **3**

Figure 1.3: A summary of the characteristics of soil organic carbon compounds, highlighting that non-humic compounds are more readily decomposable than humic compounds. Information taken from McDonald et al. (2004). **7**

Figure 1.4: The main stages of Tisdall & Oades (1982) and Six *et al.* (2000) model of soil aggregate turnover. Modified from Blanco-Canqui and Lal (2004). **15**

Figure 1.5: The impact that C-content and soil disturbance has on aggregation. Showing the prevalence of transient, persistent and temporary OC-binding agents and the impact upon proportions of microaggregates and macroaggregates, under various land-uses. W= wheat, F= fallow, P= pasture. Taken from Tisdall & Oades (1982). **19**

Figure 2.1: The methods used to undertake the main aims of the project. Aims 1 and 2 are undertaken separately in **Chapters 4 & 5** and discussed in **Chapter 6**, due to methodology setbacks it was not possible to analyse the results from Aim 3, therefore the analysis of Hoosfield soil will be briefly presented in **Appendix 3**. The results from the analysis of Broadbalk and soils are considered collectively to achieve aim 4 in **Chapter 7**. SEM-EDX = scanning electron microscopy with elemental dispersive x-ray detection, LA-IRMS = laser ablation with isotopic ratio mass spectrometry. **35**

Figure 3.1: Soil series at Rothamsted Research. Point of sampling: Broadbalk winter-wheat (x), Broadbalk Wilderness (x) and Hoosfield (x), the soil series is typical Batcombe. Taken from Rothamsted research electronic archive. **38**

Figure 3.2: Field plan of Broadbalk winter wheat experiment, at Rothamsted Research, UK. Within section zero, plots 2.2, 03 & 07 were sampled March 2007. **41**

Figure 3.4: Field plan of Hoosfield continuous Maize experiment, at Rothamsted Research, UK. Plots (*) were sampled June 2007. **42**

Figure 3.5. Sampling within thin-sections. The whole slide excluding the outer perimeter will be described at 10x magnification. Three areas of interest will be randomly positioned within thin-sections. These areas will be further described and image analysis performed at 40X. **53**

Figure. 3.6. The process of organic matter classification. Firstly the form of organic matter is assigned following the recommendations of Babel (1975). Secondly, the extent of decomposition is identified using a modified classification proposed by Fitzpatrick (1993). Organ and Tissue fragments can be either: fresh/living, moderately or strongly decomposed while amorphous forms are strongly decomposed and are further described by their colour, with yellow-black indicating greater decomposition (Bullock et al., 1985). It is the combination of these two methods which makes this organic matter classification scheme novel. **56**

Figure 3.7. Images taken in plane polarised light or cross polarised light (XPL), showing organic fragments classed according to form and extent of decomposition following the guidelines outlined by Fitzpatrick (1993) (**Table 3.3**). Images show: Fresh/living organ fragments (A-C); moderately decomposed organ fragment (D-E); Moderately decomposed tissue (F-H); Strongly decomposed organ (J); Strongly decomposed tissue (K-L) and very Strongly decomposed (M-O). **57**

Figure 4.1: Mean rank standardised differences between all treatments, used in Dunn's nonparametric multiple comparisons test. Summarising the magnitude of the difference in, **a)** soil solution pH, and **b)** bulk density (g cm⁻³) between all treatments. Values beyond the $-Z$ or Z point (dotted line) indicate differences between treatments that are significantly less or greater, respectively ($p < 0.05$). **68**

Figure. 4.2. Wetting treatment for the determination of aggregate stability (Le Bissonais, 1996), plotted against mean weight diameter (MWD) (μm). Bars represent median of MWD for soils taken from, Broadbalk Wilderness, FYM, Inorganic and NIL. Error bars represent the interquartile range. Within each wetting treatment groupings, bars with the same letter do not differ significantly from each other (kruskal-Wallis followed by Dunn's non-parametric multiple comparisons test, $p < 0.05$). **69**

Figure 4.3: Water release curve for soil removed from Broadbalk NIL, Inorganic, FYM and Wilderness plots. Each treatment is fitted with a separate logistic curve. Percentage variance accounted for by regression: NIL, 87.5% (SE 0.017); Inorganic, 84.7% (0.033); FYM, 96.8% (0.0073); Wilderness, 83.2% (0.050). Slope of curves: NIL = -3.58; Inorganic = -1.19; FYM = -1.66; Wilderness = -5.23. **71**

Figure 4.4. Total porosity measured by image-analysis software at 12.5x as percentage of the total area analysed by IA (65 mm²); for soils removed from Broadbalk Winter-Wheat and Broadbalk Wilderness. Symbol denotes mean porosity while the line represents the median value; the box represents the inter-quartile range. Box plots followed by the same letter are significantly different ($p < 0.05$). **76**

Figure. 4.5 Total porosity for pores classed by shape factor according to Bouma *et al.* (1977) , measured as a percentage of the total thin-section area (65 mm²) analysed by image-analysis at 10.25 magnification. Bars represent the median value for soils removed from Broadbalk-winter-wheat and Broadbalk Wilderness; error bars represent the first and third quartile range. Shape factor ranges from < 0.2 for **planar**, $0.2 < 0.5$ for **irregular** and > 0.5 for **rounded** pores. There is a significant difference among pore classes ($p < 0.001$), with Dun's multiple comparisons test revealing that significant differences occur between all pore classes ($p < 0.05$). **77**

Figure 4.6. Frequency of pores classed by shape factor according to Bouma *et al.* (1977) at 12.5x, for soils removed from Broadbalk-winter-wheat and Broadbalk Wilderness. Bars represent median porosity; error bars represent the first and third quartile range. Shape factor ranges <0.2 for **planar**, 0.2 <0.5 for **irregular** and > 0.5 for **rounded** pores. Significant differences were found between treatments, ($p = 0.003$); and between pore classes ($p < 0.001$). **78**

Figure. 4.7. Total porosity measured by image-analysis software at 40x as percentage of the total area analysed by IA (36 mm²); for soils removed from Broadbalk-Winter wheat and Broadbalk mown-grassland. Symbol denotes mean porosity while the line represents the median value, the box represents the inter-quartile range. There is no significant difference in total porosity (logit transformed data) between treatments ($p = 0.270$). A Significant difference was found in the variance of the original data between treatments (Levene's test of equal variance: $p > 0.05$). **79**

Figure 4.8. Total porosity for pores classed by shape factor according to Bouma *et al.* (1977) , measured as a percentage of the total thin-section area (36 mm²) analysed by image-analysis at 40x. Bars represent the median value for soils removed from Broadbalk-winter-wheat and Broadbalk Wilderness; error bars represent the first and third quartile range. Shape factor ranges from <0.2 for **planar**, 0.2 <0.5 for **irregular** and > 0.5 for **rounded** pores. There is a significant difference among pore classes ($p < 0.001$) and a significant interaction between treatment*pore-shape ($p = 0.031$). **80**

Figure 4.9 Frequency of pores classed by shape factor according to Bouma *et al.* (1977) at 40x magnification. Bars represent the mean value for soils removed from Broadbalk winter-wheat and Broadbalk Wilderness; error bars represent the 95% confidence intervals. Shape factor ranges <0.2 for **planar**, 0.2 <0.5 for **irregular** and > 0.5 for **rounded** pores. No Significant differences were found among treatments, ($p = 0.999$); significant differences are found between pore classes ($p < 0.001$) There is no significant interaction between Treatment*Pore shape ($p = 0.637$). Plots followed by the same letter are significantly different (Tukey multiple comparison test $p < 0.05$). **81**

Figure 4.10: The pore size distribution for Broadbalk treatments NIL, Inorganic, FYM and Broadbalk Wilderness at **12.5x**. **a)** shows the observed and fitted curve, for each treatment. For clarity **b)** shows the fitted curve for each treatment, without the observed values. A linear + logistic curve was fitted and accounts for 90.9% of the variation in the data. The steepness of the curve between treatments decreases from: NIL (2.90), Inorganic (2.10), FYM (2.08) to Wilderness (1.69). **84**

Figure 4.11: The pore size distribution for Broadbalk treatments NIL, Inorganic, FYM and Broadbalk Wilderness at **40x**. **a)** shows the observed and fitted curve, for each treatment. For clarity **b)** shows the fitted curve for each treatment, without the observed values. A linear + logistic curve was fitted and accounts for 93.3% of the variation in the data. The steepness of the curve between treatments decreases from: Wilderness (1.93), Nil (1.82), Inorganic (1.64) to FYM (1.51). **86**

Figure 5.1 Loss on ignition as a proxy for organic matter content. Boxes represent the interquartile range, lines represent the median value, and the symbol denotes the mean value for soils removed from Broadbalk-winter-wheat and Broadbalk mown-grassland. Plots followed by the same letter are not significantly different ($p = 0.05$). **94**

Figure 5.2 Total area cover of organic matter at 40x. Boxes represent the interquartile range, lines represent the median value, and the symbol denotes the mean value for soils removed from Broadbalk-winter-wheat and Broadbalk mown-grassland. No significant differences were found in the area of organic matter fragments between treatments ($p = 0.614$). **97**

Figure 5.3. Area cover of organic matter classed according to form and extent of decomposition at 40x magnification. Bars represent the median value for soils removed from Broadbalk-winter-wheat and Broadbalk Wilderness; error bars represent the interquartile range. No significant differences were found between organic matter classes ($p = 0.087$). Organic matter classes are coded as follows: OF =Organ-Fresh, OM = Organ-Moderate, OS =Organ-Strong, TM= Tissue-Moderate, TS =Tissue-Strong, AY =Amorphous Yellow, AR =Amorphous Red, AB = Amorphous Black. **98**

Figure 5.4: Image of an Area of interest (AOI) of a thin-section removed from Inorganic plots of Broadbalk Winter-Wheat, in Plane polarised light (PPL) (left) and as an organic-matter pore map (right). Within the OM-pore map Pixels are colour coded White = soil matrix, Black = pore, red = Amorphous black, pink = Amorphous red, Yellow =Organ Moderately-decomposed. **100**

Figure 5.5. Frequency of organic matter classed according to form and extent of decomposition, at 40x. Bars represent the median value for soils removed from Broadbalk-winter-wheat and Broadbalk Wilderness; error bars represent the interquartile range. Significant differences were found in the frequency of organic matter fragments between organic matter classes ($p < 0.001$). Organic matter classes are coded as follows: OF =Organ-Fresh, OM = Organ-Moderate, OS =Organ-Strong, TM= Tissue-Moderate, TS =Tissue-Strong, AY =Amorphous Yellow, AR =Amorphous Red, AB = Amorphous. **101**

Figure 5.6: Mean rank standardised differences between all treatments, used in Dunn's nonparametric multiple comparisons test. Showing differences between the median frequency of organic matter by decomposition class. Values beyond the $-Z$ or Z point indicate differences between treatments that are significantly less or greater, respectively ($p < 0.05$). **101**

Figure 5.7: The O:C ratio of features by treatment, classified using micromorphological methods, the atomic O:C ratio is obtained by elemental analysed using SEM-EDX. Treatments are colour coded, light yellow = NIL, gold =Inorganic, Orange =FYM, Brown = Wilderness. The box represents the interquartile range, the line represents the median value, the symbol represents the mean, error bars represent the full range of data and outliers are indicated by a star. **103**

Figure 5.8: The O:C ratio of features, classified using micromorphology methods, the atomic O:C is obtained by elemental analysed using SEM-EDX. The box represents the interquartile range, the line represents the median value, the symbol represents the mean, error bars represent the full range of data and outliers are indicated by a star. Plots followed by the same letter are not significantly different (Dunn's $p < 0.05$). **104**

Figure 5.9: The concentration of C-associated with features, classified using micromorphology methods. Carbon (mg/kg) is obtained by elemental analysis using SEM-EDX. The box represents the interquartile range, the line represents the median value, the symbol represents the mean, error bars represent the full range of data and outliers are indicated by a star. Plots followed by the same letter do not differ significantly (Dunn's $p < 0.05$). **105**

Figure 5.10: The elemental spectrums for features classified using micromorphology, obtained by elemental point analysis using SEM-EDX. The box represents the interquartile range, the line represents the median value, the symbol represents the mean, error bars represent the full range of data and outliers are indicated by a star. **107**

Figure 5.11: Loading plot showing the contribution of Si, O, Mg, Al, Fe, Na, S and C to PC axis 1 and 2. **108**

Figure 5.12: Samples plotted according to their principal components. Samples are coded according to treatment (**a, top**) and feature (**b, bottom**). **109**

Figure 5.13 a) The O:C ratio of features, identified using phase analysis, obtained by elemental analysis using SEM-EDX. **b)** The C-concentration of features, identified using phase analysis, **c)** the O-concentration of features, identified using phase analysis. The box represents the interquartile range, the line represents the median value, the symbol represents the mean, error bars represent the full range of data and outliers are indicated by a star. Plots followed by the same letter are not significantly different (Dunn's $p < 0.05$). **114**

Figure 5.14: Elemental maps showing **(a)** Black-carbon particle (*red*, $O:C = 0.1$) surrounded by matrix (*blue*, $O:C = 1.2$) and silicates (*yellow*, $O:C = 0.5$). And **(b)** an organic-matter fragment (*pink*, $O:C = 0.2$) surrounded by soil matrix (*blue*, $O:C = 0.6$) silicates (*yellow*, $O:C = 1.2$) and resin (*green* = 0.4). **115**

Figure 5.15: The elemental spectrums for features classified using micromorphology, obtained by elemental phase analysis using SEM-EDX. The box represents the interquartile range, the line represents the median value, the symbol represents the mean, error bars represent the full range of data and outliers are indicated by a star. **116**

Figure 5.16: a) The O:C ratio of features, identified using phase analysis, obtained by elemental analysis using SEM-EDX. **b)** The C-concentration of features, identified using phase analysis, **c)** the O-concentration of features, identified using phase analysis. The box represents the interquartile range, the line represents the median value, the symbol represents the mean, error bars represent the full range of data and outliers are indicated by a star. Plots followed by the same letter are not significantly different (Dunn's $p < 0.05$). **118**

Figure 5.17: (a) Back Scatter Image of an organic matter fragment. **(b)** Elemental phase map taken at 15 keV of the same organic-matter fragment (*red* $O:C = 0.42$) surrounded by soil matrix (*blue*, $O:C = 1.0$) resin (*yellow*, $O:C = 0.58$). **120**

Figure 5.18: The elemental spectrums for features classified using micromorphology, obtained by elemental phase analysis using SEM-EDX at 15keV. The box represents the interquartile range, the line represents the median value, the symbol represents the mean, error bars represent the full range of data and outliers are indicated by a star. **121**

Figure 5.19: Elemental transect of the resin standard, analysed at 15 Kev. **Left**, BSI image showing the positioning of the transect; **right**, the relative concentration of Na (pink), Mg (purple), Fe (blue), Al (turquoise), S (green), Si (lime), O (orange) and C (red). **123**

Figure 5.20: Theoretical C-distributions with distance away from organic matter and black carbon particles located within an intact soil structure. Transects will begin 30 μm within the feature of interest. Each transect will cross from the feature of interest into the soil matrix, presented schematically in the lower diagram. The Blue line represents the boundary between feature and soil matrix, dark black line represents C-concentration with features, due to topological effects there will be a drop in x-ray detection. Beyond the boundary differences in C-concentration will be detected due to the nature of C-containing features and the total C-contents of the soil. Within the graph, black dotted lines represent OM and BC features that act as a source of carbon. The magnitude of the change in C-concentration will reflect total OC-content of the soil, different dotted lines represent the different treatments (see key). Red dotted lines represent BC features that act as a store of carbon. The

magnitude of the change in C-concentration will reflect total OC-content of the soil, different dotted lines represent the different treatments (see key). The bars below the graph summarise the nature of C-containing features, when acting as a store or source of C. Black represents where C is stored, dark grey where carbon is leaking into the soil matrix, and light grey represents background levels C within the soil matrix carbon. **125**

Figure 5.21: Elemental transect away from an **organic matter** fragment within Broadbalk **NIL** treated soil. Image top shows the OM-fragment under PPL. Images to the left show OM under BSI conditions, transect positioning is superimposed. Elemental concentrations along transects are shown, right, S =blue, O =green, C =red. **127**

Figure 5.22: Elemental transect away from an **organic matter** fragment within Broadbalk **Inorganic** treated soil. Image top right shows the OM-fragment under PPL, image top left shows the OM-fragment under BSI at low magnification. Images to the left show OM under BSI conditions, transect positioning is superimposed. Elemental concentrations along transects are shown, right, S =blue, O =green, C =red. **128**

Figure 5.23: Elemental transect away from an **organic matter** fragment within Broadbalk **FYM** treated soil. Image top right shows the OM-fragment under PPL, image top left shows the OM-fragment under BSI at low magnification. Images to the left show OM under BSI conditions, transect positioning is superimposed. Elemental concentrations along transects are shown, right, S =blue, O =green, C =red. **129**

Figure 5.24: Elemental transect away from an **organic matter** fragment within **Broadbalk Wilderness** soil. Image top shows the OM-fragment under PPL. Images to the left show OM under BSI conditions, transect positioning is superimposed. Elemental concentrations along transects are shown, right, S =blue, O =green, C =red. **130**

Figure 5.25: Elemental transect away from a **Black carbon** fragment within Broadbalk **NIL** treated soil. Image top right shows the BC-fragment under PPL, image top left shows the BC-fragment under BSI under at magnification. Images to the left show BC under BSI conditions, transect positioning is superimposed. Elemental concentrations along transects are shown, right, S =blue, O =green, C =red. **131**

Figure 5.26: Elemental transect away from a **Black carbon** fragment within Broadbalk **Inorganic** treated soil. Image top shows the BC-fragment under PPL. Images to the left show BC under BSI conditions, transect positioning is superimposed. Elemental concentrations along transects are shown, right, S =blue, O =green, C =red. **132**

Figure 5.27: Elemental transect away from a **Black carbon** fragment within Broadbalk **FYM** treated soil. Image top right shows the BC-fragment under PPL, image top left shows the BC-fragment under BSI under at magnification. Images to the left show BC under BSI conditions, transect positioning is superimposed. Elemental concentrations along transects are shown, right, S =blue, O =green, C =red. **133**

Figure 5.28: Elemental transect away from a **Black carbon** fragment within Broadbalk **Wilderness** treated soil. Image top right shows the BC-fragment under PPL, image top left shows the BC-fragment under BSI under at magnification. Images to the left show BC under BSI conditions, transect positioning is superimposed. Elemental concentrations along transects are shown, right, S =blue, O =green, C =red. **134**

Figure 6.1: Demonstrating the relationship between SOC and soil porosity. Values in red represent data obtained by this study, values in blue are published values taken from: Barral *et al.*, (2007), Miralles *et al.*, (2009), Verma & Sharma (2007), Bhogal, Nicholson & Chambers (2009), Abid & Lai (2008). **142**

Figure 6.2: Examples of the porosity characteristics determined by image analysis (minimum threshold = 100 μm) . Taken from: Broadbalk NIL (*top left*), Inorganic (*top right*), FYM (*bottom left*) and Wilderness (*bottom right*) soil. **146**

Figure 6.3: SEM images showing evidence for faunal exploitation of charcoal, taken from Colluvial soils, Campo Lameiro, Spain. Images Taken from Kaal & Van Mourik, 200. **154**

Figure 6.4: Image of an area of interest (AOI) of a thin-section removed from Inorganic plot of Broadbalk Winter-Wheat. **a)** in Plane polarised light (PPL) (*top left*) and **b)** as an organic-matter pore (map *top right*). Within the OM-pore map pixels are colour coded White = soil matrix, Black = pore, red = Amorphous black, pink = Amorphous red, Yellow =Organ Moderately-decomposed. **c)** SEM-EDS phase-map showing the organic matter fragment classified as Moderately-decomposed (*bottom left*). Pixels within the phase-map are colour coded as (blue), resin (red), soil matrix (yellow) silicates (orange). **d)** back scatter electron image of Organ Moderately-decomposed (*bottom right*). **158**

Figure 6.5: Revised theoretical C-distributions with distance away from organic matter and black carbon particles located within an intact soil structure, based on preliminary data. Transects will begin 30 μm within the feature of interest. Each transect will cross from the feature of interest into the soil matrix, presented schematically in the lower diagram. The Blue line represents the boundary between feature and soil matrix, dark black line represents C-concentration with features, due to topological effects there will be a drop in x-ray detection. Beyond the boundary differences in C-concentration will be detected due to the nature of C-containing features and the total C-contents of the soil. Within the graph, black dotted lines represent BC and red represents OM features that act as a source of carbon. The bars below the graph summarise the nature of the C-signal. Black represents where C is stored, dark grey where carbon is leaking into the soil matrix, and light grey represents background levels C within the soil matrix carbon. **160**

Figure 7.1: A summary of the process of OM decomposition and its impact upon soil structure, as evident within soil thin-sections. **a)** The decomposition of particulate organic matter will lead to the formation of a pore. **b)** As decomposition proceeds OM becomes fragmented and increasingly incorporated into the soil matrix and microaggregates in the form of excremental pedofeatures are more abundant. **c)** Towards the later stages of decomposition, under the light microscope OM appears amorphous in form and is incorporated into the soil matrix away from soil pores. Amorphous OM is likely to stabilise soil structure by organo-mineral interactions and therefore itself be more chemically and physically protected from decomposition. As evident by SEM-EDS analysis there is a movement of C into the soil matrix, this may further enhance soil structural stability, for particulate OM the extent that C enters the soil matrix is greater ($>40 \mu\text{m}$) compared to more recalcitrant black carbon (20 μm). Further analysis is required to investigate the extent to which amorphous OM acts as a source or store of OC. It is hypothesised that particulate OM located within soil pores may act as a source of labile carbon for sub-soil horizons. For instance, Chabbi *et al.*, (2009) reported that OC is located within preferential flow paths of sub-soil. **164**

Figure 7.2: Back-scattered image of a black carbon particle within a soil thin-section (*top*) taken from Broadbalk Inorganic treated soil. Elemental distribution of Ca (*bottom*) determined by SEM-EDS analysis. Calcium appears to be largely associated with cracks around the edge of the black carbon particle. **166**

Tables

Table 1: Abbreviations and Definitions

Table 1.1: Emerging levels of soil structural and functional complexity in agricultural systems. **11**

Table 1.2: A functional Classification of Pore Based on Size. **13**

Table 1.3: The classification and description of organic carbon aggregate binding agents. **17**

Table 1.4: Carbon storage within a range of aggregate size classes in soils under different Management. **24**

Table 3.1: Details of treatments and rates of application, for plots sampled within the Broadbalk experiment. **39**

Table 3.2: Treatment details for Hoosfield continuous Maiz. **43**

Table 3.3: The classification for the extent of organic-matter decomposition, modified from Fitzpatrick (1993). **58**

Table 3.4: The parameter set-up of the SEM when optimizing for the collection of carbon X-rays when using. **61**

Table 3.5: O:C ratios of a range of C-containing particles, determined by elemental analysis using SEM-EDX. **63**

Table 4.1: General chemical and physical analysis of bulk soil collected from Broadbalk Winter-Wheat, and Broadbalk Wilderness. **67**

Table 4.2: Evidence of Soil Aggregation, across Broadbalk Winter-Wheat and Broadbalk Wilderness at 40x and 12.5x Magnification. **73**

Table 4.3: Abundance* of Voids by Shape Across, Broadbalk Winter-Wheat and Broadbalk Wilderness at 40x and 12.5x. **74**

Table 5.1: The Abundance of Excremental Pedofeatures, Across all Treatments. **96**

Table 5.2: Frequency* of Organic particles classed by form and decomposition and their location in relation to pores. **102**

Table 5.3: Showing the Total Variance Explained, by Eigenanalysis of the Correlation Matrix. **108**

Table 5.4: Summary of Classification Results, for Features using Elemental Data obtained by SEM-EDX. **111**

Table 7.1: Summary of EDS Analysis of Features Identified using Micromorphology Techniques. **168**

Table 1: Abbreviations and Definitions

	Abbreviation	Definition
Aggregate water stability	AWS	
Areas of interest	AOI	
Black carbon	BC	
C:f related distribution		“the distribution of individual fabric units in relation to smaller fabric units (lower limit set to 10 µm in this study) and associated pores” (Stoops, 2003). In this study the c:f related distribution is porphyric (i.e. “larger units occur in a dense groundmass of smaller units, there are several subtypes based on the relative distance between the coarser units” (Stoops, 2003)).
Calcite biospheres		“0.4-2mm in diameter, composed of an outer layer of pure coarse calcite with an incomplete radial fabric and finer crystals in the centre. They are secreted by earthworms” (Stoops, 2003).
Chambers		...”equidimensional smooth-walled pores interconnected by channels...” (Stoops, 2003).
Channels		“Tubular smooth voids with a cylindrical or arched cross section which are uniform over much of the length, they are mainly root channels or biogalleries...” (Stoops, 2003).
Coalescence		“Excrements...coalesce at their points of contact and form higher units (microaggregates). Four grades of microaggregates are identified by Bullock <i>et al.</i> (1985) 1= very porous, 2= porous, 3=dense, 4=very dense.” (Stoops, 2003).
Coatings		“Intrusive pedofeatures coating a natural surface (voids, grains, or aggregates)” (Stoops, 2003).
Conservation Tillage	CT	
Crossed polarised light	XPL	

Disintegration of pedofeatures		“Characterised by the formation of cracks, followed by a loss of shape.” There are “three grades of disintegration distinguished by the volume affected: weak (<30%), moderate (30-70%), strong (>70%) (Stoops, 2003).
Equivalent Circle Diameter	ECD	The diameter of a circle with the same area as the pore
Excremental pedofeatures		In this study refers to excrement of the mesofauna, which form discrete fabric units (see definition of pedofeatures).
Farm yard Manure	FYM	
Grade (of Aggregates)		Strongly developed: “The Soil Material is divided into a number of units each of which is entirely surrounded by features pointing to a surface of weakness” (Stoops, 2003). Moderately developed: “The soil material is divided into a number of units that are surrounded on at least two-thirds of their periphery by features pointing to a surface of weakness...” (Stoops, 2003). Weakly developed: “The soil material is divided into a number of units separable on the basis of being partially surrounded by features pointing to a surface of weakness (one-two thirds)”.
Hypo-coatings		“Matrix pedofeatures referred to a natural surface in the soil and immediately adjoining it” (Stoops, 2003).
Image analysis	IA	
Inter-Particulate Organic Matter	I-POM	
Inorganic Fertiliser (Broadbalk treatment)	Inorganic	
Laser Ablation- Isotope Ratio Mass Spectrometry	LA-IRMS	
Loss on ignition	LOI	
Manganese/iron nodules		...”Equidimensional pedofeatures that are not related to natural surfaces or voids...” (Stoops, 2003).

Mean Weight Diameter	MWD	“The MWD is the sum of the mass fraction remaining in each sieve multiple by the mean aperture of the adjacent sieve (with MWD ranging from 25 µm to 3.5 cm)” Le Bissonnais (1996).
No fertiliser application (Broadbalk treatment)	NIL	
No Tillage	NT	
Oblique incident light	OIL	
Oxygen: Carbon ratio	O:C	
Organic carbon	OC	
Organic matter	OM	
Particulate Organic Matter	POM	
Pedofeatures		“Are discrete fabric units present in soil materials that are recognisable from an adjacent material by a difference in concentration in one or more components or by a difference in internal fabric” (Stoops, 2003).
Planes		...”Flat voids, accommodating or not, smooth or rough; they are the result of shrinkage or slipping”. (Stoops, 2003).
Plane polarised light	PPL	
Quasi-coatings		“Matrix pedofeatures referred to a natural surface in the soil, but not immediately adjoining the natural surfaces” (Stoops, 2003).
Representative Elementary Area	REA	
Scanning electron microscopy	SEM	
Scanning electron microscopy energy dispersive spectroscopy	SEM-EDS	
Soil organic carbon	SOC	
Soil organic matter	SOM	
Vughs		“...Irregular voids, smooth or rough...they are the result of welding of aggregates, disruption of the microstructure or dissolution of components” (Stoops, 2003).
Wilderness (Broadbalk Grassland)	WILD	

Chapter 1: The Nature, Distribution and Significance of Organic Carbon in Soils.

1. Introduction

Within the global carbon cycle, soil represents the second largest storage component of OC (organic carbon) (**Fig. 1.1**), sequestering 1500 Pg C with the first upper meter, exceeding the quantity of carbon stored in the atmosphere and vegetation combined (IPCC, 2001). The storage of OC is not inert. C-accumulation is a balance between inputs from photosynthetically fixed-C and anthropogenic C-products and the mineralisation of these C-compounds. Additionally, environmental factors can influence C-fluxes and consequently the overall quantity of carbon sequestered within soil.

The amount of terrestrial carbon fixed globally via photosynthesis is estimated at 120 Pg C yr⁻¹ (Ciais, 1997) this is termed gross primary production (GPP). One half of GPP is incorporated into plant tissue while the remaining is released as CO₂ produced through autotrophic respiration (Lloyd & Farquhar, 1996). Only 50% of C fixed by vegetation enters the soil and this is defined as net primary production (NPP). The longevity of this sequestered-C within soil depends upon a multitude of factors (**Fig. 2**) including: the type of C-compounds, land disturbance and environmental constraints. Net ecosystem production (NEP) is the difference between NPP and C respired by heterotrophic respiration (Rh) through the decomposition of C-compounds. NEP clarifies the amount of carbon lost or gained in the absence of ecosystem disturbances (e.g. fire). The global NEP is currently estimated at 10 Pg C yr⁻¹(IPCC, 2001), although this value is possibly an over estimation given current biases of site sampling (Bolin *et al.*, 2000).

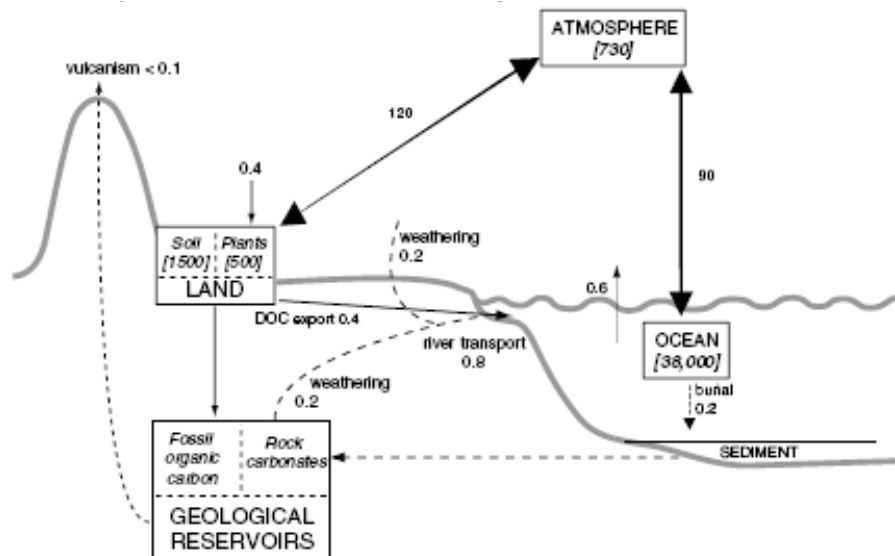


Figure 1.1: The main components of the natural carbon cycle showing, carbon storage (Pg C) and fluxes (Pg C/Yr). Thick arrows denote current important fluxes to ensure balance of CO₂ exchange including gross primary production and respiration by the land biosphere and physical air-sea exchange. Thin lines denote smaller additionally natural fluxes, with dashed lines representing fluxes of CaCO₃ CO₂ from these fluxes are balanced on longer-term scales. Also shown is river export (0.8 Pg C/yr) comprising the export of dissolved organic carbon (DOC) (0.4 Pg C/yr) and dissolved inorganic carbon (DIC) from the weathering of CaCO₃ (0.4 Pg C/yr). Once reaching the ocean DOC is respired and released into the atmosphere while only one half of DIC is returned to the atmosphere the remaining is incorporated into deep sea sediments and forms carbonate rocks. Vulkanism is responsible for 0.02-0.05 Pg C/yr (Williams et al., 1992; Brickle, 1994).

Of particular importance is net biome production (NBP), the actual remaining C-storage once all land-disturbances have been accredited. The ultimate fate of CO₂ entering the terrestrial biosphere is to return to the atmosphere, for an ecosystem to be in “steady-state” NPP all forms of C-losses must balance, thereby NBP will equal zero. In reality this scenario is not observed given the multitude of factors which influence C-inputs and losses (**Fig. 1.2**). Therefore, sequestered carbon is a product of a time-lag between C-fixed and C-returned to the atmosphere, caused by NPP exceeding the rate of C-decomposition of more recalcitrant carbon. This time-lag can persist for years to decades with the global average persisting for 20-30 years as the ecosystem gradually returns to a steady-state equilibrium (Raich & Schlesinger, 1992). Currently net global NPP exceeds NBP therefore the terrestrial biosphere is acting as a net sink for carbon, sequestering $-0.2 \text{ Pg C yr}^{-1}$ (IPCC, 2001).

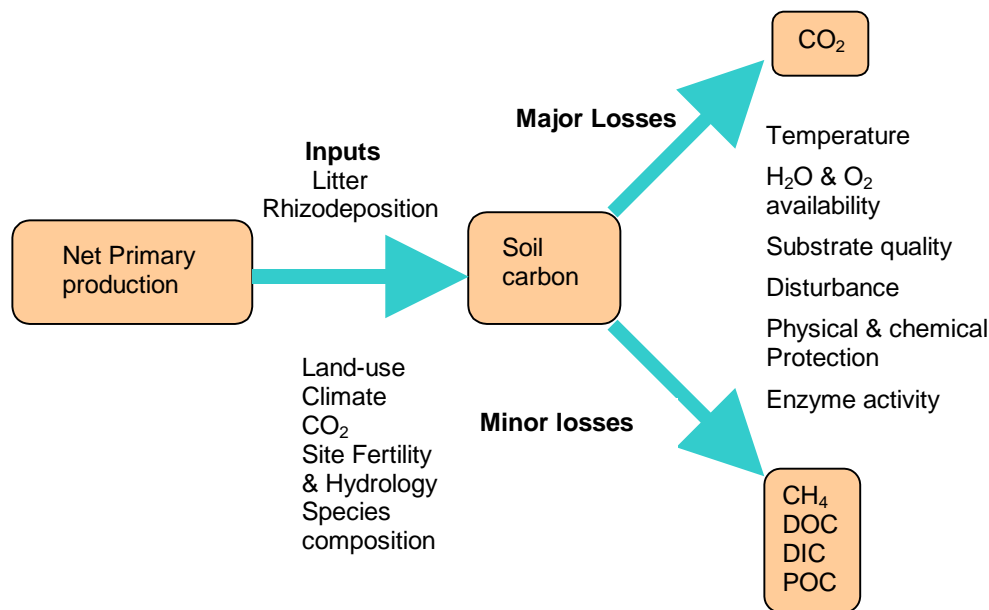


Figure 1.2: The extent to which environmental factors alter soil organic carbon storage remains ambiguous. Major OC-inputs include litter and Rhizodeposition. Major OC-losses are dominated by the gaseous release of CO₂. While minor losses include the release of methane (CH₄), dissolved organic carbon (DOC), dissolved inorganic carbon (DIC) and particulate organic carbon (POC). Adapted from Davidson & Janssens (2006).

As stated, inputs and losses of carbon are influenced by a multitude of environmental factors. However, the extent to which each alters C-storage remains ambiguous (**Fig. 1.2**). Given this, it is highly complicated to predict the impact of future environmental change and human disturbance events upon NBP. Anthropogenic exploitation of land has caused huge losses of terrestrial OC globally: from 1850 to 2000 it is estimated that 156 Pg C was emitted (Houghton, 2003). Deforestation is responsible for major carbon losses accounting for 90% of the global C lost since 1850 (Houghton, 1999). Globally, the conversion of natural vegetation to arable land is still prevalent and substantial CO₂ is released, primarily as carbon from plant biomass is lost and secondly through continued soil disturbance including tillage, irrigation and fertiliser application (Schesinger, 2000; Six *et al.*, 2000). The actual amount of C lost from soils following deforestation is dependent upon the subsequent land use. Take for example Amazonia Oxisols, which represent 8.7% of the earth's land surface and contain approximately 7.5% of all the soil organic carbon content to a depth of 1m (Eswaran, 1993). Mature forest soil is estimated to contain 96 Mg ha⁻¹ following conversion to pasture this decreases to 79.7 Mg ha⁻¹, while conversion to rubber tree plantations SOC-content can fall to 56.3 Mg ha⁻¹ (Ibraim *et al.*, 2009). Andosols (volcanic soils) and Histosols (organic soils) have the greatest potential to store organic carbon and the exploitation of these soils can lead to substantial SOC losses. Histosols are estimated to store 455 Pg C (IPCC, 2001) this large

SOC reserve is maintained through waterlogged (anaerobic) conditions. Management practises which disrupt the anaerobic conditions of Histosols (e.g. drainage) can initiate SOM decomposition and therefore substantial emissions of greenhouse gases: CO₂, CH₄ and N₂O. Of all the mineral soils Andosols have the highest organic carbon content, they are formed upon volcanic parent material, the mean SOC stock within the top 100cm is estimated to be 25.4 kg m⁻² (Batjes, 1996) and conversion to arable land leads to these soils acting as a net source of C.

The UK's voluntary low C-transition plan proposes a 6-11% reduction in C-emissions from agricultural practises (Gundula Azeez, 2009). Efficient management practices of agricultural land provide the opportunity to mitigate CO₂ emissions and to alleviate soil disturbance, ensuring overall a more sustainable approach to land-use complying with the Kyoto protocol article 3.4 (1997). Sustainable management schemes will vary regionally and will incorporate one or more of the following:

- Application of organic amendments
- Organic farming
- Conservation tillage
- Set-aside land
- Cultivation of woody bioenergy crops
- Reduced in cultivation of organic soil (ECCP, 2001)

Environmental change is expected to influence both the rate of plant photosynthesis and C-decomposition. Warming will extend the duration of both daily and seasonal plant growth in northern temperate and arctic ecosystems. This in the short-term is expected to increase both NPP and respiration (root and soil), in northern latitudes (Lloyd & Taylor, 1994). As atmospheric CO₂ increases, C₃ plants respond with an increase in the rate of photosynthesis (Norby *et al.*, 2005), alternatively plant growth may enhance due to a greater water use efficiency as stomata can be open less often to fix the same amount of CO₂ (Luo *et al.*, 1999). In temperate regions N-limitation has been elevated by N-fertilisation of biologically active NO_x and NH₄, released through anthropogenic activity. The increasing atmospheric CO₂ and N-availability has been found to have an additive effect upon forest production (Oren *et al.*, 2001). However the response of plant productivity is further complicated if other elements become limiting (Shaw *et al.*, 2003). Furthermore, the longer-term responses remain unclear due to the conglomeration of climatic changes, for instance, rainfall, solar radiation, and land disturbance frequencies and their environmental impacts (IPCC, 2001).

The impact that climate change will have on SOM (soil organic matter) decomposition is equally ambiguous. One major uncertainty is the extent to which various C pools are sensitive to changes in temperature; with models Century model: (Parton *et al.*, 1987); Roth-C model: (Coleman *et al.*, 1996) suggesting that resistant C pools are greater (Knorr *et al.*, 2005), lesser (Giardina & Ryan, 2000) or similar to the labile C-pool in its sensitivity to changes in temperature. Recalcitrant compounds are more abundant than labile C-compounds and if they are more sensitive to increases in temperature, this could lead to a greater efflux of carbon over decadal and longer time-scales (Davidson, *et al.*, 2006).

In the natural environment the response of SOM decomposition is further complicated since soil structure also influences the availability of substrates at enzyme reaction sites (Diaz and Balkus, 1996; Mayer *et al.*, 2004). For instance, micropores may physically reduce accessibility of decomposers or extracellular enzymes to substrates. Drought reduces water film thickness thereby impeding the diffusion of substrates and enzymes. Alternatively, decomposition can be chemically inhibited due to anaerobic conditions which would limit the range of reactions that can take place (Davidson, 2006). The ever changeable soil environment means that many of these constraints are transient.

Models of carbon turnover separate carbon into several “pools”, reflecting their mean residence times (MRTs). MRT is defined as the inverse of decomposition rate (K) thereby accounting for both chemical constraints (C-compound composition) and environmental limitations (Davidson, 2006). The two major C-turnover models are ROTH-C (Jenkinson, 1990) and CENTURY (Parton, 1987). The models have proven to be highly effective in predicting local turnover rates of carbon compared to models which class SOM as a single homogenous pool, however, their usefulness in predicting responses to climate change is still being debated (Davidson, 2006). Despite the effectiveness of these models one major limitation is that the precise constraints determining MRTs have not been fully explored and it is presumed that all SOM is equally sensitive to changes in temperature. Consequently, two very different carbon compounds can have the same MRT as a result of completely separate processes. For instance, no distinction is made between C-compounds that are chemically simple yet physically protected, and vice versa (Davidson, 2006). Identifying where C-compounds are sequestered within the soil structure would be a major step towards separating environmental constraints and intrinsic chemical properties of C-compounds, which together determine carbon MRT. Furthermore, Brunn *et al.*, (2010) argue that multi-component models are theoretical constructs unrelated to measurable pools of SOM, and that partitioning of SOM should be based upon SOM fractions which have functional roles within the soil. Brunn *et al.*, (2010) argue that the current separation of SOM is not realistic and methods

need to be developed which classify SOM on a continuous scale relating to their functional role. For instance even the most well defined pool e.g. black carbon is highly variable in form and composition. Thereby classifying SOM on a continuous scale related to their function will permit models to be validated which in turn will aid a more mechanistic understanding of SOM turnover (Brunn, *et al.*, 2010).

1.2 Carbon-Compounds in Soil Organic Matter.

Soil-organic-matter (SOM) is defined as “Natural-C-containing-organic materials living or dead, but excluding charcoal” (Oades, 1988). The composition of SOM is highly heterogeneous, due to the multitude of sources and extent of decomposition of OM found within the soil. SOM is an important storage component of organic nutrients, and is generally composed of 55% OC, with the remaining 45% comprising of a range of other essential nutrients including organic N, P and K (Blanco-Canqui & Lal, 2004). Since SOM is composed largely of OC it is not unusual to find the two terms used interchangeably within the literature.

As with SOM, organic-C-compounds have a highly variable structure, which, to date is incompletely known. As such, OC-compounds are grouped together into broad classes. There are several approaches for achieving this according to decomposability, molecular weight, and size. In theory, C-compounds are generally described according to their decomposability since high molecular weight and larger molecular size both contribute to recalcitrance. Conversely, in practise partitioning of C-compounds typically involves separation according to size (sieving), molecular weight (suspension), or C-functional groups (C^{13} NMR).

The basis of classifying C-compounds is to first separate according to two broad classes; non-humic and humic substances defined according to the extent of OC decomposition and MRT (**Fig. 1.3**). Non-humic C-residues typically have their original physical and chemical characteristics of their source material still identifiable, they have low molecular weights and are relatively susceptible to degradation (Schnitzer, 1991). Non-humic substances have a “known” composition which includes: polysaccharides 50-60% (Starch, cellulose, hemicellulose and pectin), lignin (15-20%), proteins polyphenols, chlorophyll, cutin, suberin, waxes and resins (10-20%). (Lützow *et al.*, 2006). Although described as having a “known” composition, the actual variability of each component of non-humic substances (e.g. lipids) is only identifiable for a small number of plant species (Lützow *et al.*, 2006). Non-humic compounds in soil have a short MRT, with decomposition taking place from hours to days for simple monomers (e.g. glucose, amino acids) extending to months for more complex polymers (e.g. cellulose) (Lützow *et al.*, 2006).

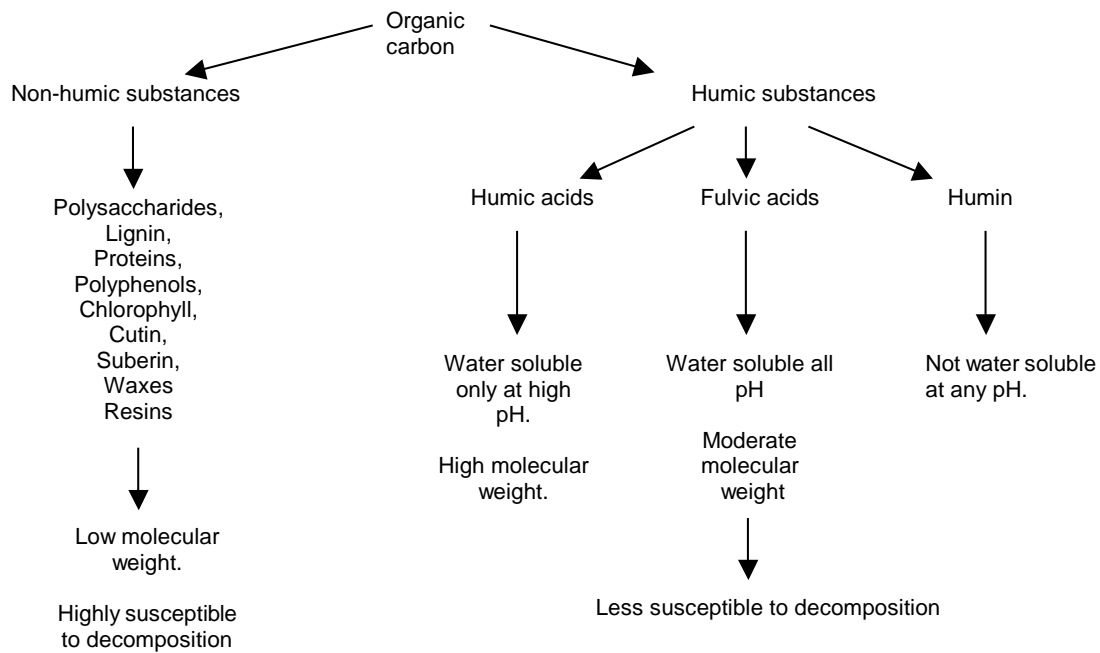


Figure 1.3: A summary of the characteristics of soil organic carbon compounds, highlighting that non-humic compounds are more readily decomposable than humic compounds. Information taken from (McDonald *et al.* (2004)).

Carbon compounds, altered chemically and physically from their original composition are an important focus when studying C-storage within soils since even minor modifications can drastically impede decomposition and mineralisation rates (Tate, 1987). Humification-represents the major pathway through which carbon is modified with processes such as combustion and the production of black carbon. Additionally, more recently it has been found that C-compounds which are synthesised specifically by microorganisms accumulate in soils (Kögel-Knaber, 2003). Consequently, microorganisms are described as having an indirect impact on OC-sequestration rather than a direct impact given their relatively low biomass (0.3-6% of total SOC) (Lutzow, *et al.*, 2006).

Humic compounds are highly decomposed and do not display any of the original physical and chemical characteristics of the source material. Humic compounds are defined as “naturally occurring, biogenic, heterogeneous organic substances... being yellow-black in colour, of high molecular weight and refractory” (McDonald *et al.*, 2004; MacCarthy *et al.*, 1990). Humic compounds are especially prolific within the soil and contribute approximately to 60-70% of bulk OC-contents (Griffith & Schnitzer, 1975), however their composition is inadequately understood. To compensate for this, humus is subdivided into three categories: humic acids, fulvic acids, and humin, each having distinct mean molecular weights, functional group content and solubility characteristics (**Fig. 1.3**) (McDonald *et al.*, 2004).

Humic compounds, or humus, is a significant contributor to OC-storage due to its abundance (Griffith & Schnitzer, 1975), highly refractory nature (Tate, 1987) and high C-content (~50%) (Schnitzer, 1991). Partially decomposed polymers form the precursors for humic polymers which are formed through condensation and polymerization reactions. Currently the precise process leading to the formation of humus is unknown, but two opposing theories of humus formation (humification) exist. Firstly that humus is formed from spontaneous heteropolycondensation which produces a C-compound with a unique chemical structure, thereby rendering it indecomposable by conventional enzymes (Heges, 1988); (Stevenson, 1994). However, evidence for the spontaneous production of new C-compounds *in-situ* is rarely evident, as indicated through ¹³C NMR studies (Hedges & Oades, 1997). An alternative hypothesis is that products from plant and animal decomposition form clusters through hydrophobic interactions and H-bonds, forming chemical recalcitrant molecules with ostensibly high macromolarities termed “Pseudo-macromolecularity” (Piccolo, 2002), but as yet there is no evidence to support this theory (Lutzow, *et al.*, 2006).

Black carbon (BC) compounds represents a major storage component of global soil C-sequestration, to the extent that BC is considered to contribute significantly to the “missing carbon” fraction within the global C-budget (González-Pérez *et al.*, 2004). BC is formed through chemical and physical modifications of organic matter caused by incomplete combustion of OM, due to limited O₂ availability. The term BC has recently been endorsed to describe the “continuum from partly charred plant material through char and charcoal to graphite and soot particles condensed from the gas phase” (González-Pérez *et al.*, 2004). Clearly BC represents a highly heterogeneous array of C-compounds the precise nature of which is influenced by fire intensity and fuel. In general though, BC is composed largely of aromatic (low energy) compounds, consequently it has a long MRT ranging from 500-10 000 years (Schmidt, *et al.*, 2002). BC is estimated to constitute 1-6% of total SOC (González-Pérez *et al.*, 2004), however within the regional scale BC can constitute a much greater proportion of total-OC. In Germany, BC can account for 45% of total OC in chernozemic soils and up to 80% (in more industrialised regions) of total OC-storage, while in Australia, BC is found to constitute around 30% in grasslands under aboriginal burning practises (Schmidt *et al.*, 1999); (Skjemstad *et al.*, 1997). Clearly these more extreme BC-contents are associated with human activities which have increased the occurrence of OM-combustion.

Recalcitrant C-compounds are also characterised by their low carbon to nitrogen ratio (C:N), since as decomposition proceeds, the C:N narrows as N is utilised by microorganisms for protein synthesis (White, 2006). The C:N ratio is often used as an indicator for the rate of decomposition, with decreasing N-availability limiting the rate of decomposition. However,

the C:N ratio is only a useful indicator of the rate of decomposition at the early stage i.e. for describing the quality of residue inputs (Melillo, *et al.*, 1982). While for the more advanced stages (i.e. recalcitrant SOM decomposition), high lignin concentrations (Fogel & Cromack, 1977) or high lignin to nitrogen ratios (Melillo, *et al.*, 1982) will retard the rate of OC decomposition. Consequently, lignin and other plant polyphenolic compounds are regarded as important compounds for SOC-storage since polyphenolics act as precursors for the production of humic compounds (Martens, 2000b; Stevenson, 1994). It is also possible to distinguish between C-compounds by their oxygen to carbon ratio (O:C). For instance, recalcitrant humic compounds consist of a greater proportion of carbon and lesser amounts of oxygen than fulvic compounds. This is attributed to fulvic acids being associated with greater amounts of carboxyl functional groups. Additionally, black carbon particles (BCP) can be characterised by low oxygen to carbon ratios, typically less than 0.15 (Stoffyn-Egli *et al.*, 1997), this is clearly distinct from the O:C ratios of humic acid (0.60) and Fulvic acid (0.98) (**Section 3.3.8 & 3.4.9**).

Clearly, recalcitrant properties of C-compounds will favour their selective preservation within the soil. However, the sequestration of C-compounds within the soil matrix is a consequence of the interactions between the inherent recalcitrant properties of C-compounds and their simultaneous interaction with soil structural components. Additionally, it is becoming increasingly evident that C-compounds, which are conventionally considered to be vulnerable to decomposition, can accumulate in the soil.

1.3 An Introduction to Soil Structure

Towards the end of the 19th century theories of pedology began to develop and it was rapidly recognised that soil is not randomly formed but is organised into structural units. Throughout this project descriptions of soil structure will encompass both aggregates, pore space and their arrangement. Soil structure is dynamic, it is continually being modified by external forces, which influence its development, as such, the condition and quality of soil is also changeable (Blanco-Conqui & Lal, 2004). The components of soil structure range over several orders of magnitude (μm to cm) (Carter, 2004) with the development of soil structure being hierarchical. As such methods of investigating soil structure can be conducted in the field, or by using microscopy or sub-microscopy techniques. Typically soil structure can be characterized by three aspects these include, geometry i.e. the arrangement and size of pore space; stability, i.e. the response of soil aggregates to external forces and resilience, which is the ability of a soil to recover its pore space following an applied stress (Kay, 1990). External forces (often termed stresses) include compaction by machinery or animals, breakage by tillage, dry-wet or freeze-thaw cycles and bioturbation by mesofauna. These factors influence the arrangement of particles into aggregates and aggregates into peds. The hierarchical nature of soil structure and the processes that soil structure influence are summarised in **Table 1.1**, it is clear that the maintenance of a good soil structure is essential to soil functionality. Soil organic matter is directly and indirectly (through microbial and mesofauna activity) responsible for aggregate development and in turn soil structure confers physical protection to SOM (**Table 1.1**). It is well accepted that soil aggregates are central to the storage of OC, with numerous studies (**Section 1.4.5 & 1.5**) demonstrating that the rate of OC-decomposition is far greater when OC is not occluded within soil aggregates, as a result much of the current research into C-storage focuses upon the role of soil aggregates, however the mechanisms involved are not yet fully understood (Besnard *et al.*, 1996). In brief organic matter plays a major role in soil structural development in all soils except oxisols. Therefore, any external forces that influence OM will consequently affect soil structure. Current research has largely focused upon the interactions between soil aggregates and SOM, by assessing aggregate turnover and stability and SOM dynamics within aggregates.

Table 1.1: Emerging levels of soil structural and functional complexity in agricultural systems.

Soil structural entities and components	Soil Functional Features and Processes
Primary Structure (scale in μm)	
Mineral-organic matter complexes	Modification of microenvironment
Uncomplexed organic matter	Surface reactivity
Microaggregates (2-250 μm in diameter)	Chemical stabilisation of organic matter
Secondary Structure (scale in μm-mm)	
Aggregated mineral-organo complexes	Physical protection of organic matter
Uncomplexed organic matter	Soil porosity and aeration
Macroaggregates (>250 μm diameter)	Pore space and continuity
Fine roots	Microfaunal habitat
Fungal hyphae	Water retention
Tertiary Structure (scale in mm-cm)	
Whole, intact soil <i>in situ</i>	Macrofauna and bioturbation
Macropores and large roots	Pore continuity and preferential flow
Macrostructure	Leaching and gaseous emissions
	Compaction and draft
Soil profile (scale in cm-m)	
Soil peds (granular, blocky, platy, columnar)	Soil disturbance and movement
	Abiotic features (freeze-thaw, Shrink-swell)
	Tillage impacts on structure

Taken from Carter (2004), originally adapted from Christensen (2001) and Carter, (2004)

1.4 The Importance of Structure for Soil Functionality

The following section will discuss the importance of structure for soil functioning. The development and functioning of soil pores will be discussed followed by theories of aggregate stability and hierarchy. Finally the current understanding of the relationship between aggregates and SOM and the approaches used for investigation will be presented.

Understanding the forces controlling soil structural development is essential due to the important effect soil structure has on biological, chemical and physical processes. In turn identifying the mechanistic control of structure upon soil function is problematic given that external forces are constantly altering soil structure in both time and space. The arrangement and size of pores and aggregates ultimately controls the dynamics of water, air and organic matter within soil. For instance, aggregation controls plant establishment, water infiltration aeration and drainage thereby creating a habitat for soil biota (Oades & Waters, 1991), in turn strength and stability of soil aggregates ensures storage of SOM (Blanco-Canqui & Lal, 2004).

1.4.1 Soil Porosity

Total porosity of a soil is dependent upon water content since the volume of pores may change due to swelling or shrinkage upon the addition or removal of water, respectively (White, 2006). Total porosity can be measured by bulk density, although the pore size distribution is more informative about the functioning of a soil. Pores are formed by abiotic and biotic processes, together these processes help to develop a range of pore sizes within the soil; the actual size of a pore determines its function. **Table 1.2** summarises the function of specific ranges of pore size and the processes, which form them and highlights that a range of soil pores are required to ensure drainage, aeration and water storage within a soil.

Soil pores control the availability of substrate, water and air to microbes and thereby the rate at which OM is decomposed (Lutzow, 2006). It has been found that with increasing depth down the soil profile, the main C inputs are via the movement of dissolved C through soil pores, and C-inputs by plant roots, thereby limiting the occurrence of preferential flow paths (Bundt *et al.*, 2001). Preferential flow paths within upper horizons are more abundant due to bioturbation or tillage in agricultural soils, meaning that there is a greater probability that any point in the soil is located near to a preferential flow path (Bundt *et al.*, 2001). Research has been conducted investigating the distribution of microbes in relation to soil pores (e.g. (Numan *et al.*, 2003) and organic matter (Gaillard, 1999). The distribution of microbes in the soil structure is a newly emerging discipline and is discussed in further detail in **Section 1.6**.

In summary the size and arrangement of pores are formed by a variety of biotic and abiotic processes. The size of a pore determines its function, whether it aids to drain, aerate, store water and determine the accessibility of substrate. However the pore size and arrangement of a soil is not only dependent upon the processes which form them, but also the stability and resilience of soil aggregates. The following section will introduce the theories behind aggregate hierarchy and stability and the interrelationship between aggregation and SOM storage.

Table 1.2: A functional Classification of Pore Based on Size

Pore Diameter (μm)	Biotic Agent and Descriptive Function
5000-500	Cracks, earthworm channels, main plant roots. <i>Aeration and Drainage</i>
500-30	Grass roots and small mesofauna <i>Normally drainage and aeration</i>
30-0.2	Fine lateral roots, fungal hyphae and root hairs. <i>Storage of "available water"</i>
<0.2	Swell-Shrink water in clays. <i>Residual or "non available" water</i>

Taken From (White (2006), originally after Greenland (1979) and (Cass *et al.*, (1993)

1.4.2 Soil Aggregation

Primary particles of clay, sand and silt combined with organic matter and exchangeable ions form the building blocks of soil aggregates. The stabilisation of clay particles (<2 μm) into floccules occurs by electrostatic forces. Floccules together with sand and silt particles further develop into stable aggregates, by the action of inorganic, organo-mineral or organic binding agents, (See Tisdall and Oades 1982 for an in depth discussion). Within the soil, aggregates can be seen as distinct units separated by natural planes of weakness (White, 2006), in the field they form larger units often termed peds (**Table 1.1**). From the shape of aggregates, inferences about the formation process can be made, producing soil thin-sections is a popular method, which permits this (**Section methods 3.4.4**). Field descriptions of the shape and grade of peds can also be conducted as outlined in (White 2006).

The physical forces (e.g. land management practises) exerted by disturbances can disrupt the organic and inorganic agents, which bind particles. Consequently, the lifecycle of an aggregate is short-circuited and aggregates breakdown into smaller structural units. Size is an important physical characteristic of soil aggregates, which cover a wide range from <2 μm to >2000 μm . Typically, within the literature aggregates are divided into two main categories macroaggregates (>250 μm) and microaggregates (<250 μm) since physical separation of these two size classes is easily achieved with sieving. However, one drawback is that this vastly over simplifies the actual range of aggregate size classes. The extent of this simplification is best observed by producing soil thin-sections, in which a whole range of aggregate sizes and shapes can be examined along with the coinciding pore system.

A soil that has stable aggregates is less likely to become compacted and is more resilient when stress is applied (Kay & Angers, 1999); it also promotes successful plant growth and a suitable habitat for mesofauna and macrofauna. A good soil structure which supports plant growth consists of aggregates between 1-10 mm diameter containing pores $>75\ \mu\text{m}$ and 30-0.2 μm in diameter, which each ensure good aeration and water retention, respectively (Tisdall & Oades, 1982). It is desirable that when aggregates breakdown (or slake when immersed in water) they disintegrate into smaller aggregates rather than into fine particles, since if the dispersion of particles is impeded this could block pores and hinder the infiltration of water and emergence of seedlings (Tisdall & Oades, 1982). Clearly, effective management of soil structure, and in particular aggregate stability, is desirable to ensure both a good soil quality, productivity, and the maintenance of SOM/SOC stocks promotes both of these attributes (Beare & Bruce, 1993; Waksman, 1961).

As outlined previously organic residue acts as a binding agent of primary soil particles thereby forming aggregates. In fact organic residue is the major binding agent of most soils with the exception of oxisols (Carter, 2004). Therefore the maintenance of SOM is fundamental to aggregate stability. The relationship between aggregate stability and SOM is reciprocal, SOM aids aggregate stability and in return SOM is protected against decomposition. Soil organic matter is required to ensure soil quality and biological functioning, specifically mesofauna and microfauna activity, this is discussed in **Section 1.6**. SOM represents the largest terrestrial storage component of organic carbon (**Section 1**), thereby aggregate stability also has important implications for C-storage (Blanco-Canqui and Lal, 2004). Clearly the interaction between SOM and aggregate stability is fundamental to soil functioning due to the numerous processes that both soil structure and SOM influence. However, elucidating the mechanisms involved in the reciprocal relationship between SOM and soil structure is problematic given that they are “two of the most dynamic properties that are extremely sensitive to crop and soil management” (Blanco-Canqui and Lal, 2004).

As aggregates destabilise, due to either a disturbance or the disintegration of organic bonds aggregates breakdown into smaller units, it has been suggested that this demonstrates a degree of aggregate hierarchy, which in turn will have important implications for soil functioning. There have been many attempts to model aggregate hierarchy focusing upon soils where OC represents the major binding agent.

The following section will present the current understanding of the interaction between soil structure and SOM. Much of the research has focused upon sampling at the aggregate and this approach relies on some form of fractionation method.

1.5 Modelling the Turnover of Aggregates.

Tisdall and Oades (1982) were the first to truly emphasise the role of SOM in binding soil aggregates. The model (**Fig. 1.4**) includes the modification made by Oades (1984) in which macroaggregates disintegrate liberating microaggregates, this contrasts to what was originally stated by Tisdall & Oades (1982) that microaggregates develop into macroaggregates. As with models predicting the turnover of carbon pools (e.g. ROTH-C), OC is divided into separate categories reflecting their resistance to disturbances (**Table 1.3**), which is especially distinct between free-OC and of that stored within aggregates (Elliot *et al.*, 1986). Macroaggregates (>250 μm) are formed by temporary agents that form a mesh-like structure as they are adsorbed to mineral particles. Temporary agents include: plant roots, fungal hyphae, mycorrhizal hyphae, bacterial cells and algae, all are highly susceptible to disturbances such as tillage, partly because of this and also due to their large size macroaggregates are highly unstable structural units.

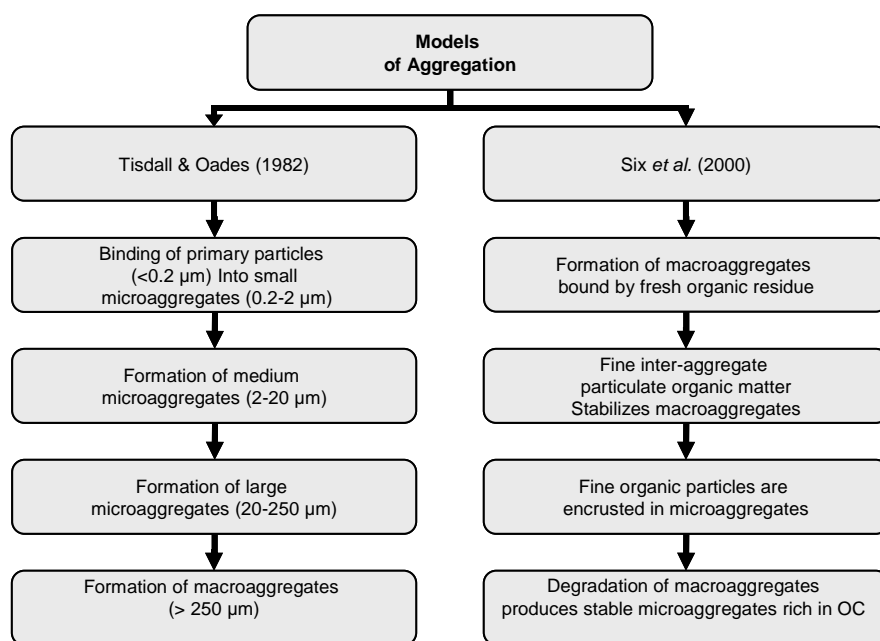


Figure 1.4: The main stages of Tisdall & Oades (1982) and Six *et al.* (2000) model of soil aggregate turnover. Modified from Blanco-Canqui and Lal (2004).

Macroaggregates breakdown and release smaller microaggregates (20-250 μm), as the temporary agents are disrupted through decomposition, tillage or rapid rainfall. Microaggregates (20-250 μm) are held together both by transient agents (polysaccharides) whose binding ability is linked to its capacity to link between mineral particles, which is ultimately determined by molecular length (Martin, 1971). Permanent binding agents

consisting of recalcitrant humus compounds are also found within microaggregates. These form organo-mineral associations e.g. via cation bridges between negatively charged organic and mineral particles through binding with polyvalent metals (e.g. Ca^{+2} , Al^{+3} , Fe^{+3}), van der waals forces or H-bonds (Blanco-Canqui & Lai, 2004). Microaggregates (20-250 μm) will also breakdown into smaller microaggregates (<20 μm) as polysaccharides are eventually utilised by decomposers leaving just permanent agents to stabilise small microaggregates (<20 μm). Microaggregates (20-250 μm) are resistant against rapid wetting and tillage and will only disintegrate under ultrasonic dispersion. Microaggregates (<20 μm) are resistant to disruption by tillage and rapid rain fall but differ from microaggregates (20-250 μm) in that they can withstand 5 minutes of ultrasonic dispersion (Tisdall & Oades, 1982). The high degree of structural stability of microaggregates (20-250 μm) is partly because of the range of physico-chemical binding agents and also due to their small size making microaggregates an important long-term storage component of OC (Tisdall & Oades, 1982). Additionally single clay crystals rather than just clay domains may also bind to organic mater though physico-chemical interactions (Edwards and Bremner, 1967). The importance of humic compounds in acting as permanent binding agents, was demonstrated in corn-soyabean rotations. The cropping of soybean (which has a significantly lower humic acid content compared to corn) led to significantly lower aggregate stability compared to corn cropping despite similarities in total SOC-content (Martens, 2000b). Furthermore, mean aggregate size was most correlated with humic acid content ($r = 0.996$, $p = 0.05$) closely followed by phenolic acid content ($r = 0.98$, $p = 0.05$) this is consistent with phenolic compounds acting as precursors for soil humic substances (Stevenson, 1994).

Table 1.3: The classification and description of organic carbon aggregate binding agents.

Binding Agent	Example	Mechanisms	Aggregates stabilise	Persistence
Temporary	Roots, Hyphae, (particularly Vesicular-arbuscular mycorrhizal hyphae), algae and bacteria	Form a visible organic skeleton that mineral particles adhere to via adsorption.	Macroaggregates (>250 μm)	Highly vulnerable to physical disturbance (e.g. tillage). If undisturbed can persist for months to years.
Transient	Polysaccharides (non-humic compound). Produced by Plants, fungi and bacteria.	Adhere to mineral particles (mainly clay) via polymer bridges.	Microaggregates (<250 μm)	Persist for several months Until they are eventually utilised as an energy source.
Persistent	Humic compounds forming organo-mineral or organic-organic complexes	H-bonds, polyvalent Cations bridges, or Van der waals	Microaggregates (<250 μm)	Highly resistant to physical disturbance also chemically recalcitrant.

Based on information taken from Blanco-Canqui and Lal (2004).

Figure 1.4 also shows the aggregate turnover as proposed by (Six *et al.* (1998)). It follows the (Oades (1984)) model that coarse-particulate organic matter (POM) (250-2000 μ m) act as nucleation sites for the formation of macroaggregates since POM represents fresh material that is readily available for microbial use and consequently produces concentration points of microbial mulches which become encrusted with mineral particles (Golchin *et al.*, 1994). Once encrusted, the POM will be located within macroaggregates and is defined as intra-particulate-organic-matter (IPOM), which, eventually fragments and forms fine IPOM that in turn act as nucleation points for the formation of microaggregates within macroaggregates. In non-tilled soils where there has been a shift in C₃ to C₄ dominate vegetation the $\delta^{13}\text{C}$ signature was measured (Six, 1998). The $\delta^{13}\text{C}$ value for fine-IPOM was -23.69 ± 0.05 and -25.27 ± 0.17 for coarse-IPOM, the less negative value of fine-IPOM indicates that it is older than coarse-IPOM. Six *et al.*, 1998 conclude that this supports the hypothesis that fine-IPOM is a product of the disintegration of coarse-IPOM. As the binding agents of macroaggregates degrade, macroaggregates will disintegrate liberating microaggregates and microbial derived products. Microaggregates will then most likely act as new nucleation sites for the production of macroaggregates (Tisdall & Oades, 1982; Six *et al.*, 1998). The OC released when macroaggregates breakdown will be a mixture of chemically recalcitrant and liable carbon compounds, the released carbon will be more susceptible to degradation since it is no longer physically protected within aggregates (Six *et al.*, 1998). The model has been validated against modes of physical disruption e.g. tillage verses non-tillage systems, also dry-wet cycles implementing isotope tracers, or the natural abundance of ^{13}C (Angers, *et al.*, 1997; Gale *et al.*, 2000; Denef *et al.*, 2001). The major assumption of the model is that macroaggregate formation will be the same between non-tilled and tilled systems since residue inputs are likely to be similar (Doran *et al.*, 1998) therefore any differences in the proportion of macroaggregates to microaggregates between systems will reflect different turnover rates (Six *et al.*, 1998).

The importance of aggregates for the storage of OC is elegantly demonstrated with the disruption of aggregates which increases the decomposition of OC compared to undisturbed aggregates (Angers & Chenu, 1998; Six *et al.*, 1999). A good correlation can typically be found between OC contents and the number of water-stable-aggregates. However, some weak correlations can be found firstly, where OC contents are so high that any further increases will not enhance the number of water stable aggregates; secondly in soils where OC is not the major aggregate binding agent. (Tisdall & Oades, 1982). Alternatively, measuring the amount of free-POM can produce a stronger correlation since this fraction acts as a substrate for microbes from which microbial “glues” (e.g. polysaccharides) are produced or because it is a measure of root and hyphae length, which mesh aggregates together (Oades, 1984; Golchin *et*

al. 1994). Microaggregates <250 μm are far more resilient against disturbance than macroaggregates due to their high molecular weight and recalcitrant nature of persistent binding agents making them an important long-term storage component of OC, especially in agricultural soils. However the compromise is that they are incapable of storing the same amounts of carbon as macroaggregates due to their smaller size. Additionally, particles between 20-250 μm contain approximately half the total carbon compared to aggregates >250 μm thus highlighting the strength of individual organic bonds in microaggregates <250 μm (Tisdall & Oades, 1982). Furthermore, the rate and amount of SOC lost from macroaggregates is much greater in comparison to losses from microaggregates in forest soils converted to agricultural use. This was demonstrated by monitoring the natural abundance of ^{13}C in systems where there has been a shift in the photosynthetic pathway of the dominant vegetation (Besnard *et al.*, 1996), therefore supporting the hypothesis that macroaggregates are far more vulnerable to disruption by tillage than microaggregates.

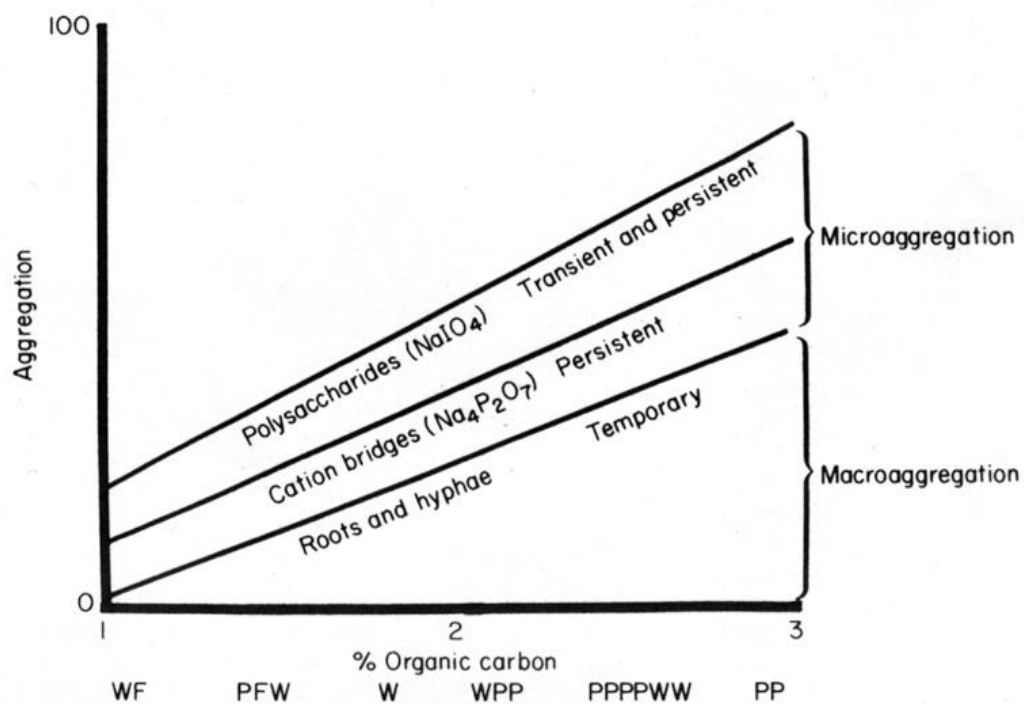


Figure 1.5: The impact that C-content and soil disturbance has on aggregation. Showing the prevalence of transient, persistent and temporary OC-binding agents and the impact upon proportions of microaggregates and macroaggregates, under various land-uses. W= wheat, F= fallow, P= pasture. Taken from Tisdall & Oades (1982).

1.6 The Spatial Distribution of Soil Biota.

The heterogeneity of the soil environment is responsible for generating and regulating the biodiversity and distribution of soil biota, in turn soil organisms control the spatial patterns of SOM decomposition and nutrient supply. A range of environmental factors which influence the spatial heterogeneity of soil biota at different scales. Clusters of soil biota have been recorded over scales from centimetres for: microbes, protozoa, nematodes (Ronn *et al.*, 1996) amoebae (Wachinger *et al.*, 2000) and earthworms (Rossi *et al.*, 1997); to meters for, nematodes (Roberston and Freckmann, 1995) earthworms (Rossi *et al.*, 1997) and collembola (Fromm *et al.*, 1993). Ettema and Wardle (2002) summarised the different scales and processes by which soil biota distribution is influenced. Large scale effects include: gradients in soil carbon or vegetation; Plot to field-scale effects include: burrowing, functional vegetation types and individual plants (e.g. trees); Microscale effects include: roots, organic particles and soil structure (Ettema and Wardle, 2002). Concurrent with environmental factors, intrinsic population/community characteristics (e.g. competition, fecundity and dispersal) also influence the distribution of soil biota.

1.7 The Spatial Distribution of Soil biota: Soil Fauna as Ecosystem Engineers

“Ecosystem engineers are organisms that directly or indirectly affect the availability of resources to other organisms through modifications of the physical environment” (Lavelle, 1998). The activities of soil fauna namely earthworms and termites influence the physical environment, creating structures that have different biological and physical properties in comparison to the bulk soil, while burrowing activity will alter soil porosity.

The burrowing activities of earthworms are shown to manipulate the soil structure by decreasing bulk-density through macro-pore formation (Francis and Fraser, 1998; Capowiez et al., 2000) and increasing macro-pore continuity (Capowiez *et al.*, 2000), while the activity of Enchytraeids increases pore space (Van Vliet *et al.*, 1993). The capability of earthworms to create macropores at a particular depth of soil is species dependent, a combination of shallow and deep burrowing earthworm species are required to improve the connectivity of both lateral and vertical pores (Lee and Smettem, 1994).

Earthworm activities enhance the incorporation of SOM into the soil (Pulleman *et al.*, 2005) and casts have proved to be advantageous to soil structural stability, with studies concluding that casts are more stable in comparison to bulk soil (Shipitalo and Protz, 1988; Marinissen and Dexter, 1990); (Marinissen et al., 1996; Winsome and McColl, 1998; Bottinelli, 2010). This increase in aggregate stability is explained in part by either an increase in either SOM content (particularly polysaccharides, which function as binding agents, **Section 1.5**) or the hydrophobic properties of SOM contained within casts. In turn this increase in aggregate stability promotes physical and chemical protection of occluded organic matter. More significant to the turnover of OC, some studies have found that labile organic matter ingested by earthworms is incorporated with soil minerals to form microaggregates, thereby protecting it against decomposition (Ladd *et al.*, 1993; Bossuyt *et al.*, 2004; Pulleman 2005). The importance of this finding is evident when considering previous studies which, have demonstrated that microaggregates are more physically stable in comparison to macroaggregates thereby functioning as long-term storage components of OC (**Section 1.5 & 1.8**).

1.7.1 The Spatial Distribution of Soil Biota: Interactions between Soil Biota and Organic Carbon

Excremental features produced by biota can constitute a significant proportional of soil structure, representing up to 80% and 50% within organic and organo-mineral horizons of upland grassland systems, respectively (Davidson *et al.*, 2004). Within organic horizons of upland-grassland soils, up to 40% of recent photosynthates can be located within excremental features as determined by laser ablation of excrements following pulse labelling (Davidson and Grieve, 2006). To further validate the location of recent photosynthates, the microbial distribution upon excremental features was determined, it was found that relative to bulk soil 25% of excremental features were colonised more heavily relative to bulk soil. Davidson and Grieve (2006) concluded that even within organic rich soils the distribution of fresh liable organic carbon can still be highly variable. This study demonstrates that food web interactions also play a significant role in determining the spatial distribution of soil biota and therefore organic carbon.

Macro and Meso-fauna are central to the first stages of OC-turnover, by incorporating organic matter into the soil matrix and initialising the first stages of decomposition. However it's the soil microbial community, which determines the majority of OC decomposition, as 80-90% of a soils' functionality. Nannipieri *et al.* (2003) discuss that a suitable microhabitat for microbial growth is dependable on a wealth of changeable environmental factors, therefore the habitats them-self are transient and consequently the available space occupied by microorganisms represents less than 5% (Nannipieri *et al.*, 2003; Ingham *et al.*, 1985). Microhabitats where elevated microbial activity or biomass (proxy for microbial activity) is detected are termed "hot-spots", these are largely associated with particulate organic matter (Gallard *et al.*, 1999), microaggregates, the soil rhizosphere (Nannipieri *et al.*, 2003) and faunal excrement (Bruneau *et al.*, 2005). The spatial extent of microbial activity is demonstrated by a study, which measured a gradient in microbial activity with distances of 3-4mm away from organic matter (Gallard *et al.*, 1999). This study performed spatial analysis of microbial activity by taking slices of soil cores produced by packing calibrated aggregates; clearly a similar approach which retains soil heterogeneity would be advantageous.

The incorporation of organic matter into the sub-soil is largely reliant upon the activity of plant roots and the leaching of dissolved OM, therefore OM is much more spatially heterogeneous in the sub-soil compared to upper horizons, as C enters the soil via paths of preferential flow (Bundt *et al.*, 2001). Concurrent with this the microbial distribution was found to be 9-92% greater in areas of preferential flow compared to bulk soil (Bundt *et al.*,

2001). Research (Chabbi *et al.*, 2009) has supported that new C-inputs enter the sub-soil via preferential flow paths by showing, within preferential flow paths modern radiocarbon dates are recorded, while in adjacent bulk soil radiocarbon dates of several thousand years are reported (Chabbi *et al.*, 2009). Interestingly, carbon sampled from preferential flow paths and bulk soil is chemically similar. While the concentration of organics lost after treatment of 10% Hydrofluoric acid (which breaks down the Si-O bonds, created through mineral stabilisation) is significantly greater in bulk soil (mean = 77%) compared to preferential flow paths (mean = 58%). Since microbial abundance in preferential flow paths is greater than bulk soil, Chabbi *et al.*, (2009) argue that this reflects a microbial preference for differences in the physical protection and not selecting for the chemical nature of C.

Studies investigating the micro-scale distribution of microbes within thin-sections have shown that, within the subsoil microbes are largely located close to pores and their abundance decreases with distance (Nunan *et al.*, 2003). Much larger densities of microbes were found in the topsoil compared to the sub-soil, reflecting the higher C-contents of the top-soil and, within the topsoil there is no relationship in microbial distribution with soil pores, however colonisation of microbes did occur in patches (Nunan *et al.*, 2003). Nunan *et al.*, (2003) concluded that microbial growth was localised to regions where substrate is available to test this they suggested that "...it would be necessary to develop methods that would allow the distribution of organic matter to be studied at scales similar to that employed in this study".

1.8 Land Management, its Consequences for SOC-Content and Soil Structure.

The exploitation of land for human resources has led to a well documented decline in total SOC content and soil erosion. However, the direct consequences of a decline in OC upon soil micro-structure is less well understood mainly due to a combination in the lack of long-term experiments as well as methodological constraints. This project will involve sampling from the long-term experimental fields at Rothamsted Research. Although sampling will be conducted on soils receiving different nutrient treatments or land-use, the aim is not to compare the impacts of land-use but rather to compare how the differences in total SOC content impact on soil structure (**Chapter 2**). However, in order to gain a full understanding of the processes involved, appreciating how land-use can impact on SOC-content and soil structure is essential.

The focus of soils as a storage component of OC has gained substantial attention largely as a result of the 1997 Kyoto protocol and the proposed use of soils to “offset” C-emissions. Soil organic carbon storage through management regimes is estimated to increase by 0.4 to 1.2 Pg C yr⁻¹, with agricultural soils having the capacity to sequester the highest proportion of carbon from 0.4 to 0.8 Pg C yr⁻¹ (Lal, 2004). Equally, under an incorrect management regime agricultural soils have the potential to substantially increase C-emissions. This is especially problematic given that the mechanisms governing C-storage remain unresolved.

Numerous studies (e.g. **Table 1.4**) have focused upon comparing the impact of different tillage practises on SOC-storage and soil structure. It is generally accepted that no-tillage (NT) soils contain substantially more OC than conventional tillage (CT) soils. For instance McCnokey *et al.*, (2003) found that NT soils contained 67-512 kg C ha⁻¹yr⁻¹ more than CT-soils. Relating this to soil structure, the lower total SOC-content of NT systems has been attributed to the faster turnover of macroaggregates in, which can store twice as much carbon than microaggregates. **Figure 1.5**, presented by Tisdall & Oades (1982), effectively presents the shift in aggregate binding agents in soils with different land use histories and clearly demonstrates that microaggregates, due to their small size and persistent binding agents, are an integral component of C-storage within agricultural soils.

Table 1.4: Carbon storage within a range of aggregate size classes in soils under different management

Location	Soil texture	Depth (cm)	Treatment	Duration of Treatment (Years)	Organic carbon content (g C m ⁻²)				Reference
					<53 μm	250-53 μm	2000-250 μm	2000-2800 μm	
France	Haplic Luvisol	20	No Tillage	32	-	-	(2.34)	(1.22)	(Oorts <i>et al.</i> , 2007)
France	Haplic Luvisol	20	Tilled	37	-	-	(1.51)	(0.86)	Oorts <i>et al.</i> , 2007
U.S	Silt loam	0-20	No tillage	33	-	21.1	30.5	30.9	(Tan <i>et al.</i> , 2007)
U.S	Silt loam	0-20	Tilled	23	-	7.8	11.9	10.6	Tan <i>et al.</i> , 2007
Argentina	Coarse loamy	0-10	No Tillage	2	27.7*	48.9* (23.5)*	56.3*	33.8* ns (32.9)*	(Bongiovanni & Lobartini, 2006)
Argentina	Coarse loamy	0-17	Tilled	50	16.9*	18.1* (7.3)*	26.7*	29.2* (19.1)*	(Bongiovanni & Lobartini, 2006)
Germany	Sandy silt loam	0-30	Tilled	37	(9.6)	(10.6)	-	(16.5)	(Yamashita <i>et al.</i> , 2006)
Germany	Sandy silt loam	10-30	Grassland	Permanent	(11.7)	(10.8)	-	(23.8)	Yamashita <i>et al.</i> , 2006
Italy	Silty Clay loam	0-10	Grassland	Permanent	75	452	3755	-	(Del Galdo <i>et al.</i> , 2003)
Italy	Silty Clay loam	0-10	Tilled	100	70	282	1858	-	Del Galdo <i>et al.</i> , 2003
Australia	Fine-silty	0-20	No tillage	28	-	(99)	(60)	-	(Six <i>et al.</i> , 1998)
Australia	Fine-silty	0-20	Tilled	28	-	(21)	(25)	-	Six <i>et al.</i> , 1998
Greece	Sandy clay loam	0-5	No tillage	19	0.63*	-	5.32*	15.60*	(Beare <i>et al.</i> , 1997)
Greece	Sandy clay loam	0-5	Tilled	19	1.15*	-	3.14*	6.48*	Beare <i>et al.</i> , 1997
France	Acidic loam	26	Tilled	7	-	(27.77)	-	(34.73)	(Besnard <i>et al.</i> , 1996)
France	Acidic loam	26	Tilled	35	-	(20.38)	-	(26.20)	Besnard <i>et al.</i> , 1996

Difference in OC-content between treatments within the same study, are statistically significant unless followed by ns.

*Carbon content values shown in g kg⁻¹

Values in red and parenthesis correspond to the mineral organic carbon content (MOC).

Values in blue and parenthesis correspond to the particulate organic carbon content (POC).

Continued focus has been placed upon assessing C-storage in different aggregate size classes thus expanding from the traditional method of assessing C-storage in whole soils or between soil horizons with particular emphasis upon agricultural management practises, especially the physical disruption caused by tillage (**Table 1.4**). There is mounting evidence supporting that macroaggregates are more susceptible to disruption via tillage than microaggregates as the turnover of macroaggregates is accelerated (Six *et al.*, 2000b). It is well established that tillage leads to the degradation of macroaggregates producing a soil that is composed of a greater proportion of microaggregates relative to macroaggregates which themselves are depleted in OC (Denef *et al.*, 2001). Earthworm abundance is dependent upon land management, as outlined in Pulleman *et al.*, (2004), tillage, manure and pesticide use each affect abundance. Typically earthworm abundance is high in grasslands and this improves productivity (Partsch *et al.*, 2006). Recently it has been demonstrated that the stability of earthworm casts is also affected by tillage applications (Bottinelli *et al.*, 2010). Bottinelli *et al.*, (2010) concluded that earthworm casts under conservation tillage are more stable than earthworm casts under mouldboard plowing; this is attributed to a greater OM content and water repellence.

Nevertheless there is evidence to suggest that microaggregates are more vulnerable to physical disruption than previously believed. In agreement with previous tillage studies, Bongiovanni & Lobartini (2006) concluded that macroaggregates are most susceptible to disruption by tillage. Interestingly, they also observed that the mineral associated organic carbon (MOC) was drastically reduced in microaggregates compared to macroaggregates, with a 69% reduction in MOC due to tillage (**Table 1.4**). Additionally, FA and more so HA within microaggregates were also found to be highly sensitive to tillage practises. The greatest losses of HA were found within microaggregates (250-53 μm) ranging from 68-71% this rate of OC-loss is equal to losses of liable C-fractions from macroaggregates suggesting that despite their chemical recalcitrance HA can be rapidly decomposed, thus challenging the extent to which microaggregates contribute to long term C-storage (Bongiovanni & Lobartini, 2006). Nevertheless, Bongiovanni & Lobartini (2006) failed to explain the possible mechanisms behind the decomposition of mineral carbon from microaggregates and largely imply that the reduction in MOC is a direct consequence of the decomposition of recalcitrant carbon. However, since the precursors of humic compounds which are composed of liable carbon are also being rapidly decomposed, a reduction in recalcitrant-C concentration is likely to be a consequence of both a decrease in humification and the oxidation of existing humic compounds (Bongiovanni & Lobartini, 2006).

Organic amendments (e.g. animal manure, sewage sludge, city refuse compost and crop residues) have long been recognised as increasing OC contents and aggregate water stability and thus reducing soil erosion (Tisdal & Oades, 1982). There are two possible mechanisms operating to cause an increase in aggregate water stability. Firstly, that fresh OM inputs provide a labile substrate promoting microbial activity and the synthesis of microbial binding agents, which in turn promote greater aggregation. Secondly, that organic amendments reduce the hydrophobic nature of aggregate surfaces thereby rendering it susceptible to slaking (Zhang, 1994). To a lesser extent inorganic fertiliser applications also enhance SOC by increasing plant C-inputs from above and below ground litter. More recent developments have found a highly positive correlation between particular C-compounds and aggregate water stability as opposed to total-C. Typically, the addition of labile C-compounds promotes rapid transient aggregation, while, recalcitrant-C favours a gradual longer-term increase in aggregation (Blair, 2006; Martens, 2000a). For instance, soils receiving organic amendments with high concentration of humic acids correlate to greater longer-term mean weight diameter (MWD) compared to those receiving lower humic acid concentrations (Martens, 2000a) or organic amendments with high carbohydrate and amino acid which only promote short-term aggregation (Martens, 2000b).

The capacity for humic acid to increase soil structural stability surpasses the capabilities of fulvic acid (Tejada, 2007) due to its higher molecular weight and greater role in forming organo-mineral complexes (Whalen, 2003). Long-term experiments of this kind are rare making it difficult to investigate the sustainability of nutrient treatments. Blair *et al.* (2006) sampled from Broadbalk experimental field at Rothamsted Research and found that after more than 100 years application of FYM OC-contents had increased by 353%. Blair *et al.* (2006) assessed the correlation between MWD and each of the following: labile carbon, non-labile carbon and total carbon contents. In soils with a low carbon content MWD was positively correlated to the labile carbon fraction, while, in soils with a high carbon content the different carbon fractions had a similar impact. Blair *et al.* (2006) suggested that this was indicative of soils with a high C-content reaching the maximum storage capacity with the possibility that any further organic additions would not lead to increases in MWD. A further consideration is the cation content of organic amendments which will also influence aggregation with monovalent cations promoting dispersion of particles while polyvalent cations enhance aggregation (Tejada, 2007; Blair *et al.*, 2006). Management practises such as cropping, fertilising and tillage each alter OC-storage, and it is hoped that a more comprehensive understanding of their impacts upon C-storage within aggregates will assist in the application of a management strategy that will sustain or even enhance soil C-stocks.

1.9 Soil Texture and Mineralogy

Soil texture also influences the C-storing capacity of soils, with fine textured soils exhibiting the greatest C-storage capacity (Hassink, 1997). Temperate clay soils are typically dominated by 2:1 clay minerals, in these soils under NT management microaggregate storage within macroaggregates can be twice as great compared to CT soils (Six, 2000b). In more weathered clay soils (such as Oxisols and Ultisols) dominated by 1:1 clay minerals, C-storage is not so closely related to water aggregate stability with aggregation largely being controlled through interactions between positively charged oxides and negatively charged mineral surfaces (Denef, 2004). The interaction between oxides and organic material remains unclear and is further complicated since these soils are highly acidic due to high Al concentrations which are toxic to plants thereby limiting the input of organic residues (Oades & Tisdall, 1982). Comparisons between three soils of different clay mineralogy (2:1, 1:1 and mixed (moderately weathered), and the impacts upon carbon storage under NT and CT management, revealed CT impacted similarly across all soil types (Denef, 2001). Nevertheless, differences in microaggregate proportions between NT and CT were minimal in the 1:1 soil except for the upper horizons, therefore CT does not prevent the formation of microaggregates by accelerating the turnover of macroaggregates across all soil types. This is consistent with oxides in 1:1 clays being more important for aggregate stability (Denef, 2001) Interestingly, the greatest microaggregate water stability was observed in the mixed soil suggesting that clay plus silt contents both influence C-aggregation. One possible mechanism is that OC is acting as a bridge between 2:1 and 1:1 clays thereby promoting greater stabilisation than is possible with either 2:1 or 1:1 clays. Furthermore, across all three soils >90% of the difference in total C-storage could be explained by the amount of C-stored in the microaggregate mineral fraction. Therefore, Denef *et al.* (2001) suggested that monitoring the changes in mineral-C in tilled soils could be developed as a useful diagnostic tool assessing changes in C-storage.

As previously highlighted the importance of aggregates for the storage of OC is elegantly demonstrated with the disruption of aggregates which increases the decomposition of OC compared to undisturbed aggregates (Angers & Chenu, 1998; Six *et al.*, 1999). Nevertheless, Besnard *et al.* (1996), found that the amount of carbon in particulate organic matter (POM) was greater than the amount of carbon occluded in macroaggregates and microaggregates in forest vertisol with a thick humic acidic loam. One explanation is that limited nutrient supply (most probably N) and high aluminium concentrations retard the rate of free-POM decomposition, as supported by the increase in free-C-POM decomposition with the liming and the application of fertilisers. Furthermore, in oxisols oxides act as the major stabilising

agent of aggregates rather than OC (Six *et al.* 2000a). Thus the mechanisms controlling the storage of carbon are most likely to be site specific, determined by the combination of a number of factors including: soil texture, nutrient availability, management and climate.

1.10 Conclusion

The storage of SOC is determined by both the intrinsic chemical decomposability of C-compounds and the apparent decomposability enforced by soil structure rendering substrate inaccessible to decomposers or extracellular enzymes. To date models predicting the turnover of OC within soils fail to distinguish between the intrinsic chemical decomposability of C-compounds and the protection enforced by the soil structure. Consequently, gaining a greater understanding of where carbon is stored within the soil structure could enhance our predictive capacities of the rate of SOC-turnover.

Soil aggregates are central to promoting OC-storage and in turn OC function as binding agents thereby enhancing aggregation. Models of aggregate turnover specify that microaggregates act as a long-term storage component of OC since they are more structurally stable than macroaggregates, due to a combination of their small size and the action of permanent OC-binding agents. However much of the current research has been performed on fractionated soil, thereby not fully accounting for the structural heterogeneity of soil.

There is growing interest to quantify the location of soil microbes within the soil. Current models of soil microbial activity presume a uniform distribution; however increasingly studies are concluding that microbes have a clustered distribution in relation to soil structural features and substrate. Therefore there is a growing need to develop methods which will permit the quantification of OM/OC at scales relevant to microbial populations.

Agricultural soil is typically comprised of a higher proportion of microaggregates to macroaggregates due to the vulnerability of macroaggregates to physical disturbance caused by tillage. Since agricultural soil has a substantial capacity to increase C-storage (0.4 – 1.2 Pg C yr⁻¹) which, under the Kyoto protocol can be counted towards offsetting C-emissions, focussing on where C is stored in soil at the micro-scale is essential to effectively calculate the extent to which C-emissions have been offset.

Additionally and equally as important, sustaining C-stocks in agricultural soils is necessary for maintaining soil quality to ensure a successful crop yield. In conclusion, a more comprehensive understanding of C-storage at the micro-scale has a dual benefit leading to a more effective offsetting of C-emissions and improving overall soil quality.

Chapter 2: Research Framework

This section briefly outlines some of the important methodological factors for consideration when investigating C-storage within soils. The research questions raised from the literature review will also be presented. The chapter will conclude with a thesis outline detailing how each research question will be addressed and presented. The chapter will include both links to previous and subsequent chapters.

2.1 Methodological Considerations for Investigating Soil Organic Carbon.

The principal aim of this project is to determine the occurrence and nature of OM and its associated organic carbon in and between soils contrasting in total OC-content. To achieve this aim, soils with a well documented land-use history are required, firstly to provide prior knowledge regarding the steady-state turnover of carbon, and secondly, to provide a full history of C-inputs into the system. The Broadbalk Winter-Wheat experiment (**Section 3.1**) will be sampled, this experiment has been ongoing for >160 years, therefore information regarding land-use and SOM inputs and C-turnover are widely documented. Poulton (1996) explains the importance of long-term experiments, for instance the OM-content of soils will change to an equilibrium value and this is dependent upon: 1, the quantity of the added OM and the rate of its decomposition, 2 the rate of decomposition for existing OM, 3 soil texture and stabilisation through OM-mineral interactions, and 4, climate. The long-term experiments at Rothamsted research are a unique occurrence where continuous experimental rigor has been applied for more than 160 years and OC-turnover is well documented (**Section 3.1.1**). Much can still be learnt from long-term experiments, particularly when considering changing climatic conditions. For instance, changes in SOC are difficult to detect after a few years, since the background level of SOC is much greater than annual inputs and losses and the continuation of long-term experiments will allow trends in C-content to be recorded in response to changing climatic conditions.

2.1.1 Soil Depth

Soil depth is a critical factor affecting C-content, typically C-content decreases with depth, as C is restricted to entering sub-soils through either leaching or via plant roots or turbation. Studies have also shown that the distribution of OM in deeper horizons is more variable compared to upper horizons, thereby creating “hotspot” of substrate availability (Bundt *et al.*, 2001). However, due to time constraints, the experimental fields will be sampled at a single

depth 25-30cm (i.e. height of the Kubiena tin) (**Section 3.1.2**). The upper soil horizon was sampled, to investigate if “hotspots” in the distribution of OM/OC still occur within the portion of soil receiving the greatest C-inputs relative to the sub-soil,

2.1.2 Carbon Amount versus Carbon Concentration.

When measuring C-contents it is essential to express C amounts as mass per unit area (**Section 4.2**), thereby taking into account any differences in the amount and density of soil sampled. If C-concentration is used to make comparisons between soils this will not take into consideration changes in C-contents due to bulk density or sampling depth, therefore changes in C-concentration will not accurately reflect the C-contents of the soil.

2.1.3 Seasonal Variability

It is not within the scope of the project to account for seasonal variability; therefore sampling will take place at a single point in time and therefore will provide a snapshot of the processes occurring. However, it is recognised that a number of factors will vary seasonally including: soil-structure, water content, bulk density and critically the distribution of OM within agricultural systems, for instance the distribution of OM maybe more variable with seasons compared to grassland because the soil is mixed by tillage and plant biomass is harvested.

2.2 Research Questions

In this section the research questions generated following the literature review are presented. Specific hypotheses will be presented at the beginning of each results chapter.

2.2.1 The Relationship between Soil Structure and Soil Organic Carbon

Section 1.4 discussed the importance of structure for soil functionality and it’s relationship with C-storage. It was also highlighted that much of the current research has focused upon the role of soil aggregates in C-storage by fractionating the soil (see review paper Blanco-Canqui & Lai, 2004), meaning that the distribution of OM/OC within intact soil is largely unexplored. By fractionating the soil much of the structure is destroyed and important processes may be overlooked, however researching OM and C-storage within intact samples poses many methodological setbacks, many of which will be addressed in this thesis. A handful of studies have used thin-sections to investigate the distribution of microbes in relation to soil structural features (Nunan et al., 2003; Bruneau et al., 2005) or the distribution of plant roots (with the surrounding degree of aggregation also described (De León-González *et al.*, 2007)). The location of microbes in relation to the soil physical environment is a significant field of research, with the heterogeneity of soil structure being responsible for generating soil

biodiversity (Young *et al.*, 2008) and accessibility to substrate (OM) creating “microbial activity hotspots” (Gaillard *et al.*, 2003; Gonod *et al.*, 2003). The location and availability of substrate may have implications for soil structural development. Therefore studying thin-sections will allow the distribution of substrate to be assessed within a heterogeneous soil environment.

It is hoped that this study will add to the field of research by quantifying OM and describing the microscale distribution of OM in relation to soil pores (**Section 3.3.4**) and subsequently the distribution of C in relation to soil structure, if successful both will substantially add to our current understanding. To achieve this, micromorphology, image-analysis and sub-microscopy with elemental analysis methods will be integrated, by doing so the thesis will also present a new protocol by which OM and OC can be investigated within intact soil samples. Since some degree of methods testing is required and due to time limitations, the project is limited in terms of the range and depth of soils investigated, but it is hoped that this work will act as a platform for future research.

2.2.2 Soil Carbon Content and Land-Use.

Broadbalk Winter-Wheat is selected as the experimental site as outlined in **Sections 2.1** and **3.1**. Treatments that have created soils with contrasting carbon contents will be sampled (NIL, Inorganic and FYM) and two different land-uses, agricultural and grassland (Wilderness) will also be compared (**Section 3.1.1**).

Previous studies have shown that with depth, as carbon content decreases, the variability of its distribution increases (Bundt *et al.*, 2001). This research will investigate the microscale distribution of OM and OC within the top 20-25cm of soils contrasting in OC-content, this horizon receives the greatest amount of OC-inputs. The structural characteristics at the microscale within the vicinity of OM fragments will also be assessed. The aim is to assess **a) whether differences in the structure of soils contrasting in total OC-content can be detected at the microscale**, and **b) determine the nature and distribution of OM within the upper horizon of soils contrasting in total OC-content**.

Land-use determines the OM/OC content of soils (**Section 2.2**), with grassland soils having a much larger OC-content compared to agricultural soils due to the greater litter inputs and absence of disruption by machinery; concurrent with this grassland soils have a greater aggregate stability particularly of larger aggregates (Six *et al.*, 2000b; Denef *et al.*, 2001) (**Section 1.4.2**). However, questions remain as to whether this translates to a difference in the

distribution of OM/OC evident at the microscale. The experimental design at Rothamsted ensures that comparisons can be made between agricultural and grassland soils which have similar clay contents and are from the same soil series (implications of soil texture for OC-storage are discussed in **Section 1.9**).

2.2.3 The Redistribution of Old versus New Carbon Inputs.

Studies examining C-isotopic natural abundance within fractionated soil have indicated that a redistribution of carbon occurs from macroaggregates as they disintegrate into microaggregates (Six, 1998; Deneff *et al.*, 2001) (**Section 1.5**). Thin-sections have previously been used to investigate the distribution of recent photosynthates within grassland soil using pulse-labelled carbon (Bruneau *et al.*, 2002). This project will implement a modified method of Bruneau *et al.*, (2002). The design of this experiment means that vegetation is manipulated to shift the photosynthetic pathway, allowing recent carbon inputs from C₄ plants (with a stable isotope ratio δ -13C 13‰) to be distinguished from older OM contents from C₃ plants (with a ratio of δ -13C 27‰). By using natural abundance rather than pulse labelled CO₂ and producing thin-sections, the longer-term redistribution of OC can be investigated within a heterogeneous soil structure (**Section 3.1.3**). However due to a number of methodological setbacks this was not possible, the results are presented in **Appendix 3**.

2.3 Summary and Research Structure

To undertake the 4 main aims of the project chemical, physical and microscopic approaches to analysing the soil have been conducted, **Fig. 2.1** summarises this research structure. The results with respect to Aim 1 “*to determine the structural characteristics of Broadbalk soils*” are presented in chapter 4, and represent the pre-requisite analysis for Aim 2.

Aim 2 “*to determine the occurrence and nature of organic matter in and between soils contrasting in total organic carbon content*”, is addressed using soil collected from Broadbalk Winter-Wheat (**Section 3.1.1**). The historic treatments applied to these soils has resulted in soil which differ in total organic carbon content. Also by comparing the FYM treated soil with the Wilderness soil comparisons can be made between soils with a similar OC-content but which are managed differently one being grassland and the other agricultural soil.

The central focus of this research is to analyse the distribution of OC in relation to soil structural features, this has been conducted using soil thin-sections produced from intact soil samples, the purpose being to develop alternative methods to soil fractionation. The methods

chosen were selected to ensure thin-sections are analysed to their full potential, whilst bulk analysis is performed to either compliment or reinforce the findings from thin-section analysis. Sampling (**Section 3.1.2**) was restricted to a single point in the soil profile, since extensive sampling down the soil profile would have limited the extent of subsequent laboratory analysis.

Aim 3 “*to examine the redistribution of OC as it is retained within the soil structure*”, will be addressed separately in **Appendix 3**, using soil from Hoosfield Continuous Maize experiment (**Section 3.1.3**). Due to a number of methodological setbacks it is not possible to analyse the results and consequently form a discussion. Therefore for future reference the results from laser-ablation isotope ratio mass spectrometry (LA-IRMS) will be presented in **Appendix 3**.

The results will be discussed in **Chapter 6** according to the aims and hypotheses as presented at the beginning of each results chapter (**Chapter 4.1**) (**Chapter 5.1**), also the effectiveness of thin-sections as an alternative approach to investigating the distribution of OC in relation to soil structural features will be assessed. It is hoped that by considering the conclusions collectively the fourth aim, “*to explore the processes controlling carbon storage*”, can be explored in **Chapter 7**.

In summary, the specific aims, objectives and hypotheses are outlined at the beginning of each results chapter, and will end with a discussion of the results. Within a separate final discussion chapter the fourth aim will be discussed along with the wider significance of the findings and recommendations for future research.

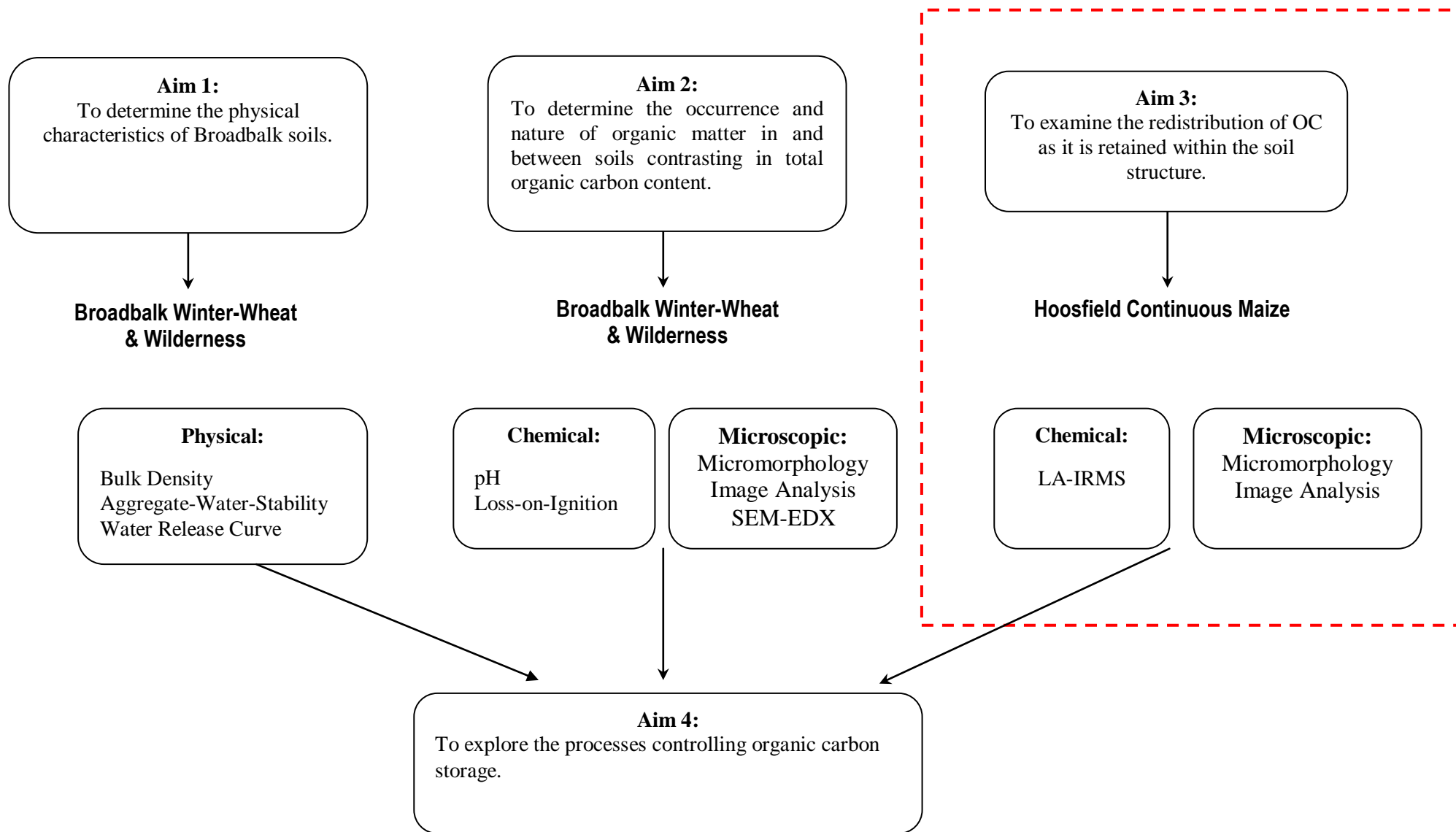


Figure 2.1: The methods used to undertake the main aims of the project. Aims 1 and 2 are undertaken separately in **Chapters 4 & 5** and discussed in **Chapter 6**, due to methodology setbacks it was not possible to analyse the results from Aim 3, therefore the analysis of Hoosfield soil will be briefly presented in **Appendix 3**. The results from the analysis of Broadbalk and soils are considered collectively to achieve aim 4 in **Chapter 7**. SEM-EDX = scanning electron microscopy with elemental dispersive x-ray detection. LA-IRMS = laser ablation with isotopic ratio mass spectrometry.

Chapter 3: Field Sites and Methodology

The project was split into three distinct components: firstly to characterise the structural complexity of Broadbalk Winter-Wheat and Broadbalk Wilderness soils which contrast in total OC-content (Objectives & Hypotheses: **Chapter 4.1**), Secondly to investigate the distribution of OC in relation to soil structure within Broadbalk Winter-Wheat and Broadbalk Wilderness soils (Objectives & Hypotheses: **Chapter 5.1**). Finally, the distribution of old versus. new carbon in soil collected from Hoosfield Continuous Maize (Objectives & hypotheses: **Appendix 3.1**). Due a number of methodology problems it was not possible to assess the distribution of old versus. new carbon, therefore this section will be presented in **Appendix 3**. The protocols are presented below in a single chapter. This chapter will conclude by presenting the research design, explicitly outlining the main aims of the project and the manner by which these are undertaken.

3.1 Field-Descriptions

The field sites selected are the Broadbalk Winter-Wheat, Broadbalk Wilderness and Hoosfield continuous maize experiment at Rothamsted Research, UK. At the experimental site climatic conditions are temperate cool with a mean annual temperature of 9.1°C and mean annual rainfall of 693mm. All sites were sampled between March & June 2007.

3.1.1 Broadbalk Winter-Wheat and Broadbalk Wilderness

The Broadbalk Winter-Wheat- experiment was established in 1843 with *Triticum aestivum* first harvested the following year. The experimental design consists of 10 sections, with each section further subdivided into up-to 20-strips, with each strip receiving a different fertiliser treatment. Although these treatments are repeated within each section there is no true replication within the Broadbalk experiment since each section receives an overall unique treatment, typically manipulation of crop rotation. Although described as a continuous experiment the treatments have not remained static and have been modified in response to modern agricultural challenges. Consistent with this endeavour the winter-wheat cultivar has been changed every 5-10 years, with the current wheat variety being Hereward seeds treated with Redigo twin.

The soil is flinty-silty clay loam over clay with flints, Batcombe soil series (WRB classification: Luvisol (LV)) (**Fig. 3.1**). The clay content across the whole field ranges from 18-38%, however, the clay content for the plots sampled span a much narrower range of 23.8-

26.4 % (Watts et al., 2006). Profile descriptions have shown the upper horizons to be: 0-20cm, Ap, dark brown (10YR 4/3) slightly flinty, slightly calcareous, silty clay loam; 20-51cm, 2Bt (g)1, yellowish red to strong brown (5-7.5 yr 5/6-8), very slightly flinty clay, with few to common red mottles and paler brown ped faces (Avery & Catt, 1995). The SOM contents have remained constant for approximately 100 years with plots receiving fertiliser having a slightly higher OM-content than plots receiving no treatments (Poulton, 1996). Annual additions of Farm-yard-manure have produced the most noticeable difference in SOM-content due to the large amounts added ($35 \text{ t ha}^{-1} \text{ yr}^{-1}$) (Watts et al., 2006). Monitoring of the SOM-accumulation in the top 23cm of soil has showed at first a rapid increase in SOM, then a change towards a more gradual increase in SOM content (Poulton, 1996). As Poulton emphasises this change in the rate of SOM accumulation occurred over 130 years with the most rapid increase in SOM content occurring within the first 60-70 years of the experiment being established. Clearly this trend in SOM accumulation may not be evident in shorter term experiments.

Soil from section zero, plots 2.2, 03 and 07 (**Fig. 3.2**) were sampled in March 2007. The overall treatment across section zero is the incorporation of straw which has been applied annually since autumn 1986. Plot 2.2 receives inputs of farm-yard-manure (**FYM**); plot 03 receives no additional nutrient inputs (**NIL**); plot 07, receives inputs of N, P, K, Na and Mg inorganic fertiliser (**Inorganic**) (**Table 3.1**). In addition to the wheat-plots on Broadbalk, the adjacent grassland was also sampled.

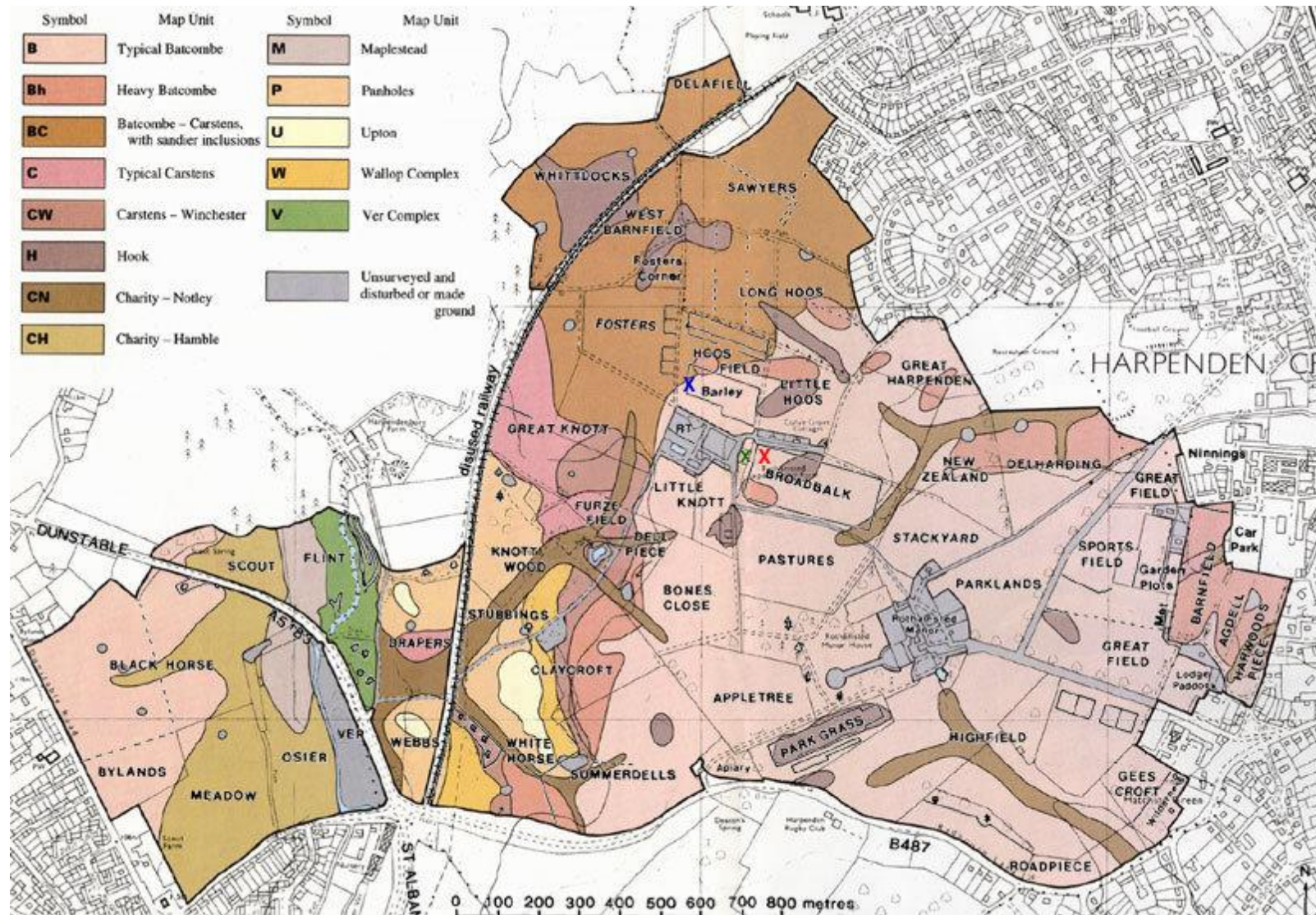


Figure 3.1: Soil series at Rothamsted Research. Point of sampling: Broadbalk winter-wheat (x), Broadbalk Wilderness (x) and Hoosfield (x), the soil series is typical Batcombe. Taken from Rothamsted research electronic archive.

The area known as Broadbalk wilderness was originally part of, the winter-wheat experiment, however, it was fenced off in 1882. Today three distinct sections exist within Broadbalk Wilderness. A deciduous woodland consisting of: mainly ash, sycamore and hawthorn; a grassland portion (with hogweed and nettles) and a scrub region. It was the grassland portion which was sampled, this area was initially mown from 1957-1961, from 1962 to 2000 it was maintained by sheep grazing and since 2001 the grassland has been managed by mowing. Profile descriptions from 1953 show the soil series and texture (with a clay content of approximately 27%) to be the same as Broadbalk, in 1953 horizon development was much the same as Broadbalk winter wheat experiment (Avery & Catt, 1995) which is logical given that the area was yet to be converted into managed grassland. At the time of sampling (2007) when the upper 30 cm was exposed, this revealed a thin litter horizon (Lf) 0-8cm was followed by an Ao-horizon. These soils were selected for their similar textures and contrasting OC-contents with the Grassland, FYM, Inorganic and NIL plots containing 3.05, 2.91, 1.22, and 0.93% OC, respectively.

Table 3.1: Details of treatments and rates of application, for plots sampled within the Broadbalk experiment.

Plots (section*)	Treatment	Abbreviation	Dimensions (m)	Treatment details	Last Application**
2.2 (0)	Farm-yard-manure	FYM	15.24 x 4	35 t ha yr ⁻¹	4/10/06
03 (0)	No inputs	NIL	15.24 x 6	-	-
07 (0)	Inorganic fertiliser	Inorganic	15.24 x 6	N: 96 Kg ha yr ⁻¹ as, ammonium nitrate P: 35 Kg ha yr ⁻¹ as, triple superphosphate K: 90 Kg ha yr ⁻¹ as, potassium sulphate Na: 16 Kg ha yr ⁻¹ as, sodium sulphate until 1973 Mg: 12 Kg ha yr ⁻¹ as, kieserite	14/03/07
Broadbalk Wilderness	Mown grassland	Grassland		Mown	

* Overall treatment to whole section is the incorporation of straw last straw ploughed in 14/10/06

**Refers to the last application before sampling in March 2007.

Wheat harvested 23/8/06, wheat sown 2/11/06

3.1.2 Sampling Protocol

Sampling was along the edges of the experimental plots (1m in from the buffer strips separating each plot), this permitted Kubiena tins to be collected in the harvested region while the digging of soil pits was largely restricted to the buffer zone thereby minimising any damage to the harvested crop. Sampling on Broadbalk was done, 1.7m apart along, 1 edge of plot 2.2 and 3m apart where both edges of the plot were sampled along plots 03 and 07 (**Fig. 3.2**). The wilderness was sampled in a grid pattern, each sample 6m apart. Sampling consisted of intact soil samples removed using Kubiena tins, and loose bulk samples, both were taken from each sampling point. Shallow soil pits (approximately 30cm deep) were dug in order to expose the upper horizons, again taking care to minimise disturbance to the experimental plots, Kubiena tins (75 x 55 x 40 mm) were pushed into the soil profile in a horizontal orientation allowing a depth of 15-20cm to be sampled. This depth corresponded to the Ap horizon within Broadbalk-winter-wheat and the upper Ao horizon within the grassland site. Particular care was taken when sampling the grassland, firstly the turf was peeled away, secondly sampling at a depth of 15-20 cm ensured that the soil removed was well within the boundaries of the A horizon and therefore the upper Lf horizon was not sampled. In total 7, 5, 4 & 5 Kubiena and bulk samples were removed from the Wilderness, FYM, NIL and Inorganic plots, respectively. A greater number of samples were removed from the grassland to account for the larger variability expected across this plot. The number of samples removed from each of the agricultural plots was less than the agricultural soil since the management aims to ensure a more homogenous soil. Only four Kubiena tins were removed from the Nil treated soil due to the difficulty in removing intact samples due to the high abundance of flints.

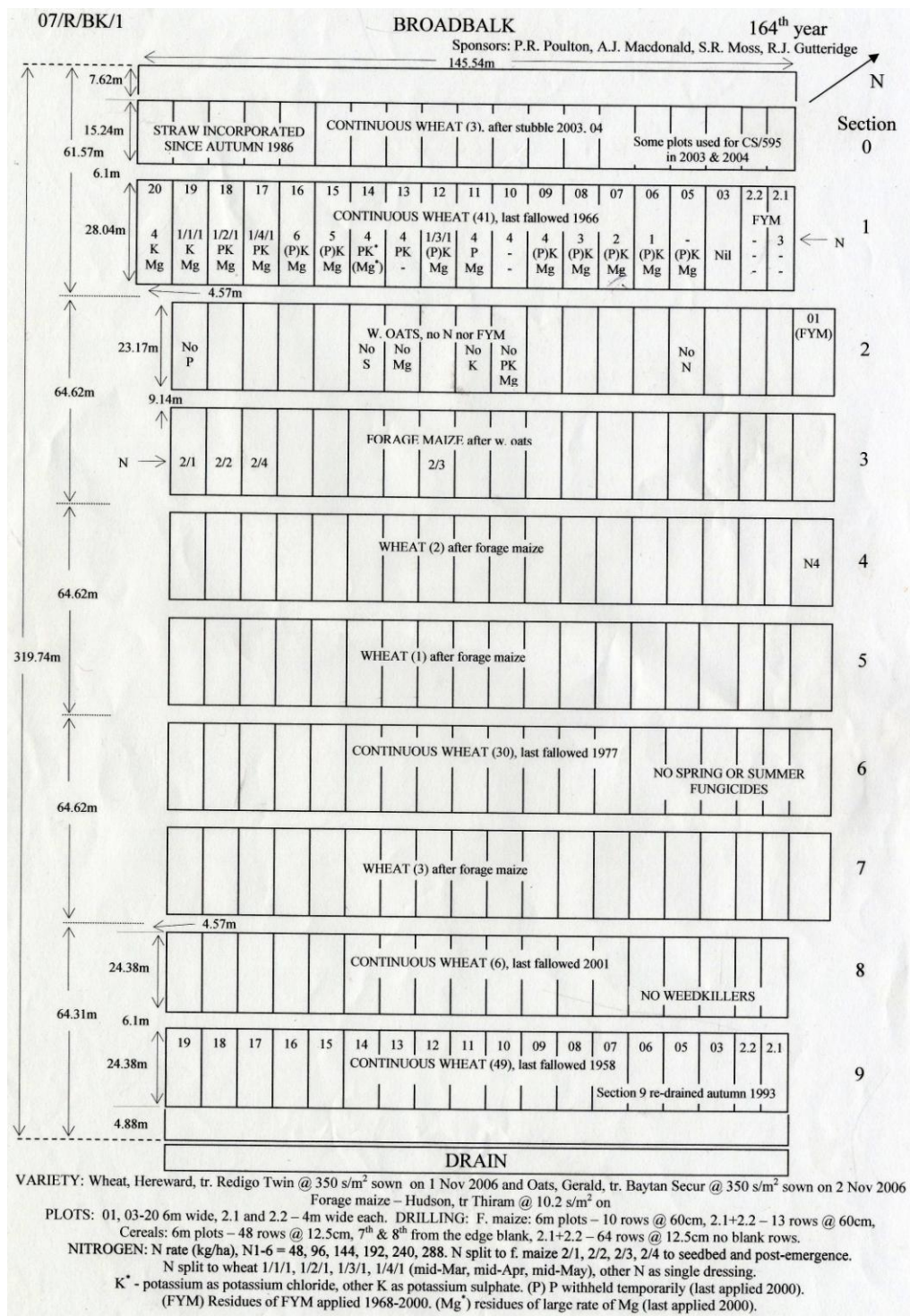
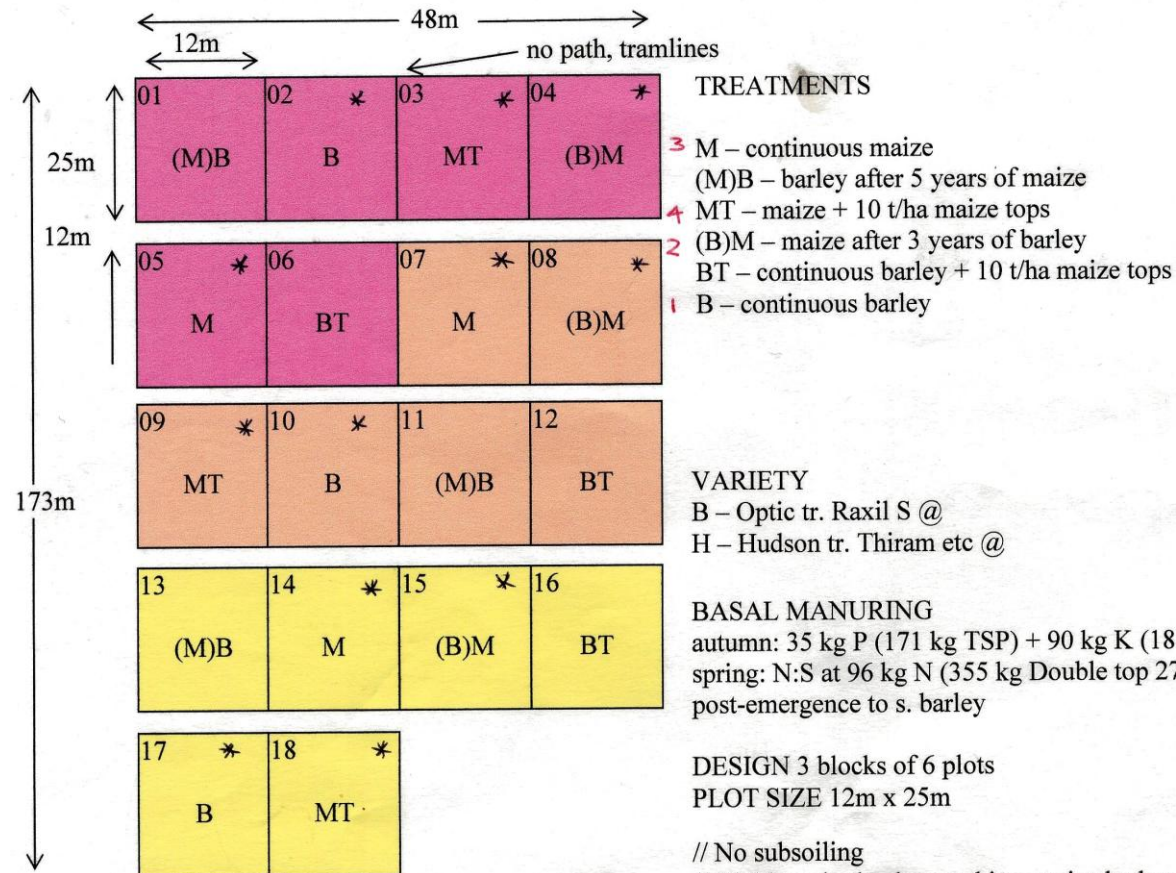


Figure 3.2: Field plan of Broadbalk winter wheat experiment, at Rothamsted Research, UK. Within section zero, plots 2.2, 03 & 07 were sampled March 2007.

Sponsors: P.R. Poulton, A.J. Macdonald



code	M	MT	MB	BM	BT	B
year						
	5,7,14	3,9,18	1,11,13	4,8,15	6,12,16	2,10,17
1997	M	M	M	B	B	B
1998	M	M	M	B	B	B
1999	M	M	M	B	B	B
2000	M	M	M	M	B	B
2001	M	M	M	M	B	B
2002	M	M	B	M	B	B
2003	M	M	B	M	B	B
2004	M	M	B	M	B	B
2005	M	M	B	M	B	B
2006	M	M	B	M	B	B
2007	M	M	B	M	B	B
2008	M	M	B	M	B	B
2009	M	M	B	M	B	B
2010	M	M	B	B	B	B
2011	M	M	B	B	B	B

Signed

Date

RO no.

D.P. Yeoman, 17.7.06

Figure 3.4: Field plan of Hoosfield continuous Maize experiment, at Rothamsted Research, UK. Plots (*) were sampled June 2007.

3.1.3 Hoosfield Continuous Maize

Established in 1997 “Hoosfield Continuous Maize” consists of 6 treatments with 3 replicates in a randomised block design (**Fig. 3.4**) Each plot is 12m x 25m and receives a basal manuring of N, P & K. Treatments involve the manipulation of vegetation, four were sampled, they include: continuous barley, continuous maize, maize after 3 years of barley and maize receiving additional Maize tops (**Table 3.2**, for full treatment details). Two samples were removed from each of the plots across all 3 blocks in June 2007, sampling was positioned approximately 2m from the plot edge. Soil pits were dug and samples removed as on Broadbalk (see above). The soil is similar to that seen at Broadbalk with the soil being flinty-silty clay loam over clay with flints. The experiment overlaps two soil series, Batcombe, and Batcome-Carstens series (**Fig. 3.1**), the difference between the two series is negligible with Batcome-Carstens series containing occasional sandy inclusions. Since the Hoosfield soil is similar to that found at Broadbalk experiment, for a profile description it is recommended to refer to the Broadbalk soil horizon description (**Section 3.1**) (Electronic Rothamsted Archive, Rothamsted Research). The varieties of *Hordeum vulgare* (barley) and *Zea mays* (maize) grown are Optic, (treated with Raxil pro) and Hudson (treated with Thiram) respectively.

Table 3.2: Treatment details for Hoosfield continuous Maize

Treatment	Abbreviation	Plot sampled	Basal manuring	Application*
Continuous Barley	B	02, 10, 17	35 kg P/ha (171 kg Triple superphosphate),	
Continuous Maize	M	05, 07, 14	90 kg K/ha (181 kg/ha Muriate of Potash)	P & K: 12/10/06
Maize after 3 years of Barley	(B)M	04, 08, 15	N:S at 96 kg N/ha (355 kg Double top 27% N)	N: 25/04/07
Maize + Maize tops (10t ha ⁻¹ yr ⁻¹)	MT	03, 09, 18		

*Refers to the last application before sampling in June 2007.

3.2 Chemical Analysis

3.2.1 Soil pH

Soil solution pH is measured using a combination electrode, by mixing air-dried soil with water (1:2.5 ratio) following the standard method outlined in Black (1988). The pH was measured for each bulk sample and then repeated once 0.01 M CaCl₂ is added. The effect of soil dilution is to increase the pH of the soil solution, due to the addition of neutral salts, while the addition of 0.01 M CaCl₂ is almost approximate to the total electrolyte concentration and therefore represents more accurately field conditions (Peech, 1965). The difference between the pH measured in water and in salt solution is known as the “salt effect”. The measurement of pH is one of the most widely measured chemical properties of soil and yet it is difficult to designate a concrete conclusion, due to the vast array of factors causing variability in pH. Briefly, Natural weathering, OM-decay, chemical fertiliser, tillage and acid deposition can all alter pH. In turn, pH affects a multitude of chemical, physical and biological properties including plant nutrient availability and microbial activity (Brady, 1999) and consequently the decomposition of OM. For instance, acidic soil conditions reduce the rate of OM-decomposition, particularly in the early stages (Russel, 1988; Jenkinson, 1977).

3.2.2 Loss-on-Ignition

Loss-on-ignition is a rather simple yet robust method for estimating OM-content providing suitable precautions are applied. Soil is prepared by passing through a 2mm sieve and dried to a constant weight at 105 °C for 24 hours. A sub-sample of 10g is analysed as recommended by Cambardella *et al.* (2001).

Samples are ignited in a muffle furnace. 10 g of soil is heated at 450 °C for 4 hours, this temperature is thought to be the most appropriate since the clay content of these soils to be analysed is high and more critically varies between samples (ranging from 23.8-26.4%), a 10-fold difference in clay content of soils can generate errors due to the loss of structural water in the region of 4-5% (Ball, 1964). Consequently heating above 500 °C could lead to some variation in the loss of structural water between samples (Rowell, 1994). SOM content will then be calculated as outlined in Rowell (1994).

3.2.3 Laser Ablation and Isotope-Ratio Mass Spectrometry (LA-IRMS)

The following method was used to analyse soil collected from Hoosfield Maize experiment (3.1.3).

By the use of stable-isotope ratio mass spectrometry (IRMS), quantification of the extent that stable isotopes of carbon (^{12}C & ^{13}C) in organic samples have fractionated is possible. The spatial distribution of carbon isotopes can be determined by targeted analysis using a laser with controlled combustion in an oxygen environment. The $\delta^{13}\text{C}$ values are calculated relative to the Pee dee belemnite standard (PDB), $\delta^{13}\text{C}$ values are presented in ‰ (parts per thousand) as outlined by Boutton, (1998).

This method has previously been successfully applied to investigate the $\delta^{13}\text{C}$ of $^{13}\text{CO}_2$ pulse labelled plant-soil blocks allowing the distribution of recent photosynthates to be identified within soil thin-sections (Bruneau *et.al.*, 2002). Only through natural abundance of ^{13}C is the distribution of older carbon identified. Differences in the photosynthetic pathway of C_3 and C_4 vegetation, due to the activity of different enzymes and the limitation of CO_2 diffusion into the leaf (O' leary, 1988) creates a distinct non overlapping $\delta^{13}\text{C}$ signature that can be tracked from plant to soil with $\delta^{13}\text{C}$ values differing by approximately 14 ‰ (Boutton, 1996) (Boutton, 1998). Within C_3 plants the first C-product is produced by the enzyme RuBP-carboxylase this enzyme discriminates against ^{13}C with $\delta^{13}\text{C}$ values ranging from -32 to -20 ‰, averaging -27 ‰ (Boutton, 1998). Within C_4 plants the first C-product is produced by PEP-carboxylase and this enzyme does not discriminate against ^{13}C and therefore has a higher $\delta^{13}\text{C}$ value between -17 to -19 ‰ averaging -13‰ (Boutton, 1998). The isotopic composition of SOM is not well known (Boutton, 1998) and differences can occur between certain biochemical fractions (for example lignin and cellulose), due to differences in the rate of decomposition. Clearly differences within fractions may occur as decomposition proceeds (Boutton, 1998). Despite this it is well accepted that the isotopic composition will reflect the photosynthetic pathway of the dominant vegetation (Boutton, 1998). Since soil sampling was restricted to one depth, further complications due to potential differences in $\delta^{13}\text{C}$ down the soil profile (due to enrichment by ^{13}C of 1-3‰) (Boutton, 1996) are avoided. Long-term experiments have made use of this distinct signal to track the distribution of older versus newer carbon inputs by changing the photosynthetic pathway of the dominant vegetation. This analysis was conducted at SUERC in East Kilbride in collaboration with Prof. Tony Fallick. Loose soil samples (closed tube-combustion) and thin-sections (laser-ablation) were analysed for both Hoosfield and pot-experiment soil. Closed-tube combustion was performed

in order to obtain reference $\delta^{13}\text{C}$ values for PEG resin, soil and the root and shoots of *H. vulgare* and *Z. Mays* in order to verify the $\delta^{13}\text{C}$ values obtained by laser ablation. Closed-tube combustion of graphite has shown the reproducibility of results to be ± 0.05 ‰ with standard deviations of $< 0.3\%$ (Boutton, 1996). Previous analysis showed that PEG resin has a $\delta^{13}\text{C}$ value of -30.4 ‰ ± 0.5 (Bruneau *et al.*, 2002), indicating no overlap with the $\delta^{13}\text{C}$ values of carbon compounds from C_3 or C_4 plants. Closed tube-combustion was performed by placing 5g of air-dried sample in evacuated quartz-tubes containing fired-cupric oxide, as an O_2 source which was combusted at 850°C for 6-hours and a conventional glass extraction line was then used to purify the CO_2 . The extraction line consisted of a CO_2 / acetone spiral slush trap, to remove any water and a liquid N_2 spiral trap to freeze-down SO_2 and CO_2 , allowing non-condensable gases to be pumped away. The amount of CO_2 gas extracted was measured using a capacitance manometer, for which the isotopic composition was measured using a VG Isogas Sira II dual inlet isotope ratio mass spectrometer. The extracted *purified* CO_2 would only contain CO_2 with a mass of 44 ($^{12}\text{C } ^{16}\text{O } ^{16}\text{O}$), 45 ($^{12}\text{C } ^{16}\text{O } ^{17}\text{O}$) and 46 ($^{12}\text{C } ^{16}\text{O } ^{18}\text{O}$). The $\delta^{13}\text{C}$ values are calculated relative to the Pee dee belemnite standard (PDB), corrections are made for ^{17}O contributions and $\delta^{13}\text{C}$ values are presented in ‰ (parts per thousand).

Laser-ablation of targets within thin-sections is performed using a modified Leitz Metallux 3 microscope system. The system ensures a controlled combustion, through a focused beam with a spot diameter of $100 \mu\text{m}$ and a further well area of $30 \mu\text{m}$ (Bruneau, 2002; Kelley & Fallick, 1992). The laser current ranges from $4\text{-}9 \times 10^{-10}$ A, this variation in ion current caused $< 0.25\%$ variation in $\delta^{34}\text{S}$ measurements when analysing natural sulphide minerals showing that the values are highly reproducible (Kelly & Fallick, 1990). The CO_2 collected is purified to remove any Sulphurs, O_2 , H_2O and hydrocarbons originating from the resin. The CO_2 extraction line is modified to include a furnace where the gas is contained and combusted at 800°C for 5 minutes before being released into the conventional extraction line. Ideally single targets should be burnt and the gas isolated before sampling another region within the thin-section, thus ensuring that, the source and location of CO_2 was accurately identified in subsequent evaluation. However, preliminary analysis found that burning multiple targets was required to obtain enough CO_2 ($> 15 \mu\text{m}$) for subsequent mass spectrometer analysis. However the amount of CO_2 was often too low to be run manually instead CO_2 was frozen down into the cold finger using liquid N_2 . Targets were identified during prior micromorphological analysis of the thin-sections as in **Section 3.4**.

3.3 Physical Analysis

3.3.1 Bulk Density

Bulk density is defined as “the mass of a unit volume of dry soil” (Brady, 1999). Bulk density measurements are taken using Kubiena tins sampling is positioned as explained in **Section 3.1.2**. Dry bulk density was calculated once soil samples were dried to a constant weight (105 °C). More routinely carbon stocks are calculated using both bulk density and C-concentration measurements, although some recent studies have made estimates of C-contents based solely upon C-concentration (Arrouays *et al.*, 2006; Bellamy *et al.*, 2005) this approach is extremely problematic since both OC-concentration and bulk density are variable in time and space. Organic carbon concentration is sensitive to biotic processes, while bulk density is a product of parent material, soil genesis and aggregate formation and therefore any processes which alters aggregate formation (Don *et al.*, 2007). Furthermore Don *et al.*, (2007) argue that despite a strong negative correlation between OC-concentration and bulk density the scale and magnitude of change for these two variables may also differ.

3.3.2 Aggregate Water Stability

The assessment of a good soil structure can be measured through aggregate stability, since the stability of aggregates influences many aspects of soil physical behaviour (in particular water infiltration and soil erosion) and biological quality (e.g. the storage of SOC). SOC is recognised as an important indicator of soil physical quality (Watts & Whalley *et. al.*, 2001). SOC acts as a binding agent between soil particles, its contribution to aggregate stability varies at different scales, as outlined by Tisdall & Oades (1982). Additionally SOM protects the soil surface against raindrop impact, improves water infiltration and aids hydrophobic characteristics that inhibit soil wetability and slaking (Le Bissonnais, 1996; Mcghie & Posner, 1990; Sullivan, 1990).

In general agricultural soil in good physical condition should be strong when wet and weak when dry. Thus providing protection from collapse and crusting when wet, and a lower resistance to root penetration and improved workability when dry (Watts and Whalley, 2001). There are several mechanisms of aggregate breakdown, as outlined in more detail by Le Bissonnais (1996):

1. Slaking, caused by the compression of entrapped air upon wetting.
2. Breakdown by differential swelling, i.e. the swell-shrinkage of clays.
3. Physico-chemical dispersion, due to the reduction in attractive forces between colloidal particles
4. Breakdown by raindrop impact.

As a reflection there are numerous methods testing AWS which place a varying emphasis upon testing each of the breakdown mechanisms.

Aggregate water stability was performed for each of Le Bissonnais wetting treatments, since it is possible that only one treatment will provide sufficient distinction between treatments, dependent on soil type (Le Bissonnais, 1996). The treatments included: fast wetting- the immersion of aggregates in water; Slow wetting with controlled tension- to stimulate a more gentle rain and mechanical breakdown after pre-wetting- which tests the wet mechanical cohesion of aggregates independent of slaking. Calibrated aggregates were analysed, these are 2-8 mm in diameter and dried at 40 °C for 24 hours to a constant matric potential.

Mean weight diameter (MWD) and fragment size distribution (FSD) are measured to record the breakdown of aggregates following treatment. This involves passing soil through a 50 µm sieve and moving the sieve up and down (mimicking a yoder apparatus) while submerged in methylated spirit, thus separating the <50 µm from the > 50 µm fraction. Sieving in methylated spirit reduces further breakdown of soil aggregates. Once dried the soil is then passed through a nest of sieves (2000, 1000, 500, 200, 100 and 50 µm) this must be done gently again to avoid further breakdown of aggregates. The FSD measures the mass percentage of soil for each of the 7 size class (with the <50 µm fraction calculated by the difference of the initial mass and the sum of the 6 other fractions). “The MWD is the sum of the mass fraction remaining in each sieve multiple by the mean aperture of the adjacent sieve (with MWD ranging from 25 µm to 3.5 cm)” Le Bissonnais (1996).

3.3.3 Water-Retention-Characteristics

Water-retention-characteristics or water-release-curves describe the basic relationship between water content and matric potential Ψ , thus permitting an indirect behavioural assessment of the pore size distribution. The water release characteristic is measured using intact soil cores and allows a rapid indirect method of assessing the pore-size distribution. Water is held within the soil at a negative pressure (to atmospheric pressure) through forces controlling the extent of adhesion between water molecules and cohesion of water molecules to particle surfaces. By applying pressures greater than soil water pressure, water can be removed (e.g. uptake by plant roots). In short, at increasing pressures water will first drain from larger pores, by increasing pressure, air-water interfaces retract back and successively smaller pores are drained, until at the most negative pressure water is retained only within the narrowest of pores (Marshall & Holmes, 1979) (Rowell, 1994).

The volumetric water content (cm cm^{-3}) for each treatment will be plotted. At the lower end of the water release curve (i.e. at less negative pressures) the water holding capacity is largely governed by adsorption to particle surfaces and is therefore more greatly affected by soil structure. While at higher pressures and within smaller pores water storage is primarily controlled by capillary effect, here it is soil texture which has the overriding control (Hillel, 1982). Nevertheless, other factors may alter the water holding capacity of a soil such as the shrink-swell history (Hillel, 1982) and root exudation which has been found to alter the surface tension (Read & Gregory, 1997) this can then be reflected in the water-retention-curve by reducing water content at any given water potential (Read *et al.*, 2003; Whalley *et al.*, 2005).

Since pore size distribution will be determined by both image analysis and water-retention data, it will be possible to compare the curves proposed by the two methods, as has previously been achieved in separate studies, (e.g. Crawford, 1995). By comparing the two methods it may become apparent that pore size distributions proposed by water release data may underestimate the size of pores, this is possible if larger pores tend to empty through smaller pores, Crawford *et al.*, (1995) suggest that only at high pressures where smaller pores are empty is the water release accurate reflection of pore size.

Water retention was measured from soil cores 7.61cm^3 and 76.03 cm^{-3} in volume. Soil cores were sampled from Broadbalk Winter wheat in March 2009, being the same time of year the Kubienia tins were removed two years previously. The soil profile was exposed to allow sampling at 20cm depth using the same approach previously explained (see 3.1.2). The water

content was measured from fresh (wet) soil cores (7.61cm^3) after 3-weeks of equilibration following exposure to -1, -5, -10, -15 kPa using pressure-plate apparatus. After removal from the pressure plate the wet soil core weight was measured while the dry soil weight was measured after drying at 105°C . From these results both gravimetric (g g^{-1}) and volumetric water content (cm cm^{-3}) and differential water capacity (cm cm^{-3}) was calculated. For pressures of 0, 0.2 & 0.5 kPa soil cores of 76.03 cm^{-3} (3 from each Broadbalk treatments) were placed on a sand table and allowed to equilibrate for several days this was checked by weighing, if the core weight did not change ± 0.1 it was taken that the soil had equilibrated to the set matric potential. To ensure that a good contact with the soil and sand table is maintained the base of the soil core was coated in calcium sulphate (plaster of Paris) mixed with distilled water to a 1:1 ratio. This was done by displacing a small volume of soil from the core, the displacement height measured 0.6mm using callipers and the volume filled with Plaster of paris. By weighing the core after soil displacement and again once the plaster had been applied the wet soil weight and plaster contribution was known. The water content and volume of plaster was also calculated, with the volume of plaster calculated from its wet bulk density 1.39 g cm^{-3} knowing that plaster has a particle density of 2.54 g cm^{-3} . Knowing the contributions made by the plaster it is then possible to calculate the actual water and volumetric water content of the soil core.

3.4 Microscopy and Sub-Microscopy with Elemental Analysis

The following section describes the analysis of thin-sections performed at the microscopy and sub-microscopy level. The application of image analysis and micromorphology was applied to thin-sections collected from Broadbalk Winter-Wheat, Broadbalk Wilderness and Hoosfield continuous maize while, elemental analysis using SEM-EDS was restricted to Broadbalk and Wilderness slides.

3.4.1 Micromorphology

Micromorphology permits the study of soil and the spatial arrangement of soil components in a relatively undisturbed state. Micromorphology is conventionally based upon the description of soil thin-sections under the light microscope however, more frequently descriptions act as a sound basis for additional analysis including: Image-analysis, electron microscopy, EDS, and LA-IRMS.

The origins of micromorphology date back to 1935 after the publication of papers by W.L. Kubiëna. Over the last 74 years the application of micromorphology is far reaching featuring in numerous disciplines e.g. Archaeology, engineering, geomorphology, soil microbiology, as such, due to the discursive nature of this method a vast array of terminology and classification techniques exist and are ever generating. To ensure effective understanding and transfer of research findings the description of thin-sections has been conducted using several core texts including (Stoops, 2003; Fitzpatrick, 1993; Babel, 1975).

3.4.2 Summary of Thin-Section Analysis:

- The largest units of structure and OM will be described across the whole thin-section, using a light box and a hand-held magnifying lens (10 x).
- Thin sections will be sub-sampled by randomly positioning 3 areas of interest (AOI), to determine the intra-sample variability. The size AOI was determined by calculating the representative elementary area (REA).
- Using a polarizing microscope at 40 x a conventional description of thin-sections will be made, aiding the overall interpretation of micromorphological findings.
- Image analysis software will be utilised to provide quantitative information on the abundance, size and distribution of pores and OM-categories at 40 x.
- Finally AOI will undergo quantitative elemental micro-analysis using SEM-EDS.

3.4.3 Thin-Section Production

Thin-sections (5 x 7 cm) were produced at The University of Stirling Thin-Section Production Laboratory, from undisturbed soil blocks sampled using Kubiena tins (Murphy, 1985). Water was removed from the soil blocks using the solvent exchange method, this is ideal for soils with either a high clay or OM content. Water replacement was performed by enclosing the sample in an environment of vaporised acetone. Following this soil blocks (from Wilderness and Broadbalk) were impregnated with crystic resin. Once cured the soil blocks are cut and bonded to glass slides after which they are lapped and polished to 30µm. Since these thin-sections are to be analysed under the SEM these slides were not cover-slipped. Full details of standard thin-section production can be found at: <http://www.thin.stir.ac.uk/>.

For Hoosfield soils for which LA-IRMS was to be performed, these soil blocks were impregnated with polyethylene glycol (PEG) as previously performed by Bruneau *et al.*, (2002). PEG is miscible with water meaning that removal of water by acetone replacement was not required, this has the advantage of reducing the loss of solvent-sensitive carbon namely root exudation (Bruneau *et al.*, 2002). When heated to 60°C PEG liquefies and has a similar viscosity to crystic resin and can be poured into the soil block. To ensure complete impregnation of PEG samples are kept in an oven at 60°C for approximately 3 weeks. Once cooled soil blocks are hardened at room temperature in approximately 24 hours. The thin-sections are then cut and ground smooth, by hand, to between 30-60 µm thick using medium to fine abrasive paper.

3.4.4 Micromorphology Description

A general description of thin-sections was made at both 10x (whole thin-section) and in more detail at 40x (within AOI) using a polarised microscope (Olympus BX50) under plane polarised light (PPL), cross polarised light (XPL) and oblique incident light (OIL). At 40x magnification estimates of abundance were made using abundance diagrams (Stoops, 2003, pg.43) from which summary tables were produced (**Appendix 1**). These conventional descriptions were made following guidelines recommended by Stoops (2003) and included the assessment of mineral, organic (**Section 3.4.6**), porosity, pedofeatures (namely excremental). Since estimates of abundance for both organic matter and porosity were made within each AOI this permitted a direct comparison with quantitative results derived from image analysis. This is especially relevant with soil pores since descriptions of pores can give an indication of their genesis (e.g. planes form by shrink swell processes, while channels from biological). In comparison image analysis will provide an assessment of pore shape (e.g.

pores are either: planular, irregular or rounded) which is more limited in its implication of pore genesis. Upon preliminary investigation it was found that it was not possible to identify discrete aggregates at 40 x magnification this was also true for the wilderness slides and therefore not restricted to the agricultural soil. As such structural assessments were made upon the extent and nature of porosity.

3.4.4. Procedure for Sub-Sampling within Thin-Sections.

A grid was placed over each slide, each grid measures 5 mm², giving a total of 165 grids (area of thin-section 55 x 75 mm), the grid acts as a guide when describing the thin-sections particularly at high magnifications. The thickness of thin sections is strictly maintained between 25-30 µm since the thickness of the slide will influence a number of significant properties including colour, and wedging effects. Inspection of thin-sections taken from Broadbalk revealed a thinning around the edges of the thin-section this is largely restricted to the outer 0-3 mm perimeter. When viewing at higher magnifications there is a clear difference in both colour and resolution of finer materials compared to central regions of the thin-section, therefore the outer perimeter will be discarded from any analysis (**Fig. 3.5**).

To ensure that grid lines are not included when automatically setting phases using image analysis and more importantly that the acetate grid does not interfere with the direction of the light beam when viewing samples under XPL, acetate covering AOI will be cut away.

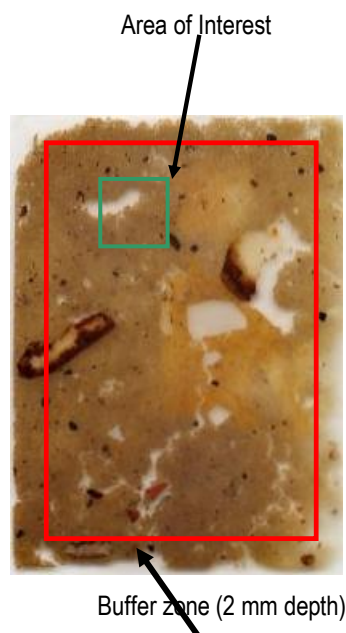


Figure 3.5. Sampling within thin-sections. The whole slide excluding the outer perimeter will be described at 10x magnification. Three areas of interest will be randomly positioned within thin-sections. These areas will be further described and image analysis performed at 40X.

Randomly designating areas of interest (AOI) at low magnification (10 x) rather than restricting analysis within discrete grid squares is considered to be the most appropriate method of sub-sampling within thin sections, as this will ensure that larger components (e.g. earthworm channels which can span >4 mm in diameter (Jongmans, 2003) are included in the analysis. Additionally the size of AOI will be determined by calculating the representative elementary area (REA) that accounts for all spatial heterogeneity of pore size within the scale of interest (scale referring to the actual size of features being measured). The REA has been defined as “the minimum area of a soil sample required from which a given soil parameter measurement becomes independent of the size of the sample” (VandenBygaart & Protz, 1999). Pore area was measured using image analysis (for methods see **Section 3.4.7**) in a series of successively larger areas and the REA selected when measurements in 3 consecutive areas did not change $\pm 10\%$ (VandenBygaart & Protz, 1999). Variation in pore area was consistently <10% when the area of the thin section analysed approached 0.3 % therefore, the size of each AOI was set at 12 mm². With a total of 3 AOI analysed within each thin-section, image analysis was performed upon 0.9% of the total thin-section area. Clearly the larger the features of interest the greater the REA will be. Since multiple images of the same area are required to separate pores from quartz grains (**Section 3.4.7**), a large computer memory is also required, therefore computer memory also limits the maximum size of Areas of interest. As a consequence the criterion for setting the size of AOI was principally based upon calculating the REA with consideration given to the software capacity for processing images.

When measuring and counting objects within defined areas objects often overlap the edge of images, this may become critical when measuring the size and shape of pores, by elevating the occurrence of non continuous pores (e.g. poroids). To control for “edge effects” which could create a bias in the size and shape of objects measured, only objects that cross the upper and left edge of a mosaic image will be counted (adapted from Ringrose-Voase, 1996).

3.4.5. Procedure for Sub-Sampling within Hoosfield Thin-Sections.

The approach used to analyse Hoosfield slides differs to the method used to analyse samples removed from Broadbalk due to the differences in the manufacture process (**Section 3.4.3**). To recap, samples from Hoosfield were grounded to 30µm using a bench sander. The manufacture of thin-sections created artefacts including, loss of soil material, variable slide thickness and surface abrasions. To control for this variability areas of the thin-section were selected for analysis. Due to the limited regions within thin-section suitable for analysis, micromorphology was performed at 20x and restricted to identifying and describing features of interest, the area of features were calculated using image analysis (**Appendix 3**). Three features were identified across all treatments this included microaggregates (<2mm diameter) macroaggregates (>2mm diameter) and black carbon (**Appendix 3**).

3.4.6 The Classification of Organic-Matter

Micromorphological descriptions will focus upon the form and distribution of OM-fragments within thin-sections, from which the extent of decomposition and modes of transport can be discerned. Descriptions will comprise of plant (organ/ tissue) or their more decomposed forms, since sections though animals are rare (Stoops, 2003).

It is possible to identify plant tissue and organ types (Stoops, 2003); (Fitzpatrick, 1993); (Babel, 1975); however due to limited access to reference material this approach seemed ambitious and overtly open to misinterpretation. In addition as decomposition proceeds different tissue types may converge in their appearance (Babel, 1975). Because of the potential problems with identifying tissue and organ types it was decided to describe organic fragments according to their form and extent of decomposition (**Fig. 3.7** for the classification examples): furthermore this method of description is in accordance with the aims of the project, **Fig. 3.6** shows the summary of OM classification.

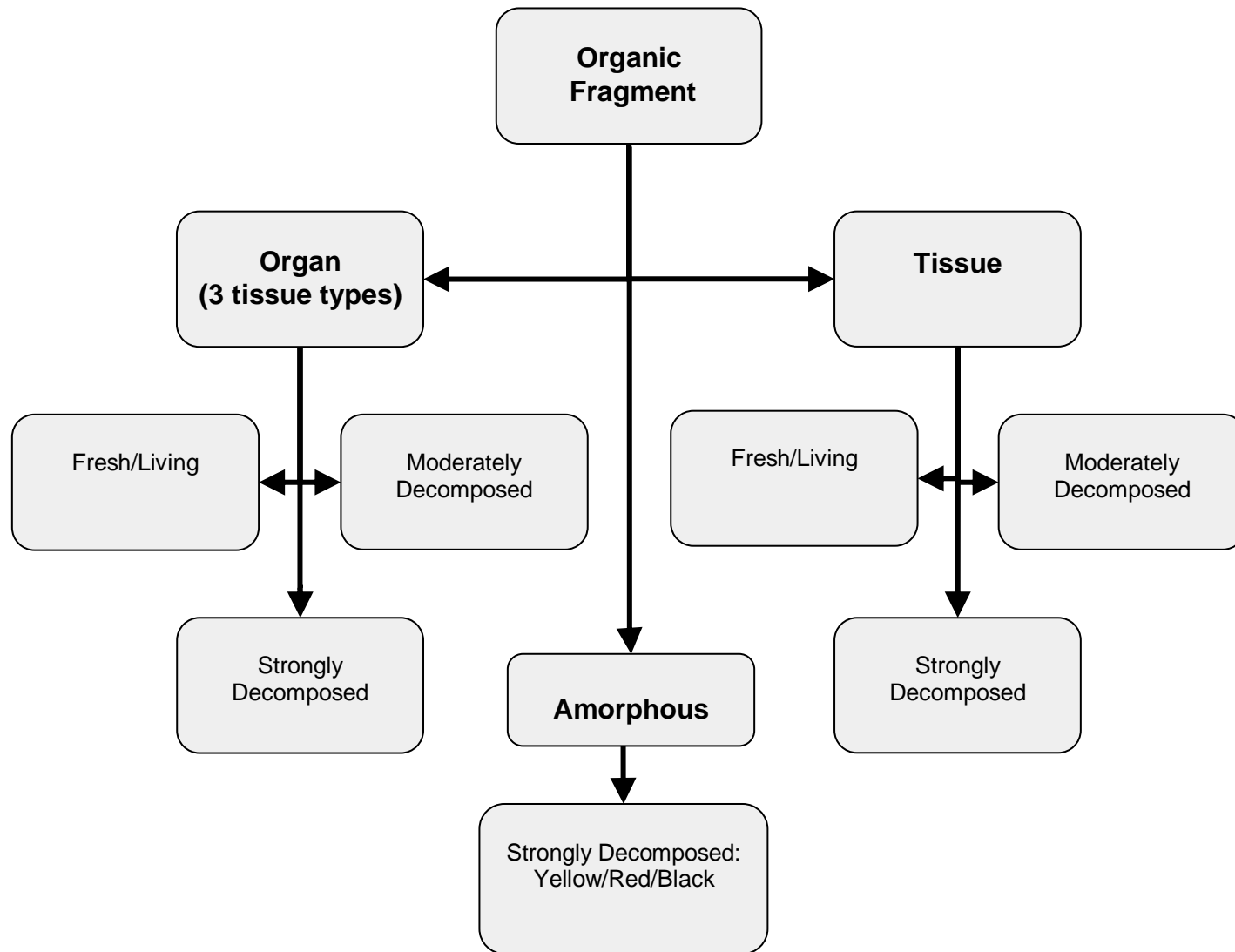


Figure. 3.6 The process of organic matter classification. Firstly the form of organic matter is assigned following the recommendations of Babel (1975). Secondly, the extent of decomposition is identified using a modified classification proposed by Fitzpatrick (1993). Organ and Tissue fragments can be either: fresh/living, moderately or strongly decomposed while amorphous forms are strongly decomposed and are further described by their colour, with yellow-black indicating greater decomposition (Bullock et al., 1985). It is the combination of these two methods which makes this organic matter classification scheme novel.

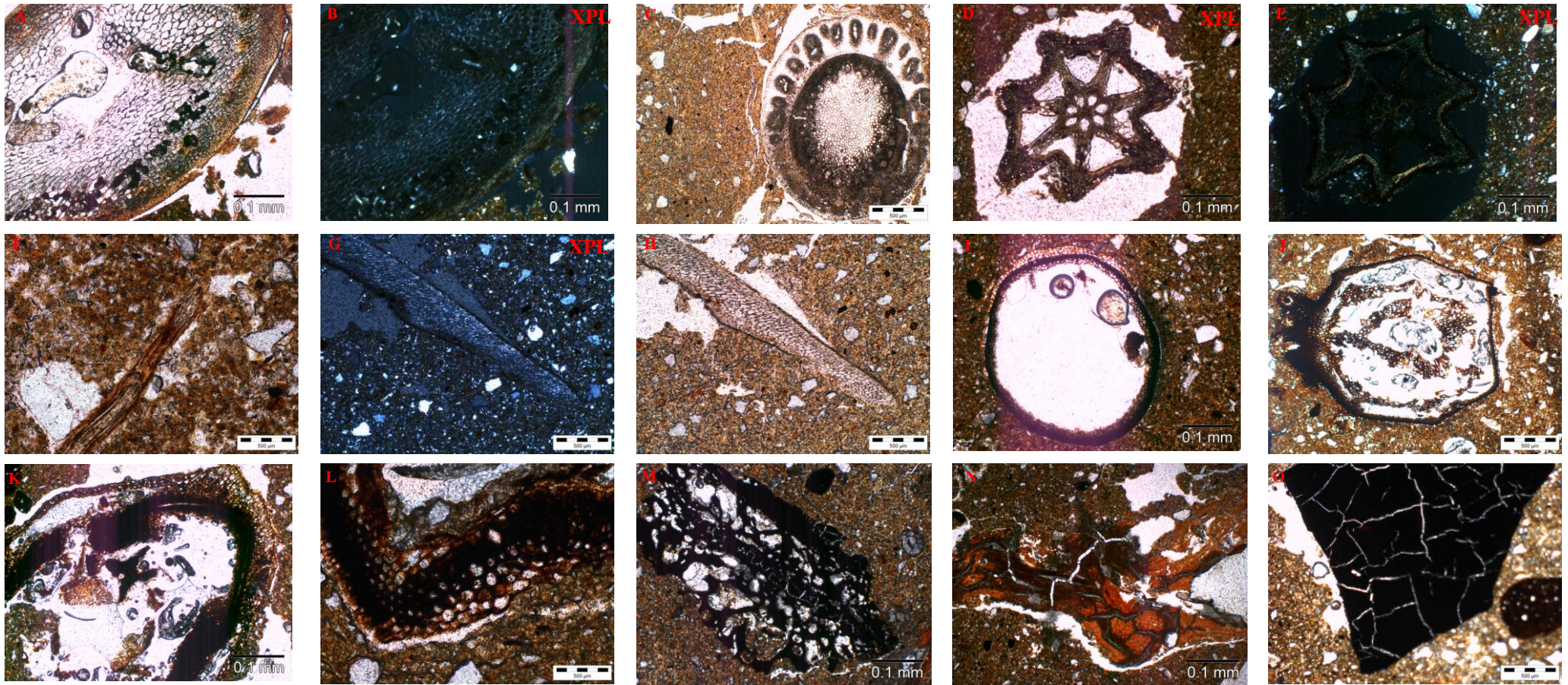


Figure 3.7. Images taken in plane polarised light or cross polarised light (XPL), showing organic fragments classed according to form and extent of decomposition following the guidelines outlined by Fitzpatrick (1993) (**Table 3.3**). Images show: Fresh/living organ fragments (**A-C**); moderately decomposed organ fragment (**D-E**); Moderately decomposed tissue (**F-H**); Strongly decomposed organ (**J**); Strongly decomposed tissue (**K-L**) and very Strongly decomposed (**M-O**).

Organic matter will first be described according to its form whether it occurs as organ (>1 tissue type) tissue (>10 cells of one tissue type) or as fine residue/ amorphous (<10 cells or where no cellular structure can be identified) (Stoops, 2003; Babel, 1975). As with organ and tissue types fine residue/ amorphous can be further sub-classified (e.g. punctuations and organic pigment) however, this is highly difficult due to the unavailability of reference material. Therefore further description of amorphous forms will be based upon its colour whether fragments occur as yellow, red, or black forms, with yellow to black indicating an increase in decomposition due to autoxidative and microbial processes (Bullock *et. al.*, 1985). In addition restricting extensive classification of OM ensures more accurate descriptions that are readily comprehensible to non-micromorphologists due to the cross-disciplinary use of definitions such as organ and tissue.

Once an OM-fragment has been identified in terms of its form it is then further described according to the extent of decomposition (**Table 3.3**), following a modification of the classification proposed by Fitzpatrick (1993). The classification was altered to prevent misinterpretation between very similar stages of decomposition by reducing the number of stages from 4 to 6, thus ensuring that the 4-stages of decomposition are distinct and thus OM-fragments could be readily assigned to a decomposition stage.

Table 3.3. The classification for the extent of organic-matter decomposition, modified from Fitzpatrick (1993).

Decomposition Stage	Description
Living/fresh	Live/ dead at the time of sampling, very slightly decomposed, <25% fine residue. Showing interference colours and primary fluorescence.
Moderately decomposed	Plant material is still recognisable showing loss of structure and fragmentation, 25-55% fine material. Showing interference colours, in association with undecomposed cellulose.
Strongly decomposed	Plant material that is just recognisable and has lost most of its structure, 55-70% fine residue.
Very strongly decomposed	Amorphous remains of plant material, generally isotropic with >70% fine residue

3.4.7 Image Analysis

Image analysis permits a quantitative assessment of features occurring within thin-sections and is routinely applied to calculate and characterise soil porosity. High resolution image mosaics were produced to form the contiguous area required to meet the REA (**Section 3.4.4**), images were taken using a polarised microscope (Olympus BX50), fitted with a motorised stage (Lang, Hüttenberg) the images were stitched together using the “multiple image alignment” function image analysis software (analySIS pro, version 5) as described in Adderley *et al.*, (2002).

Images can be segmented allowing measurements to be made on discrete features, this can be achieved by applying colour or shape thresholds if these characteristics are uniform between features of interest. Since neither shape nor colour is confined or systematic to organic fragments, segmenting images using semi-automatic thresholds is not possible. Instead organic components can be distinguished using image analysis software by manually delimitating features. The identification of organic residue using conventional micromorphology is well established, applying these guidelines it is possible to achieve a systematic method of phasing different organic components. Once images were segmented, (selecting for organic fragments), measurements included: frequency and area of organic fragments. By exporting images into an image manipulation program (GIMP 2.6) organic features could be colour coded according to the extent of their decomposition and a map showing the distribution of organic matter in relation to soil pores produced.

By taking multiple images of the same AOI under both PPL and XPL light it was possible to measure porosity and distinguish between pores and quartz, since both are translucent under PPL. multiple images under XPL at 0, 5 and 15° allowed the high interference colours of quartz to be visible. By subtracting XPL images from the PPL image and applying colour thresholds (R: 0-255 G: 0-255, B: 54-255) meant quartz grains could easily be removed. Although time consuming this method was highly effective, and meant that adding dye to the soil that would have caused further complications in subsequent elemental analysis was avoided. Colour images were binarised, pores are represented by white and the soil matrix by black pixels. Using the “edit image” tool any artefacts of slide production were removed (converted from black to white pixels) and any remaining quartz grains removed (converted from white to black pixels). To exclude any electronic noise and difficulties in removing quartz, the minimum size for detecting pores was set at 100 μm^2 . Image analysis software performed a number of direct measurements, including area, perimeter and X, Y coordinates. Derived measurements include shape factor (Horgan, 1998). With values ranging from 0-1,

the lower the value the more convoluted the pore (Horgan, 1998). Shape factor will be used in conjunction with pore area, enabling the pore size and shape distribution to be assessed.

3.4.8 Some Considerations for the Classification of Organic Matter.

When classifying the very-strongly decomposed organic material no distinction has been made between black carbon, humified and melanised organics, therefore these are grouped together in the amorphous black category. All of the above will occur either as distinct units or in combination as aggregates (Kaal & Movick, 2008).

Kaal & Movick (2008) highlighted the problem in identifying BC from the non-charred dark (brown-black) organo-mineral amorphous fraction, using micromorphology techniques. The occurrence of dark organic particles can be due to either, carbonisation, humification or melanisation of organic matter. Increasingly microscopy techniques are being used to identify BC in either thin-sections (Kaal & Movick, 2008) or in fractionated bulk soil. As Kaal & Movick (2008) highlighted caution is needed when identifying BC using colour thresholds due to the multiplicity of darkened organic particle generation. Furthermore separation of these forms at the light microscope level based upon descriptions of structure is also difficult, with only plant derived (charcoal) displaying a discrete structure. However, some melanised OM has been found to display a very similar structure to charcoal being deep black and having sharp boundaries (Van Mourik 1985). Therefore to make accurate distinctions between the amorphous black forms both micromorphological and elemental data from SEM-EDS is required.

3.4.9 Protocol for SEM-EDS

Thin-sections which are polished to 30 μ m and non-cover slipped, can be analysed under the scanning-electron-microscope (SEM) and elemental data can be collected using the energy-dispersive x-ray (EDS) detector. The SEM operational parameters applied to ensure optimal X-ray detection impairs imaging, however the location and full extent of features can be located using OM-pore maps generated by image analysis. For this project the principal element of interest is carbon, as such the set-up of the microscope is maintained to ensure optimal C-detection for this system (**Table 3.4**). This requires using an accelerating voltage of 5 kv, a process time of 5 and a working distance of 10mm, (all live times given below will be according to this set-up and a spot-size between 64- 68). The penetration of the EDS probe will vary depending upon the accelerating voltage. The maximum accelerating voltage to be used is 15 keV, at which the EDS probe has a depth and lateral resolution of 1 μ m x 1 μ m.

Elemental analysis utilised a range of sampling approaches, from targeted point and ID, elemental mapping and line/point transects. Point and ID permits more quantitative data to be gathered providing a minimum of 100,000 counts per analysis is collected (process time approximately 10mins). Elemental mapping gathers qualitative data, with a minimum of 500 frames collected (live time: 1 hour). For more detailed elemental maps approximately 1500-2000 frames are required, however this has the disadvantage of requiring much longer acquisition times (live time: 3 hours). The acquisition time needed to accrue sufficient x-rays is also dependent upon the conductivity of the sample and the presence of charging at the sample's surface, the spotsize can be lowered to reduced charging, however this also has the drawback of limiting x-ray production and as a consequence longer live-times will be required. Alternatively, charging can be reduced by coating, either with Au or C, clearly it is preferable to avoid C-coating when mapping carbon and Au has the draw back that it will absorb some of the low-energy x-rays such as those originating from C-atoms.

Table 3.4: The parameter set-up of the SEM when optimizing for the collection of carbon X-rays when using EDX.

Parameter	Constraint
Sample Tilt	0.0°
Accelerating potential	5 keV
Magnification	200-1000
Working distance	10 mm
Spotsize	60-68
Aperture	3
Process time	5
Number of frames for linescan or mapping	min. 500
Number of counts for point and ID	min. 100,000

Thin-sections have been analysed using Jeol SEM systems (JSM-6360LV) linked to an oxford instruments INCA X-sight detector with a Si/Li crystal, thin film window. The analysis was performed on JSM-6360 LV (Rothamsted Research Imaging facilities) which requires the thin-sections to be cut isolating AOI as identified by micromorphology and image analysis, due to the smaller stage size (stage can accommodate a stub size of 2.5 cm in diameter).

Prior to analysis of the thin-sections a blank polished crystic resin standard was analysed. Using this standard and existing published standards the O:C ratios of different C-phases can be separated in point and ID analysis, **Table 3.5**. Studies have found the low O:C ratio determined by elemental analysis particularly useful for identification of carbonised particles (Davidson 2006; Brodowski, 2005; Stoffyn-Egli *et al.*, 1997). Using the O:C ratio it is also possible to separate Black carbon from other organic matter fractions (Glaser *et al.*, 2000) with O:C ratios been proposed for several non-carbonised carbon materials (**Table 3.5**). This approach is powerful enough to identify BC-particles when it occurs within complexes of other OM fragments and minerals (Brodowski *et al.*, 2005). Following from this it should be possible to use the O:C ratio, to differentiate between OM and crystic resin, from which distinct phases can be produced within elemental maps. Since detailed maps of the nature and location of OM are produced, using image analysis, it will then be possible to assess the validity of phase separation between OM and resin using elemental data gathered by SEM-EDS.

3.4.10. Alternative SEM-EDS System.

Towards the end of this project an alternative SEM-EDS system became available for use, Zeiss (EVO MA15). This system has two advantages firstly it has the option of performing analysis under low vacuum variable pressure conditions thereby reducing surface charging of samples. In addition it is fitted with an INCA X-sight detector (80mm) the larger crystal means that x-ray counts can be collected much quicker thereby more than halving process times. Due to the reduced charging under low vacuum pressure imaging was significantly improved (**Discussion 7.5**), this enable greater precision for targeted sampling. This system was used to perform elemental mapping (**Section 5.5.6**) and transects (**Section 5.5.7**) at a higher accelerating voltage of 15 keV. A higher accelerating voltage was applied in order to excite heavier elements to improve phase analysis.

Table 3.5: O:C ratios of a range of C-containing particles, determined by elemental analysis using SEM-EDX.

Carbon Particle	O:C ratio		
	Mean	St. deviation	Range
Black-C Particles			
Oil combustion	0.03	0.01	0.02-0.04
Coal combustion	0.03	0.02	0.02-0.06
Charcoal	0.05	0.01	0.03-0.08
Softwood combustion	0.11	0.02	0.09-0.15
Non-Black-C particles			
Sedimentary organic particles	0.30	0.01	0.28-0.31
Chitin	0.62	–	–
Cellulose	0.83	–	–
Lignin	0.37	–	–
Waterless wood	0.87	–	–
Diatoms	0.48	–	–
Peridinians	0.54	–	–
Resin Blank			
Crystic resin (polished)	0.14	0.02	0.12-0.16

O:C ratios of Black-C and non Black-C taken from Stoffyn-Eggi *et al.* (1997). O:C ratios of resin blanks determined from own analysis.

Areas-of-interest for which micromorphology and image analysis has been performed were analysed under the SEM-EDS, AOI are located using the OM-pore-maps and images of the AOI. It was found that the most efficient way to locate each AOI is to set the SEM to back-scatter-mode, selecting for contrast between elemental composition and guided by photos taken under the light-microscope look for distinct features; the precise nature and extent of organic fragments are more clearly discerned from the OM-pore maps. The difficulty in locating features within thin-sections means it's essential for AOI to be thoroughly imaged and mapped using the light-microscope. This itself is time consuming however, is essential for efficient and more importantly for a comprehensive and accurate analysis at the sub-microscope level.

The use of SEM-EDS in analysing soils is an emerging field with interests spanning across mineralogy, archaeology and soil science. Although the majority of studies have analysed loose usually fractionated soil under the SEM-EDS or SEM with microprobe, soil thin-sections are increasingly being utilised (for example, Davidson *et al.*, (2006) & Wilson *et al.*, 2005). Thin-sections are ideal for SEM-EDS since they are flat, polished samples eliminating much of the topography problems we would otherwise face with loose soil samples. Much of the research using SEM-EDS has focused upon sampling single points upon a surface, few have attempted to quantitatively measure the chemical composition of a specimen surface since, to obtain detailed maps long acquisition times are required (e.g. 500 frames requires a live-time of approximately 60 minutes). As such interpreting elemental maps must be done with care. For instance Brodowski *et al.*, (2005) found that BC-particles were more highly oxidised at the surface and a positive correlation between the degree of surface roughness and the extent of oxidation, although plausible, since this assessment was made on non-flat unpolished samples questions about topological effects are raised. In a separate study Laird *et al.*, (2008) looked at the occurrence of BC and humic carbon upon clay surfaces and mapped C-distributions upon non-flat samples, which resulted in poor quality maps although this could also have been a consequence of short run times especially as single element maps in particular need longer runs (Wilson, per. com.)

3.5 Statistical Analysis

Statistical analysis was performed using either Minitab (version 15) or Genstat (version 11). A range of statistical tests are applied including Kruskal-Wallis, general linear models, multiple comparisons, non linear regression and multivariate tests including cluster and discriminate analysis. Full details and rationale of the tests applied are given in conjunction with the results.

Chapter 4: The Structural Characteristics of Broadbalk Soils Contrasting in Total Organic-Carbon Content.

The following section recaps the study aims and introduces their specific objectives and the hypotheses that will be tested. The density, porosity and aggregate stability of Broadbalk NIL, Inorganic, FYM and Broadbalk Wilderness soils (**Section 3.1.1**) are presented.

4.1. Specific Objectives and Hypotheses

Aim 1: To assess the contribution of organic-carbon in determining the physical properties of soils.

Objective 1.1: The density of soils contrasting in total organic carbon content will be compared

Objective 1.2: The contribution of organic-carbon content to water-aggregate-stability will be determined.

Objective 1.3: The nature and grade of aggregation will be determined using micromorphology.

Objective 1.4: Total macro-porosity and total macro-porosity by shape, in soils contrasting in total organic carbon content, will be compared at 12.5x and 40x.

Objective 1.5: The pore size distribution of soils contrasting in total organic carbon content will be compared at 12.5x and 40x.

Objective 1.6: Porosity characteristics as proposed by both water release and image analysis methodologies will be compared?

Hypothesis 1.1: Soils with higher carbon content will have a lower bulk density.

Hypothesis 1.2: Water-aggregate stability is positively associated with total soil-organic-carbon-content.

Hypothesis 1.3: There will be a greater occurrence of strongly developed aggregates within the grassland (Wilderness) soil compared to agricultural treatments (NIL, Inorganic, FYM).

Hypothesis 1.4: Aggregates in the grassland soil will typically be granular in shape (reflecting greater biological activity).

Hypothesis 1.5: Differences in porosity characteristics between treatments will be evident at both 12.5x and 40x.

Hypothesis 1.6: Soils receiving the highest C-inputs (e.g. FYM & Wilderness) have a greater proportion of pores of biological origin, through the decomposition of organic-matter, worm-burrowing and root penetration.

Hypothesis 1.7: The pore size distribution is better at discriminating between soils contrasting in total organic carbon content than total macro-porosity.

4.2 General Chemical and Physical attributes of Broadbalk Winter-Wheat and Broadbalk Wilderness.

The results from pH and bulk density analysis are presented in **Table 4.1** for soils collected from Broadbalk Winter Wheat and Broadbalk Wilderness. The SOC for treatments are presented in **Section 3.1**.

The pH of the soil solution measured in distilled water is significantly different among treatments (Kruskal-Wallis: $H = 20.91$, $d.f = 3$, $p < 0.001$). The pH of soil solution once 0.01 M CaCl_2 is added also shows significant differences (Kruskal-Wallis: $H = 19.56$, $d.f = 3$, $p < 0.001$). For pH measured before and once KCl was added, Dunn's multiple comparisons test (**Fig. 4.1a**) reveals significant differences exist between, the Wilderness which has a significantly lower pH compared to NIL ($p < 0.001$) and FYM soil ($p = 0.021$); while NIL soil has a significantly higher pH compared to Inorganic treated soil ($p = 0.01$).

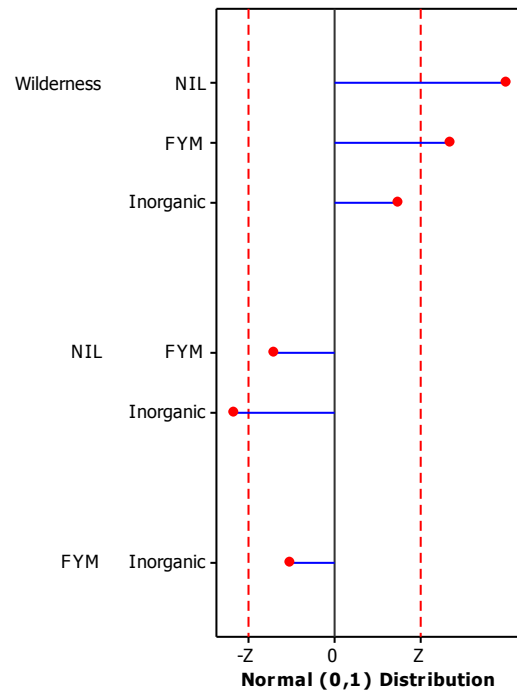
Bulk density is significantly different among treatments (Kruskal-Wallis: $H = 14.15$, $d.f = 3$, $p < 0.01$). Dunn's multiple comparisons test (**Fig. 4.1b**) specifies that the Wilderness soil has a significantly lower bulk density compared to NIL ($p < 0.01$) and FYM treated soil ($p = 0.02$). Interestingly Inorganic treated soil has a significantly higher bulk density compared to NIL ($p > 0.01$) despite no difference in LOI between these two treatments (**Chapter 5.2**). From the bulk density results a much larger confidence interval can be seen from the Wilderness and NIL compared to the FYM and Inorganic soils.

Table 4.1. General Chemical and Physical Analysis of Bulk Soil collected from Broadbalk Winter-Wheat, and Broadbalk Wilderness.

Treatment	pH (H ₂ O)	pH (CaCl ₂)	Δ pH	Bulk density (g cm ⁻³)	Total Porosity (cm ³ cm ⁻³)
Wilderness	6.4 (0.19)	7.4 (0.21)	0.9	1.40 (0.09)	0.47
FYM	7.8 (0.03)	8.4 (0.05)	0.6	1.44 (0.06)	0.46
Inorganic	7.4 (0.04)	8.12 (0.14)	0.8	1.61 (0.06)	0.39
NIL	8.2 (0.12)	8.9 (0.09)	0.7	1.57 (0.11)	0.41

Means are presented with the 95% confidence intervals (0.05) shown in parenthesis.
 Δ pH, represents the difference between pH measured in distilled water and 0.1 M KCl solution, also known as the salt effect.
 Total porosity calculated assuming dominance of quartz which has a density of 2.65 g cm⁻³

a)



b)

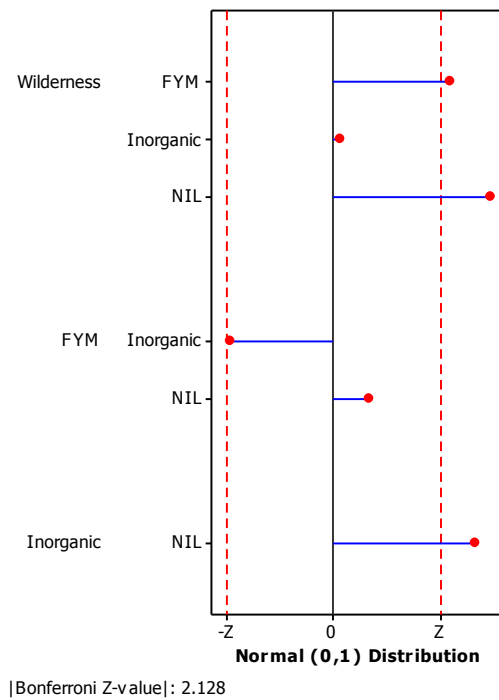


Figure 4.1: Mean rank standardised differences between all treatments, used in Dunn's nonparametric multiple comparisons test. Summarising the magnitude of the difference in, **a)** soil solution pH, and **b)** bulk density (g cm^{-3}) between all treatments. Values beyond the $-Z$ or Z point (dotted line) indicate differences between treatments that are significantly less or greater, respectively ($p < 0.05$).

4.3 Aggregate Water Stability.

Aggregate water stability results (**Fig. 4.2**) from the fast wetting treatment are significantly different among treatments (Kruskal-Wallis: $H = 12.56$, $d.f = 3$ $p < 0.05$). The pattern of aggregate stability reflects SOC-contents, with aggregate stability being greatest in soils with the highest C-content and lowest in soils containing the least amount of C. However significant differences, revealed by Dunn's multiple comparisons test, only exist between the MWD of Broadbalk Wilderness (1716.4 μm) and Broadbalk NIL (602.8 μm) ($p < 0.01$) and Inorganic (737.2 μm) ($p < 0.01$). There are no significant differences in MWD between Broadbalk Wilderness and Broadbalk FYM (932.8 μm) ($p > 0.05$) and between Inorganic and NIL soils ($p > 0.05$). There are no significant differences in MWD among any of the soils after receiving the slow wetting treatment (Kruskal-Wallis: $H = 1.76$, $d.f = 3$, $p = 0.624$). Pre-wetting results followed by mechanical disruption are inconsistent with results after fast wetting treatment, indicating that aggregate stability is greatest in soil collected from Broadbalk plot FYM with a MWD of 2533 μm and lowest in the Wilderness soil with a MWD of 2030.3 μm . Multiple comparisons reveal that the MWD of FYM is significantly higher than the MWD of soil collected from Broadbalk Wilderness ($p < 0.01$). However the MWD of Broadbalk FYM does not differ significantly from the MWD of Broadbalk Inorganic and NIL soil ($p > 0.05$), which have a MWD of 2533 μm and 2117 μm respectively. As with the fast wetting treatment, no significant differences in aggregate stability occur between Inorganic and NIL treated soil ($p > 0.05$).

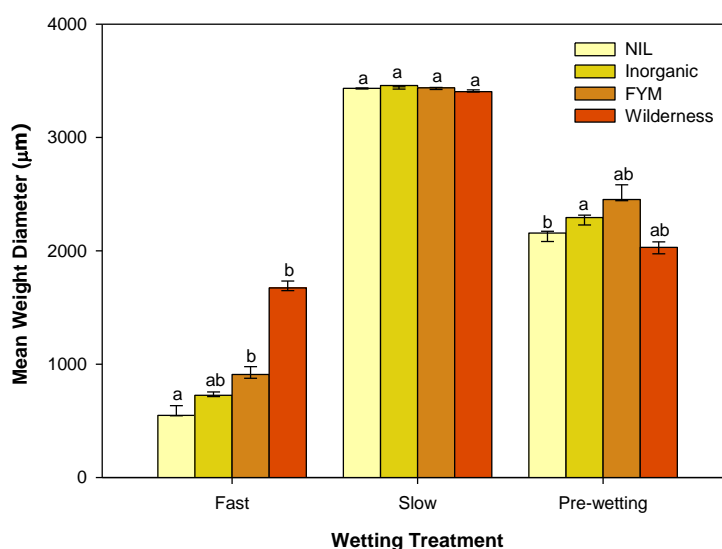
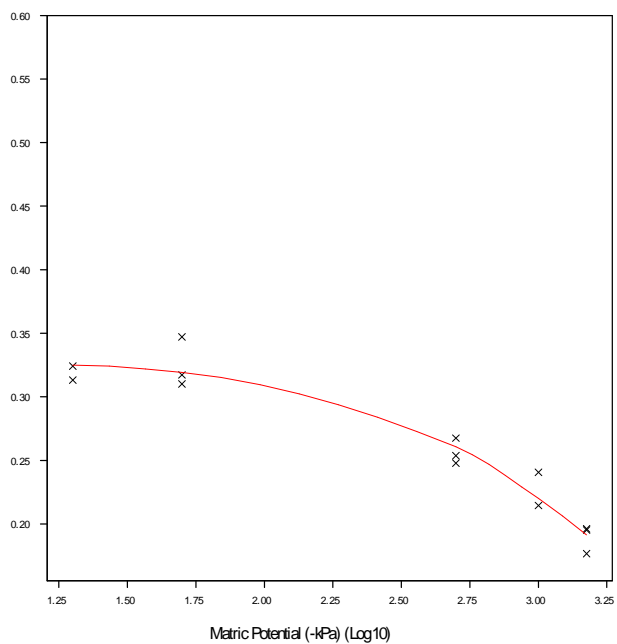


Figure. 4.2. Wetting treatment for the determination of aggregate stability (Le Bissonais, 1996), plotted against mean weight diameter (MWD) (μm). Bars represent median of MWD for soils taken from, Broadbalk Wilderness, FYM, Inorganic and NIL. Error bars represent the interquartile range. Within each wetting treatment groupings, bars with the same letter do not differ significantly from each other (kruskal-Wallis followed by Dunn's non-parametric multiple comparisons test, $p < 0.05$).

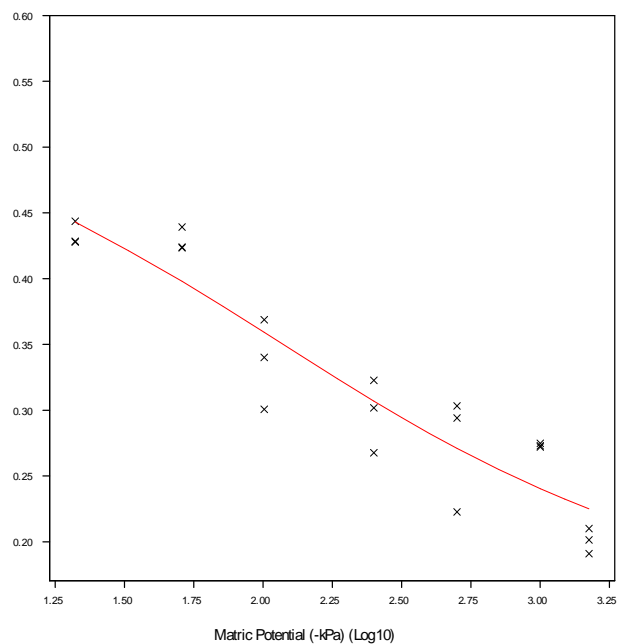
4.4 Water Release Characteristics

The water release characteristic was measured from intact soil cores removed from Broadbalk treatments, NIL, Inorganic, FYM and Wilderness in June 2009 as outlined in **Section 3.3.3**. The results were analysed in Genstat using an unbalanced ANOVA, the analysis concluded that there is a significant effect of matric potential (ANOVA: $H = 67.38$, $d.f = 6$, $p < 0.001$), and treatment upon water release (ANOVA: $H = 44.62$, $d.f = 3$, $p < 0.001$) and there is a significant interaction between treatment and matric potential (ANOVA: $H = 5.01$, $d.f = 18$, $p < 0.001$). A common logistic regression model could not be fitted to the data, however a separate model for each of the treatments explained a significant amount of the variation, thereby confirming that the soil from each of the treatments behaves differently in terms of water release (**Figure 4.3**). The slope of the curve decreases from Wilderness (-5.23), NIL (-3.582), Inorganic (-1.1876) to FYM (-1.66) soils; meaning that at a given matric potential soils with a steeper slope will release more water.

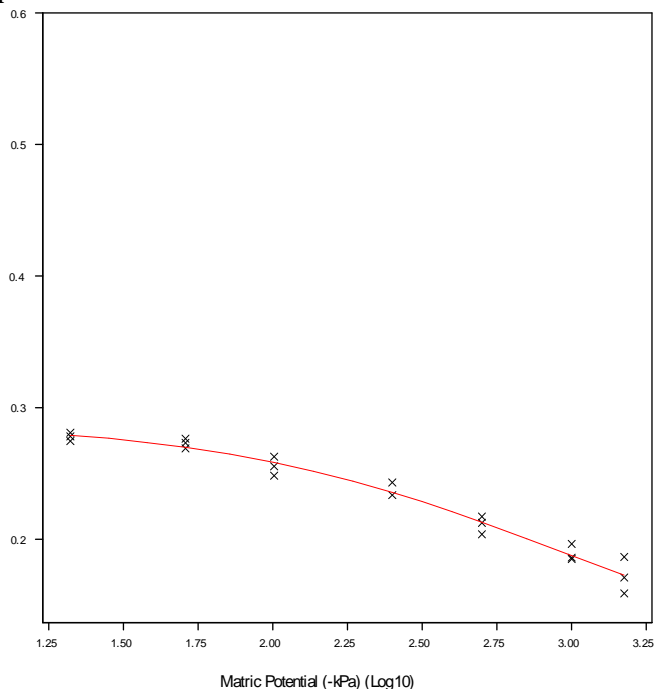
NIL



Inorganic



FYM



Wilderness

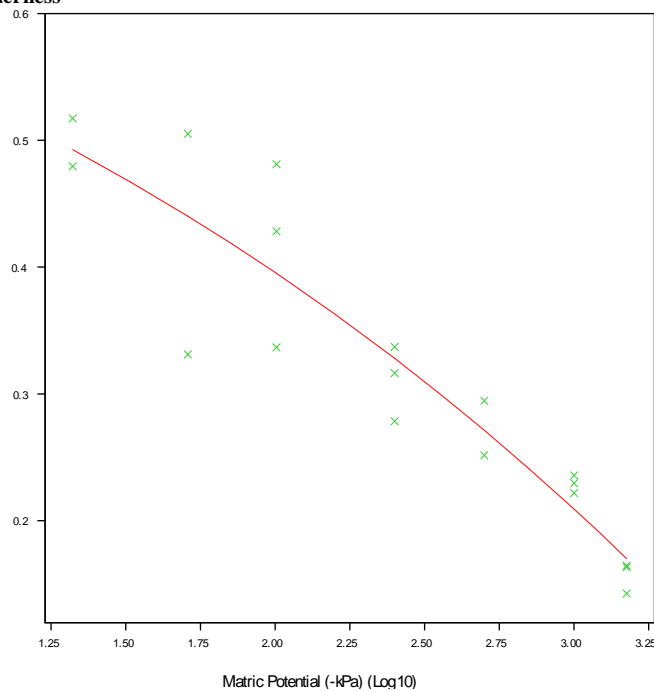


Figure 4.3: Water release curve for soil removed from Broadbalk NIL, Inorganic, FYM and Wilderness plots. Each treatment is fitted with a separate logistic curve. Percentage variance accounted for by regression: NIL, 87.5% (SE 0.017); Inorganic, 84.7% (0.033); FYM, 96.8% (0.0073); Wilderness, 83.2% (0.050). Slope of curves: NIL = -3.58; Inorganic = -1.19; FYM = -1.66; Wilderness = -5.23

4.5 Micromorphology Descriptions

This section presents the micromorphology results; descriptions were made at magnifications of 12.5x and 40x, micromorphology descriptions made at 40x were performed in conjunction with Image analysis. The results will be discussed in terms of both the overall pattern between and within treatments. Summary diagrams showing abundances for each sample can be found in **Appendix 1**.

4.5.1 Coarse and Fine Mineral Material.

There are no distinct differences in micromass (<10 µm) between treatments. Soil collected from NIL, Inorganic, FYM and the Wilderness has a brown stipple-speckled micromass. There are a couple of exceptions in samples collected from FYM treated soil, where slight differences in colour suggest a dark-stipple-speckled micro-mass. The stipple speckled term by definition indicates a micromass that consists of individual, isolated clay domains which are randomly arranged (Stoops, 2003).

The coarse mineral material was briefly investigated. Across all samples collected from NIL, Inorganic, FYM and Wilderness soil, similar proportions of calcite and quartz are present, having abundances from <5-30% in the field of view. Calcite-biospheres are also present in FYM treated soil, however their abundance is low (<5%) and infrequent across samples, being present in just 2 samples.

4.5.2 Soil Structure

This section will describe the shape and grade of aggregation (**definition: Table 1**). There is no convincing evidence of aggregation within NIL treated soil. In the rare incidence blocky or granular shaped aggregates are recognised these occur in isolated patches and therefore are not typical of NIL-treated soil. Evidence of aggregation is more frequent within inorganic than NIL soil, however consistent with other treatments, aggregation is restricted to isolated patches and is not a common attribute of Inorganic treated soil. Within FYM samples aggregation is rarely evident, when identified, aggregates are granular or sub-angular blocky in shape and moderate or weakly developed. Within Broadbalk Wilderness when evident soil aggregation is sub-angular or granular in shape and is weakly to strongly developed. In

summary, evidence of aggregation across samples from all treatments is infrequent at both 12.5x and 40 x (**Table 4.2**).

The coarse: fine (c: f) (fine material < 10µm) related distribution (**definition: Table 1**) across all thin-sections is porphyric. The relative distance between coarser units is variable within treatments, as such the c:f related distribution ranges from single-spaced to open porphyric, with no distinct patterns between treatments.

Table 4.2: Evidence of Soil Aggregation, across Broadbalk Winter-Wheat and Broadbalk Wilderness at 40x and 12.5x Magnification.

Sample	Mag.	AOI	Treatment	Aggregation	Grade
1	10		NIL	Blocky	Strong
1	40	1	NIL	x	x
1	40	2	NIL	x	x
1	40	3	NIL	x	x
2	40	1	NIL	x	x
2	40	2	NIL	x	x
2	40	3	NIL	Granular	Weak
1	40	1	Inorganic	Granular	Weak
1	40	2	Inorganic	x	x
1	40	3	Inorganic	x	x
2	40	1	Inorganic	x	x
2	40	2	Inorganic	x	x
2	40	3	Inorganic	Granular	Weak
3	40	1	Inorganic	x	x
3	40	2	Inorganic	Sub-angular	Weak
3	40	3	Inorganic	x	x
4	40	1	Inorganic	x	x
4	40	2	Inorganic	Granular	Weak
4	40	3	Inorganic	Sub-angular	Weak
1	10		FYM	sub-angularblocky	Weak
1	10	1	FYM	x	x
1	10	2	FYM	x	x
1	10	3	FYM	x	x
2	10		FYM	Granular	Weak
2	40	1	FYM	Granular	Moderate
2	40	2	FYM	Granular	Weak
2	40	3	FYM	x	x
4	40	1	FYM	Granular	Weak
4	40	2	FYM	x	x
4	40	3	FYM	x	x
5	10		FYM	sub-angular	Weak
5	40	1	FYM	x	x
5	40	2	FYM	Sub-angular	Weak
5	40	3	FYM	x	x
3	10		Wildemess	Sub-angular	Strong
3	40	1	Wildemess	x	x
3	40	2	Wildemess	x	x
3	40	3	Wildemess	x	x
4	10		Wildemess	Sub-angular	Weak
4	40	1	Wildemess	x	x
4	40	2	Wildemess	x	x
4	40	3	Wildemess	x	x
5	10		Wildemess	Sub-angular	Weak
5	40	1	Wildemess	x	x
5	40	2	Wildemess	x	x
5	40	3	Wildemess	x	x
7	20		Wildemess	Granular	Moderate
7	40	1	Wildemess	x	x
7	40	2	Wildemess	Granular	Moderate
7	40	3	Wildemess	Granular	Moderate

Only samples with evidence of aggregation at either 40X or 12.5X are presented.
X = no soil aggregation.

Porosity was recorded using both micromorphology techniques and image analysis. Unlike image analysis, micromorphology description will provide an indication of the formation processes of soil pores. Using micromorphology description pores are classed into one of the following vughs, channels, chambers or planes (**definition: Table 1**). Image analysis focuses upon quantifying shape i.e. pores are rounded, irregular or planar in shape. An additional drawback of IA, is it is unable to detect planes with a narrow throat width, therefore micromorphology is particularly useful in providing estimates in area cover for this pore shape. **Table 4.3** shows the average porosity results measured at 40x and 12.5x for each sample across all treatments.

At 40x, channels have a greater occurrence and area cover in Wilderness and FYM, than in NIL and Inorganic treatments. However, at 12.5x the abundance of channels across treatments is evenly spread. Chambers are most abundant in the Wilderness at both 40x and 12.5x, covering 5-15% of the field of view. Across all treatments the occurrence of planes is much higher at 40x than 12.5x, except for the Wilderness in which there is little difference in the abundance of planes between 40 and 12.5x, with planes typically covering <5% of the field of view. In FYM treated soil the area cover of planes at 40x is much higher than in other treatments typically within the region of 15-30%.

Table 4.3: Abundance* of Voids by Shape Across, Broadbalk Winter-Wheat and Broadbalk Wilderness at 40x and 12.5x.

Sample	Treatment	Voids 40x				Voids 10.25x			
		Vughs	Channels	Chambers	Planar	Vughs	Channels	Chambers	Planar
1	NIL	●		†	○	●	●	●	
2	NIL	○		○	●	●	○	●	
3	NIL	○		●	●	○	●	○	
4	NIL	○		○	●	○	○	○	
5	NIL	○	○			○	●	†	
1	Inorganic	●	●	●	●	●	○	○	
2	Inorganic	●		○	●	●	○	○	
3	Inorganic	○		●	○	○	○	○	
4	Inorganic	●		○	●	○	○	○	
1	FYM	○	○	○	†	○	○	●	
2	FYM	○	○	○	†	○	○	○	
3	FYM	○	○	●	●	○	○	○	
4	FYM	○	●	●	†	●	○	●	
5	FYM	○		●	†	○	○	○	
1	Wilderness	○	○	●	●	●	●	○	
2	Wilderness	○	○	●	●	○	○	○	
3	Wilderness	○	●		○	●	○	○	
4	Wilderness	●	○	●	○	○	○	○	
5	Wilderness	●		●	○	○	●	○	
6	Wilderness	○		●	○	○	○	○	
7	Wilderness	○		●	○	○	○	○	

*Abundance across field of view:
 <5 % ○; 5-15% ●; 15- 30% †

In summary soils with a lower OC-content (NIL and Inorganic) aggregation is mainly evident at 40x while soils with a higher OC-content aggregation is more frequently found at 12.5x, particularly in the Wilderness soil. At 12.5x the abundance of channels is evenly spread across treatments, while at 40x channels are largely confined to FYM and Wilderness soils. These results suggest that differences in soil structure due to OC-content have been detected; however the scale of detection is inconsistent. Furthermore, there are inconsistencies between the nature of porosity and the occurrence of aggregation recorded at the same scale. For instance in NIL and Inorganic treatments, aggregation is predominately evident at 40x, in agreement with this is a higher incidence of planes at 40x. However, where planes are most abundant at 40x, within FYM samples, this does not translate to a greater incidence of aggregation. In summary the micromorphology results show, there is no synergy between the nature of aggregation and porosity characteristics across treatments and that differences in soil structure due to OC-content are evident but at different scales. Micromorphology analysis has also detected some differences between the land-use of soils, chambers tend to be more frequent in the grassland (Wilderness) soil, while in the agricultural soil planes are more abundant, particularly at 40x. The high abundance of planes with no strong evidence of aggregation in agricultural soil could indicate that planes are often non-continuous.

4.6 Image Analysis: Porosity at 12.5x.

The image analysis results are presented below. Porosity was measured at both 12.5x and 40x magnification. A minimum detection limit was applied to image analysis (IA) (3.4.5) Therefore at 12.5x, pore area ranged from 259.2 μm^2 to 1.23 mm^2 equivalent to an ECD of 18.2 μm (1.3 \log_{10} ECD) to 1.25 mm (3.09 \log_{10} ECD). The smallest mean feret diameter (mean of minimum and maximum distance of opposite tangents) recorded is 20 μm . Therefore according to the functional classification of pores based upon pore diameter (Greenland, 1981 and Crass et al., 1993), IA at 12.5x can detect down to pores formed by fine lateral roots which function as water storage micro-pores.

4.6.1 Porosity by Treatment and Pore Shape.

Total macro-porosity (%) for each treatment is presented below (Fig. 4.4). The data are not normally distributed and transformations (including logit transformation) failed to normalise the data. Therefore a non-parametric Kruskal Wallis test is used to analyse the original data. Two runs of Kruskal-Wallis are required opposed to the single run if using ANOVA, therefore the level of significance is reduced using the Bonferroni procedure, giving a p -value of 0.03. Total median porosity is not significantly different between treatments (Kruskal Wallis: $H= 4.88$, $p = 0.181$, $d.f = 3$). Levene's test (which tests the null hypothesis that variance is equal) can be applied to data that is not normally distributed (Minitab help, "Barlett versus Levene's tests", Minitab 15), this revealed that variance among treatments is not eq

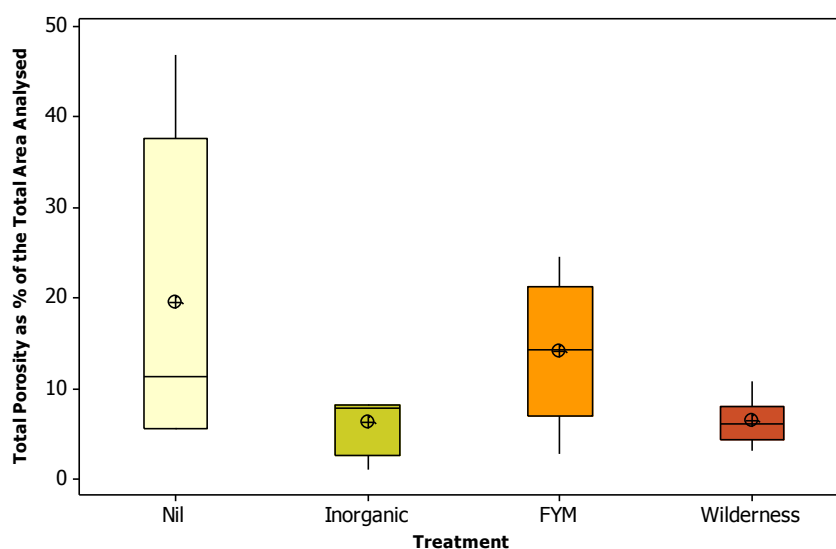


Figure 4.4. Total macro-porosity measured by image-analysis software at 12.5x as percentage of the total area analysed by IA (65 mm^2); for soils removed from Broadbalk Winter-Wheat and Broadbalk Wilderness. Symbol denotes mean porosity while the line represents the median value; the box represents the inter-quartile range. Box plots followed by the same letter are significantly different ($p < 0.05$)

Using the shape factor proposed by Horgan (1998) and subcategorised according to Bouma *et al.*, (1977) (section 3.4.7), porosity (%) was measured by first classing pores according to their shape. With planes having a shape factor of <0.2, irregular 0.2- <0.5 and rounded pores >0.5. **Figure 4.5** presents soil pores classed by shape and treatment. Significant differences were found in pore area (%) among pore shapes (Kruskal-Wallis: $H= 37.32$ $p < 0.001$, d.f= 2). Dunn's multiple comparisons test revealed that significant differences exist between all pore shapes, with the area of planes (5.9 %) being 73% and 93% greater than irregular and rounded pores and the area of irregular shaped pores (1.6 %) being 75% greater than rounded pores ($p < 0.05$). Levene's test revealed that the variance in pore area is not equal among pore shapes ($p = 0.069$). Since there is no well established non-parametric equivalent of a 2-way-ANOVA (Zar, pg 90), it is not possible to test for an interaction between treatments and pore shape, and its effect upon pore area.

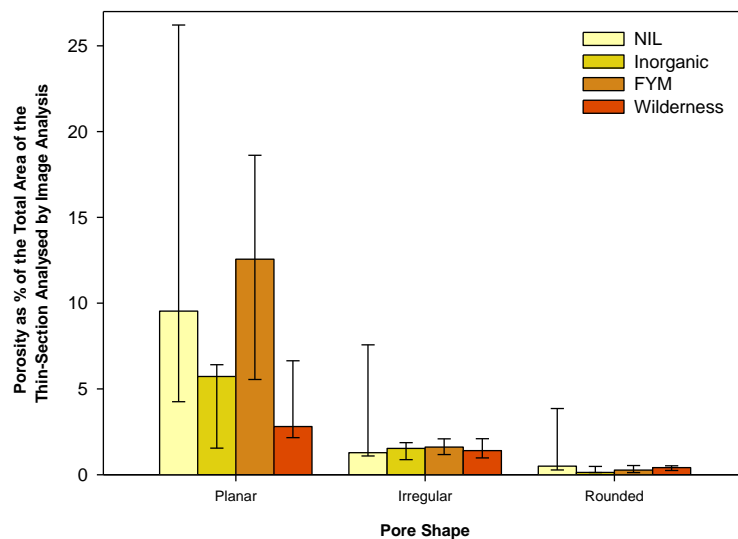


Figure. 4.5 Total macro-porosity for pores classed by shape factor according to Bouma *et al.* (1977) , measured as a percentage of the total thin-section area (65 mm²) analysed by image-analysis at 10.25 magnification. Bars represent the median value for soils removed from Broadbalk-winter-wheat and Broadbalk Wilderness; error bars represent the first and third quartile range. Shape factor ranges from <0.2 for **planar**, 0.2 <0.5 for **irregular** and > 0.5 for **rounded** pores. There is a significant difference among pore classes ($p < 0.001$), with Dun's multiple comparisons test revealing that significant differences occur between all pore classes ($p <$

4.6.2 Image Analysis: Pore Frequency by Treatment and Shape.

The frequency of pores in treatments and by shape was counted using Image analysis software (Fig. 4.6) differences in the frequency of pores by shape and treatment is analysed by Kruskal-Wallis, while Chi-square is applied to test for an association between the two factors. The original data set is not normally distributed and transformations failed to normalise the data, therefore 2 Kruskal-Wallis tests are performed using the original data, and the p -value is reduced to 0.03. The frequency of pores among treatments is significantly different (Kruskal-Wallis: $H=9.97$ $p=0.019$, d.f= 3), with the frequency of pores in the Wilderness soil being 6.6% higher than Inorganic plot (Dunn's test: $p < 0.05$). While no significant differences exist between agricultural treatments with the maximum differences in pore frequency being <33 % (Dunn's test: $p = 0.003$). The frequency of pores among pore shapes is significantly different (Kruskal-Wallis: $H= 14.39$ $p = 0.001$, d.f= 2). Dunn's multiple comparisons test revealing that significant differences exist between planes (median frequency: 45), which are 44% less frequent than irregular pores ($p = 0.0002$). While irregular pores are 26% more frequent than rounded pores ($p = 0.02$).

Chi-square test showed that there is an association between pore shape and treatment ($X^2 = 179.911$, $p > 0.001$, d.f = 6). Inspection of Chi-square values indicate that the biggest contribution comes from Irregular and rounded pores from NIL treated plots. In NIL treated soil, the occurrence of irregularly shaped pores is far less common, and the occurrence of rounded pores far more common than expected if there were no association between factors.

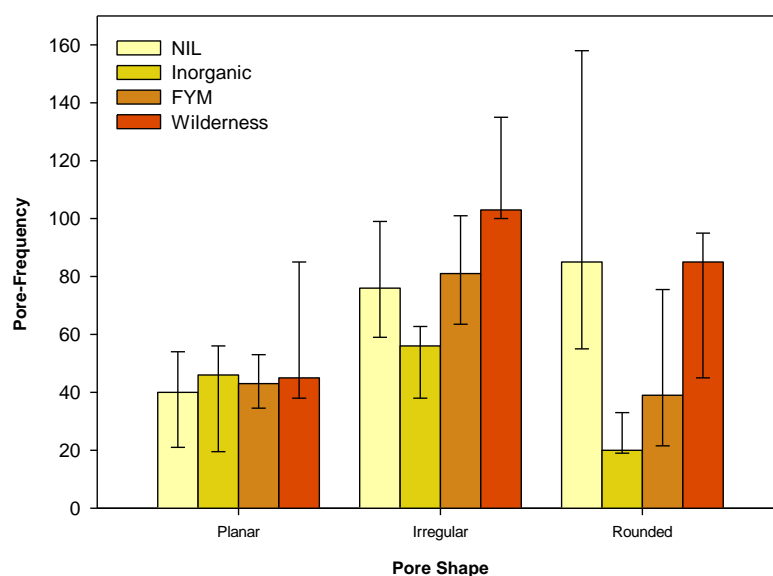


Figure 4.6. Frequency of macro-pores classed by shape factor according to Bouma *et al.* (1977) at 12.5x, for soils removed from Broadbalk-winter-wheat and Broadbalk Wilderness. Bars represent median porosity; error bars represent the first and third quartile range. Shape factor ranges <0.2 for **planar**, 0.2 < 0.5 for **irregular** and > 0.5 for **rounded** pores. Significant differences were found between treatments, ($p = 0.003$); and between pore classes ($p < 0.001$).

4.6.3 Image analysis: Porosity at 40x.

A minimum detection limit was applied to image analysis (3.4.4) Therefore at 40x, pore area ranged from $150\mu\text{m}^2$ to $1600\mu\text{m}^2$ equivalent to an ECD of $13.8\mu\text{m}$ ($1.17\log_{10}$ ECD) to 1.42mm^2 ($3.15\log_{10}$ ECD). The smallest and largest mean ferret diameter (mean of minimum and maximum distance of opposite tangents) recorded is $16.9\mu\text{m}$ and 1.28mm , respectively. Therefore, according to the functional classification of pores based upon pore diameter (Greenland & Crass et. al., 1993), IA at 40x can detect pores which, are formed by fine lateral roots (and function as water storage micropores), cracks, earthworm channels and pores formed by main plant roots (which aerate and aid rapid drainage of the soil).

Porosity (%) data from image analysis is normalised, using a logit transformation. The variability in pore area data is significantly different between treatments (Levene's test of equal variance: test statistic = 0.182, $p=0.05$), and a logit transformation helped to reduce this variance. The transformed data is analysed using a general linear model (GLM), testing for differences in macro-porosity between treatments and pore shape and testing for an interaction between treatment and pore shape. Total macro-porosity between treatments is not significantly different (GLM: $F = 1.34$, $p = 0.270$, d.f = 3). **Figure 4.7** presents the untransformed data for total macro-porosity between treatments by treatment.

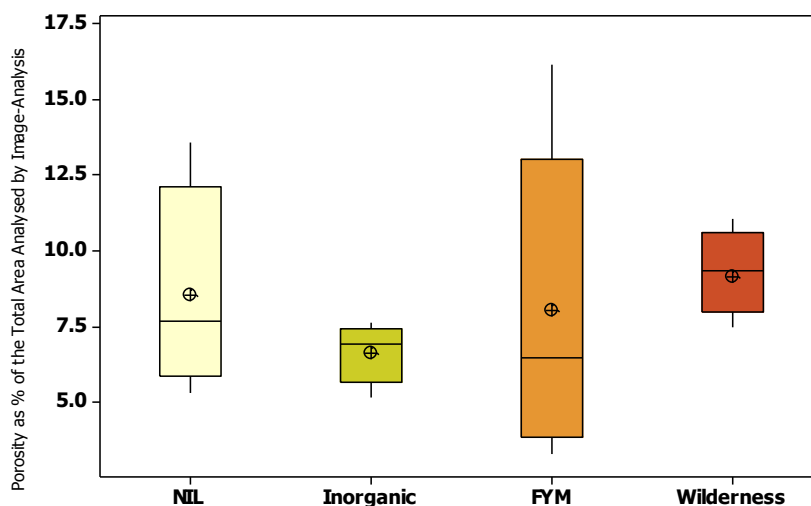


Figure. 4.7. Total macro-porosity measured by image-analysis software at 40x as percentage of the total area analysed by IA (36mm^2); for soils removed from Broadbalk-Winter wheat and Broadbalk mown-grassland. Symbol denotes mean porosity while the line represents the median value, the box represents the inter-quartile range. There is no significant difference in total porosity (logit transformed data) between treatments ($p=0.270$). A Significant difference was found in the variance of the original data between treatments (Levene's test of equal variance: $p > 0.05$).

Porosity (%) by pore class is determined by first grouping pores according to their shape. Planes have a shape factor of <0.2 , Irregular shaped pores $0.2- <0.5$ and rounded pores >0.5 . Porosity is significantly different among pore shapes (GLM: $F = 140.41$, $p < 0.001$, $d.f = 2$). Tukey multiple comparisons test revealed that significant differences occur between all pore shapes ($p < 0.001$), with the area of planes being 83% and 92% larger than irregular or rounded shaped pores, respectively (**Fig. 4.8**).

The GLM also tested for any interaction between treatment and pore shape and its effect upon pore area, thereby investigating if the effect of treatment upon pore area is different between pores having different shapes. The results showed that there is a significant interaction between treatment and pore shape (GLM: $F = 2.55$ $p = 0.031$, $d.f = 6$). Tukey multiple comparisons revealed that when pore area is grouped according to shape and treatment (**Fig. 4.8**) significant differences occur between the broad grouping of planar and irregular/rounded shaped pores ($p < 0.001$). Rounded pores from Wilderness soil are significantly smaller than irregular shaped pores from all soil treatments ($p < 0.05$). The only significant difference within the same treatment between irregular and rounded shaped occurs within the Wilderness soil, where the area of irregular shaped pores is 74% greater than rounded shaped pores ($p < 0.05$).

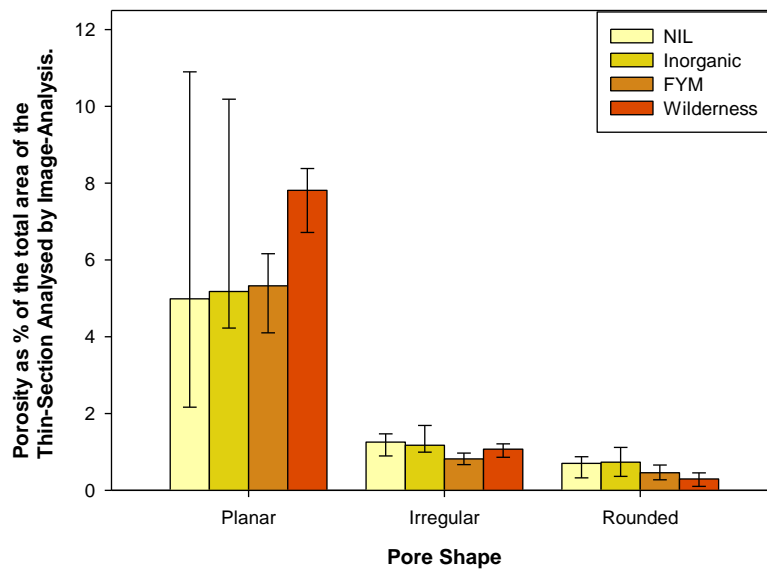


Figure 4.8. Total macro-porosity for pores classed by shape factor according to Bouma *et al.* (1977), measured as a percentage of the total thin-section area (36 mm^2) analysed by image-analysis at 40x. Bars represent the median value for soils removed from Broadbalk-winter-wheat and Broadbalk Wilderness; error bars represent the first and third quartile range. Shape factor ranges from <0.2 for **planar**, $0.2 < 0.5$ for **irregular** and > 0.5 for **rounded** pores. There is a significant difference among pore classes ($p < 0.001$) and a significant interaction between treatment*pore-shape ($p = 0.031$).

4.6.4 Image Analysis: Pore Frequency by Treatment and Shape.

Pore frequency is analysed using a GLM testing for differences in the frequency of pores between treatments and pore shape, and for the presence of an interaction between treatment and pore shape (**Fig. 4.9**). There is no significant difference in pore frequency among treatments (GLM: $F = 2.20$, $p = 0.999$, $d.f = 3$). The frequency of pores between shape classes is significantly different (GLM: $F = 21.01$, $p < 0.001$, $d.f = 2$), the frequency of irregular and rounded shaped pores is more than double that of planes ($p < 0.001$), there is no difference in the frequency of irregular or rounded shaped pores ($p > 0.05$). The results from GLM also indicate that there is no significant interaction between treatment and pore shape (GLM: $F = 0.72$, $p = 0.637$, $d.f = 6$). However, When randomly selecting 4 slides from each treatment, Chi-square test showed that there is an association between pore shape and treatment ($X^2 = 245.232$, $p > 0.001$, $d.f = 6$). Inspection of the chi-square values indicate that the biggest contributions come from planar and rounded pores from the Wilderness soil. The occurrence of planes in Wilderness soil are far more common and the occurrence of rounded pores far less common than expected if there was no association between factors.

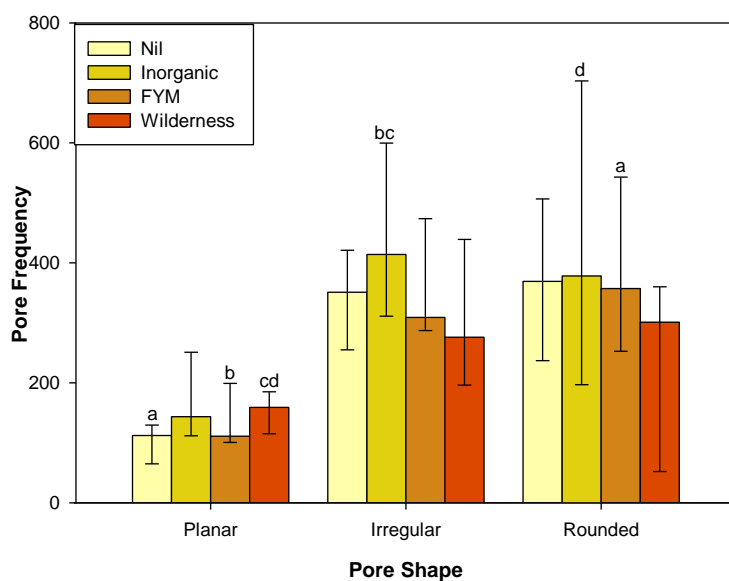


Figure 4.9 Frequency of macro-pores classed by shape factor according to Bouma *et al.* (1977) at 40x magnification. Bars represent the mean value for soils removed from Broadbalk winter-wheat and Broadbalk Wilderness; error bars represent the 95% confidence intervals. Shape factor ranges < 0.2 for **planar**, $0.2 < 0.5$ for **irregular** and > 0.5 for **rounded** pores. No Significant differences were found among treatments, ($p = 0.999$); significant differences are found between pore classes ($p < 0.001$) There is no significant interaction between Treatment*Pore shape ($p = 0.637$). Plots followed by the same letter are significantly different (Tukey multiple comparison test $p < 0.05$).

4.7 Image Analysis: Comparison of Porosity Characteristics between 12.5x and 40x.

Image analysis for the measurement of porosity was performed at both 12.5x and 40x magnification in order to assess whether scale dependent differences exist. The following section will compare the results from analysis performed at 12.5x and 40x.

The analysis revealed that there is no significant difference in total macro-porosity by treatment at either 12.5x or 40x. Furthermore at both 12.5x and 40x, the data are not equally distributed with porosity being highly variable across NIL and FYM plots. Porosity by pore shape follows a consistent pattern at both 12.5x and 40x, with area cover being significantly different between all pore shapes, area decreases from planes, irregular to rounded shapes. At both 12.5x and 40x the total area of planes is more variable between treatments compared to irregular or rounded shaped pores. Porosity at 40x could be normalised by logit transformation, therefore a GLM could be applied. The GLM found a significant interaction between shape and treatment. However few differences were found in total area when classed by treatment and shape.

Pore frequency by treatment is not significantly different at 40x. However at 12.5x pore frequency is significantly different between Wilderness and Inorganic soil, there are no significant differences in pore frequency between agricultural treatments. Pore frequency by shape is significantly different between all shapes at 12.5x; at 40x there is no significant difference between the frequency of irregular and rounded pores. Chi square analysis concluded that there is an interaction between treatment and shape in determining pore frequency at both 40x and 12.5x.

4.8 Image Analysis: Pore Size Distribution.

The pore size distribution is determined for Broadbalk Winter-Wheat and Broadbalk Wilderness soils using the data gathered by image analysis. This is to investigate if more gradual differences in porosity are detected between soils contrasting in total OC-content, which would otherwise be overlooked if simply total porosities are assessed.

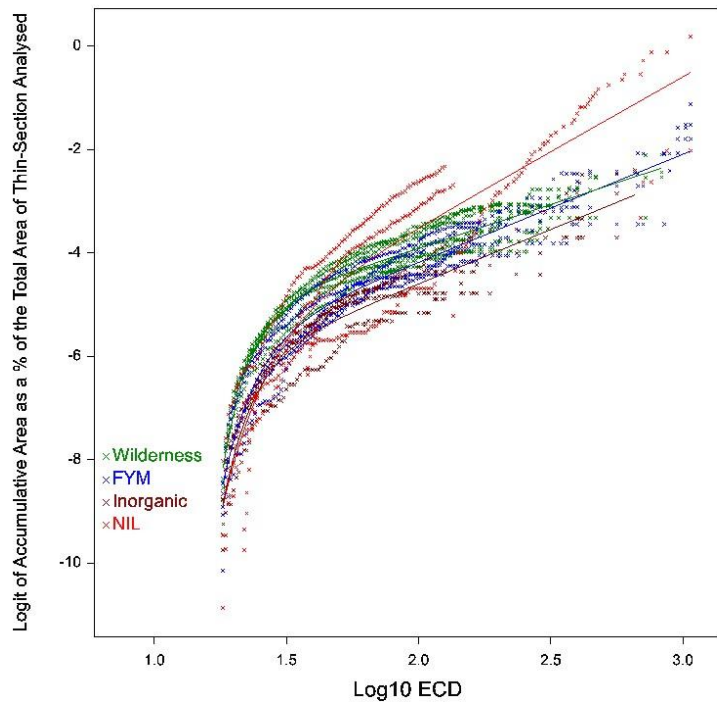
4.8.1 Image Analysis: Pore Size Distribution at 12.5x

Presented in **Figures 4.10 a-b**, is the pore size distribution for each treatment categorised by equivalent circular diameter (ECD) (i.e. the diameter of a circle with the same area as the pore). ECD has been logged to the base of 10 and accumulative area calculated as a percentage of the total area of thin-section analysed. Accumulative area is logit transformed and non linear regression applied to help describe the differences between treatments. A linear + exponential curve is fitted, the analysis revealed that a common curve cannot be fitted to all the treatments, however separate linear + exponential curves by treatment explained 90.9% of the variance. The steepness of the curve between treatments decreases from: NIL (2.90), Inorganic (2.10), FYM (2.08) to Wilderness (1.69).

By calculating accumulative pore area the pore size distribution is analogous to water release curves (**Section 4.4**). Accumulative porosity was calculated for each slide to account for within treatment variability. The effect of slide was not included in the model, due to complications arising from having a different number of slides per treatment, however the effect of slides is minimal as the model explained 90.9% of the variance in the data. Furthermore the curve is fitted to help explain differences in pore size distributions between treatments and is not used to make predictions about pore size.

The fitting of a linear + exponential curve demonstrates that at 12.5x the pore size distribution is bimodal, which suggests that separate processes are occurring to produce smaller and larger sized pores. At 12.5x NIL treated soil has the steepest curve thereby indicating that it has the largest sized pores. while the Wilderness soil has the shallowest slope therefore the maximum pore area is smallest in the Wilderness soil.

a)



b)

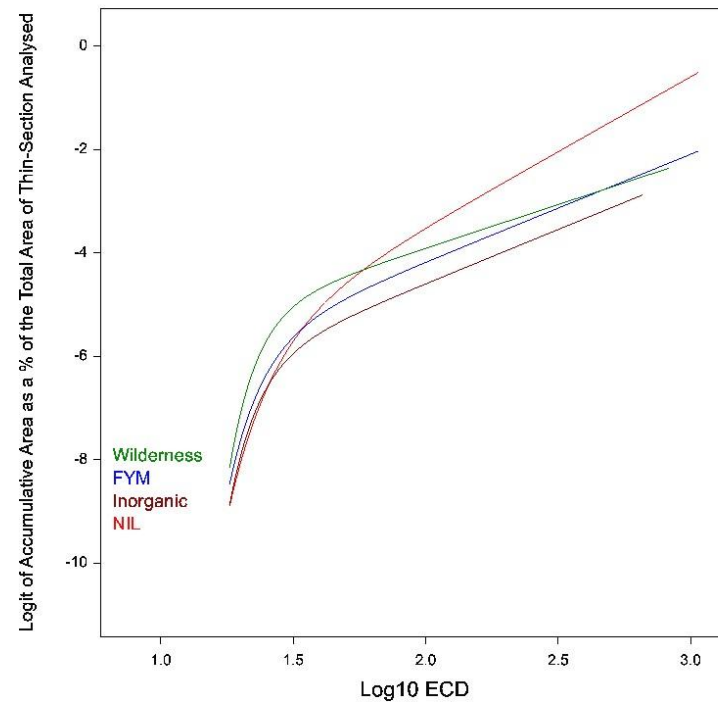


Figure 4.10: The pore size distribution for Broadbalk treatments NIL, Inorganic, FYM and Broadbalk Wilderness at **12.5x**. **a)** shows the observed and fitted curve, for each treatment. For clarity **b)** shows the fitted curve for each treatment, without the observed values. A linear + logistic curve was fitted and accounts for 90.9% of the variation in the data. The steepness of the curve between treatments decreases from: NIL (2.90), Inorganic (2.10), FYM (2.08) to Wilderness (1.69).

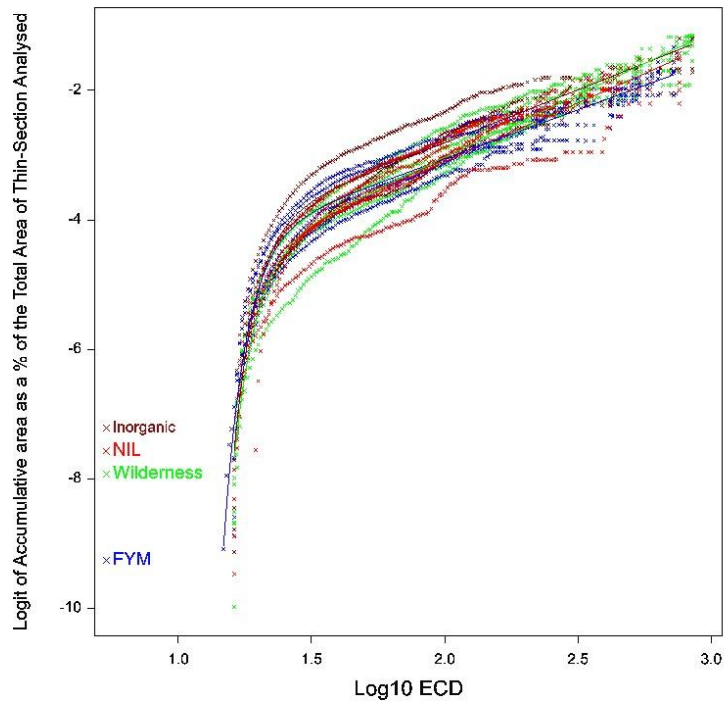
4.8.2 Image Analysis: Pore Size Distribution at 40x

Presented in **Figures 4.11 a-b**, is the pore size distribution for each treatment categorised by equivalent circular diameter (ECD) (i.e. the diameter of a circle with the same area as the pore). ECD has been logged to the base of 10 and accumulative pore area for each slide calculated as a percentage of the total area of thin-section analysed. Accumulative area is logit transformed and non linear regression applied to help describe the differences between treatments. A linear + exponential curve is fitted, the model took into account treatment but not slide effects. The analysis revealed that a common shape parameter can be fitted to all the treatments ($R = 0.96$), however separate linear and curve parameters were required for each treatment, in doing so the linear + exponential curves by treatment explained 93.3% of the variance. The steepness of the curve between treatments decreases from: Wilderness (1.93), Nil (1.82), Inorganic (1.64) to FYM (1.51).

As for 12.5x, the effect of slide was not included in the model, due to complications arising from having a different number of slides per treatment, however the effect of slides is minimal as the model explained 93.3% of the variance in the data. As intended for the analysis conducted at 12.5x the fitted curve is used to describe differences between treatments and not to make predictions about pore size.

The fitting of a linear + exponential curve demonstrates that at 40x the pore size distribution is bimodal, which suggests that separate processes are occurring to produce smaller and larger sized pores. In brief at 40x the Wilderness soil has the steepest slope therefore between the treatments this soil has the largest sized pores, while FYM soil has the shallowest slope therefore the maximum pore area is smallest in this treatment.

a)



b)

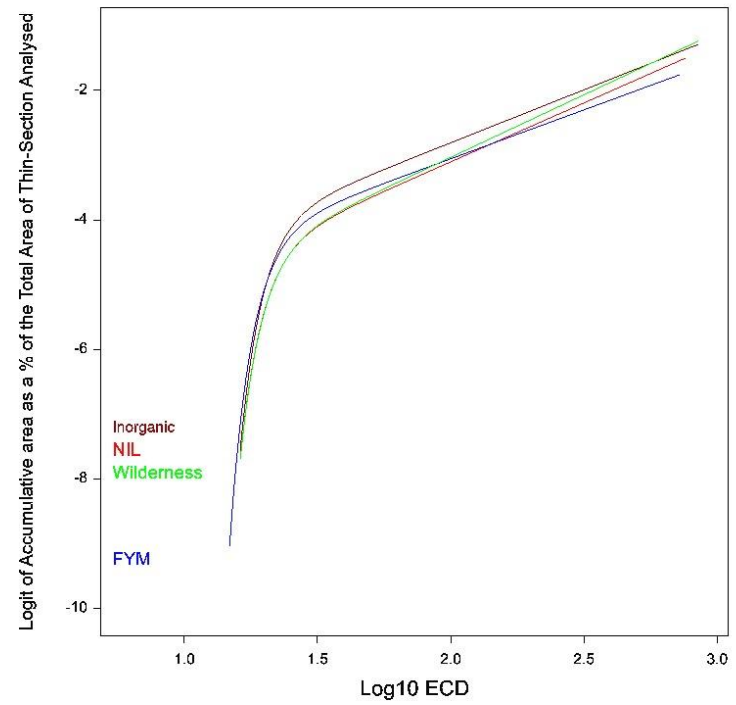


Figure 4.11: The pore size distribution for Broadbalk treatments NIL, Inorganic, FYM and Broadbalk Wilderness at 40x. **a)** shows the observed and fitted curve, for each treatment. For clarity **b)** shows the fitted curve for each treatment, without the observed values. A linear + logistic curve was fitted and accounts for 93.3% of the variation in the data. The steepness of the curve between treatments decreases from: Wilderness (1.93), Nil (1.82), Inorganic (1.64) to FYM (1.51).

4.8.3 Image Analysis: Comparison of Pore Size Distribution at 12.5x and 40x.

At both 12.5x and 40x the pore size distributions of the Broadbalk treatments are different. There are some similarities between the treatments at 40x as the same shape parameter can be fitted to all the curves. The relative differences between treatments also varies at 12.5x and 40x, indicating that there is no consistent pattern in pore size distribution between treatments at different scales. However linear + exponential curves could be fitted at both 12.5 and 40x and accounted for >90% of the variation in data, which suggests that at both magnifications, for all treatments, separate processes are occurring to produce smaller and larger sized pores.

4.9 Summary of Results

Presented below is the summary of results each of which will be discussed in chapter 6.

4.9.1 Bulk Analysis

- The Wilderness soil has a significantly lower bulk density compared to NIL and FYM treated soil.
- Interestingly Inorganic treated soil has a significantly higher bulk density compared to NIL despite no difference in LOI between these two treatments (**Section 5.2**).

4.9.2 Aggregate Water Stability

- Aggregate water stability results from the fast wetting treatment are significantly different among treatments. The pattern of aggregate stability reflects SOC-contents, with aggregate stability being greatest in soils with the highest C-content and lowest in soils containing the least amount of C.
- Significant differences, only exist between the MWD of Broadbalk Wilderness and Broadbalk NIL and Inorganic.
- There are no significant differences in MWD between Broadbalk Wilderness and Broadbalk FYM and between Inorganic and NIL soils.
- There are no significant differences in MWD among any of the soils after receiving the slow wetting treatment.
- Pre-wetting results followed by mechanical disruption are inconsistent with results after fast wetting treatment, indicating that aggregate stability is greatest in soil collected from Broadbalk plot FYM and lowest in the Wilderness soil.
- The MWD of FYM is significantly higher than the MWD of soil collected from Broadbalk Wilderness.
- After the pre-wetting treatment there are no significant differences in MWD between agricultural treated soils.

4.9.3 Water Release Characteristics

- The water release characteristic results concluded that there is a significant effect of matric potential and treatment upon water release and there is a significant interaction between treatment and matric potential.
- A common logistic regression model could not be fitted to the data, however a separate model for each of the treatments explained a significant amount of the variation, thereby confirming that the soil from each of the treatments behaves differently in terms of water release.
- The slope of the curve decreases from Wilderness (-5.23), NIL (-3.582), Inorganic (-1.1876) to FYM (-1.66) soils; meaning that at a given matric potential soils with a steeper slope will release more water.
- A less negative matric potential will be required to drain the largest pores within the Wilderness and NIL, compared to Inorganic and FYM soils.

4.9.4 Describing Soil Structure

- There are no distinct differences in micromass (<10 μm) between treatments. Soil collected from NIL, Inorganic, FYM and the Wilderness has a brown stipple-speckled micromass.
- The coarse mineral material was briefly investigated. Across all samples collected from NIL, Inorganic, FYM and Wilderness soil, similar proportions of calcite and quartz are present.
- In soils with a lower OC-content (NIL and Inorganic) aggregation is mainly evident at 40x while soils with a higher OC-content aggregation is more frequently found at 12.5x, particularly in the Wilderness soil.
- At 12.5x the abundance of channels is evenly spread across treatments, while at 40x channels are largely confined to FYM and Wilderness soils.
- These results suggest that differences in soil structure due to OC-content have been detected; however the scale of detection is inconsistent.
- There are inconsistencies between the nature of porosity and the occurrence of aggregation recorded at the same scale.

- Micromorphology results show, there is no synergy between the nature of aggregation and porosity characteristics across treatments and that differences in soil structure due to OC-content are evident but at different scales.
- Differences between the land-use of soils were detected, chambers tend to be more frequent in the grassland (Wilderness) soil, while in the agricultural soil planes are more abundant, particularly at 40x.

4.9.5 Image Analysis of Soil Porosity

- The analysis revealed that there is no significant difference in total macro-porosity by treatment at either 12.5x or 40x.
- At both 12.5x and 40x, the data are not equally distributed with porosity being highly variable across NIL and FYM plots.
- Porosity by pore shape follows a consistent pattern at both 12.5x and 40x, with area cover being significantly different between all pore shapes, area decreases from planes, irregular to rounded shapes.
- At both 12.5x and 40x the total area of planes is more variable between treatments compared to irregular or rounded shaped pores.
- Pore frequency by treatment is not significantly different at 40x.
- At 12.5x pore frequency is significantly different between Wilderness and Inorganic soil, there are no significant differences in pore frequency between agricultural treatments.
- Pore frequency by shape is significantly different between all shapes at 12.5x; at 40x there is no significant difference between the frequency of irregular and rounded pores.
- Chi square analysis concluded that there is an interaction between treatment and shape in determining pore frequency at both 40x and 12.5x.

4.9.6 Image Analysis: Pore Size Distributions

- At both 12.5x and 40x the pore size distributions of the Broadbalk treatments are different.

- There are some similarities between the treatments at 40x as the same shape parameter can be fitted to all the curves.
- Linear + exponential curves could be fitted at both 12.5 and 40x and accounted for >90% of the variation in data, which suggests that at both magnifications, for all treatments, separate processes are occurring to produce smaller and larger sized pores.

Chapter 5: The Distribution and Significance of Organic Matter and Organic Carbon, in Broadbalk Soils.

Section 5.1 recaps the main study's aims and introduces the specific objectives and hypotheses that will be tested in this chapter. The results are presented from the analysis of organic matter and organic carbon in soil sampled from Broadbalk-winter-wheat treatments: NIL, Inorganic and FYM and Wilderness (full details of treatments can be found in **Table 3.1** the chapter concludes with a discussion where the findings will be examined.

5.1. Specific Objectives and Hypotheses

Aim 2: To determine the occurrence within the soil structure and nature of organic matter and its associated organic carbon in and between soils contrasting in total organic-carbon content.

Objective 2.1: Organic matter frequency, form and extent of decomposition will be determined, comparisons will be made between soils contrasting in total organic-carbon content.

Hypothesis 2.1: The volume of organic-matter is positively associated with total soil-organic-carbon content (3.1.1)

Objective 2.2: The occurrence of excremental pedofeatures within soils will be assessed.

Hypothesis 2.2a: The occurrence of excremental pedofeatures will be greater in soils with a higher OC-content

Hypothesis 2.2b: A greater variety of excremental pedofeatures will be associated with the Wilderness soil compared to soils from Broadbalk Winter-Wheat.

Objective 2.3: The location of organic-matter (of varying form and decomposition) within thin-sections will be identified.

Hypothesis 2.3: Organic-matter fragments of varying form and decomposition differ in their distribution in relation to soil structural features, with more decomposed organic matter being located away from soil pores.

Objective 2.4: The distribution of organic-carbon (associated with organic matter) will be assessed and soils contrasting in total organic-carbon content are compared.

Hypothesis 2.4a: Classes of organic-matter classified using micromorphology have a distinct O: C ratios.

Hypothesis 2.4b: A Higher amount of elemental C will be associated with organic matter fragments.

Hypothesis 2.4c: Features classified using micromorphology will have a distinct elemental signature.

Hypothesis 2.4d: A gradient in elemental C exists, with the concentration of C decreasing with increasing distance away from organic-matter and BC fragments. In addition the gradient in elemental C will be steeper in soils with a lower total C-content (NIL & Inorganic) compared with soils with a higher total C-content (FYM & Wilderness).

Objective 2.6: Elemental distributions will be mapped within areas of interest, previously analysed by micromorphological and image-analysis methods.

Hypothesis 2.6: Features previously classified using micromorphological classification, can be identified using the relative concentration of C:O:Si.

Objective 2.5: The location of organic-carbon (associated with organic matter) in relation to soil structural features will be identified.

Hypothesis 2.5: A gradient in elemental C exists, with the concentration of C decreasing with increasing distance away from soil pores.

5.2 Total Organic Matter Content

The percentage LOI, which acts as a proxy for organic matter content (3.2.2), is significantly different among treatments (Kruskal-wallis: $H = 78.57$, $d.f = 3$, $p = 0.001$). The amount of SOM, is in accordance with the total OC-content previously determined (3.1.1), with the organic matter content in the grassland soil being twice as great compared to the NIL soil. Dunn's multiple comparisons test (Fig. 5.1) revealed significant differences between the LOI of the wilderness with NIL ($p < 0.001$) and Inorganic soil ($p < 0.002$), while no significant differences exist between the Wilderness and the FYM treated soils ($p > 0.05$). Significant differences in LOI occur between NIL and FYM soils ($p = 0.013$), however there is no difference between NIL and Inorganic soils ($p > 0.05$).

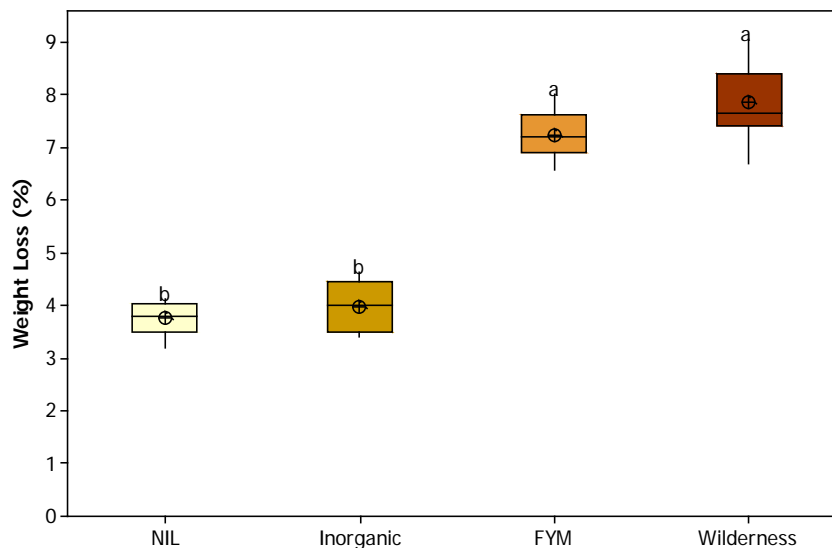


Figure 5.1 Loss on ignition as a proxy for organic matter content. Boxes represent the interquartile range, lines represent the median value, and the symbol denotes the mean value for soils removed from Broadbalk-winter-wheat and Broadbalk mown-grassland. Plots followed by the same letter are not significantly different ($p = 0.05$)

5.3 Micromorphology: Pedofeatures

This section presents the micromorphology results (3.4.4), which were made at 12.5x and at 40x; micromorphology descriptions at 40x were performed in conjunction with image analysis. The results will be discussed in terms of both the overall pattern between and within treatments. Summary diagrams showing abundances for each sample can be found in **Appendix 1**

Excremental pedofeatures (**definition: Table 1**) can be seen across all treatments, but are more consistently found in samples from FYM and Wilderness soils (Table 4.2). Typically, spheroid and cylindrical forms are present and within sample abundance is <5-15% across all treatments. Soils with the highest OC-content (FYM and Wilderness) have a greater variety in the types of pedofeatures, with mammilated forms also being present in low abundance (<5%). Within FYM and NIL soils, disintegration of excremental (**definition: Table 1**) pedofeatures is largely moderate to strong and excrement is frequently situated within pores or near to OM. In the Inorganic treated soil, excremental pedofeatures are found in just two samples, and at low abundance (<15%), in the form of dense microaggregates (**coalescence definition: table 1**) and located within pores or associated with OM. Within the Wilderness soil excremental pedofeatures are highly disintegrated and are commonly located in the soil matrix or in pores; they are often found in association with amorphous-yellow-OM.

Manganese/iron oxide nodules (**definition: Table 1**) are frequently present in samples across all treatments. Within sample abundance varies between soils. In samples from NIL and Inorganic soil, abundance is more variable ranging from <5-30%, while in samples from FYM and wilderness, abundance is <5% and <5-15%, respectively.

Fe coatings, hypo-coatings and/or quasi-coatings (**definition: Table 1**) were identified across all NIL samples. The abundance of coatings and hypo-coatings within NIL samples is <5%, while the abundance of quasi-coatings ranged from <5% up to 30-50%. Clay coatings are present within NIL samples, however these are rare. Within Inorganic treated soil, both Fe and clay coatings are consistently found across all samples; abundance is low, typically between <5 -15%.

Clay and Iron coatings are common in FYM samples, with coatings and hypo-coatings being the most frequent forms and their abundance can be up to 15-30%, however abundances of <5% are more typical. In the Wilderness samples some form of coating is consistently present, mainly being composed of clay or Fe which occur as coatings, hypo-coatings or quasi-coatings; within sample abundance is typically between <5 -10%, but in some cases can be up to 35%.

Table 5.1: The Abundance of Excremental Pedofeatures, Across all Treatments.

Sample	AOI	Treatment	Mammilate	Location	Coalescence	Cylindrical	Location	Coalescence	Spheroid	Location	Coalescence
2	1	NIL									
2	2	NIL							○	OM	3
2	3	NIL									
4	1	NIL							○	OM+P	2
4	2	NIL									
4	3	NIL									
5	1	NIL									
5	2	NIL							†	P	2
5	3	NIL									
1	1	Inorganic							○	P	3
1	2	Inorganic									
1	3	Inorganic									
3	1	Inorganic							●	OM+P	1+3
3	2	Inorganic									
3	3	Inorganic									
1	1	FYM							○	P	3
1	2	FYM									
1	3	FYM									
2	1	FYM									
2	2	FYM							○	M	2
2	3	FYM									
3	1	FYM									
3	2	FYM							●	P	2
3	3	FYM							○	M	2
4	1	FYM	○	M	1+2				○	M	1+2
4	2	FYM	○	P	2				●	OM	2
4	3	FYM							○	P	1
5	1	FYM									
5	2	FYM	○	P	2	○	OM	2			
5	3	FYM									
1	1	Wilderness				●	OM*	3			
1	2	Wilderness	○	M	3						
1	3	Wilderness							○	M	3
2	1	Wilderness									
2	2	Wilderness									
2	3	Wilderness				○	M	3	○	M	3
3	1	Wilderness							○	P+M	3
3	2	Wilderness	○	M	3	○	M	3			
3	3	Wilderness									
4	1	Wilderness									
4	2	Wilderness	○	M	3	○	M	3			
4	3	Wilderness									
6	1	Wilderness									
6	2	Wilderness							●	OM*	2
6	3	Wilderness							○	OM*	2
7	1	Wilderness							●	P	3
7	2	Wilderness									
7	3	Wilderness									

Pore location: P = pore; M = Matrix; OM = Organic Matter; OM* = Amorphous Yellow.

Coalescence: 1 = very porous microaggregates; 2 = porous microaggregates; 3 = dense microaggregates.

Only samples containing Excrements are displayed.

5.4 Image Analysis: Total Organic Matter at 40x.

The data for organic matter area (%), measured by image analysis is presented in **Figure 5.2**. The data are not normally distributed and transformations (including logit transformation) failed to normalise the data. Therefore, the non parametric Kruskal Wallis test is used to analyse the original non-transformed OM-area (%) data. Since 2 Kruskal Wallis tests are required the p -value is reduced using the Bonferroni method, giving a p -value of 0.03.

There is no significant difference in the total area of organic matter among treatments (Kruskal Wallis: $H = 2.27$, $p = 0.519$, $d.f = 3$). Levene's test for equal variances indicates that the variance in organic matter area is not equal between treatments (Levene's: test statistic = 0.93, $p = 0.423$), with the percentage area of organic matter area being most variable from FYM-treated soil.

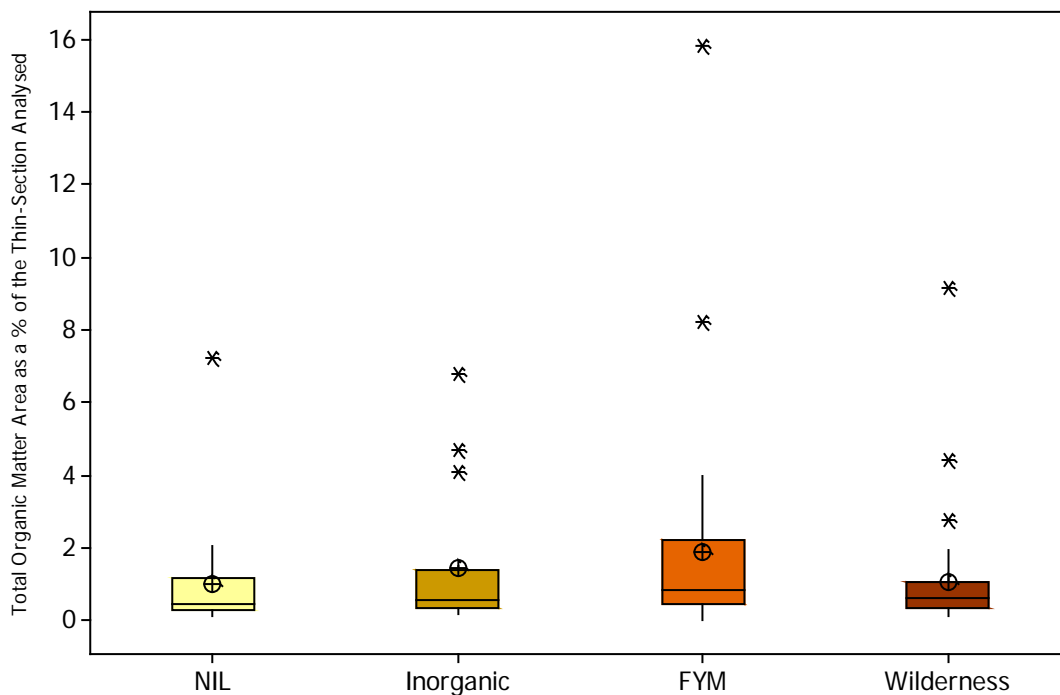


Figure 5.2 Total area cover of organic matter at 40x. Boxes represent the interquartile range, lines represent the median value, and the symbol denotes the mean value for soils removed from Broadbalk-winter-wheat and Broadbalk mown-grassland. No significant differences were found in the area of organic matter fragments between treatments ($p = 0.614$)

5.4.1 Image Analysis: Organic Matter by Form and Decomposition.

Organic matter fragments were classed according to their form and extent of decomposition (3.4.6), and image analysis was used to calculate the area cover (%) of fragments (Figure 5.4). There are no significant differences in area cover among organic matter classes (Kruskal Wallis: $H = 12.52$, $p = 0.085$, $d.f = 7$) (Fig. 5.3).

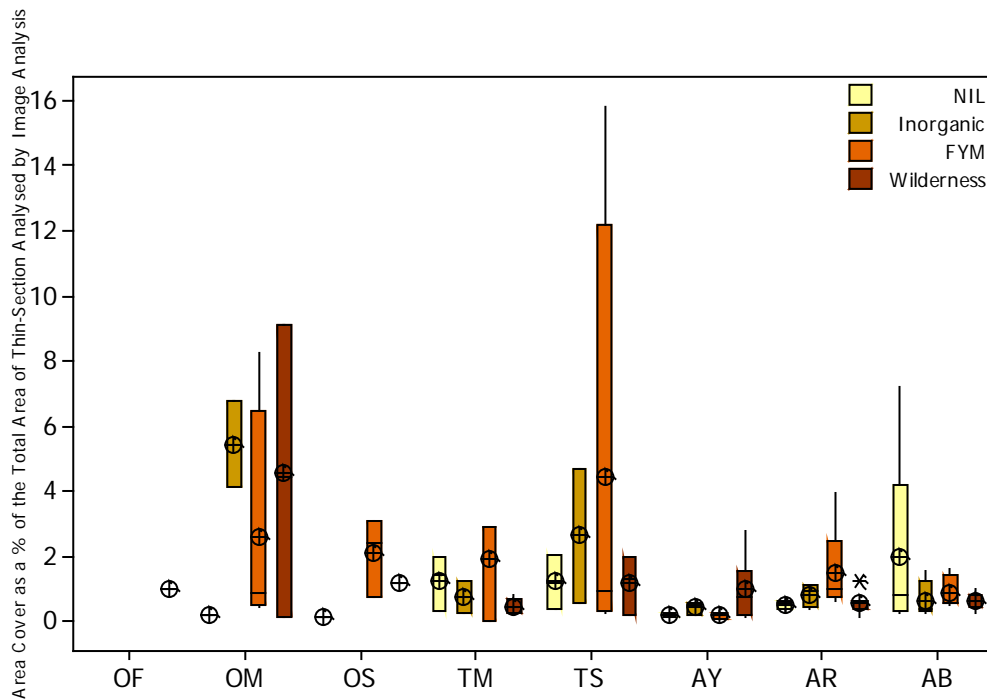


Figure 5.3. Area cover of organic matter classed according to form and extent of decomposition at 40x magnification. Bars represent the median value for soils removed from Broadbalk-winter-wheat and Broadbalk Wilderness; error bars represent the interquartile range. No significant differences were found between organic matter classes ($p = 0.087$) Organic matter classes are coded as follows: OF = Organ-Fresh, OM = Organ-Moderate, OS = Organ-Strong, TM = Tissue-Moderate, TS = Tissue-Strong, AY = Amorphous Yellow, AR = Amorphous Red, AB = Amorphous Black.

The frequency of organic matter was also analysed by image-analysis. The frequency data are not normally distributed, and could not be normalised by transformation, therefore, the original data were analysed using the non-parametric test Kruskal Wallis. Since two Kruskal Wallis tests are required, the p -value is reduced using the Bonferroni method, giving a p -value of 0.03. There is no significant difference in the frequency of organic matter among treatments (Kruskal Wallis: $H = 0.60$, $p = 0.897$, $d.f = 3$). The frequency of organic matter among OM-classes (Fig. 5.5) is significantly different (Kruskal Wallis: $H = 82.88$, $p < 0.001$, $d.f = 7$). Across all treatments black and red amorphous OM-

forms are significantly more frequent than either organ and tissue forms (**Fig. 5.6**). Within the amorphous class, black and red forms (93% and 82%) are more frequent than amorphous yellow (median area cover = 7%). The area of amorphous forms is very small covering < 5% of the slide analysed, therefore amorphous organic matter occur as numerous but small fragments.

Since there is no well established non-parametric equivalent of a 2-way-ANOVA, it is not possible to test for an interaction between treatment and organic matter class, and its effect upon organic matter frequency.

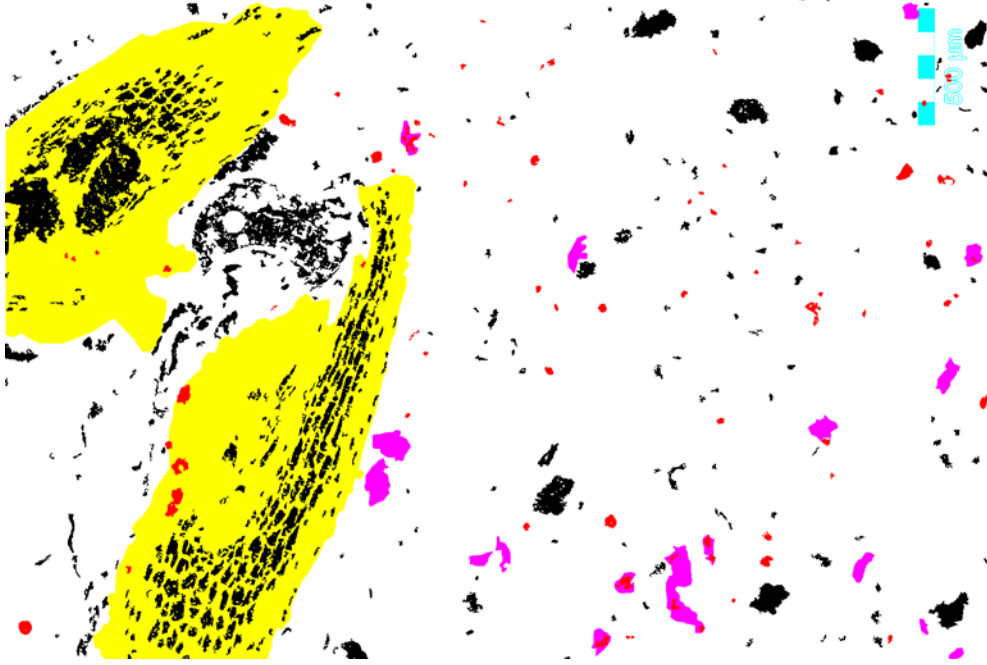
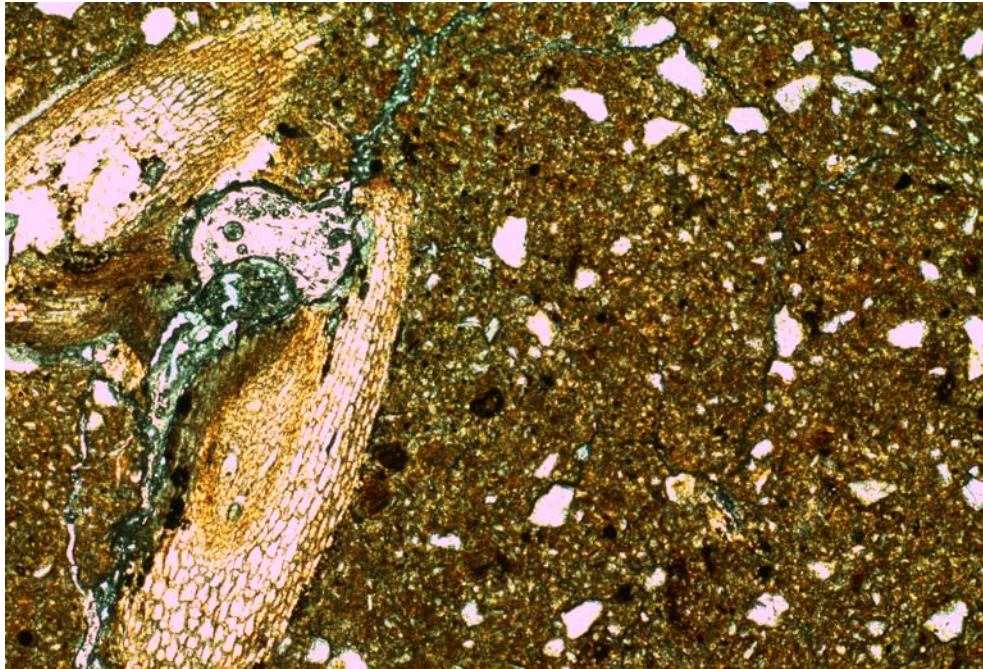


Figure 5.4: Image of an Area of interest (AOI) of a thin-section removed from Inorganic plots of Broadbalk Winter-Wheat, in Plane polarised light (PPL) (left) and as an organic-matter pore map (right). Within the OM-pore map Pixels are colour coded White = soil matrix, Black = pore, red = Amorphous black, pink = Amorphous red, Yellow =Organ Moderately-decomposed.

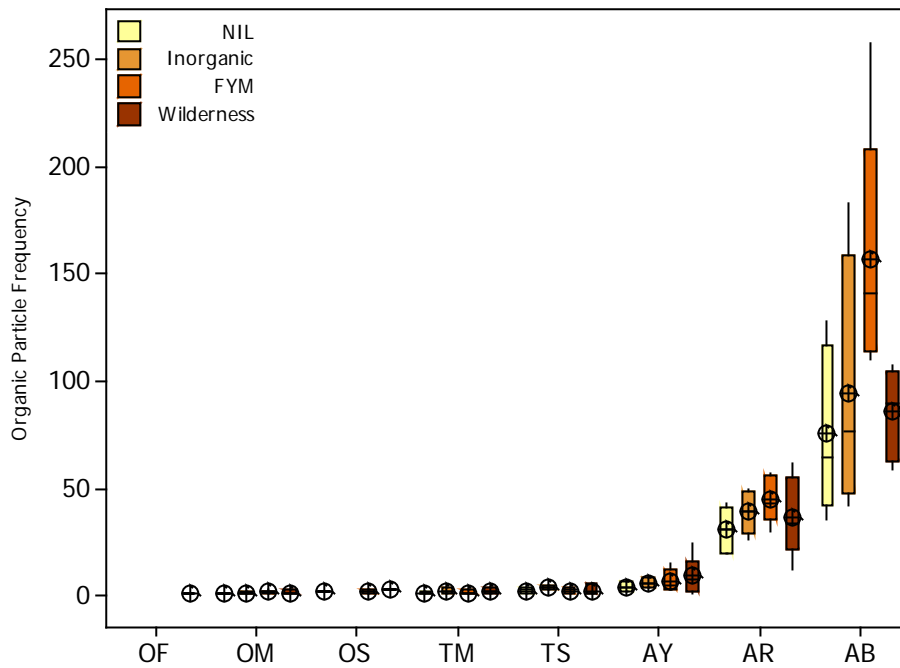


Figure 5.5. Frequency of organic matter classed according to form and extent of decomposition, at 40x. Bars represent the median value for soils removed from Broadbalk-winter-wheat and Broadbalk Wilderness; error bars represent the interquartile range. Significant differences were found in the frequency of organic matter fragments between organic matter classes ($p < 0.001$). Organic matter classes are coded as follows: OF = Organ-Fresh, OM = Organ-Moderate, OS = Organ-Strong, TM = Tissue-Moderate, TS = Tissue-Strong, AY = Amorphous Yellow, AR = Amorphous Red, AB = Amorphous Black.

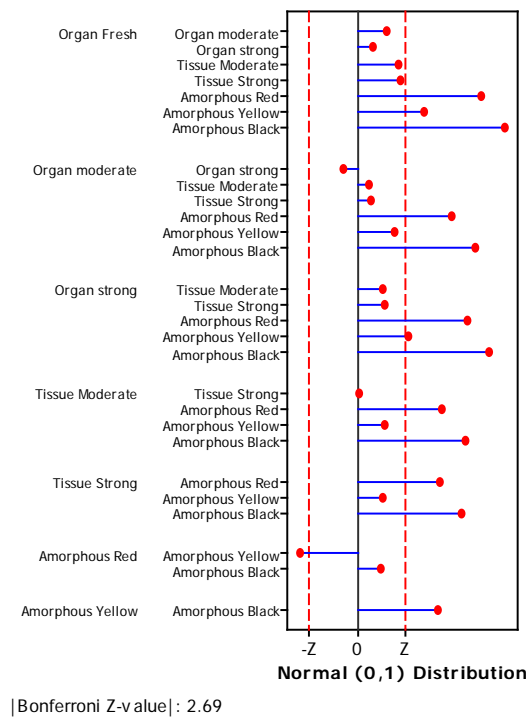


Figure 5.6: Mean rank standardised differences between all treatments, used in Dunn's nonparametric multiple comparisons test. Showing differences between the median frequency of organic matter by decomposition class. Values beyond the $-Z$ or Z point indicate differences between treatments that are significantly less or greater, respectively ($p < 0.05$).

5.4.2 The Location of Organic Matter in Relation to Soil Pores.

By utilising intact soil samples it is possible to investigate the distribution of organic matter fragments in relation to soil structural features (**Objective 2.3**). Since, no clear aggregation is evident within the agricultural or grassland soil (**4.5.3**), the location of OM-fragments is described in relation to soil porosity. It is not possible to use IA-software to analyse the location of OM-fragments in relation to soil pores, therefore the location of OM was assessed using micromorphological techniques at 40x (**Section 3.4.6.1**).

There are few differences in the location of organic matter fragments in relation to soil pores between treatments (**Table 5.2**). Across OM-fragment classes a broad distinction in the location of organic matter can be seen between the less decomposed (organ & tissue) and the more decomposed amorphous forms. Across all treatments organ and tissue fragments at all stages of decomposition are typically located within soil pores. Typically very-strongly decomposed amorphous forms are located near to, or within the soil matrix. However one striking difference is that amorphous-yellow OM within the grassland soil is located within soil pores, while across other treatments it is situated within the soil matrix.

Table 5.2. Frequency* of Organic particles classed by form and decomposition and their location in relation to pores

Field	Organ residue			Tissue (> 5 cells)			Fine Organic matter (< 5 cells)		
	Living / Fresh	Moderately decomposed	Strongly decomposed	Living / Fresh	Moderately decomposed	Strongly decomposed	Amorphous red	Amorphous yellow	Amorphous black
Nil	1	2		4	9		31	2	76
FYM	10	4		10	12		45	6	157
Inorganic	3			4	9		39	5	80
Wilderness	1	6	3	9	10		36	8	86

Green: Located within a pore

Blue: Located near to a pore

Brown: Located within the soil matrix

* Counted by image-analysis software

5.5 The Distribution of Elemental Carbon.

The distribution of elemental C was measured using SEM-EDS (3.4.9). The following section will begin by presenting the O:C ratio of features to determine whether features can be distinguished by O:C ratios as previously concluded for BC (Stofin-Egli *et al.*,1997), and also to assess if the O:C ratio of the same features differs between treatments. The amount of C (mg/kg) associated with features will also be presented. The full spectrum of elements will then be investigated to determine whether an elemental signature exists for features. As a result it should be established if features identified and classed according to micromorphological methods are chemically distinct. Comparisons are made between SEM-EDS analysis performed at 5 and 15 keV, allowing the most effective protocol to be developed.

5.5.1 Elemental O:C Ratios of Features Analysed at 5 keV.

The O:C ratios of organic matter features are presented in **Figure 5.7**. When using SEM-EDS to determine C-distributions, image quality is reduced due to the required microscope set-up to optimise C- detection (**Section 3.4.5**), therefore hindering the identification of features. To ensure features viewed under the SEM are correctly identified a number of procedures such as performing micromorphology, image analysis (Including, ascertaining the location and extent of features of interest) and determining the O:C of blank resin (**Table 3.5**), have been performed prior to elemental analysis, therefore it is possible to target analysis for particular features. It should be assumed that resin impregnates all but the smallest of micropores, therefore the area cover of resin is effectively a measure of soil porosity. Particular care should be taken to sample within solid regions of OM (i.e. the cell wall opposed to more readily decomposable regions) The mean O:C ratio of blank resin was recorded as 0.14 (standard deviation ± 0.02). When comparing the O:C ratio of blank crystic resin to O:C values previously published there is some overlap between resin and the values recorded for softwood combustion (Stoffyn-Eggi *et al.*,1997). Furthermore, variations in the O:C ratio of crystic resin are to be expected between batches.

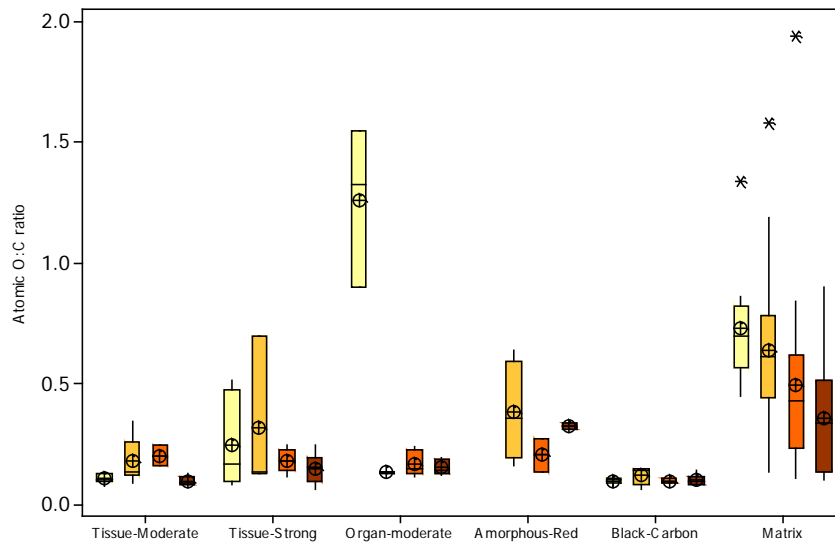


Figure 5.7: The O:C ratio of features by treatment, classified using micromorphological methods, the atomic O:C ratio is obtained by elemental analysed using SEM-EDS. Treatments are colour coded, light yellow = NIL, gold =Inorganic, Orange =FYM, Brown = Wilderness. The box represents the interquartile range, the line represents the median value, the symbol represents the mean, error bars represent the full range of data and outliers are indicated by a star.

In practise it was not possible to sample all classes of organic matter features as identified by micromorphology, possibly due to the porous nature of more decomposed OM. From the above results it is clear that the O:C ratio of organic features is very similar to crystic resin however, controls put in place such as targeting features using the OM-pore maps and images from micromorphological analysis, ensure that sampling is positioned on features that can be confidently identified. Furthermore, the analysis of blank crystic resin (**Table 3.5**) revealed that aside from C and O, other elements are not detected at an accelerating voltage of 5-15 keV. Therefore targeted sampling and checking the spectrum for the minimal presence of elements in addition to C and O, the user can be confident that an organic matter fragment has been analysed.

It is not possible to use a GLM to test for differences in the O:C ratio among features since the data are not normally distributed and there are few samples in feature*treatment combinations. Therefore, a Kruskal Wallis test was applied and the p -value reduced to 0.03. The analysis revealed that there are significant differences in the O:C ratio among features (Kruskal Wallis: $H = 85.23$, $d.f = 5$, $p < 0.0001$) (**Fig. 5.8**). Dunn's multiple comparisons revealed that, the soil matrix has a significantly higher O:C ratio compared to BC, Tissue-moderate, Tissue-strong ($p < 0.0001$) and Organ-moderate ($p = 0.01$). The O:C ratio of BC was also found to be significantly lower than Amorphous-red ($p < 0.0001$), Organ moderate ($p < 0.001$) and Tissue-strong ($p < 0.005$). Finally Amorphous red has a significantly greater O:C ratio compared to Tissue-moderate ($p = 0.002$). No differences in the O:C ratio were found between any of the organic matter fragments ($p > 0.03$). The range of O:C ratio values for organic matter features is wide, while for BC it is much narrower, in accord with previous studies (Stoffyn-

Eggi *et al.*,1997; Davidson *et al.*, 2006) which have successfully distinguished BC by O:C values alone. Through mapping it will be possible to ascertain whether O:C ratios of OM are highly variable both across and between fragments.

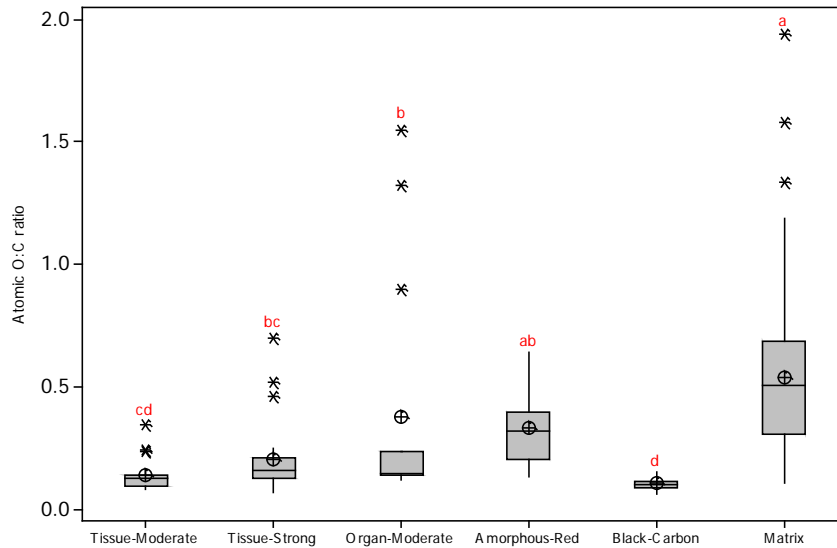


Figure 5.8: The O:C ratio of features, classified using micromorphology methods, the atomic O:C is obtained by elemental analysed using SEM-EDS. The box represents the interquartile range, the line represents the median value, the symbol represents the mean, error bars represent the full range of data and outliers are indicated by a star. Plots followed by the same letter are not significantly different (Dunn's $p < 0.05$).

The O:C ratio of the soil matrix shows distinct differences between soil treatments (**Fig. 5.7**), with the O:C ratio increasing as the organic carbon content of the soil increases. The O:C ratio of the Wilderness soil is significantly greater than NIL ($p = 0.001$) and Inorganic ($p = 0.01$). NIL matrix has a significantly lower O:C ratio compared to FYM soil ($p = 0.004$). Interestingly there are no differences in the O:C ratio of the two lowest OC-containing (NIL and Inorganic) and two the highest OC containing soils (FYM and Wilderness), although it is recognised that contributions of O could be originating from mineral components (e.g. $\text{Fe}(\text{OH})^3$) and C and O from CaCO_3 . Across all the elemental spectrums the detection of Ca was minimal, rarely reaching 30 mg/kg, but due to the low weight of Ca it is not possible to quantify for the contribution of C within the matrix by CaCO_3 , although this is likely to be minimal. In addition the significantly higher O:C ratio of the Wilderness soil matrix compared to NIL and Inorganic treatments may reflect the greater micro-porosity of this soil; due to imaging imitations sampling micropores (and their resin contents) is unavoidable and this should be considered before interpretation of the result, although the depth and lateral ($1 \times 1 \mu\text{m}$) resolution ensure high precision in sampling of surface features.

5.5.2 The Concentration of Carbon Associated with Features, Analysis at 5 keV.

Although the total C-content of features can not be determined since x-rays are only generated from the surface of features at 5 keV point analysis determination of C will reveal whether differences in the O:C ratio are also reflected by differences in the concentration of C (mg/kg) associated with features (**Fig. 5.9**). There is a significant difference in the concentration of C among treatments (Kruskal Wallis: $H = 84.73$, $d.f = 5$, $p < 0.0001$). The Matrix has a significantly lower C-concentration compared to Tissue-moderate, Tissue-organ, BC ($p < 0.0001$) and Organ-moderate ($p = 0.0006$). Black carbon has a significantly higher C-content compared to Amorphous-red ($p = 0.0001$), Tissue strong ($p = 0.0004$) and Organ-moderate ($p = 0.0008$). Amorphous-red has a significantly lower C-concentration compared to Tissue-moderate ($p = 0.002$).

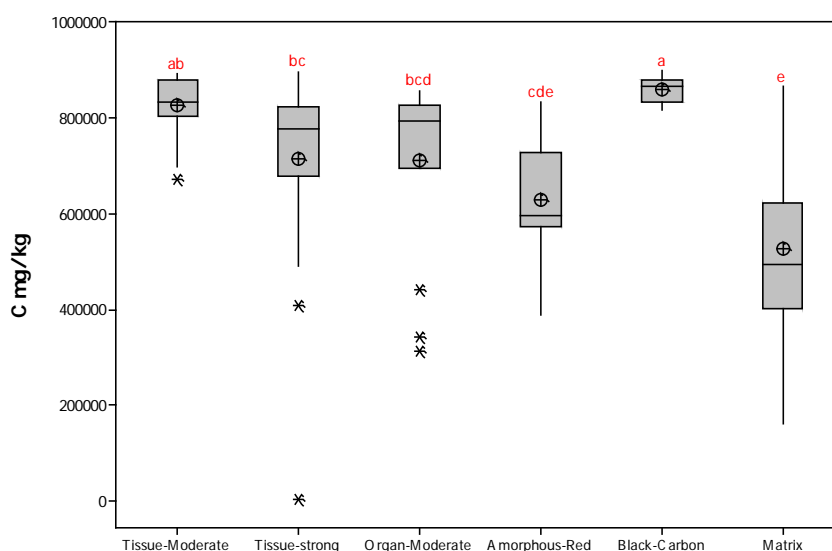


Figure 5.9: The concentration of C-associated with features, classified using micromorphology methods. Carbon (mg/kg) is obtained by elemental analysis using SEM-EDS. The box represents the interquartile range, the line represents the median value, the symbol represents the mean, error bars represent the full range of data and outliers are indicated by a star. Plots followed by the same letter do not differ significantly (Dunn's $p < 0.05$).

5.5.3 The Elemental Signature of Features.

The elemental spectra recovered from the SEM-EDS analysis included C, O, Fe, Al, Si, Na, S and Mg. **Figures 5.10 (a-f)** present spectrums for each of the features across all treatments. It is immediately clear that the elemental spectrum of BC shows the least variability, in addition low amounts of elements other than C and O are in association with BC making it simple to identify BC using SEM-EDS. The marginal amounts of Si and S in association with BC, is consistent with the findings of Stofin-Egli *et al.*, (1997). When analysing BC, the presence of elements other than O and C, reinforces that BC has been sampled rather than resin, since there is some overlap in the O:C ratio of BC and Resin (**5.5.1**). The variability of elements in spectrums removed from organic features may mean that it is not possible to identify these features solely by elemental analysis, and further supports the need to produce OM-pore maps. In the following section PCA and discriminant analysis will be applied to test these assumptions.

Principal component analysis (PCA) was performed prior to discriminate analysis, in order to assess which elements account for the maximum amount of variance between individual samples and to help explain the reduction in data in subsequent stepwise discriminate analysis. Principal component 1 accounts for 40% of the variability, the amount of variability explained by subsequent principal components decreases rapidly, with PC2 accounting for just 16% (**Table 5.3**). Within PC 1 there is a high negative weighting of C (-0.417) contrasting against a high positive weighting for Al (0.428) and O (0.366), Si (0.355) and Fe (0.378), while PC 2 is dominated by a high negative weighting for O (-0.434) and S (-0.594), Mg (0.383) and C (0.355). This is summarised in the loading plot (**Fig. 5.11**) which demonstrates how most of the variability between samples is explained by PC 1; furthermore it highlights, the concentration of Al, O, Si and Fe change in the same direction and by a similar extent. The score plot (**Fig. 5.12a**) shows that samples from across all treatments are spread along PC1 when the same samples are plotted according to feature type (**Fig. 5.12b**); the data spread along PC 1 have mainly originated from matrix features. Therefore since the mineral component of the soil has been sampled this explains the proportional weighting of Al, O, Si and Fe. Furthermore, **Figure 5.12a** shows that samples originating from Black-carbon and Tissue-moderate features form discrete clusters.

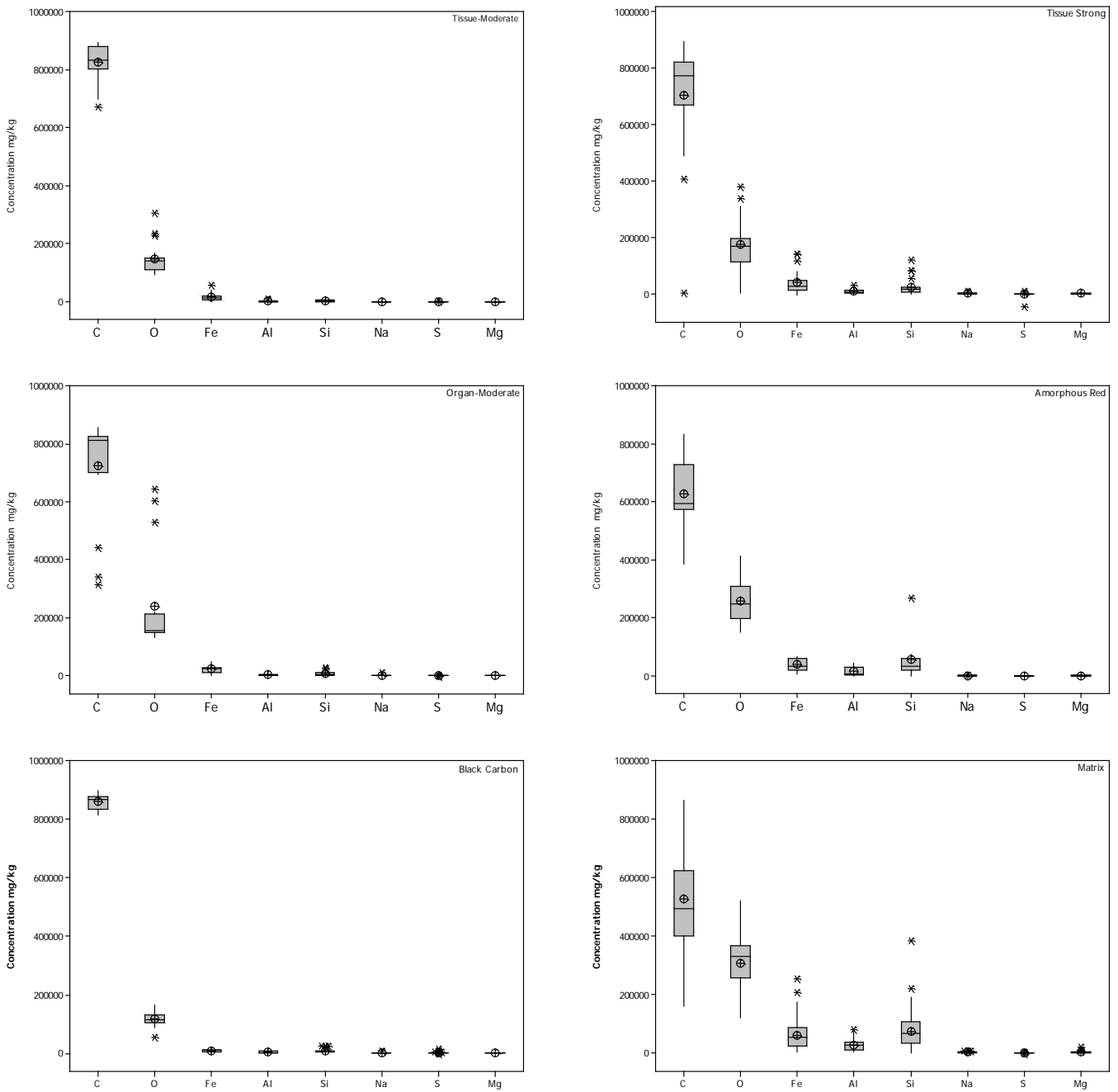


Figure 5.10: The elemental spectrums for features classified using micromorphology, obtained by elemental point analysis using SEM-EDS. The box represents the interquartile range, the line represents the median value, the symbol represents the mean, error bars represent the full range of data and outliers are indicated by a star.

Table 5.3: Showing the Total Variance Explained, by Eigenanalysis of the Correlation Matrix.

	PC1	PC2	PC3	PC4	PC5	PC6	PC7	PC8
Eigenvalue	3.1954	1.3038	1.0779	0.9180	0.6237	0.3937	0.2770	0.2105
Proportion	0.399	0.163	0.135	0.115	0.078	0.049	0.035	0.026
Cumulative	0.399	0.562	0.697	0.812	0.890	0.939	0.974	1.000

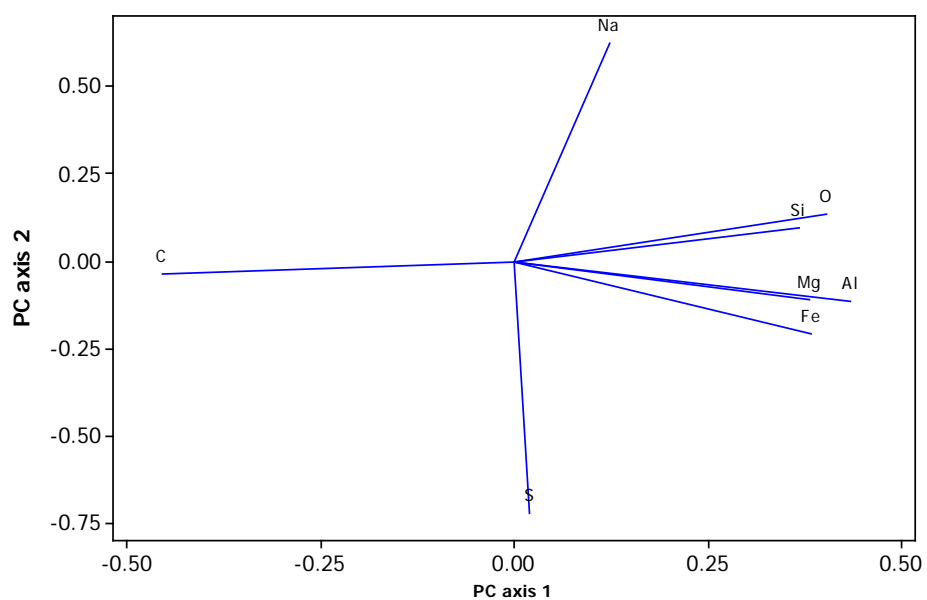


Figure 4.25: The elemental spectrums obtained using SEM-EDS, for features across all treatments, classified using micromorphology techniques. The box represents the interquartile range, the line represents the median value, the symbol represents the mean, error bars represent the full range of data and outliers are indicated by a star.

Figure 5.11: Loading plot showing the contribution of Si, O, Mg, Al, Fe, Na, S and C to PC axis 1 and 2.

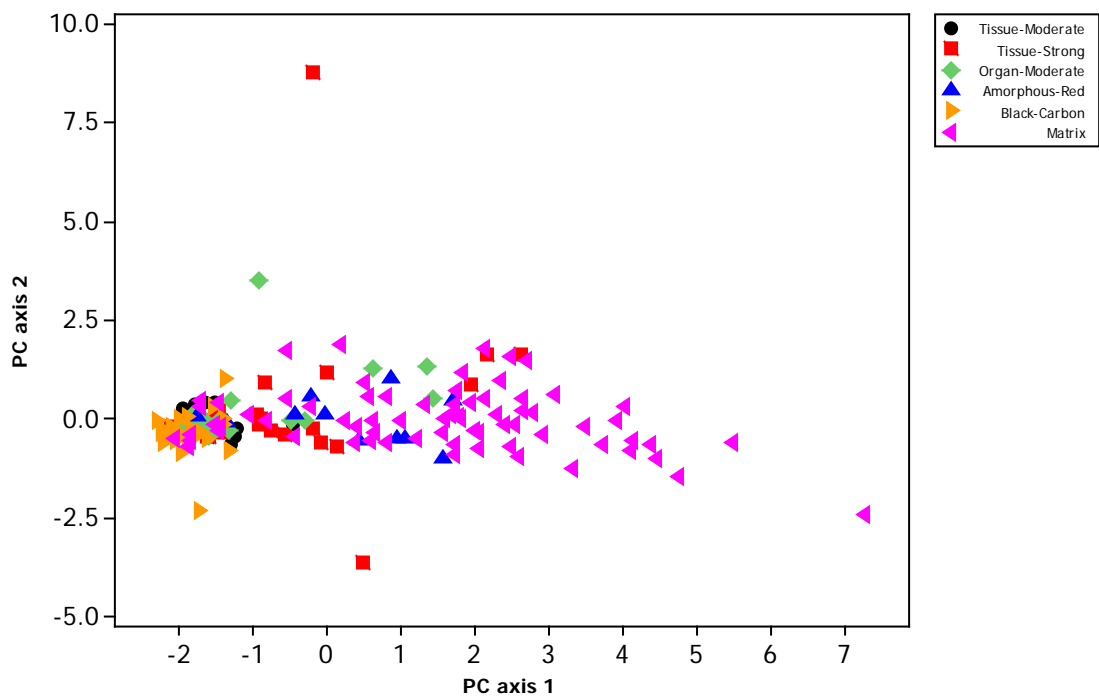
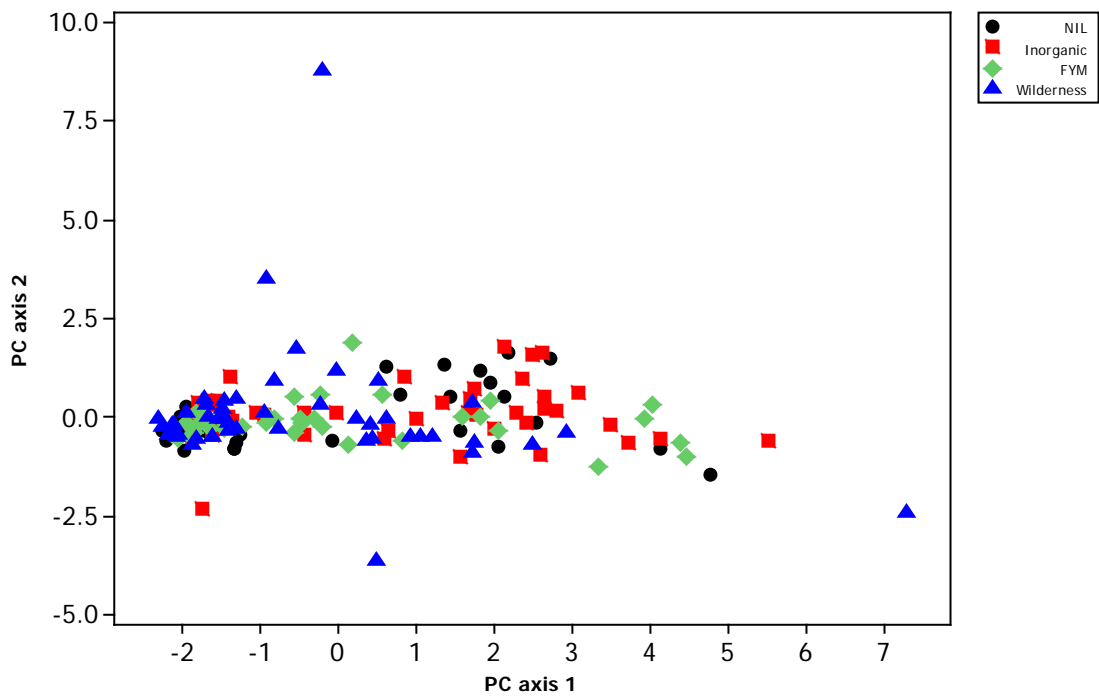


Figure 5.12: Samples plotted according to their principal components. Samples are coded according to treatment (a, top) and feature (b, bottom).

Discriminant analysis is performed to assess whether the classification of features, based upon form and extent of decomposition, would hold true when using elemental data to discriminate between groups. A stepwise method is applied whereby only elements that explained the maximum difference between groups are included in the model. The results for the stepwise model show that C and O are used to discriminate between groups in order to reduce multicollinearity between elemental data sets. The results from PCA help to clarify why just C and O were included in the discriminant analysis. The PCA demonstrated how elements were largely changing in the same direction and proportion; it is argued that this is a result of chemical analysis being performed at high magnifications where x-rays are probably generated from the same/similar compounds, and furthermore the SEM-EDS was optimised for C detection.

The results from discriminant analysis demonstrate that 52.4% of the original data is correctly classified (**Table 5.4**). Groups containing the highest percentage of correctly classified samples include: BC (76%), Matrix (66%), Amorphous-red (45.5%) and Tissue-moderate (42.1%). The high percentage of BC and to a lesser extent Tissue-moderate is expected, given the tight clustering of data observed from the PCA analysis (**Fig. 5.12b**). Due to the high variability and overlap in O & C contents of OM features (**Fig. 5.10 a-c**), the low success rate in the classification of Tissue-strong (24%) and Organ-moderate (13%) according to O and C concentration is expected.

In summary it is not possible to distinguish between OM features based upon O:C ratios alone ($p > 0.03$). However, it is possible to differentiate between organic matter, Black-carbon and the Matrix ($p < 0.03$). Interestingly, the O:C ratio of the Matrix decreases across treatments in the order of NIL, Inorganic, FYM and Wilderness, although there will be inputs of O and C from mineral and CaCO_3 sources. The carbon concentration of the Matrix is lower than all other features sampled while, the C-content of BC is greater than Tissue-strong and Organ-moderate features. Stepwise discriminant analysis was used to assess whether samples could be classified by feature using C and O concentration (mg/kg). The analysis showed that samples placed in either BC or the Matrix were the most correctly categorised; this further supports the view that the O:C ratios can be used to differentiate these features. The capability of discriminant analysis to distinguish between matrix and BC particles is expected given that these features contrast the most in terms of O and C concentration. Furthermore, the high variability in the concentration of all elements within the matrix may reflect the range materials located within this feature and despite dense areas of Silicates and Mn/Fe nodules were not sampled fine particles maybe included within the analysis. Aside from BC it is not possible to find an elemental signature for OM features classes by form and decomposition. This is due to the high variability of elements C and O (**Fig. 5.10**) and the proportional changes in other elements as highlighted by PCA (**Fig. 5.11**). Since it is not possible to differentiate between OM features solely by elemental analysis, this further supports the need for prior micromorphological analysis and the production of OM-pore maps.

Table 5.4: Summary of Classification Results, for Features using Elemental Data obtained by SEM-EDS.

Classification Results ^a

Feature			Predicted Group Membership ^c					Total	
			Tissue moderate	Tissue Strong	Organ Moderate	Amorphous Red	Black Carbon		Matrix
Original ^b	Count	Tissue Moderate	8	0	2	1	8	0	19
		Tissue Strong	9	6	1	1	5	3	25
		Organ Moderate	9	1	2	1	0	2	15
		Amorphous Red	2	1	2	5	0	1	11
		Black Carbon	6	0	0	0	19	0	25
		Matrix	6	0	5	9	4	47	71
	%	Tissue Moderate	42.1	.0	10.5	5.3	42.1	.0	100.0
	Tissue Strong	36.0	24.0	4.0	4.0	20.0	12.0	100.0	
	Organ Moderate	60.0	6.7	13.3	6.7	.0	13.3	100.0	
	Amorphous Red	18.2	9.1	18.2	45.5	.0	9.1	100.0	
	Black Carbon	24.0	.0	.0	.0	76.0	.0	100.0	
	Matrix	8.5	.0	7.0	12.7	5.6	66.2	100.0	

a. 52.4% of original grouped cases correctly classified.

b. Original data represent features classified using micromorphology methods

c. Predicted group membership, samples placed into feature classes according to elemental data.

5.5.4 Elemental Maps, at 5 keV.

Elemental distributions are mapped and features separated using the phase mapping function within the INCA software (Oxford Instruments). Distinct phases are identified based upon the relative concentration of O:C:Si allowing features (i.e. areas with the same ratio of O:C:Si) to be located and their corresponding spectrums acquired. Maps are produced showing the different phases, and features identified using the corresponding elemental spectra (**Fig. 5.14**). Organic-matter features, were not categorised according to form and decomposition when mapping, since there are few data and previous point analysis revealed no significant difference in the O:C ratio between organic matter classes.

Once features are separated using phase mapping the atomic O:C ratio is calculated, thus allowing for comparison with the analysis of the O:C ratios from point analysis. There is a significant difference in the O:C ratios among features (**Fig. 5.13a**) (Kruskal Wallis: $H=35.40$, $d.f=4$, $p < 0.0001$). Dunn's test for multiple comparisons revealed that significant differences exist between silicate features which have a higher O:C ratio compared to OM ($p < 0.0001$), BC ($p > 0.0001$) and resin ($p = 0.0017$), while the soil matrix has a significantly higher O:C ratio compared to OM ($p = 0.0001$) and BC ($p = 0.0005$). There is a significant difference in the C-content among features (**Fig. 13b**) (Kruskal Wallis: $H=35.40$, $d.f=4$, $p < 0.0001$). Dunn's multiple comparisons test revealed that significant differences exist between silicate features which have a lower C-concentration compared to resin ($p < 0.0001$), OM ($p = 0.0002$) and BC ($p = 0.0004$). The soil matrix has a significantly lower C-concentration compared to resin ($p < 0.0001$), OM ($p = 0.0062$) and BC ($p = 0.0092$).

There is a significant difference in the C concentration among features (**Fig. 5.13a**) (Kruskal Wallis: $H=34.04$, $d.f=4$, $p < 0.0001$). Dunn's test for multiple comparisons revealed that significant differences exist between silicate features which have a higher O-concentration compared to OM ($p < 0.0001$), BC ($p > 0.0001$) and resin ($p = 0.0040$), while the soil matrix has a significantly higher O-concentration compared to OM ($p = 0.0001$) and BC ($p = 0.0005$).

Interestingly there is no significant difference ($p > 0.05$) in either the O:C ratio, or O and C-concentration between OM and BC.

5.5.5 Elemental Signature Obtained by Phase Analysis, at 5 keV.

As for point analysis the elemental spectrums recovered by phase analysis included C, O, Fe, Al, Si, Na, S and Mg. **Figure 5.15 a-d** presents the spectrums for features across all treatments. Consistent with the findings from point analysis the elemental spectrum for BC shows the least variability. Phase analysis using the relative concentration of C:O:Si to differentiate between features has allowed areas densely occupied by silicates (e.g. quartz) to be separated from the Matrix, this has helped to reduce some of the variability in the elemental spectrums recovered from the Matrix. In addition the mapping of OM has reduced the variability of O and C associated with OM-fragments. In conclusion, the elemental spectrums of features recovered by both point and phase analysis are consistent i.e. elements have the same relative contribution to feature spectrums.

5.5.6 Comparison of Point and Mapping Analysis at 5 keV

Organic-matter features, were not categorised according to form and decomposition when mapping, since there are few data and previous point analysis revealed no significant difference in the O:C ratio between organic matter classes. Mapping of OM-fragments revealed a much narrower range of O:C ratios (0.1-0.3) compared to point analysis (0.07-1.0). The range of O:C values recorded for the matrix by mapping (0.40-1.6) is much narrower compared to point analysis (0.08-1.6); this is because phase mapping has allowed the soil matrix to be distinguished from areas which are densely occupied by silicates (e.g. quartz) as previously identified by micromorphology (4.5.1). The Kruskal Wallis test revealed that there are no significant differences among the O:C ratio of the soils matrix by treatment (Kruskal Wallis: $H= 4.61$, $d.f= 3$, $p = 0.203$), and no consistent pattern within the O:C ratio of soils with different total C-contents; this contrasts with the results obtained by point analysis (5.5.1). It is possible that the pattern of results seen in the O:C ratios of the Matrix recorded by point analysis was created by sampling a different mixture of quartz and matrix samples across treatments.

Point analysis revealed that BC has a significantly lower O:C ratio compared to some OM fragments: organ moderate ($p < 0.001$) and tissue-strong ($p < 0.005$). However mapping revealed no significant difference in the O:C ratio between OM and BC ($p < 0.005$). Results from point analysis revealed that BC has a significantly higher C-content compared to Tissue-strong ($p = 0.0004$) and Organ-moderate ($p < 0.0008$), while the results from mapping analysis concluded that there is no significant difference in the C-concentration OM and BC ($p > 0.05$).

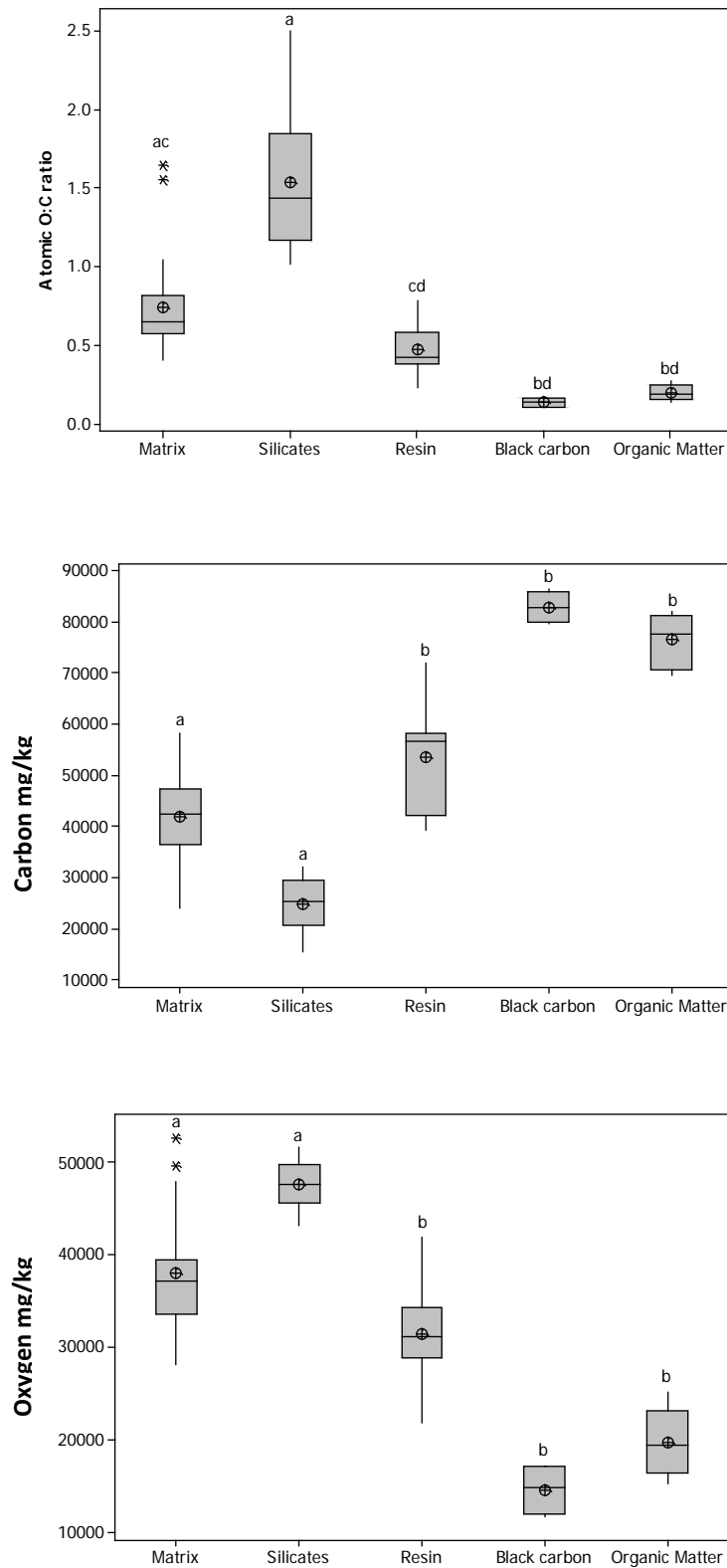


Figure 5.13 a) The O:C ratio of features, identified using phase analysis, obtained by elemental analysis using SEM-EDS. **b)** The C-concentration of features, identified using phase analysis, **c)** the O-concentration of features, identified using phase analysis. The box represents the interquartile range, the line represents the median value, the symbol represents the mean, error bars represent the full range of data and outliers are indicated by a star. Plots followed by the same letter are not significantly different (Dunn's $p < 0.05$).

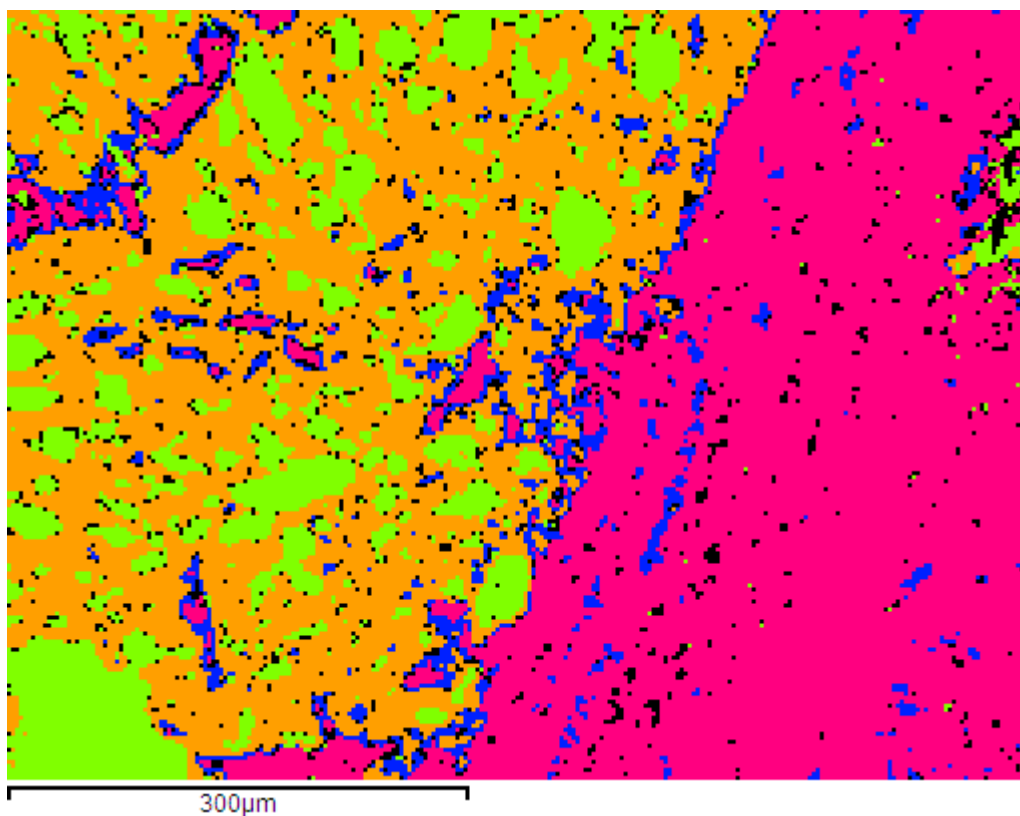
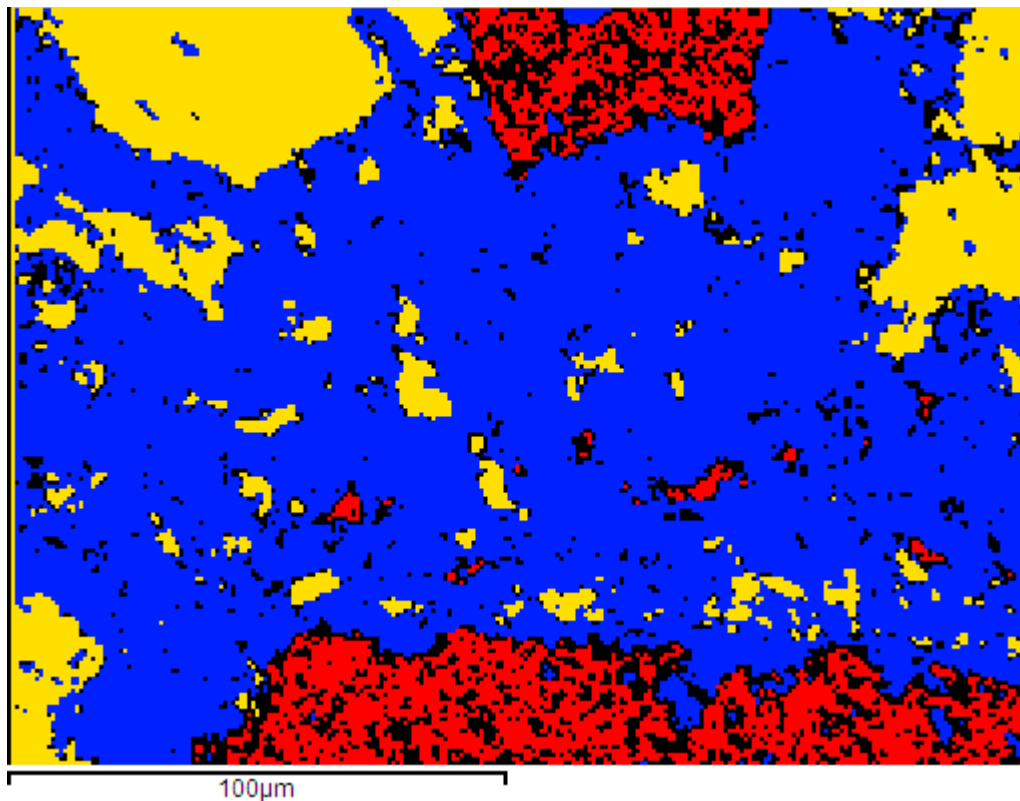


Figure 5.14: Elemental maps showing (a) Black-carbon particle (*red*, $O:C = 0.1$) surrounded by matrix (*blue*, $O:C = 1.2$) and silicates (*yellow*, $O:C = 0.5$). And (b) an organic-matter fragment (*pink*, $O:C = 0.2$) surrounded by soil matrix (*blue*, $O:C = 0.6$) silicates (*yellow*, $O:C = 1.2$) and resin (*green* = 0.4).

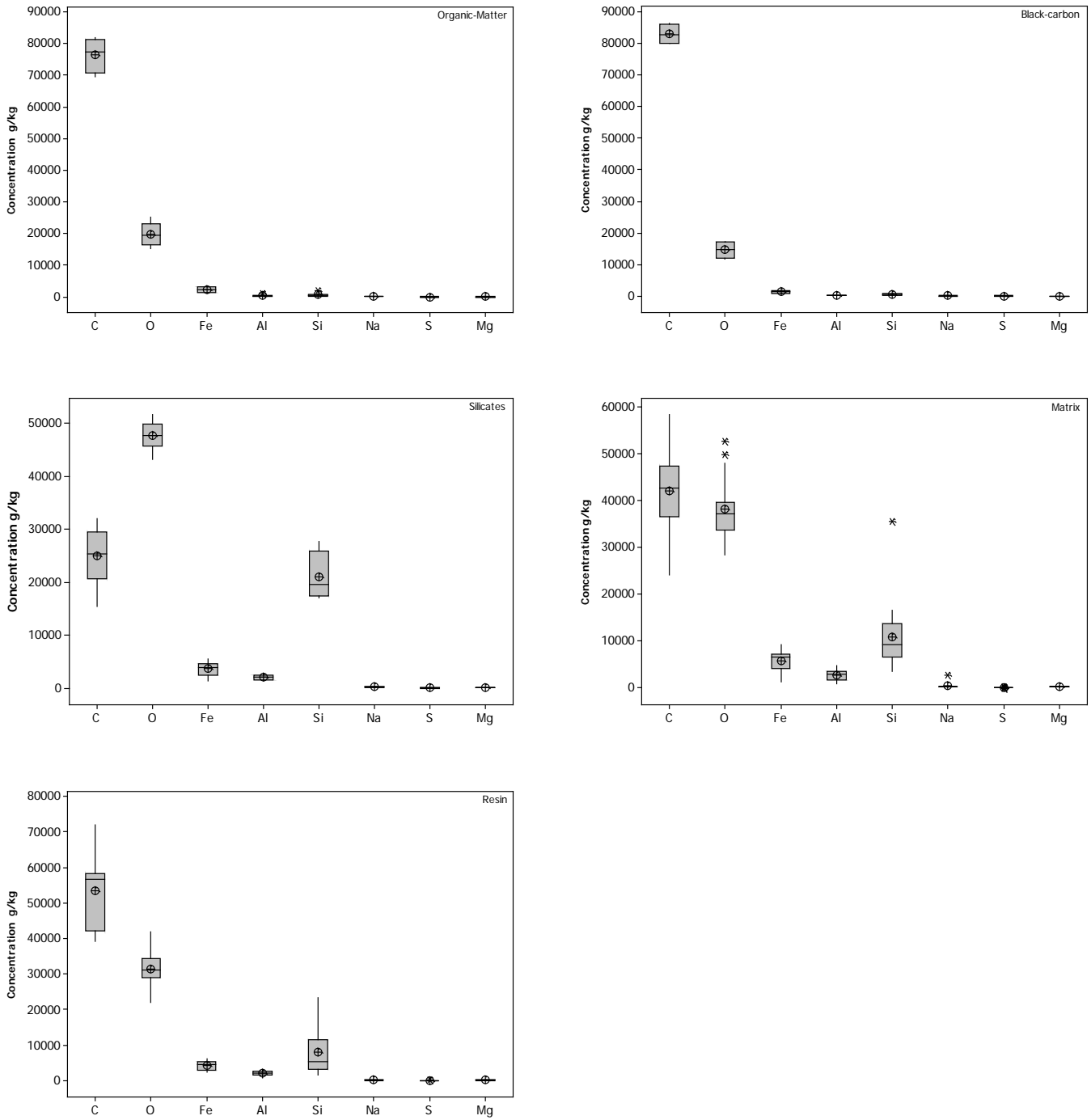


Figure 5.15: The elemental spectrums for features classified using micromorphology, obtained by elemental phase analysis using SEM-EDS. The box represents the interquartile range, the line represents the median value, the symbol represents the mean, error bars represent the full range of data and outliers are indicated by a star.

5.5.7 Elemental Mapping at 15 keV

Since there is no formal methodology for analysing C-distributions within soil thin-sections, modifications of the methodology is to be expected subsequent to data analysis. When analysing soil thin-sections using an accelerating voltage of 5 keV it was sometimes difficult to phase the resin from other features. Therefore in order to further excite heavier elements (e.g. O and Si), some of the mapping analysis was repeated at a greater accelerating voltage of 15 keV. In addition a modified SEM-EDS system became available, which reduces the electrical charging of systems by implementing a variable pressure. It is initially concluded that when C-coating is not appropriate, a combination of a higher accelerating voltage (15 keV) and a system with variable pressure, is far more effective. The following section will present the mapping results collected by implementing the alternative SEM-EDS system (**Methods 3.4.10**).

Once features are separated using phase mapping (**Fig. 5.17**) the O and C concentration (g kg^{-1}) atomic O:C ratio of features is calculated. There is a significant difference in the O:C ratios among features (**Fig. 5.16a**) (Kruskal Wallis: $H= 34.31$, $d.f= 3$, $p < 0.0001$). Dunn's test for multiple comparisons revealed that significant differences exist between the soil matrix which has a significantly greater O:C ratio compared to BC ($p < 0.0001$) OM ($p > 0.0001$) and resin ($p = 0.0093$). The O:C ratio of BC is significantly lower than resin ($p = 0.0093$). There is a significant difference in the C-content among features (**Fig. 5.16b**) (Kruskal Wallis: $H=34.22$, $d.f= 3$, $p < 0.0001$). Dunn's multiple comparisons test revealed that the C-concentration of BC is significantly greater than matrix ($p > 0.0001$) and resin ($p = 0.01$). The C-content of Matrix is significantly less than OM ($p > 0.0001$) and resin ($p = 0.003$).

Consistent with the analysis of O:C and C content; O-concentration is significantly different among features (Kruskal Wallis: $H = 33.08$, $d.f = 3$; $p > 0.0001$). With Dunn's multiple comparisons revealing that the O-concentration of BC is significantly lower than the Matrix ($p > 0.0001$) and resin ($p = 0.01$). The O-content of the soil matrix is significantly greater than OM ($p > 0.0001$) and resin ($p = 0.0008$).

Dunn's multiple comparisons test concluded that there is no significant difference in the O-concentration, C-concentration or O:C ratio between OM and BC. However, there are few samples within the OM and BC classes, therefore it is not possible to test for a significant difference between these two classes and the Dunn's result is invalid. When comparing the O-concentration, C-concentration and O:C ratio of OM and BC, there are pronounced differences. Therefore it is concluded that using an accelerating voltage of 15 keV differences in the C and O concentration of OM and BC, can be detected.

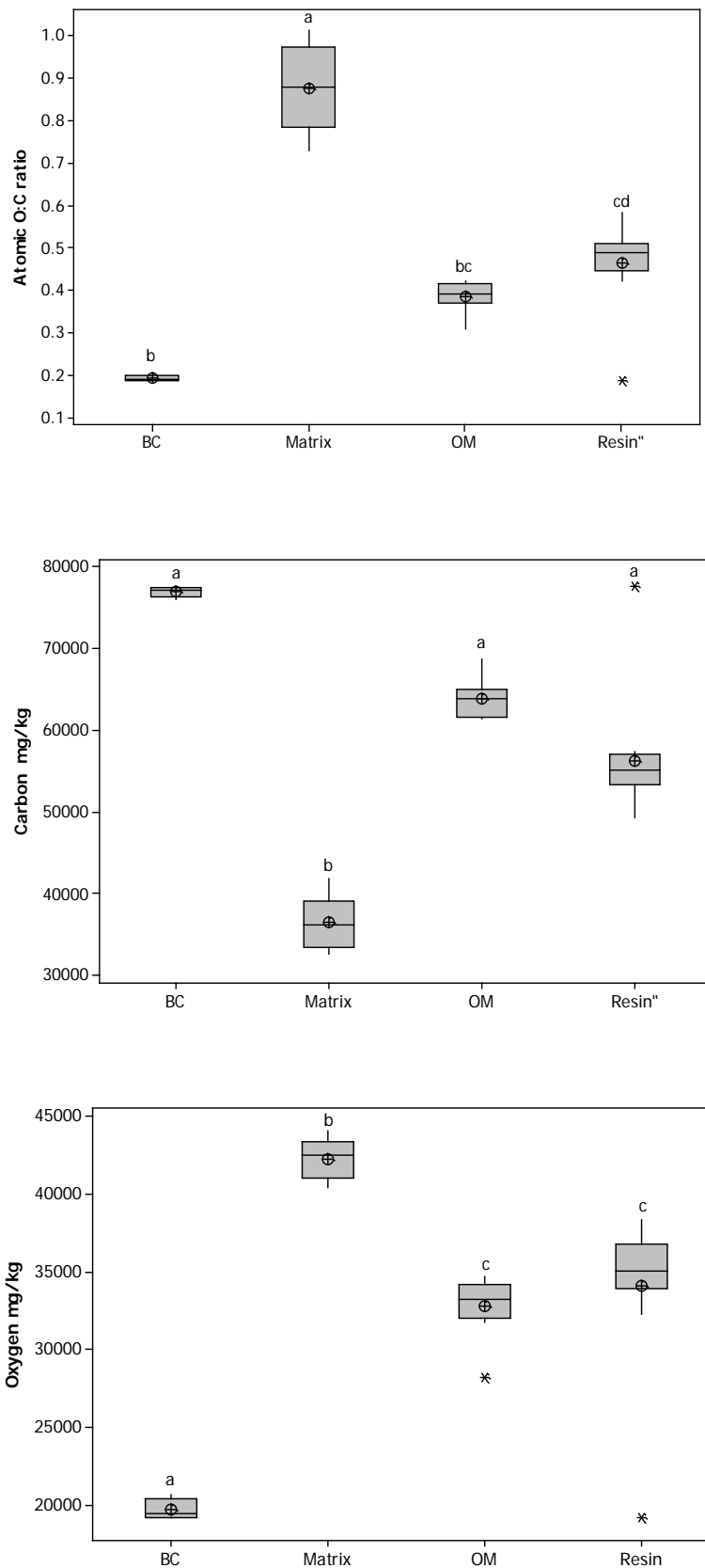


Figure 5.16: a) The O:C ratio of features, identified using phase analysis, obtained by elemental analysis using SEM-EDS. b) The C-concentration of features, identified using phase analysis, c) the O-concentration of features, identified using phase analysis. The box represents the interquartile range, the line represents the median value, the symbol represents the mean, error bars represent the full range of data and outliers are indicated by a star. Plots followed by the same letter are not significantly different (Dunn's $p < 0.05$).

5.5.8 Elemental Signatures Obtained by Phase Analysis at 15 keV

The elemental spectrums recovered by phase analysis included C, O, Fe, Al, Si, Na, S and Mg. **Figure 5.18 a-e** presents the spectrums for features across all treatments. The elemental spectrum for BC shows the least variability. Phase analysis using the relative concentration of C:O:Si to differentiate between features and has allowed areas densely occupied by silicates (e.g. quartz) to be separated from the Matrix, this has helped to reduce some of the variability in the elemental spectrums recovered from the Matrix. The resin spectrum shows the most variability in terms of O and C concentrations, the contribution of other elements to the resin spectrum is minimal. Nevertheless, the contribution of Si to the resin spectrum is slightly higher, than other elements. It is possible when phasing for resin some matrix features are included, this would help explain the high variability in O and C concentrations. However overall matrix and resin have very different spectrums as supported by the analysis of total O, C and the O:C ratio (**Section 5.5.7**).

5.5.9 Comparison of Elemental Mapping Performed at 5 and 15 keV.

By increasing the accelerating voltage from 5 to 15 keV it was much easier to pull out resin using phase analysis. Furthermore there is a significant difference in the O:C ratio of BC and resin ($p = 0.0093$) at 15 keV but not at 5keV. No significant differences were found in the O-concentration, C-concentration or O:C ratio between OM and BC, despite the distribution of the values being very different, this is due to the low number of samples within both the OM and BC classes. Therefore it is not possible to test for a significant difference between these two classes and the Dunn's result is invalid. Therefore it is concluded that by using an accelerating voltage of 15 opposed to 5 keV differences in the C and O concentration of OM and BC, can be detected.

By implementing a higher accelerating voltage and a system with variable pressure it was possible to map elemental-C within soil thin-sections, furthermore differentiating between different C-containing features was more successful.

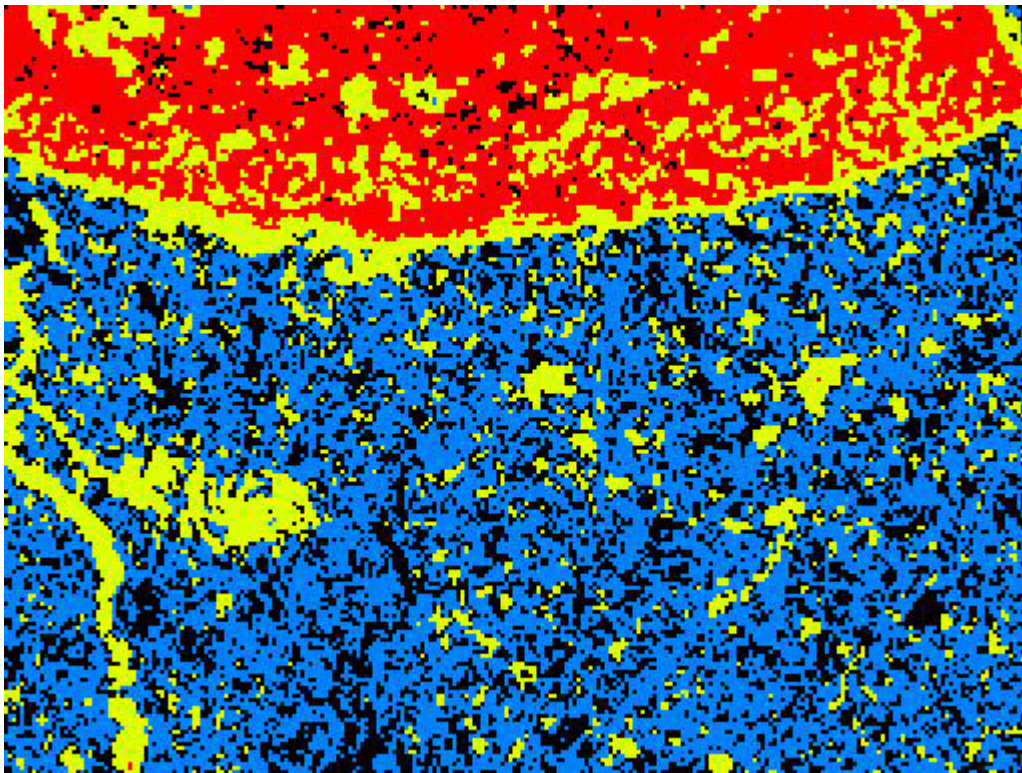
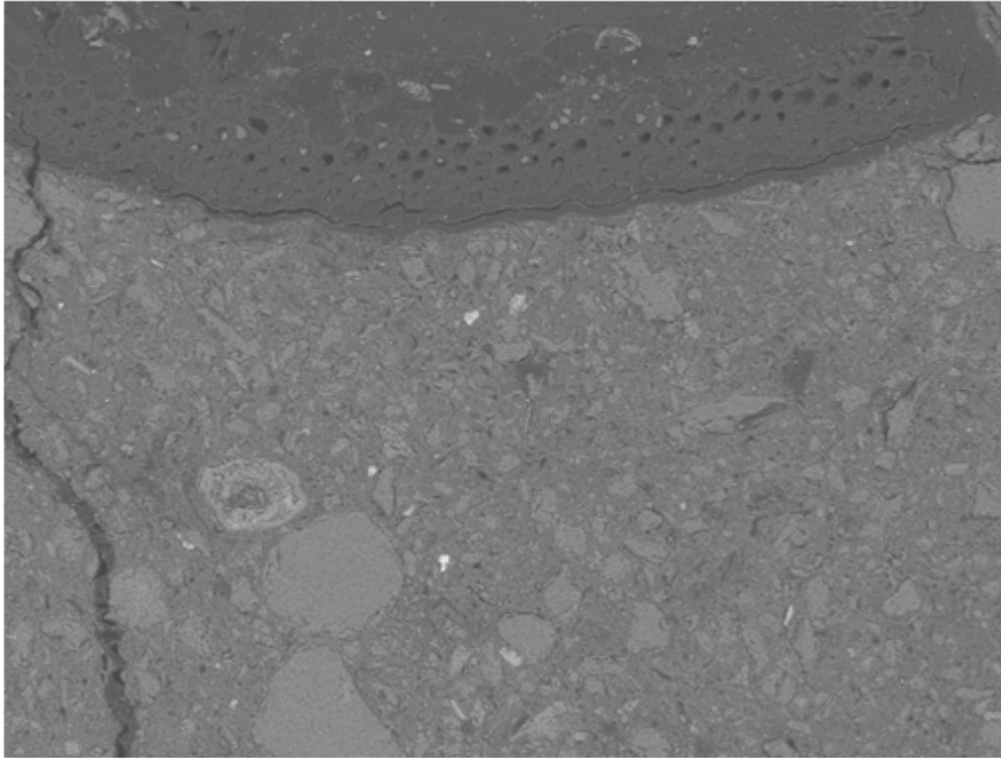


Figure 5.17: (a) Back Scatter Image of an organic matter fragment. (b) Elemental phase map taken at 15 keV of the same organic-matter fragment (*red* $O:C = 0.42$) surrounded by soil matrix (*blue*, $O:C = 1.0$) resin (*yellow*, $O:C = 0.58$)

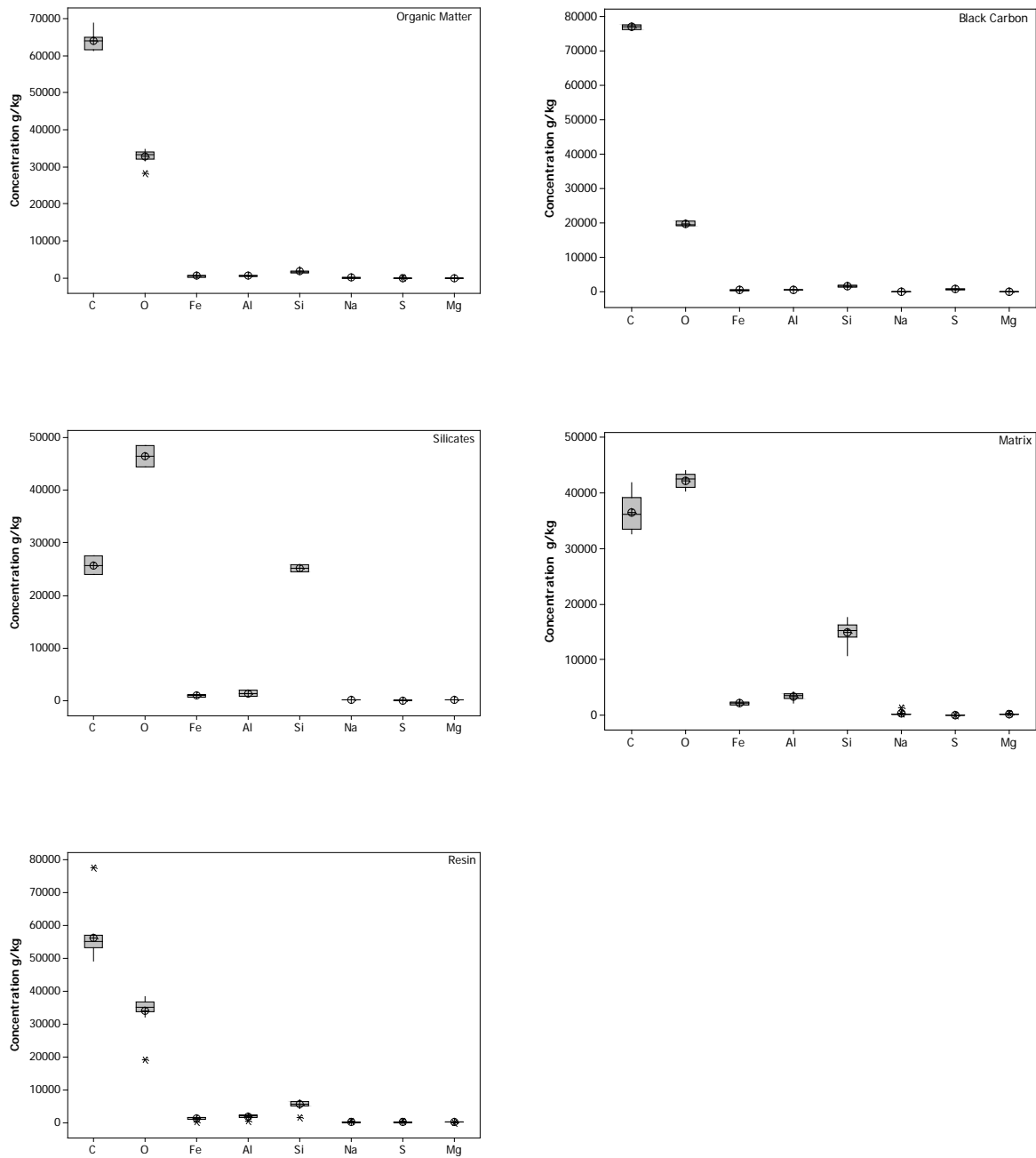


Figure5.18: The elemental spectrums for features classified using micromorphology, obtained by elemental phase analysis using SEM-EDS at 15keV. The box represents the interquartile range, the line represents the median value, the symbol represents the mean, error bars represent the full range of data and outliers are indicated by a star.

5.6 Introduction and Methodology, to Investigate C-Distribution within an Intact Soil Structure.

To investigate the distribution of C within an intact soil structure a series of elemental transects were sampled. This section describes the procedure developed to map C-distributions, away from OM and BC particles using soil thin-sections sampled from Broadbalk Winter-Wheat and Broadbalk Wilderness samples. The section will conclude by presenting some initial findings.

It was found that mapping elemental concentrations across whole areas (at 15 keV) and performing phase analysis to identify features (5.5.7) was the best practise. It is not possible to subtract the C-contribution of resin due to multiple factors, which include: non-uniform x-ray generation across samples (e.g. black pixels where no x-ray information has been collected), the nature of x-ray data (e.g. counts) and the non uniform distribution of resin. Since it is not possible to subtract the C-contribution by resin, regions densely occupied by resin can be identified by phase analysis and avoided when positioning transects. Furthermore, since resin will impregnate all pores except very small micropores (e.g. <10 μm) it is important that when analysing OM the probe is positioned within the cell wall and porous cell vacuoles are avoided, however phase analysis will confirm the location of resin. To further account for the C-contribution from resin, a blank polished crystic resin was sampled, the results demonstrate that within resin there are no pronounced changes in C-concentration with distance (**Fig. 5.19**). In addition **Fig. 5.19** demonstrates there is a minimal contribution of Si to the resin, while in OM and BC Si occurs in slightly greater concentrations and is most prominent in the soil matrix. Therefore as a control Si will be included in the elemental analysis, its presence will further confirm that solid soil material has been sampled and resin avoided.

All transects show background oscillations in elemental concentration, possibly reflecting minor changes in topography or charging of the sample, therefore only pronounced changes in elemental concentration are assessed. In this situation pronounced differences are identified as a trend for a decrease or increase in C-concentration, which is not consistent with background oscillations. It is not possible to assign a numerical upper and lower limit because; the magnitude of change in elemental concentration will vary between areas of interest as concentrations are relative. By incorporating these controls it will be possible to investigate changes in C-concentration away from OM and BC features.

Transects have been positioned to investigate the concentration of C away from OM-fragments and BC secondly. Elemental transects are show in **Figures 5.21-5.28**; the positioning of transects are superimposed onto SEM images while the elemental concentrations are shown to the left, this is the standard out put from INCA software. Elements are colour coded as: C=red, O =blue, Si =green. The start of each transect is positioned 30 μm within the feature of interest, each transect is approximately 150 μm in length and 5 pixels in diameter.

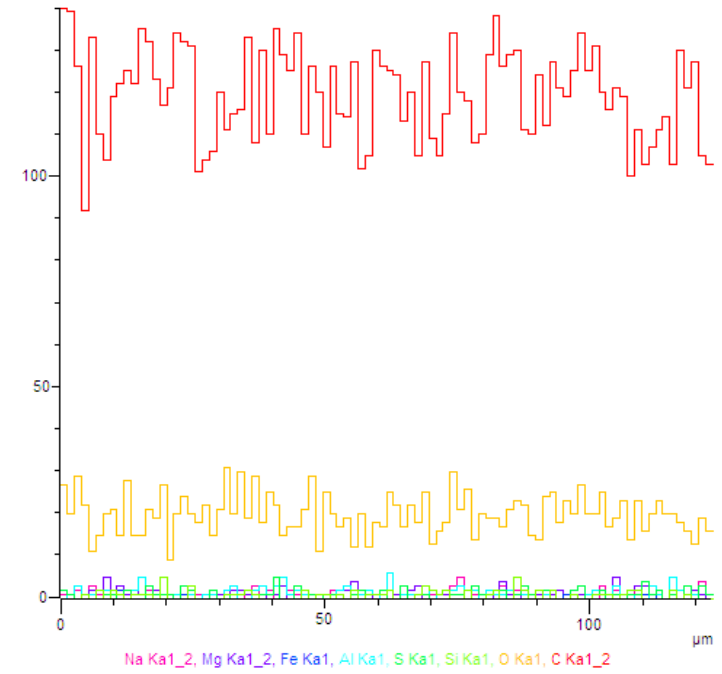
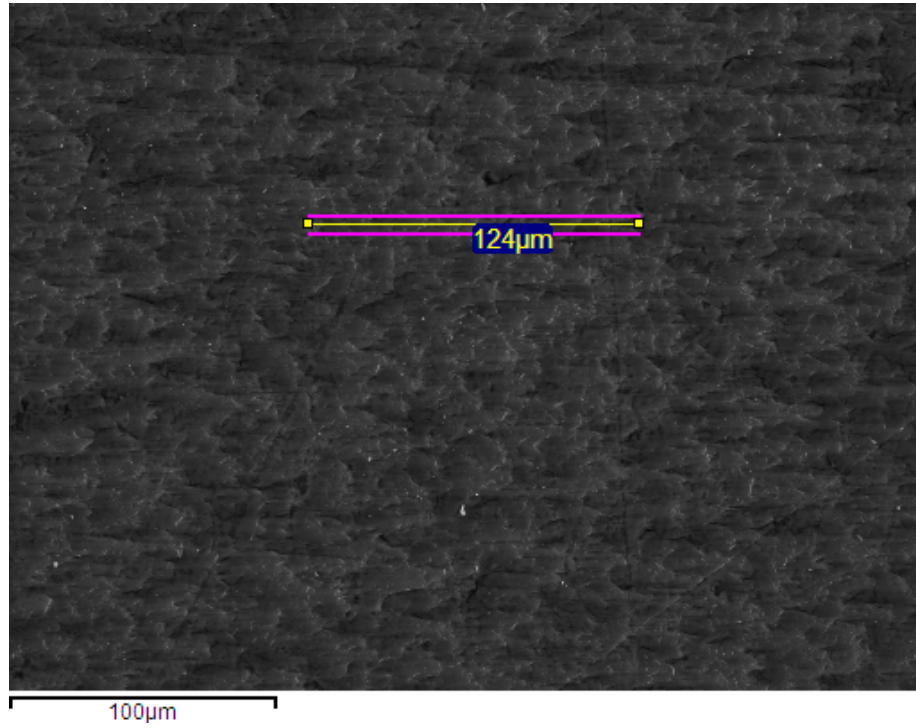


Figure 5.19: Elemental transect of the resin standard, analysed at 15 Kev. Left, BSI image showing the positioning of the transect; right, the relative concentration of Na (pink), Mg (purple), Fe (blue), Al (turquoise), S (green), Si (lime), O (orange) and C (red).

5.6.1 A Theoretical Model of the change in C-Distribution away from Organic Matter and Black Carbon Particles.

A theoretical model showing the change in C-concentration away from BC and OM particles is shown in **Figure 5.20**. The model represents the change in C-concentration away from OM or BC particles, the change in C-concentration away from BC particles can follow one of two scenarios depending on whether BC is acting as a source or store of C. The sudden decrease in C-concentration represents the reduction in X-ray detection due to boundary effects, past the boundary C-concentration is plotted for soils removed from Broadbalk Winter-Wheat and Broadbalk Wilderness. **Figure 5.20** shows that for all soils there is a gradual decrease in C-concentration away from OM or BC particles (when BC is a source of C), but the overall magnitude of C-concentration will differ between treatments, reflecting differences in total SOC content. However if BC is acting as a store of C (e.g. chemically recalcitrant) then beyond the boundary, C-concentration will drop suddenly until reaching an equilibrium. The overall magnitude of C-concentration will differ between treatments reflecting differences in total SOC-contents.

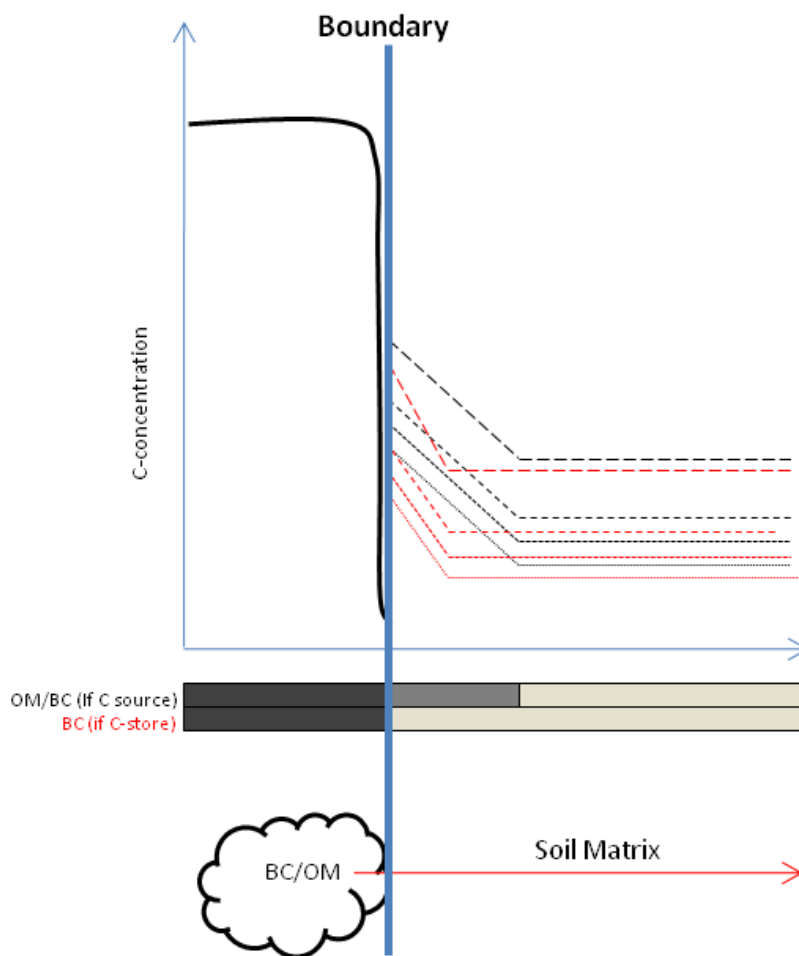


Figure 5.20: Theoretical C-distributions with distance away from organic matter and black carbon particles located within an intact soil structure. Transects will begin 30 μm within the feature of interest. Each transect will cross from the feature of interest into the soil matrix, presented schematically in the lower diagram. The Blue line represents the boundary between feature and soil matrix, dark black line represents C-concentration with features, due to topological effects there will be a drop in x-ray detection. Beyond the boundary differences in C-concentration will be detected due to the nature of C-containing features and the total C-contents of the soil. Within the graph, black dotted lines represent OM and BC features that act as a source of carbon. The magnitude of the change in C-concentration will reflect total OC-content of the soil, different dotted lines represent the different treatments (see key). Red dotted lines represent BC features that act as a store of carbon. The magnitude of the change in C-concentration will reflect total OC-content of the soil, different dotted lines represent the different treatments (see key). The bars below the graph summarise the nature of C-containing features, when acting as a store or source of C. Black represents where C is stored, dark grey where carbon is leaking into the soil matrix, and light grey represents background levels C within the soil matrix carbon.

5.6.2 Elemental Transects of Broadbalk Soils.

Figures 5.21 & 5.24 demonstrate the change in elemental C-concentration away from OM-particles. The start point for each transect was position 30 μm within each OM particle, the sharp drop in all elements corresponds with the boundary between OM and the soil matrix. **Figure 5.21** shows the elemental transects away from an OM-fragment contained within NIL treated soil. The results show that there is a gradual decrease in C-concentration extending approximately 40 μm beyond the boundary. Carbon transects from the OM-fragment sampled from within Inorganic soil (**Fig. 5.22**) show a more rapid decrease in C-concentration occurring approximately 20 μm beyond the boundary; the same pattern in C-concentration away from an OM-fragment is seen in FYM soil (**Fig.5.23**). Carbon transects from the OM-fragment sampled from within the Wilderness soil (**Fig. 5.24**) show a more variable pattern with oscillations in C-concentration, the overall magnitude of C-concentration remains high once entering the soil matrix compared to other treatments. There maybe some mixing with resin, however there is a strong Si signal throughout the transects.

Figures 5.25 & 5.28 demonstrate the change in elemental C-concentration away from BC-particles. The start point for each transect was position 30 μm within each BC particle, the sharp drop in all elements corresponds with the boundary between BC and the soil matrix. **Figure 5.25** shows the elemental transects away from an BC-fragment contained within NIL treated soil. The results show that there is a gradual decrease in C-concentration extending approximately 20 μm beyond the boundary. Elemental transects away from BC particles within Inorganic, FYM and Wilderness soil (**Fig. 5.26-5.28**), show an immediate reduction in C-concentration 0-10 μm beyond the OM-matrix boundary.

In summary there appear to be a gradual decrease in C beyond the boundary of both OM and BC particles. However from the few features sampled it appears that C from OM extends further into the soil matrix than C originating from BC particles.

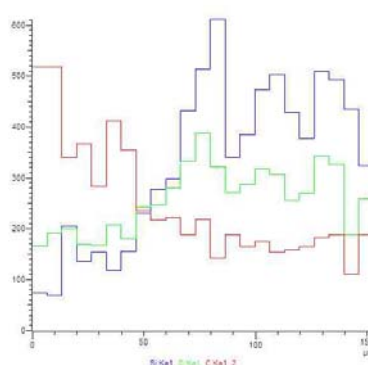
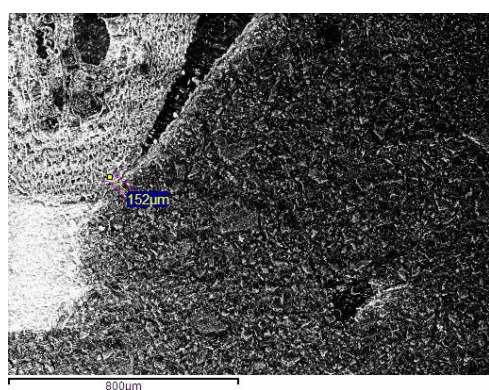
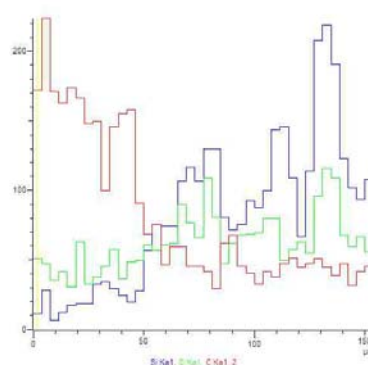
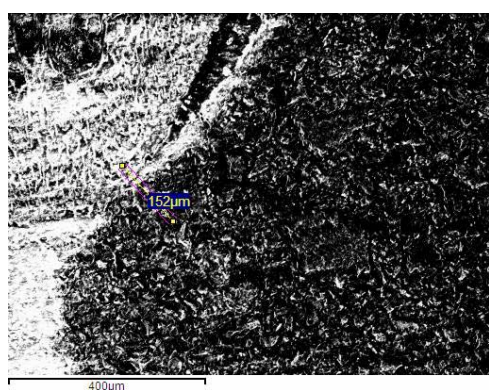
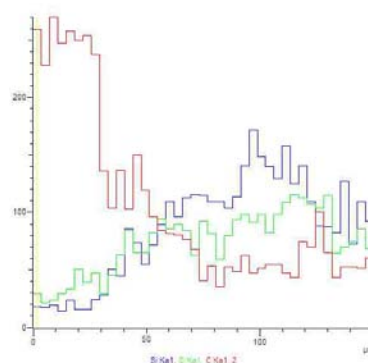
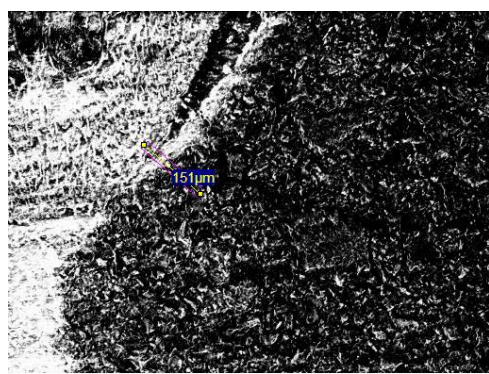
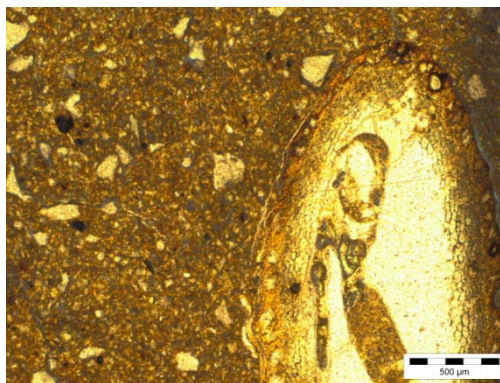


Figure 5.21: Elemental transect away from an **organic matter** fragment within Broadbalk **NIL** treated soil. Image top shows the OM-fragment under PPL. Images to the left show OM under BSI conditions, transect positioning is superimposed. Elemental concentrations along transects are shown, right, Si =blue, O =green, C =red (from organic matter (0μm) to Matrix (150μm)).

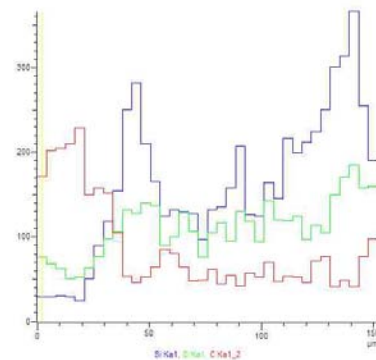
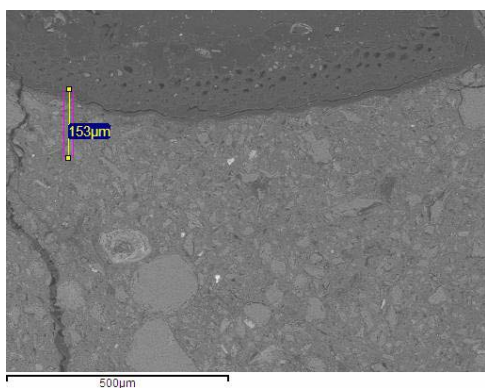
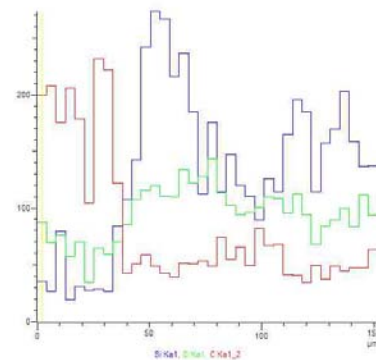
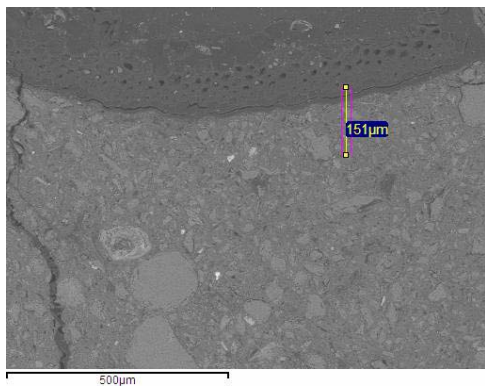
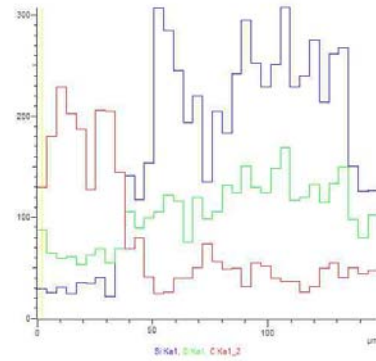
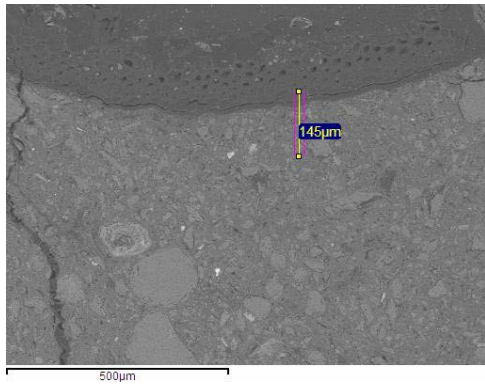
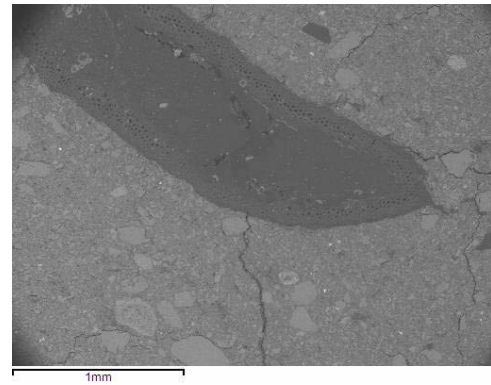


Figure 5.22: Elemental transect away from an **organic matter** fragment within Broadbalk **Inorganic** treated soil. Image top right shows the OM-fragment under PPL, image top left shows the OM-fragment under BSI at low magnification. Images to the left show OM under BSI conditions, transect positioning is superimposed. Elemental concentrations along transects are shown, right, **Si =blue**, **O =green**, **C =red** (from organic matter (0μm) to Matrix (150μm)).

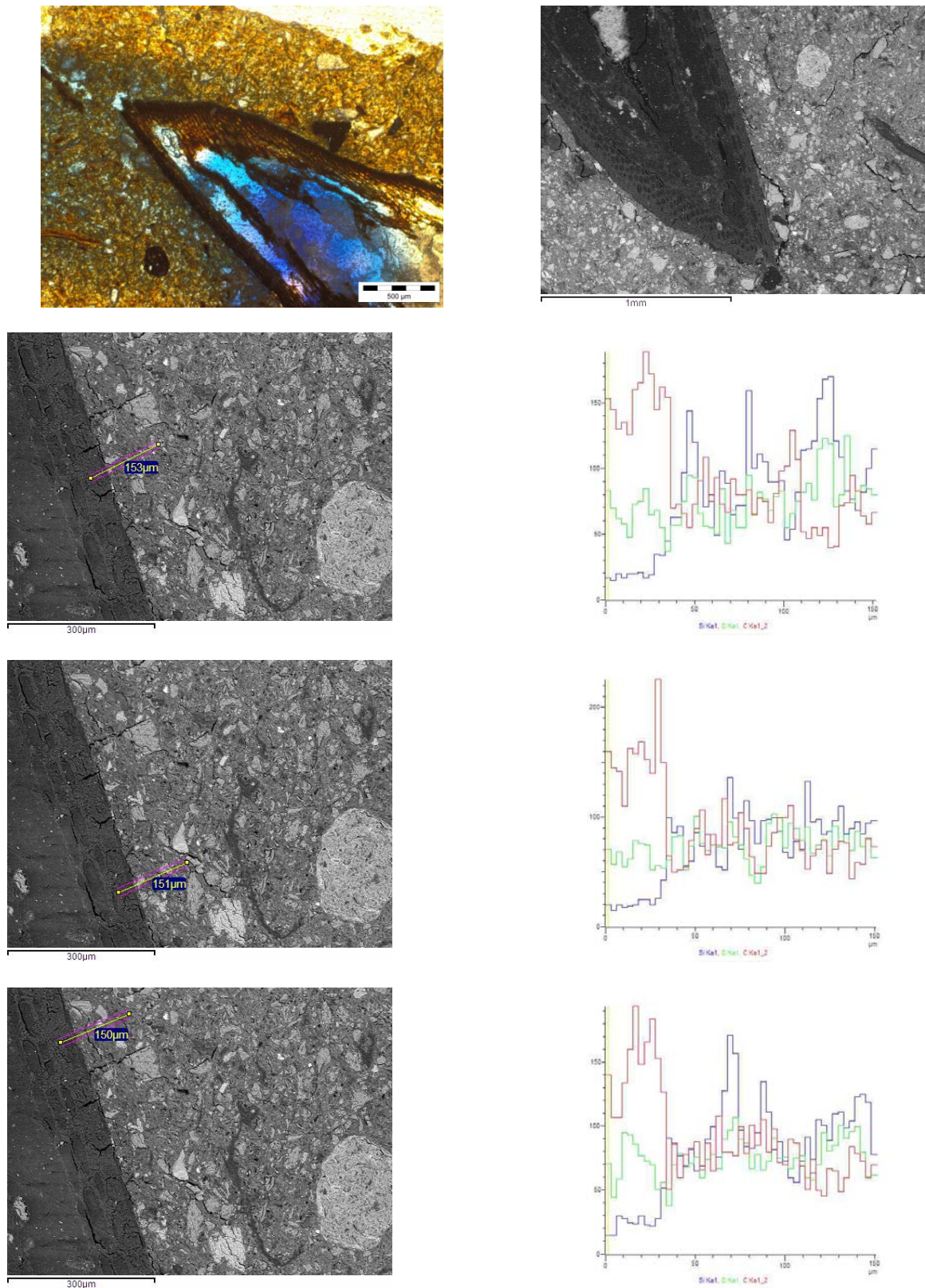


Figure 5.23: Elemental transect away from an **organic matter** fragment within Broadbalk **FYM** treated soil. Image top right shows the OM-fragment under PPL, image top left shows the OM-fragment under BSI at low magnification. Images to the left show OM under BSI conditions, transect positioning is superimposed. Elemental concentrations along transects are shown, right, Si =blue, O =green, C =red (from organic matter (0 μ m) to Matrix (150 μ m)).

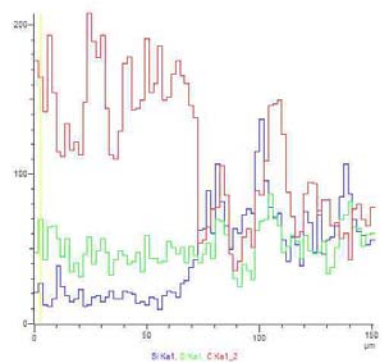
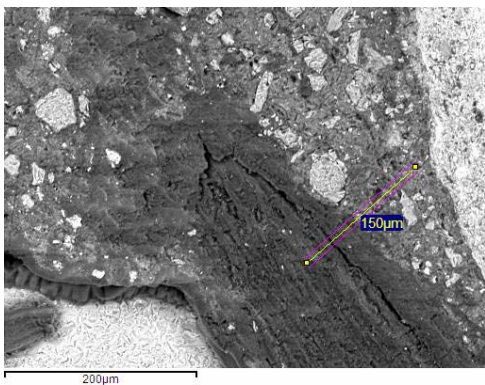
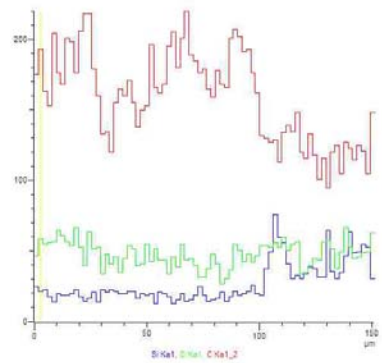
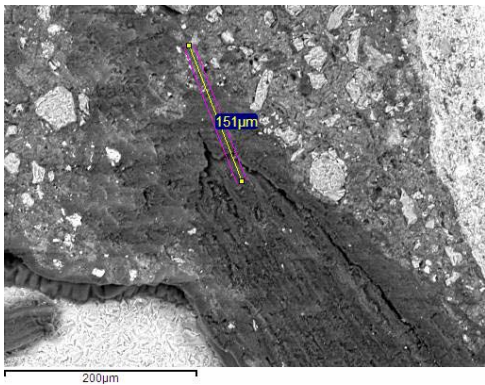
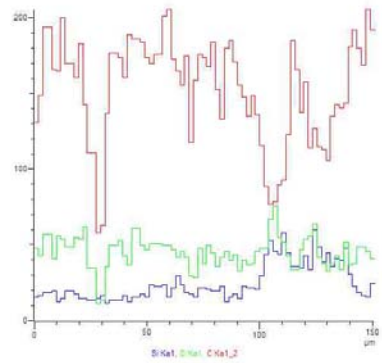
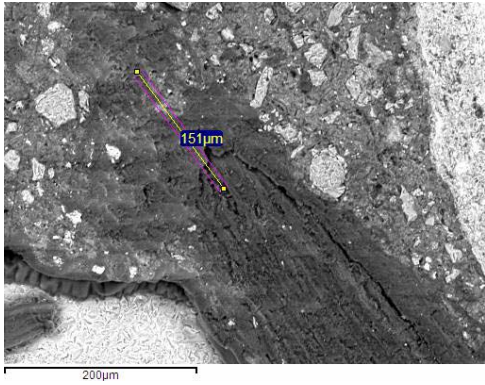
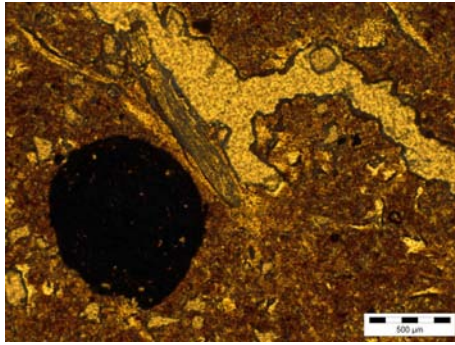


Figure 5.24: Elemental transect away from an **organic matter** fragment within **Broadbalk Wilderness** soil. Image top shows the OM-fragment under PPL. Images to the left show OM under BSI conditions, transect positioning is superimposed. Elemental concentrations along transects are shown, right, Si =blue, O =green, C =red (from organic matter (0μm) to Matrix (150μm)).

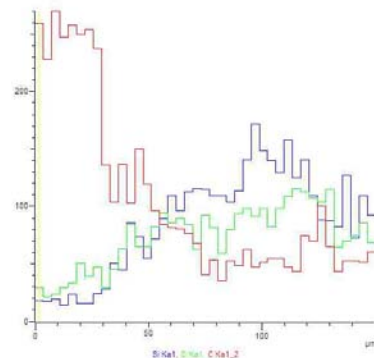
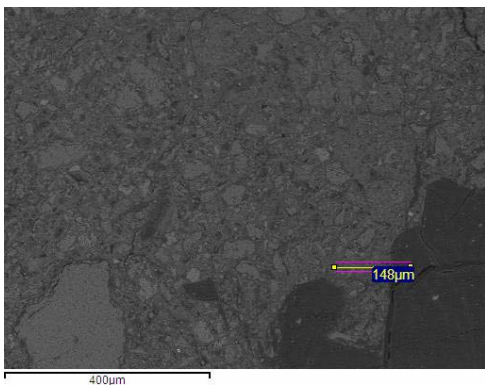
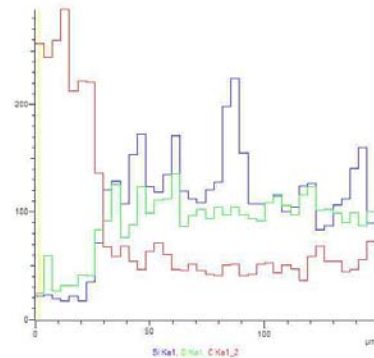
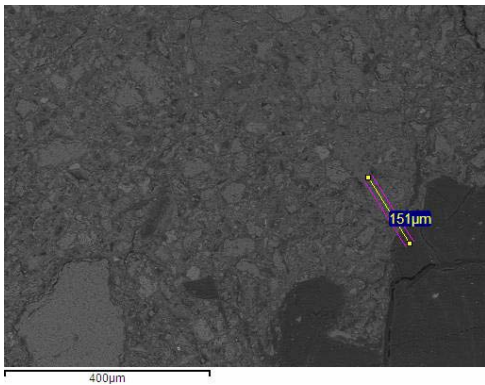
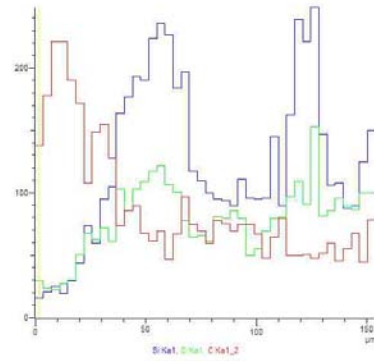
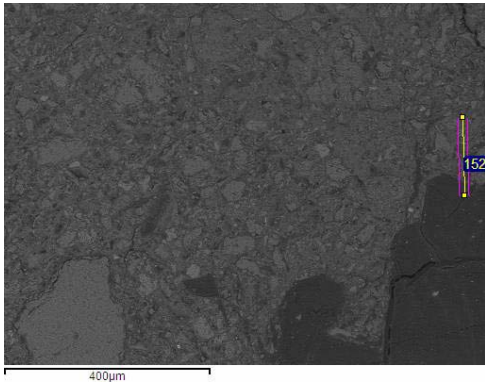
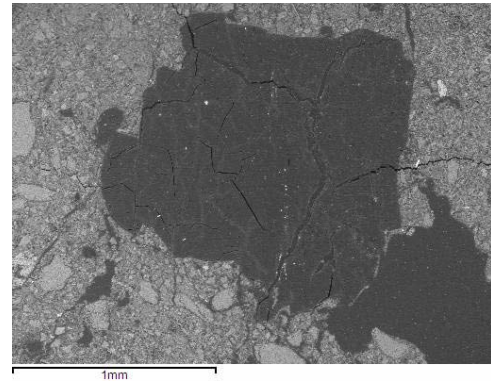
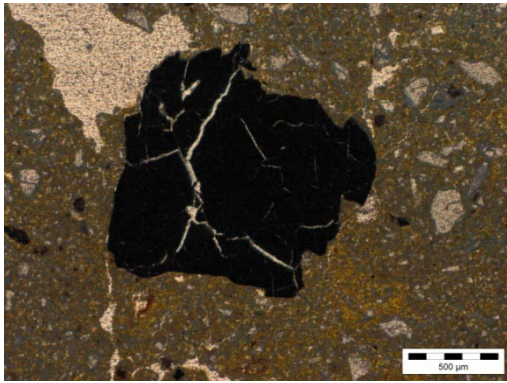


Figure 5.25: Elemental transect away from a **Black carbon** fragment within Broadbalk **NIL** treated soil. Image top right shows the BC-fragment under PPL, image top left shows the BC-fragment under BSI under at magnification. Images to the left show BC under BSI conditions, transect positioning is superimposed. Elemental concentrations along transects are shown, right, Si =blue, O =green, C =red (from BC (0μm) to Matrix (150μm)).

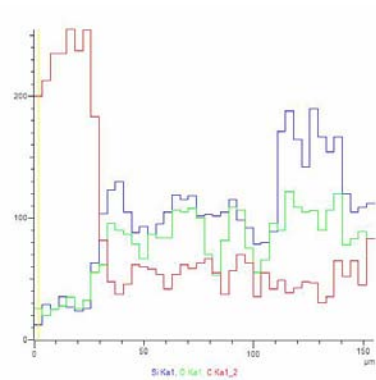
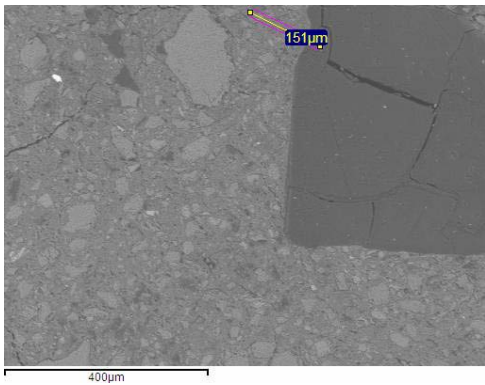
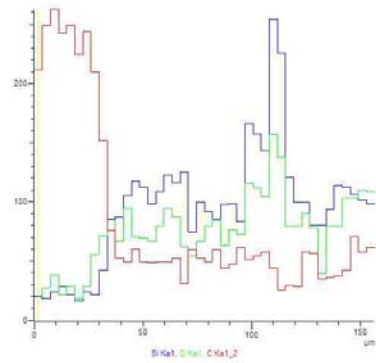
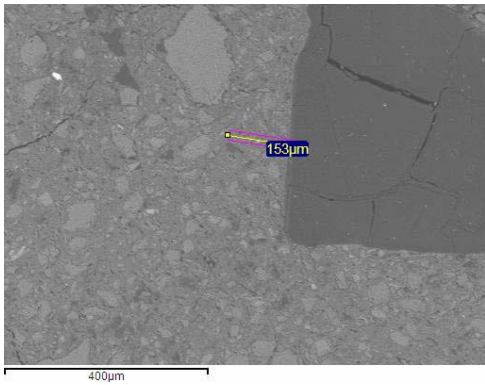
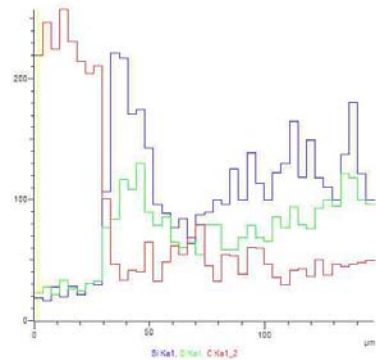
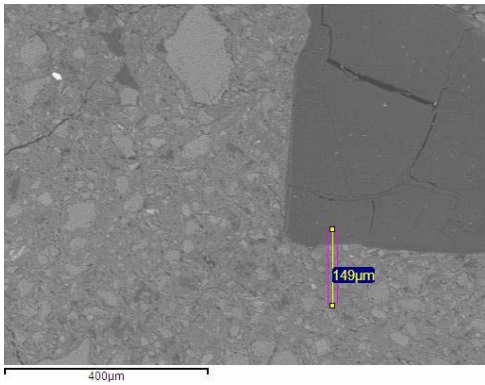
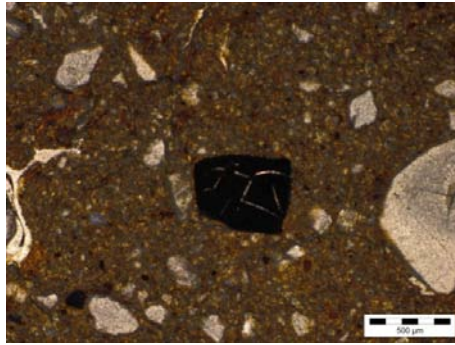


Figure 5.26: Elemental transect away from a **Black carbon** fragment within Broadbalk **Inorganic** treated soil. Image top shows the BC-fragment under PPL. Images to the left show BC under BSI conditions, transect positioning is superimposed,. Elemental concentrations along transects are shown, right, Si =blue, O =green, C =red (from BC (0μm) to Matrix (150μm)).

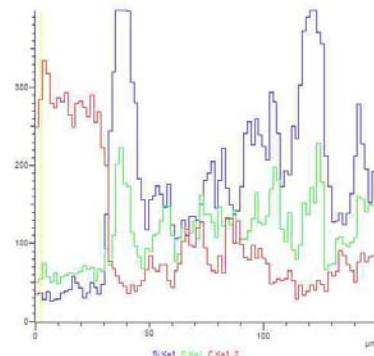
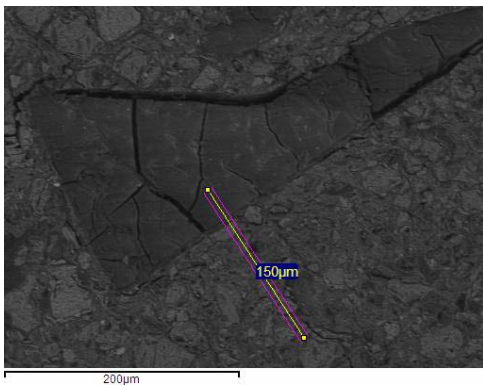
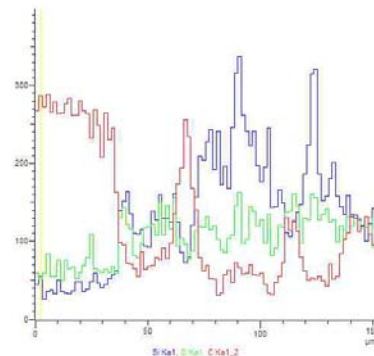
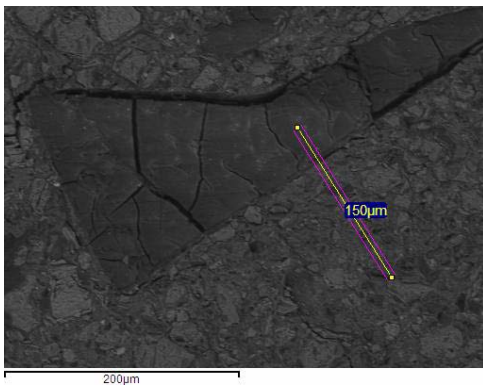
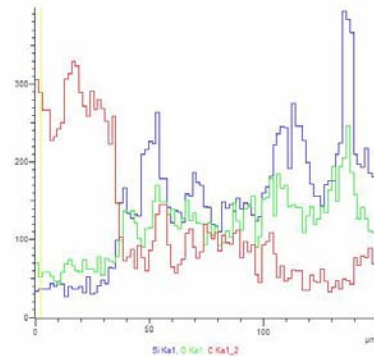
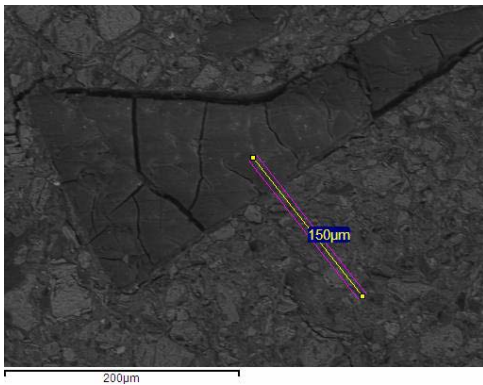
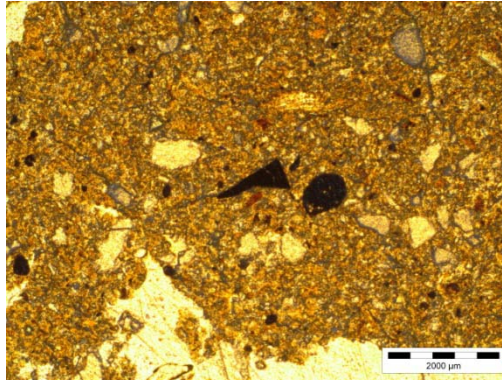


Figure 5.27: Elemental transect away from a **Black carbon** fragment within Broadbalk **FYM** treated soil. Image top right shows the BC-fragment under PPL, image top left shows the BC-fragment under BSI under at magnification. Images to the left show BC under BSI conditions, transect positioning is superimposed. Elemental concentrations along transects are shown, right, Si =blue, O =green, C =red (from BC (0μm) to Matrix (150μm)).

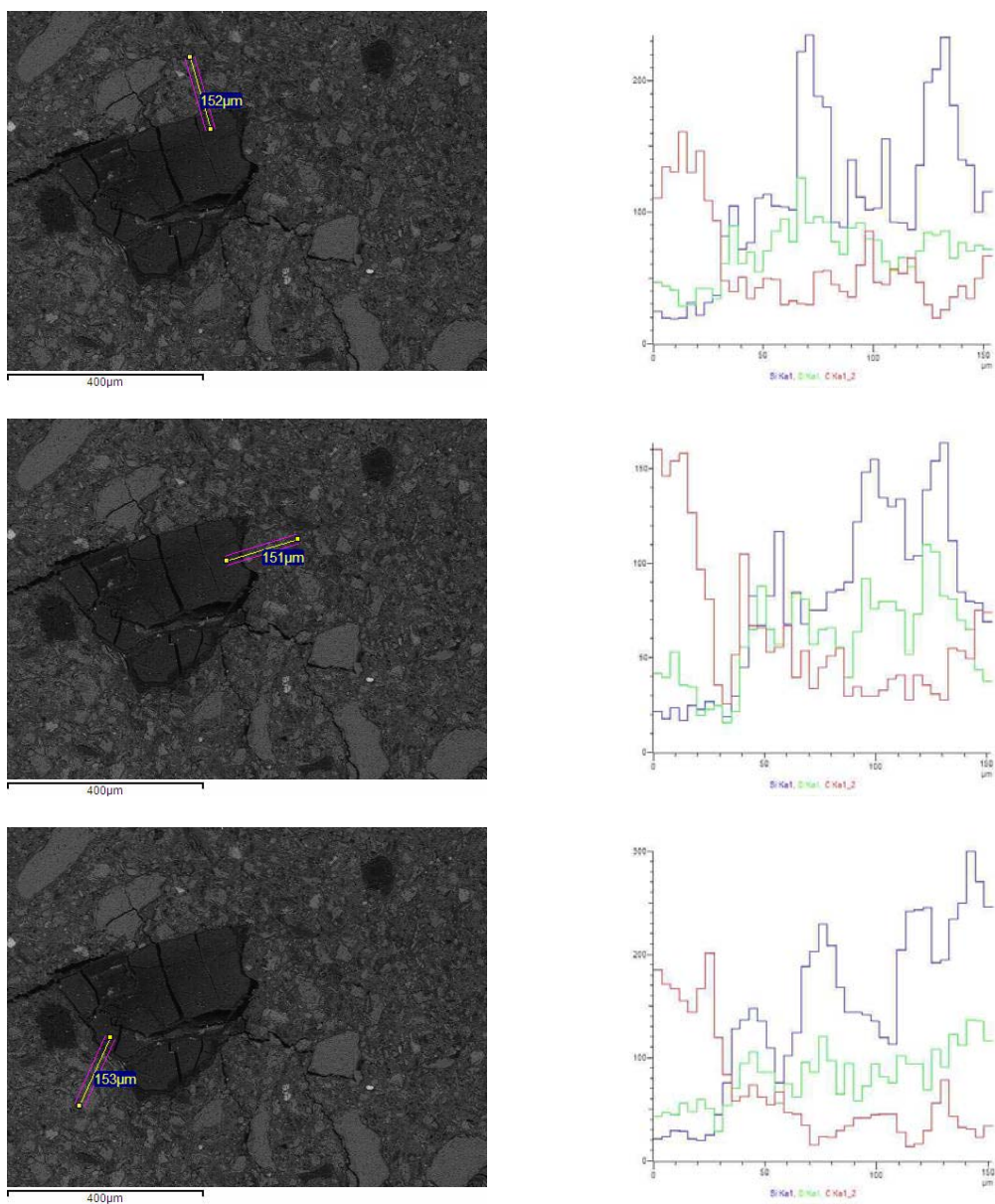


Figure 5.28: Elemental transect away from a **Black carbon** fragment within Broadbalk **Wilderness** treated soil. Image top right shows the BC-fragment under PPL, image top left shows the BC-fragment under BSI under at magnification. Images to the left show BC under BSI conditions, transect positioning is superimposed. Elemental concentrations along transects are shown, right, **Si =blue**, **O =green**, **C =red** (from BC (0µm) to Matrix (150µm)).

5.7 Summary of Results

5.7.1 Total Organic Matter content

- The amount of SOM, is in accordance with the total OC-content.
- There is a significant difference in the LOI of between the wilderness, NIL and Inorganic soil.
- Significant differences in LOI also occur between NIL and FYM soils.

5.7.2 Micromorphology results

- Excremental pedofeatures can be seen across all treatments, but are more consistently found in samples from FYM and Wilderness soils.
- Soils with the highest OC-content (FYM and Wilderness) have a greater variety in the types of pedofeatures.
- Within FYM and NIL soils, disintegration of excremental pedofeatures is largely moderate to strong and excrement is frequently situated within pores or near to OM.
- In the Inorganic treated soil, excremental pedofeatures are found in just two samples, and at low abundance and located within pores or associated with OM.
- Within the Wilderness soil excremental pedofeatures are highly disintegrated and are commonly located in the soil matrix or in pores; they are often found in association with amorphous-yellow-OM.

5.7.3 Images Analysis of Organic Matter

- There is no significant difference in the total area of organic matter among treatments.
- The variance in organic matter area is not equal between treatments, with the percentage area of organic matter area being most variable from FYM-treated soil.
- There are no significant differences in area cover among organic matter classes.
- There is no significant difference in the frequency of organic matter among treatments.
- The frequency of organic matter among OM-classes is significantly different.
- Across all treatments black and red amorphous OM-forms are significantly more frequent than either organ and tissue forms.
- Within the amorphous class, black and red forms are more frequent than amorphous yellow.
- The area of amorphous forms is very small covering, therefore amorphous organic matter occur as numerous but small fragments.

5.7.4 The location of Organic Matter

- There are few differences in the location of organic matter fragments in relation to soil pores between treatments.
- Across all treatments organ and tissue fragments at all stages of decomposition are typically located within soil pores.
- Typically very-strongly decomposed amorphous forms are located near to, or within the soil matrix.
- Amorphous-yellow OM within the grassland soil is located within soil pores, while across other treatments it is situated within the soil matrix.

5.7.5 SEM-EDS: Point Analysis at 5 keV.

- The soil matrix has a significantly higher O:C ratio compared to BC, Tissue-moderate, Tissue-strong and Organ-moderate. The O:C ratio of BC was also found to be significantly lower than Amorphous-red, Organ moderate and Tissue-strong.
- Amorphous red has a significantly greater O:C ratio compared to Tissue-moderate.
- No differences in the O:C ratio were found between any of the organic matter fragments.
- The range of O:C ratio values for organic matter features is wide, while for BC it is much narrower.
- The Matrix has a significantly lower C-content compared to Tissue-moderate, Tissue-organ, BC and Organ-moderate.
- Black carbon has a significantly higher C-content compared to Amorphous-red, Tissue strong and Organ-moderate.
- Amorphous-red has a significantly lower C-content compared to Tissue-moderate.

- The elemental spectrum of BC shows the least variability, in addition low amounts of elements other than C and O are in association with BC making it simple to identify BC using SEM-EDS.
- The variability of elements in spectrums removed from organic features may mean that it is not possible to identify these features solely by elemental analysis, and further supports the need to produce OM-pore maps.
- It is not possible to distinguish between OM features based upon O:C ratios alone. However, it is possible to differentiate between organic matter, Black-carbon and the Matrix.
- The carbon content of the Matrix is lower than all other features sampled while, the C-content of BC is greater than Tissue-strong and Organ-moderate features.

- Stepwise discriminant analysis showed that samples placed in either BC or the Matrix were the most correctly categorised; this further supports the view that the O:C ratios can be used to differentiate these features.
- The capability of discriminant analysis to distinguish between matrix and BC particles is expected given that these features contrast the most in terms of O and C contents.

5.7.6 SEM-EDS: Mapping

- Since it is not possible to differentiate between OM features solely by elemental analysis, this further supports the need for prior micromorphological analysis and the production of OM-pore maps.
- Organic-matter features, were not categorised according to form and decomposition when mapping, since there are few data and previous point analysis revealed no significant difference in the O:C ratio between organic matter classes.
- Phase mapping has allowed the soil matrix to be distinguished from areas which are densely occupied by silicates (e.g. quartz).

5.7.7 SEM-EDS: Comparison of Mapping at 5 and 15 keV

- By increasing the accelerating voltage from 5 to 15 keV it was much easier to pull out resin using phase analysis.
- Furthermore there is a significant difference in the O:C ratio of BC and resin ($p = 0.0093$) at 15 keV but not at 5keV.
- No significant differences were found in the O-content, C-content or O:C ratio between OM and BC, despite the distribution of the values being very different, this is due to the low number of samples within both the OM and BC classes.
- Phase analysis using the relative concentration of C:O:Si to differentiate between features, was more successful at 15 than 5 keV, due to the excitation of heavier elements.

5.7.8 Elemental Transects: Methods and Theoretical Model for Changes in C-Concentration.

- It was found that mapping elemental concentrations across whole areas (at 15 keV) and performing phase analysis to identify features (5.5.7) was the best practise.
- Since it is not possible to subtract the C-contribution by resin, regions densely occupied by resin can be identified by phase analysis and avoided when positioning transects.
- A blank polished crystic resin was sampled, the results demonstrate that within resin there are no pronounced changes in C-content with distance.

- There is a minimal contribution of Si to the resin, while in OM and BC Si occurs in slightly greater concentrations and is most prominent in the soil matrix. Therefore as a control Si is included in the elemental analysis, its presence will further confirm that solid soil material has been sampled and resin avoided.
- In this situation pronounced differences are identified as a trend for a decrease or increase in C-concentration, which is not consistent with background oscillations. It is not possible to assign a numerical upper and lower limit because; the magnitude of change in elemental concentration will vary between areas of interest as concentrations are relative.
- A theoretical model is presented showing the change in C-concentration away from BC and OM particles.
- The model represents the change in C-concentration away from OM or BC particles, the change in C-concentration away from BC particles can follow one of two scenarios depending on whether BC is acting as a source or store of C.
- It was hypothesised that there will be a gradual decrease in C-concentration away from OM or BC particles (when BC is a source of C).
- However if BC is acting as a store of C (e.g. chemically recalcitrant) then beyond the boundary, C-concentration will drop suddenly until reaching an equilibrium.
- The overall magnitude of C-concentration will differ between treatments reflecting differences in total SOC-contents.

5.7.9 Elemental transects: Initial results

- In summary there appear to be a gradual decrease in C beyond the boundary of both OM and BC particles. However from the few features sampled it appears that C from OM extends further into the soil matrix than C originating from BC particles.

Chapter 6 Discussion: The Structural Characteristics of Broadbalk Soils Contrasting in Total Organic-Carbon Content.

In this section the structural differences of Broadbalk soils will be considered. The discussion will compare **a)** the structural differences between soils contrasting in total organic carbon content, and **b)** the structural characteristics proposed by the different analysis; in doing so each of the objectives and hypothesis presented in **Section 4.1** will be addressed.

6.1 Describing the Structural Characteristics of Intact Samples.

Soil aggregation, is infrequent and poorly defined across NIL, Inorganic, FYM and Wilderness soils, and it is difficult to characterise differences in aggregation between these soils which, contrast in total OC-content. Therefore, ***Hypothesis 1.3:** There will be a greater occurrence of strongly developed aggregates within the grassland (Wilderness) soil compared to agricultural treatments (NIL, Inorganic, FYM)* is not accepted. Some broad differences can be distinguished, for instance; in soils with low-OC-contents (NIL and Inorganic) aggregation was more evident at 12.5x, while soils with a high OC-content (FYM and Wilderness) aggregation was more evident at 40x magnification. However aggregation is typically isolated to patches within thin-sections. Due to the infrequency of aggregation, it is difficult to ascertain the scale dependent differences, between soils contrasting in total OC.

Typically granular shaped excrement are frequently identified across all treatments except NIL, the shape and size is indicative of faunal excrement (Stoops, 2003). Interestingly granular aggregates are found within the grassland soil as proposed by ***Hypothesis 1.4:** Aggregates in the grassland soil will typically be granular in shape (reflecting greater biological activity)* but they are not markedly more abundant compared to other treatments. The greater abundance of excremental pedofeatures within grassland soil was expected due to high OC-contents (White, 2006) and undisturbed nature of the system (Pulleman, 2005). However, the absence of a significant difference between treatments in the abundance of excremental features may reflect a seasonal effect. Previous studies have shown that recent C-inputs can be associated with meso/macro-fauna excrement (Davidson and Grieve 2006), therefore greater evidence of faunal activity maybe evident if sampling was performed further into the growing season when rhizodeposition and root turnover is more prevalent. However, the grassland soil (Wilderness) has an established undisturbed root system but shows no marked increase in aggregation hence it is possible that as the root systems of the winter-wheat crop develop, the grade and frequency of aggregates observed within thin-sections removed from agricultural treatments may not differ drastically with seasons. In support of this researchers have argued that “aggregation does not

necessarily imply the development of distinct soil aggregates within the soil profile” (Young *et al.*, 2001).

It is clear that within thin-sections of the Broadbalk soils, it is not possible to define aggregates based on size-classes as is routinely performed for size fractionation of loose soil. Clearly, when fractionating aggregates the size classes retrieved will depend on the force applied (Young *et al.*, 2001) and the strength and nature of OC binding agents. Models of aggregate turnover argue that macroaggregates form around particulate organic matter (Six *et al.*, 1998; Oades, 1984), since aggregates are not evident in thin-sections of Broadbalk soils, there is no evidence that organic matter acts as a nucleation site (**Chapter 5**). These results suggest that, models of aggregate turnover based upon fractionation of the soil do not reflect the true heterogeneity of soil and, therefore, may not fully appreciate the processes of soil structural development.

The abundance and nature of porosity differs with treatment and magnification. The higher abundance of chambers and channels within the Wilderness and FYM soils is indicative of greater biological activity as reported previously (Edwards and Bohlen, 1996; Francis and Fraser, 1998; VandenBygaert *et al.*, 2000; Grieve *et al.*, 2005). This is consistent with these soils receiving greater inputs of SOC and supports **Hypothesis 1.6: Soils receiving the highest C-inputs (e.g. FYM & Wilderness) have a greater proportion of pores of biological origin, through the decomposition of organic-matter, worm-burrowing and root penetration.**

Across all treatments the abundance of planes is greater at 40x than 12.5x, indicating that the throat width of these planes may not be resolved by a hand-held lens. However, the greater incidence of planes at 40x magnification does not translate into a greater occurrence of aggregation. For example, within FYM soil the abundance of planes at 40x (15-30%) is much greater compared to other treatments, however aggregation remains infrequent and weakly defined suggesting these planes are discontinuous. The opposite was found in a separate study, in which no difference in pore structure was evident between soils with an aggregated and massive structure (Pagliai *et al.*, 1981). It is possible that some of the fine planes observed may be an artefact of slide production. However since the abundance of micro-cracks are much greater in FYM, it is probable that they are created by differences in the shrink swell of this soil due to additions of OM. Studies have concluded that organic residue aid the formation of micro-cracks which form around fragments of OM, due to differences in wetting and drying cycles associated with the addition of OM (Garnier *et al.*, 2004; De Gryze *et al.*, 2006). Furthermore, because these planes have a very narrow throat width it is not possible to include them in subsequent image analysis.

In conclusion structural differences between treatments determined by micromorphological analysis provided some evidence for greater biological activity within Wilderness and FYM soils, this is consistent with these soils having a greater SOC content. However, the results are highly variable and suggest that even within the top 25-30cm, regardless of OC-content, biological activity and its impact on soil structure, within both agricultural and grassland soil, is not uniform. To account for any seasonal variability additional sampling would be required later into the growing season.

6.2 Structural Characteristics Determined by Bulk Analysis

The bulk density values determined for Broadbalk soils are consistent with the consensus that bulk-density is negatively correlated with OC-content (Lai and Kimble, 2001), thereby supporting *Hypothesis 1.1: Soils with higher carbon content will have a lower bulk density*. This also reinforces the need to account for the amount and density of soil sampled when calculating SOC-contents (Lai and Kimble, 2001; Don *et al.*, 2007). Structural characteristics of Broadbalk soils from plots FYM and Wilderness, are consistent with them having a higher OC-content, i.e. that the bulk density of the soils is low and there is a greater incidence of pores formed through biological activity; as has been reported in previous studies (Edwards and Bohlen, 1996; Francis and Fraser, 1998; VandenBygaart *et al.*, 2000; Grieve *et al.*, 2005). Previous studies have demonstrated a positive relationship between SOC-content and soil porosity (e.g. Zawadzki, 1970), it was not possible to run a correlation analysis due to the size of the data set. However **figure 6.1** demonstrates the relationship between SOC and soil porosity are consistent with previous studies.

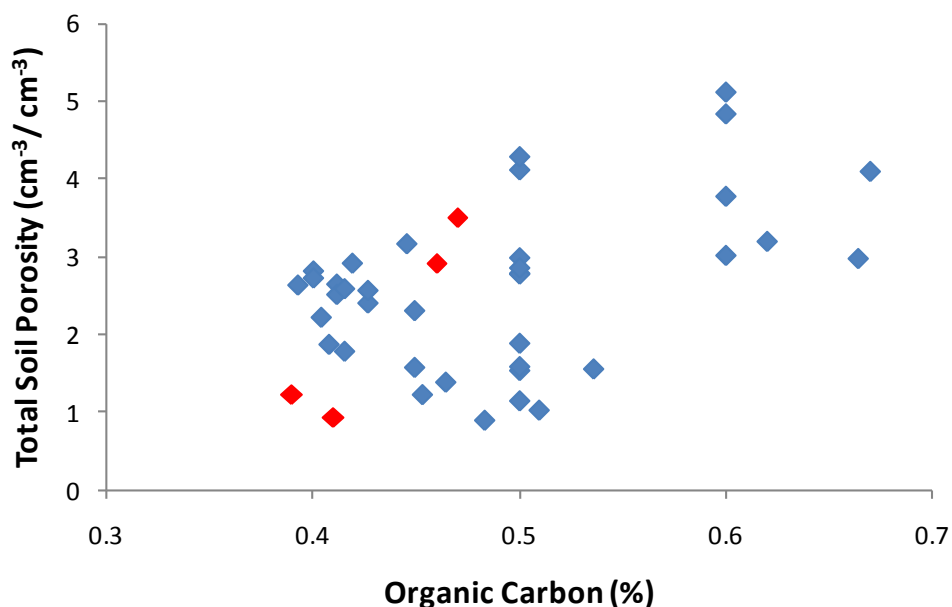


Figure 6.1: Demonstrating the relationship between SOC and soil porosity. Values in red represent data obtained by this study, values in blue are published values taken from: Barral *et al.*, (2007), Miralles *et al.*, (2009), Verma & Sharma (2007), Bhogal, Nicholson & Chambers (2009), Abid & Lai (2008).

Differences in aggregate water stability following the fast wetting treatment are consistent with OC-content, i.e. aggregate stability increases with SOC-content. In addition calcite (pg. 72) is observed in all treatments which, in turn could aid soil structural stability. No significant differences were found between soils with the lowest OC-contents (NIL and Inorganic) and the highest OC-contents (FYM and Wilderness). Previous studies have show that the fast-wetting treatments are best at discerning differences between soils with contrasting OC-contents, however this method may overemphasise slaking of soils (Grieve, 1980; Le Bissonnais, 1996). Previous analysis of the Broadbalk soils reported the same pattern of aggregate stability NIL (MWD =0.66 mm), Inorganic (MWD =1.09 mm), FYM (MWD =1.11 mm), Wilderness (MWD =1.62 mm) (Blair *et al.*, 2006); however unlike the results presented here, Blair *et al.*, found no significant difference in the MWD between Inorganic and FYM treated soils. The greater aggregate stability of the grassland (Wilderness) soil may be a consequence of these soils receiving higher inputs of labile carbon, the labile OC-fraction within the Wilderness soil can be up to 85% greater than Broadbalk agricultural soils (Blair *et al.*, 2006). Blair *et al.*, (2006) argue any further additions of liable carbon to agricultural soils will increase MWD, however in the Wilderness this will not be the case as aggregate stability has neared its maximum. In addition the lower pH of the wilderness compared to other treatments (pg. 67) indicates that decarbonation is occurring and in conjunction with Ca^{2+} (as calcite observed within soil thin-sections pg. 72) this favours humification and therefore soil aggregation.

In this study no comparison was made between soils both with and without straw applications and all of the agricultural soils analysed in this study received additions of straw. Blair *et al.*, (2006) reported that soils treated with straw have a greater MWD compared to those not receiving straw. Some studies have shown that additions of FYM can lead to a decrease in aggregate stability, due to the high prevalence of monovalent cations which promote the dispersal of soil colloids (Nymangara *et al.*, 2001). However, consistent with the results from Blair *et al.*, (2006) the addition of FYM to Broadbalk soils increased aggregate stability.

Differences in aggregate stability between soils was also discerned by the pre-wetting treatment followed by mechanical disruption, however the pattern of aggregate stability does not reflect the OC-contents of the soil, with the Wilderness soil having the lowest MWD while no significant differences were detected between agricultural soils. This result may reflect the hydrophobic nature of OM contained within aggregates which could be aiding aggregate stability by reducing soil wettability as concluded in previous studies (Bartoli, *et al.*, 1988a). For instance straw additions may be aiding water repellence in agricultural soils (Blair *et al.*, 2006), this may explain why after pre-wetting followed by mechanical disruption, it was found that agricultural soils have a greater MWD compared to the grassland soil. Therefore, **Hypothesis 1.2: Water-aggregate stability is positively associated with total soil-organic-carbon-content**, is accepted. However, the processes occurring remain unclear;

it is likely that OC has a dual role by enhancing bonds between soil particles and the hydrophobic nature of aggregates.

6.3 Quantifying Porosity within Structurally Intact Soil.

The majority of studies applying image analysis to thin-sections have done so to investigate differences in porosity between different tillage practises, few have investigated differences between grassland and cultivated soils or between soils contrasting in total OC-content.

Image-analysis at 12.5x and 40x revealed no differences in the macro porosity and frequency of pores between treatments (see **Fig. 6.2** for an example). Interestingly, at both magnifications macro porosity across soils removed from NIL and FYM plots showed the most variability, these agricultural soils contain the lowest and highest amount of OC, respectively. This indicates that, total macro-porosity is highly variable at the plot-scale within NIL and FYM plots and additional sampling is required to fully account for this variability. The variability in total macro-porosity across the FYM plot is consistent with field observations that FYM was not evenly incorporated. These results are not consistent with previous findings; Emerson and McGarry (2003) reported an increase in porosity with SOC-content. However, studies investigating the effect of SOC upon porosity at the microscale are limited.

It was decided that pore shape is the most valid attribute to compare porosity characteristics between soils. This is because shape is indicative of pore function and genesis; typically matter is transported within Planes and stored within Irregular and Rounded pores (Pagliai *et al.*, 2004). Pore area for pores classified by shape was significantly different at both 12.5x and 40x, with pore area decreasing from planes to irregular to rounded pores. This is expected given the large area to perimeter ratio of planes and is consistent with previous findings (Pachepsky *et al.*, 1996; Chun *et al.*, 2008). Furthermore a significant difference was found in the frequency of pores between planes and smaller pores (irregular and rounded shapes) at both 12.5x and 40x; this is expected given that the number of pores decreases exponentially as size increases (Edwards *et al.*, 1988; Chun *et al.*, 2008). At 40x there is an interaction between treatment and pore shape, it is not possible to test for an interaction for data recorded at 12.5x (and therefore differences in area between pore shape*treatment combinations) as the data are not normally distributed and transformations failed to normalise the data. The interaction between pore shape and treatment at 40x, translated into few pronounced differences between treatment*pore shape combinations. In summary it was found that, the areas of rounded pores from the Wilderness are significantly smaller than irregular pores from all other treatments. One possibility is that these smaller rounded pores are formed by fine plant roots or small burying animals which would be less frequent in agricultural systems due to tillage activities and time of sampling (i.e. the root system of

the winter-wheat was largely undeveloped). However, the area cover of rounded pores is small (less than 2%), this may simply reflect their orientation within the 2D sample or that pores produced by plant roots are still occupied by roots at the time of sampling.

It is assumed that cultural practises mainly affect pores $>30\ \mu\text{m}$, (Hubert, 2007). The minimum pore size detected in this study is $20\ \mu\text{m}$. No differences in porosity were detected between agricultural soils, this could be a result of agricultural practises overriding any differences between soils due to OC-content. For instance Drees (1994) concluded that tillage activities considerably masked the effect of earthworms upon soil structure. However, this does not explain why differences in porosity characteristics between grassland (Wilderness) and agricultural soil are not detected as concluded by previous research. For instance, Blank and Fosberg (1989), found that within the upper horizon of cultivated soils, total macro-porosity was lower compared to adjacent virgin fields, they attributed this to a lower abundance of interpedal packing voids, which are found within aggregated soil. In addition, it has also been shown that total macro-porosity of pastures can be twice that of adjacent cropped fields (Putenes and Wilding, 1990) and that the activities of earthworms can increase macroporosity within grassland soils (Capoweiez *et al.*, 2000; Grieve *et al.*, 2005).

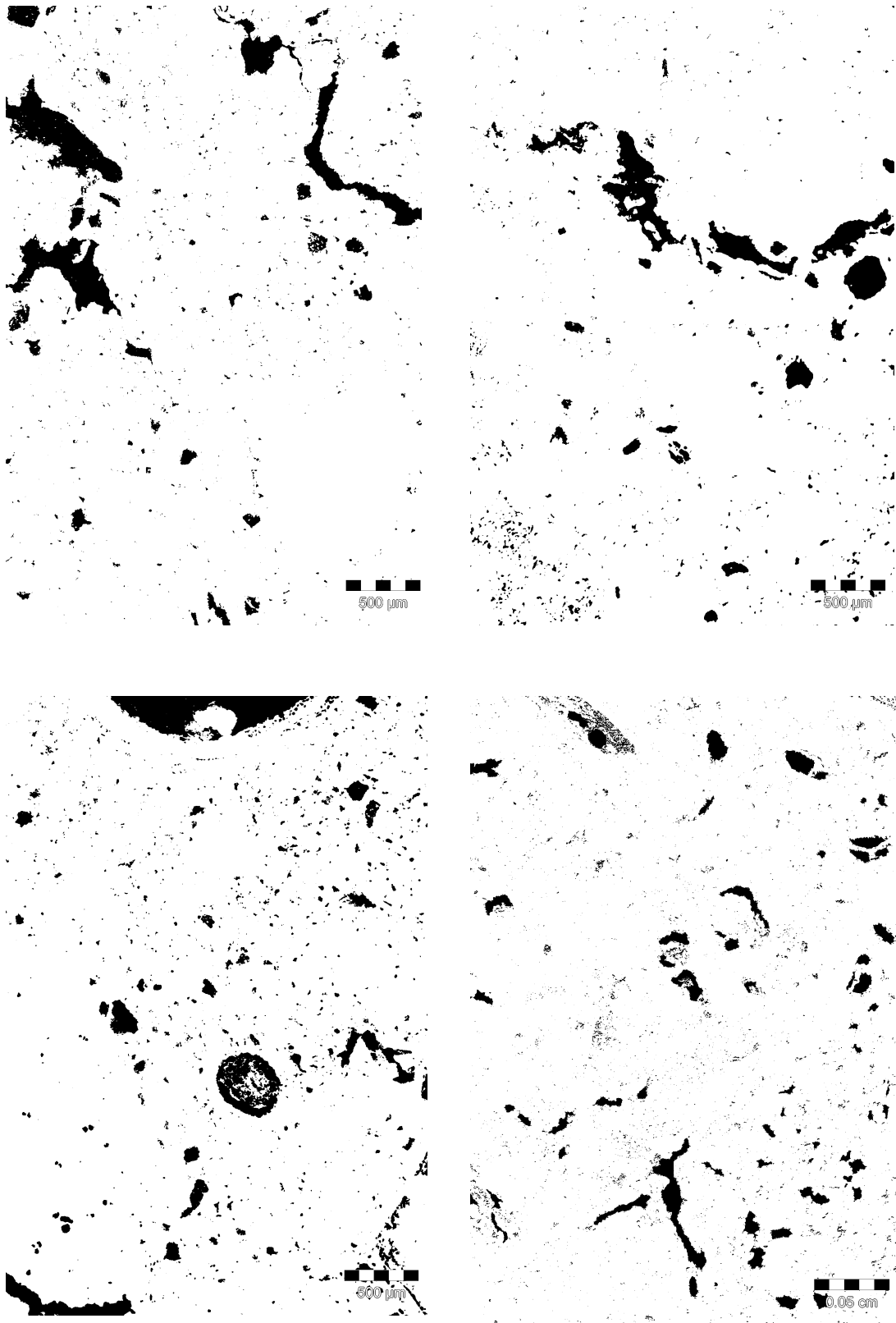


Figure 6.2: Examples of the porosity characteristics determined by image analysis (minimum threshold = 100 μm) . Taken from: Broadbalk NIL (*top left*), Inorganic (*top right*), FYM (*bottom left*) and Wilderness (*bottom right*) soil.

It could be argued that, the regularity of porosity characteristics is consistent with micromorphological evidence that there is no difference in aggregation across treatments. However previous research has concluded that total macro-porosity and aggregation are not necessarily related (Li *et al.*, 2004). Since previously, pronounced differences in porosity between land-use have been detected, and studies have shown inconsistencies with total macro-porosity and aggregation (Li *et al.*, 2004), it is argued that total macro-porosity may not be reliable statistic for quantifying differences in porosity between soils. An alternative explanation could be that the REA of the slide analysed was inadequate for detecting differences between treatments, for instance Bartoli *et al.*, (2005) concluded that the mean porosity calculated by image-analysis to be similar to bulk density values. Consistent with this, the bulk density of the Wilderness is significantly lower than FYM treated soil, indicating that much of the differences in density is created by micro-pores (<100 μm) excluded from image-analysis.

6.3.1 Quantifying Porosity within Structurally Intact Soil: Pore Size Distribution.

Since no difference in total macro-porosity is detectable between treatments, pore size distributions determined by image analysis were compared to investigate if more discrete differences could be detected. Taking into consideration that pore size distributions are typically highly skewed due to the relationship between the volume and frequency of pores (Chun *et al.*, 2008), it is reasonable to expect that pore size distribution will be a more sensitive parameter than total macro-porosity.

Pore-size distribution curves were fitted with a linear + exponential curve, for treatments using data collected at 12.5x. The results showed that a common curve could not be fitted to the treatments and that separate curves account for 90.9% of the variance. The same procedure was repeated for pores analysed at 40x. The curves fitted explained 93.3% of the variance; it was found that a common shape parameter could be fitted to all treatments while separate linear and curve parameters were required.

In summary, at 12.5x and 40x, across all treatments, accumulative area rapidly increases when pores size is $<1.5 \log_{10}\text{ECD}$, this reflects the high frequency of smaller pores. Total macro-porosity area and frequency analysis demonstrated that smaller pores are predominantly irregular or rounded in shape (**Section 4.6**). As pore size increases there is a marginal decrease in the rate of accumulative area, reflecting that larger sized pores are less frequent as supported by total area and frequency by shape analysis which showed planes to large but less frequent.

As summarised, a common curve could not be fitted to the pore size distributions measured at 12.5x. When comparing the curves it is clear that FYM and Inorganic have a similar pore size distribution. In the Wilderness rounded and irregular pores, which are in size, contribute more to total macro porosity in comparison to other treatments. In the NIL soil it is clear that larger shaped pores make a greater

contribution compared to other treatments, reflecting the large upper-quartile range of planes within NIL soil as presented in **Section 4.6**. At 40x a common curve could be fitted to all treatments, although a different shape parameter was required. In general at 40x smaller pores account for a much larger proportion of the total macro-porosity compared to the results from 12.5x, this is expected given the higher resolution at 40x. As previously outlined in **Section 4.8.1**, the fitting of a linear + exponential curve demonstrates that at both 12.5x and 40x pore size distribution is bimodal, which suggests that separate processes are occurring to produce smaller and larger sized pores. The bi-model nature of pore size distributions has been attributed to the presence of interaggregate macropores and the interaggregate micropores (Brewer, 1964; Bartoli *et al.*, 2005).

These results indicate that soils contrasting in total OC-contents and soils that have similar OC-contents (FYM and Wilderness) but differ in land-use (agriculture versus grassland), have different porosity characteristics, though this appears to be scale dependent. These results appear to contradict the findings from analysis of total macro-porosity, however it is argued that this further supports that total macro-porosity is not sensitive at quantifying differences between soils contrasting in total OC-content and land-usage. Therefore, **Hypothesis 1.7: The pore size distribution is better at discriminating between soils contrasting in total organic carbon content than total macro-porosity**, is accepted.

6.3.2 Quantifying Porosity within Structurally Intact Soil: Differences with Scale.

Since there is a synergy between the total macro-porosity results collected at 12.5x and 40x, this suggests that scale effects are not influencing porosity, however there is an overlap in the range of pore sizes measured at both magnifications and as highlighted previously, total macro-porosity is not the most sensitive parameter to use to investigate differences in porosity. Alternatively it is likely that the REA used to measure macroporosity at 12.5x was insufficient at incorporating the variability of larger sized pores.

When plotting the PSD at 12.5x a common shape parameter could not be used to fit the curve, when comparing the curves (**Fig. 4.15b**) it is clear that soils with the lowest and highest carbon content differ the most. At 40x all parameters, except shape, used to plot a common curve are the same. Therefore, the PSD highlights that there are some differences in porosity characteristics at different scales, are detectable between Broadbalk soils and that by using total macro-porosity alone this may have been overlooked.

6.4 Water Release Characteristics.

It was found that a common logistic regression curve could not be fitted to the treatments. The initial water loss at -100 kPa indicates that water loss was greatest from soils in the order of: FYM > NIL > Inorganic > Wilderness. The greater initial loss of water from FYM compared to other treatments may be indicative of the greater abundance and nature of organic matter inclusions, which alter the daily shrink-swell properties of the soil possibly creating the planes observed in the soil by micromorphology, but excluded from image analysis. The initial high loss of water from NIL treatments is consistent with the pore size distribution, which demonstrates that this soil has a higher occurrence of planes, but image analysis showed this to be variable across plots. While the small initial loss of water from the Wilderness soil, is consistent with image-analysis results that the area cover of planes is smallest within this soil. This variability may reflect the inherent shrinkage properties of the soil and how the greater OM content of the grassland enhances its resilience to stress as has been previously concluded by Gregory *et al.*, (2010). For instance, the greater OM-content, means that a range of pore sizes occur within the grassland soil and as a result show this soil is not dominated by large planes as is evident within the NIL treatment.

However the slope of the curve decreases from Wilderness (-5.23), NIL (-3.582), Inorganic (-1.1876) to FYM (-1.66) soils; meaning that at a given matric potential, soils with a steeper slope will release more water. The water release curve is a function of not only the size and shape of pores but also the connectivity of pores (Whalley *et al.*, 2005). For instance soils may contain pores which themselves are too small to drain, but act as passage for water to drain out of larger pores (Hillel, 1982). Alternatively, image analysis quantifies a narrow pore range and many small and large sized pores are excluded from the analysis. It is not possible to fully compare the results from PSD and WRC due to differences in the timing of soil sampling. However overall, the water release characteristics indicate that the soils behave differently in the way that they release water, and that the size and arrangement of pores in 3D soils may be far more different than suggested by image analysis of 2D thin sections.

6.5 The Occurrence and Nature of Organic Matter in and between Soils Contrasting in Total Organic Carbon Content.

In this section the nature and distribution of organic matter and organic carbon between soils contrasting in total organic carbon content will be discussed; in doing so a new method for examining the distribution of OM and OC within intact soil samples will be assessed. Each of the objectives and hypotheses presented in **Section 5.1** under **aim 2** will be addressed.

6.5.1 Describing Organic Inclusions within Intact Samples.

Excremental features have previously been discussed in terms of their impact upon soil structure (**Section 6.1**). The abundance of excremental features is also used as a proxy for the biological activity of soil biota. In this section the abundance, form and location of excremental features occurring in soils contrasting in total OC-content will be discussed.

As outlined in **Section 6.1** the abundance of excremental pedofeatures is greatest within soils with the highest total organic carbon content (FYM and Wilderness). Therefore **Hypothesis 2.2a:** *The occurrence of excremental pedofeatures will be greater in soils with a higher OC-content*, is accepted. This is expected given that organic matter and organic carbon acts as a “hot spot” for faunal activity (Barrios, 2007). Across all treatments excremental features are located either within pores or near to organic matter fragments. Notably, within the Wilderness soil excremental features are associated with amorphous yellow OM. The location of excremental features is consistent with soil macrofauna initialising decomposition by breaking organic matter into smaller fragments (Barrios, 2007).

The diversity and abundance of biota within a soil is dependent upon productivity (resource availability) and disturbance (which can be biological, physical or chemical in nature) (Cole *et al.*, 2008). Within agricultural systems the diversity and abundance of meso and macro fauna is typically less than that observed within grassland soils. For instance earthworm abundance in agricultural soil is lower than grasslands and it has been shown that tillage practises can alter earthworm abundance and diversity (Chan, 2001). In this study, it was found that the variety of excremental features (indicative of faunal diversity) was greatest within FYM and Wilderness compared to Inorganic and NIL soils. However, there was not a marked difference in the variety of excremental features between different land usages as predicted. Therefore **Hypothesis 2.2b:** *A greater variety of excremental pedofeatures will be associated with the Wilderness soil compared to soils from Broadbalk Winter-Wheat*, is rejected. However, disintegration of excrements with age may have limited the identification of different forms; this is consistent with excremental pedofeatures located within the Wilderness soil being highly disintegrated.

Excremental pedofeatures have an important impact upon soil structure, the magnitude of which is dependent upon the system, for instance within upland grasslands excrements can constitute up to 80% of organic horizons (Davidson, 2007). These results suggest that within agricultural and mown grassland systems the contribution of excrement to soil structure is spatially variable, with excremental pedofeatures occurring within distinct patches largely associated with organic matter fragments.

6.5.2 The Nature and Quantification of Organic Matter within Intact Samples.

The area cover of organic matter was quantified using image analysis. There is no difference in the area cover or frequency of OM among treatments; this is inconsistent with the results from LOI analysis (proxy for OM-content), which found that LOI was significantly different between the two highest and the two lowest OC-containing soils (**Section 5.2**). Based on the image analysis results, *hypothesis 2.1: The volume of organic-matter is positively associated with total soil-organic-carbon content*, is rejected. However, this discrepancy is likely to be caused by an error when calculating the REA on which to perform IA because the REA was calculated based upon variations in pore area and not OM. Therefore, only with further analysis in which the variation of pore and OM area is accounted for when setting the REA, can it be determined whether IA of thin-sections can demonstrate the differences in SOM content between soils as indicated by traditional analysis. The variability between samples was greatest for soils with the highest compared to the lowest OC-contents, therefore further supporting that the REA may not have been appropriate. The high variability in the area cover of OM within samples removed from FYM treated soil is consistent with field observations which showed FYM to be unevenly incorporated at the field level.

Micromorphological analysis revealed that OM occurs at a range of decomposition stages across all treatments and that there is no significant difference in the area cover among OM classes. However, fresh/living organ and tissue OM-forms are noticeably absent from all treatments; one exception being, the occurrence of Organ Fresh/living fragments within the Wilderness soil. The absence of Fresh/living OM is likely to reflect a seasonal effect, specifically at the time of sampling the inputs of fresh OM into the soil may have been limited because the plant growing season initialises in March (Patra *et al.*, 1990).

Interestingly, the frequency of OM is significantly different between classes, with Amorphous red and black being most frequent across all treatments compared to Organ and Tissue forms. Therefore the very strongly decomposed forms of OM are more frequent than the less decomposed organ and tissue forms. This could be a consequence of the decomposition process, i.e. reflecting that as OM is decomposed by meso/macro fauna it is disintegrated into many smaller fragments (Barrios, 2007).

The median area of amorphous black is greatest in FYM treated soil, compared to other treatments, although this difference is not significant. Subsequent elemental analysis (SEM-EDS) of black particles reveals some of these inclusions to be coal due to the presence of S however; this is not consistent across all black particles. An alternative hypothesis is that some of the black particles were added to the soil with past applications of FYM. Archaeological studies of past human waste procedures have revealed that burnt waste material from household hearths are added to dung heaps before being distributed onto nearby fields (Davidson, *et al.*, 2006) (Davidson *et al.*, 1996). The

continuous exploitation of Broadbalk for agricultural experimentation explains why BC is located within the upper horizons and is continuously redistributed through the plough horizon.

6.5.3 The location of Organic Matter within Intact Samples.

The location of OM was described in relation to soil pores and there are few differences in the location of OM between treatments. Across OM classes a broad distinction in the location of OM can be seen between less decomposed (Tissue and Organ) and more decomposed (amorphous) forms. It was found across all treatments that organ and tissue forms are typically located within pores while amorphous OM is located near to pores or incorporated into the soil matrix. One exception is amorphous-yellow OM, within the grassland soil it is located within soil pores, while in all other treatments it is situated within the soil matrix. Therefore, *Hypothesis 2.3: Organic-matter fragments of varying form and decomposition differ in their distribution in relation to soil structural features, with more decomposed organic matter being located away from soil pores*, is rejected. Although this hypothesis is rejected the results indicate that a simplified hypothesis would have sufficed, since OM which contrasts broadly in terms of form (e.g. Organ and tissue versus amorphous) are situated differently in the soil. It is argued that differences in location of OM by form will largely be a consequence of decomposition processes, however it is likely that several processes are occurring simultaneously, these will be discussed below.

The location of organ and tissue forms indicates in-situ decomposition; as decomposition proceeds a pore forms around OM-fragments, this has benefits for enhancing water and air flow (Batey, 1988).

The differing location of OM may be a product of earthworm activity. For example, as organ and tissue forms are ingested, OM is intimately mixed with mineral particles (Brown *et al.*, 2000), with disintegration of excremental pedofeatures amorphous organic matter is consequently incorporated within the soil matrix. Therefore, the digestion of OM results in OM that is completely reconstructed, not only by the actions of macro and meso fauna but also microorganisms. This creates amorphous OM which is intimately associated with the soil matrix. In 2:1 clay dominated soils, like at Broadbalk, amorphous OM functions as a binding agent by creating polyvalent-OM complexes, which then bind with negatively charged clay surfaces (Six *et al.*, 2000c). In turn these organo-mineral complexes confer protection to OM from further decomposition (Baldock and Skjemstad, 2000; Oades, 1988), this protection is likely to be a temporary rather than permanent thereby leading to a reduction in the rate of decomposition compared to an equivalent form of unprotected OM (Baldock and Skjemstad, 2000). The ability of OM to adsorb to mineral surfaces within Broadbalk soils is demonstrated by the high total clay content, but also the presence of amorphous Fe oxides as indicated by micromorphological analysis. The microscopic analysis revealed that Fe and clay coatings are common across all treatments (**Section 5.3**).

The process of decomposition from the initial stages to the incorporation of OM into the soil matrix and the physical protection conferred by organo-mineral associations explains why amorphous forms of OM are more frequent (than organ and tissue) and are much smaller in size. It also indicates that a continuum of OM decomposition occurs, from unaltered OM structures to highly decomposed amorphous forms which are smaller in size (Baldock and Skjemstad, 2000). This is well accepted and studies using loose soil, fractionate OM into particulate organic matter (POM) and amorphous forms (Baldock *et al.*, 1992; Hassink *et al.*, 1997; Six *et al.* 2000a). Future studies researching OM within thin-sections will need to implement a similar method which retains this distinction (**Section 7.6**), while having the added advantage of ascertaining the location of OM in relation to soil structure. Furthermore the finding that amorphous OM forms are intimately associated with mineral particles (and therefore more likely to receive protection by forming organo-mineral complexes); is consistent with the increasing evidence that, microbially and faunally derived OM constitutes a greater proportion of the stable OM fraction (see the review by Lutzow *et al.*, 2006).

The location of OM is consistent across both agricultural and grassland soil, therefore the redistribution of amorphous OM into the soil matrix is not solely a consequence of tillage activities. Interestingly, within the Wilderness soil amorphous yellow is located within soil pores this is not observed in any of the agricultural soils. One hypothesis is that within the grassland soil OM-fragments are more rapidly decomposed in-situ, due to the higher inputs of labile carbon as reported by Blair *et al.*, (2006) i.e. creating a priming effect. This is supported by the greater incidence of excremental features associated with Amorphous-Yellow forms in grassland compared to agricultural treatments. Alternatively, it may also reflect that OM within the agricultural system is more rapidly incorporated into the soil matrix due to cultivation, which in turn stimulates decomposition (Batey, 1988).

The SEM-EDS analysis of amorphous black particles confirmed that many of the features identified under the light microscope have an O:C ratio consistent with particles that had been formed by pyrolysis (0.02-0.15). Interestingly BC is consistently incorporated into the soil matrix across all treatments. Despite the reported recalcitrant nature of BC and potential C-sink within soils (Goldberg, 1985), previous studies have shown that lightly charred BC can be exploited by decomposers (Kaal & Van Mourik, 2008) (**Figure 6.3**). The evidence that BC can be decomposed is further indicated by the range in form of BC, for instance BC can exhibit cellular structure (e.g. charcoal) or be amorphous and form complexes with organo-mineral OM. Clearly the ability of organisms to exploit BC will vary with the extent of charring. Alternatively, within agricultural soils, BC may be incorporated into the soil matrix as a result of cultivation activities. The intimate contact of BC particles with the soil matrix indicates that some form of interaction with soil minerals is likely. This is consistent with

findings from Kaal & Van Mourik (2008), who concluded due to the morphology and location of BC within thin-sections it is probable that BC is resistant to decomposition through a combination of chemical recalcitrance (Krull *et al.*, 2003), sorptive interactions (Czimcik & Masiello, 2007) and inclusion within microaggregates (Brodowski, *et al.*, 2006). However, the degree of interaction of BC particles is influenced by the type of biomass and temperatures used to create it (Binh *et al.*, 2010) (discussed in Section 7.3).

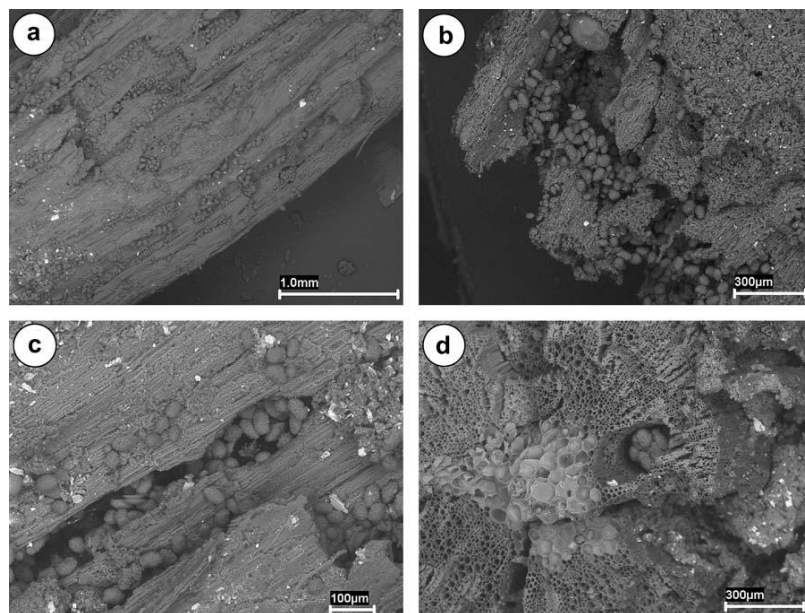


Figure 6.3: SEM images showing evidence for faunal exploitation of charcoal, taken from Colluvial soils, Campo Lameiro, Spain. Images Taken from Kaal & Van Mourik, 2008.

6.6 Identifying Features within Intact Samples using SEM-EDS

The following section will discuss the use of SEM-EDS to identify OM features within thin sections. The method has previously been used to identify black carbon within loose and thin-sectioned soil samples, as yet no previous studies have investigated the use of SEM-EDS to identify and map OM features within soil thin-sections.

6.6.1 Elemental Analysis of Features at 5 keV

Previous studies have reported that using the atomic O:C ratio is an effective method to identify BC features within loose and thin-sectioned soil samples. One objective of this study is to investigate if this approach can be extended to the identification of OM features within soil thin-sections.

Consistent with previous studies it is possible to identify BC particles based upon O:C ratios. Point analysis of BC revealed that it has a significantly lower O:C ratio compared to the Matrix, Amorphous-Red, Organ-Moderate and Tissue-Moderate features, this is due to a significantly higher C-concentration. However, there is an overlap in the O:C ratio of BC and OM features with resin. Analysis of OM also showed a limited difference in the O:C ratios between different forms and classes of decomposition. The only significant difference was found between Amorphous-Red which had a significantly lower O:C ratio than Tissue-Moderate. The concentration of elemental C associated with OM is greater than matrix features. However the concentration of elemental C associated with BC is greater than all OM classes (except Tissue-Moderate), therefore **Hypothesis 2.4b**: *A Higher amount of elemental C will be associated with organic matter fragments*, is rejected. Consistent with the O:C results the only significant difference in elemental C among OM classes is between Amorphous-Red and Tissue-Moderate classes. In conclusion, it is not possible to distinguish between OM features based upon O:C ratios alone ($p > 0.03$), therefore, **Hypothesis 2.4a**: *Classes of organic-matter classified using micromorphology have a distinct O: C ratios*, is rejected. However, grouping point data into a broad classification it is possible to differentiate between organic matter, Black-carbon and the Matrix ($p < 0.03$), therefore there is some scope in applying SEM-EDS analysis to assist with the coarser classification of features.

Elemental spectrums were compared to investigate if features differed in their chemical signatures, however few differences between features in their elemental composition were found. Stepwise discriminant analysis was used to investigate whether features had been correctly classified according to their elemental spectrum collected by point analysis; the stepwise function works by only testing for differences using factors that are most variable between classes. Stepwise discriminant analysis reduced the elemental spectrum to just C and O concentration (mg/kg), reflecting that the hardware was optimised for C detection. The analysis concluded that features placed into either BC or the Matrix were the most correctly categorised. The capability of discriminate analysis to distinguish between matrix and BC particles is expected given that these features contrast the most in terms of O and C concentrations, this further supports that the O:C ratios can be used to differentiate between these features (Davidson 2006; Brodowski, 2005; Stoffyn-Egli et al., 1997). According to discriminate analysis, Tissue-strongly decomposed had the greatest proportion of correctly classified features among all the OM classes. Therefore **Hypothesis 2.4c**: *Features classified using micromorphology will have a distinct elemental signature*, is rejected in that only BC and Matrix features can be systematically classified according to chemical composition.

Due to the few elemental differences between OM fragments detected by point analysis and difficulties in identifying some amorphous forms of OM, when mapping, OM features are not categorised according to form and decomposition. Phase analysis using the relative concentration of C:O:Si was found to be a very effective method for differentiating between features and **Hypothesis**

2.6: *Features previously classified using micromorphological classification, can be identified using the relative concentration of C:O:Si, is accepted.*

There is a discrepancy in the results between those collected by point and phase analysis. In summary, point analysis revealed that BC has a significantly lower O:C ratio compared to some OM fragments: Organ-Moderate and Tissue-Strong. However mapping revealed no significant difference in the O:C ratio between OM and BC. One explanation is that the lack of elemental differences amongst features by phase analysis maybe due to edge effects, i.e. border pixels may contain x-ray data from two different phases. However, phase analysis of features is consistent with the extent of features identified within BSI mode and by image analysis. However at 5 keV there was some difficulty in phasing resin this was resolved by using an accelerating voltage of 15 keV.

Most interesting are the results from black carbon analysis. The association of elements in addition to O and C with BC is inconsistent between particles analysed. Previous studies have reported BC to be an important store of elements, with S, Ca, Si being associated with the surfaces of BC (Davidson et al., 2006) (Stoffyn-Egli et al., 1997). Analysis of BC within this study revealed that S and Si are inconsistently detected at the surface of BC particles. In addition there are few differences in the O:C ratio and C-concentration between BC and organic features when mapping. In addition, between BC and tissue-strongly decomposed fragments, there is an overlap in the O:C ratio and chemical signature, revealed by Dunn's and principle component analysis, respectively. However, mapping at 15 keV at a higher resolution produced more pronounced differences in the O:C ratio between these features (**Section 5.6.4.2**). Therefore it is argued that while it is possible that some BC particles have been misclassified, the success of mapping at 15 keV (at a higher resolution) further supports that edge effects are largely responsible for the overlap in the O:C ratio of BC and OM with mapping at 5 keV, the low resolution mapping means that when phase mapping pixels may contain x-ray information from several sources. This suggests that with further investigation a more precise methodology could be developed to identify BC and amorphous black organic particles not produced by pyrolysis. (**Section 3.4.8**)

6.6.2 Elemental Analysis of Features at 15 keV

It is not possible to isolate the C signal from resin, instead resin can be separated from other features by phase analysis. However at 5 keV there was some difficulty in separating the resin from OM and BC features. To improve separation a higher accelerating voltage was used (15 keV), which is still within the limits recommended by Goldstein (2003) and ensures heavier elements associated with OM and BC features are excited. In conclusion, the most successful phase mapping was achieved using an accelerating voltage of 15 KeV, a spot-size between 750-800 and a map resolution of 525 x 525 pixels (pixel = $1.9\mu\text{m}^2$) (**Figure 6.4**). This set-up combined with a variable pressure SEM system meant image quality is vastly improved and as surface charging is prevented resolves any need for sputter

coating. Due to time limitations the amount of analysis that could be performed was limited, therefore analysis was restricted to testing mapping and transect data collection.

The success of phase analysis meant that differences in the O:C ratio between BC, OM and resin are more pronounced, although it is not possible to test for significant differences between OM and BC due to small and uneven sample sizes. This difference supports that when BC occurs in complexes it can be differentiated from OM using the O:C ratio as argued by (Brodowski et al., 2005) but also thin-sections as achieved in previous studies by point analysis (Davidson et al., 2006). The O:C ratio of OM and resin are similar but this is consistent with resin containing a plant derived polymer. This drawback was overcome by phase analysis which at 15 keV was very effective at separating OM and Resin features (**Figure 6.4**)

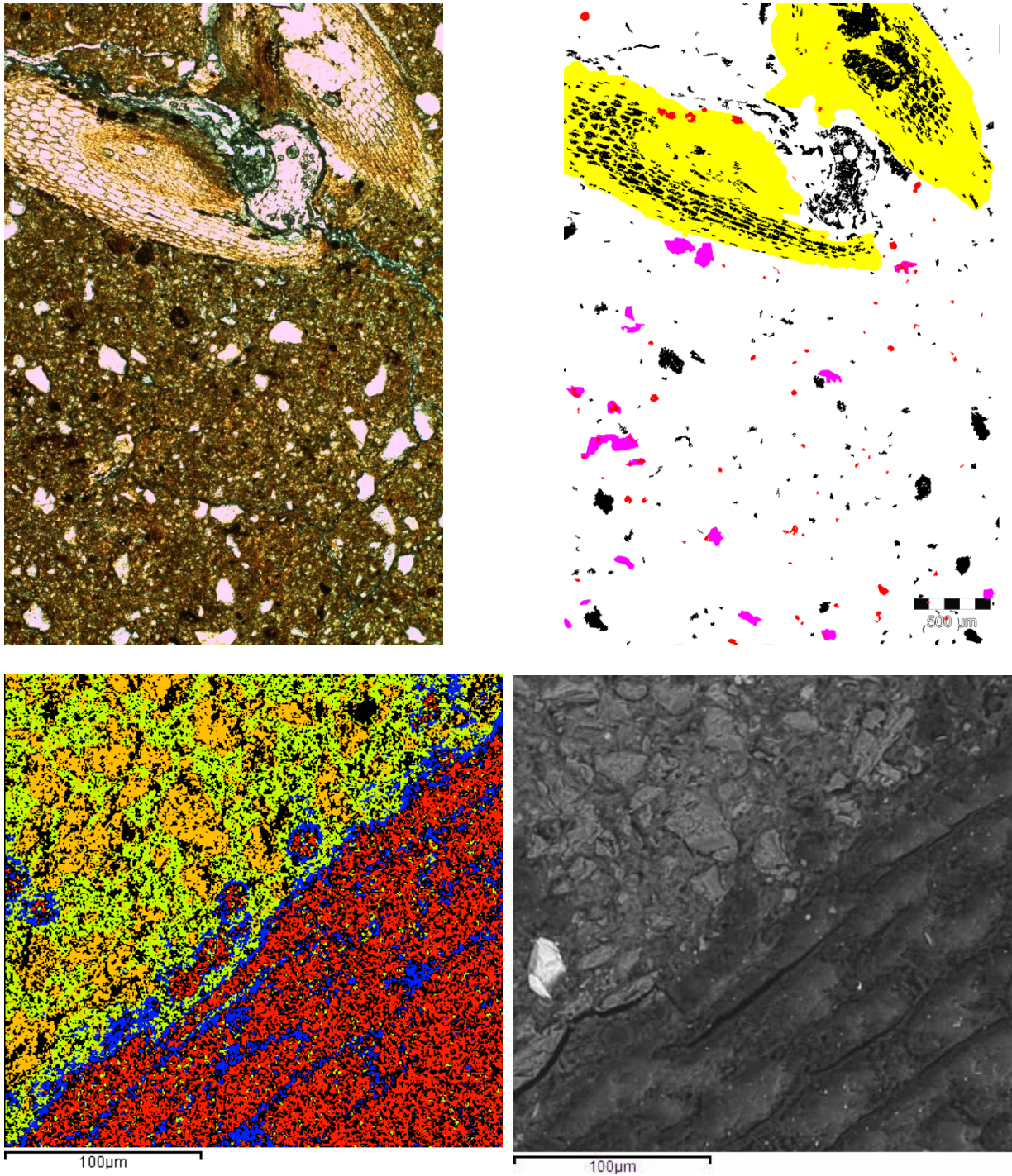


Figure 6.4: Image of an area of interest (AOI) of a thin-section removed from Inorganic plot of Broadbalk Winter-Wheat. **a)** in Plane polarised light (PPL) (top left) and **b)** as an organic-matter pore (map top right). Within the OM-pore map pixels are colour coded White = soil matrix, Black = pore, red = Amorphous black, pink = Amorphous red, Yellow =Organ Moderately-decomposed. **c)** SEM-EDS phase-map showing the organic matter fragment classified as Moderately-decomposed (bottom left). Pixels within the phase-map are colour coded as (blue), resin (red), soil matrix (yellow) silicates (orange). **d)** back scatter electron image of Organ Moderately-decomposed (bottom right).

6.7 The change in C-concentration within an intact Soil Structure.

Elemental transects allow changes in the concentration of elements to be detected that would otherwise be masked by the mapping of whole areas (Goldstein, 2003). However prior to the interpretation of transects, phase analysis should be performed to identify features. This ensures that any changes in C-concentration can be fully explained. Consistent with the results from mapping it is not possible to subtract the C-contribution made by resin. However, the absence of a strong Si signal from resin, meant that when Si peak was detected the user can be sure that solid matrix rather than resin has been sampled.

Figure 6.5, presents the proposed theoretical changes in C-concentration away from features in the different treated soils. However, the results suggest that changes in C-concentration amongst treatments are similar and that C-concentration with distance from OM features is variable while C-concentration from BC reaches a plateau once entering the soil matrix; therefore a revised model is proposed (**Figure 6.5**). In summary, the preliminary results suggest that the loss of C from OM (organ/tissue) fragments extends much further into the soil matrix than C originating from BC. There is little difference in the overall magnitude of C-concentration between treatments; such differences may not be detectable by small scale analysis. With increasing distance from features it is increasingly probable that the C-signal will receive contributions from other sources, therefore it is only feasible to explain any initial changes in C-concentration away from features. Therefore, ***Hypothesis 2.4d: A gradient in elemental C exists, with the amount of C decreasing with increasing distance away from organic-matter and BC fragments. In addition the gradient in elemental C will be steeper in soils with a lower total C-content (NIL & Inorganic) compared with soils with a higher total C-content (FYM & Wilderness)*** is rejected and further analysis is required to validate the preliminary results that OM is more likely to act as a source of C compared to BC.

Although the differences appear to be small they are consistent with previous studies which concluded microbial distribution is random within thin-sections of topsoil (Nunan et al., 2003). For instance, the availability of substrate (including the diffusion of substrate) is one factor which will influence the distribution of microbes. The results here show that even OM fragments believed to be more decomposed are acting as a source of OC by releasing C into the soil matrix, therefore it is hypothesised that the release of C from OM in turn dilutes the aggregation of microbes. Clearly further investigation would be required combining the investigation of OM with the distribution of microbes within soil thin-sections to confirm this hypothesis. The results demonstrate the applicability of using thin-sections under SEM-EDS to investigate changes in C-concentration within an intact soil structure and opens up a range of future research possibilities (**Section 7.7**).

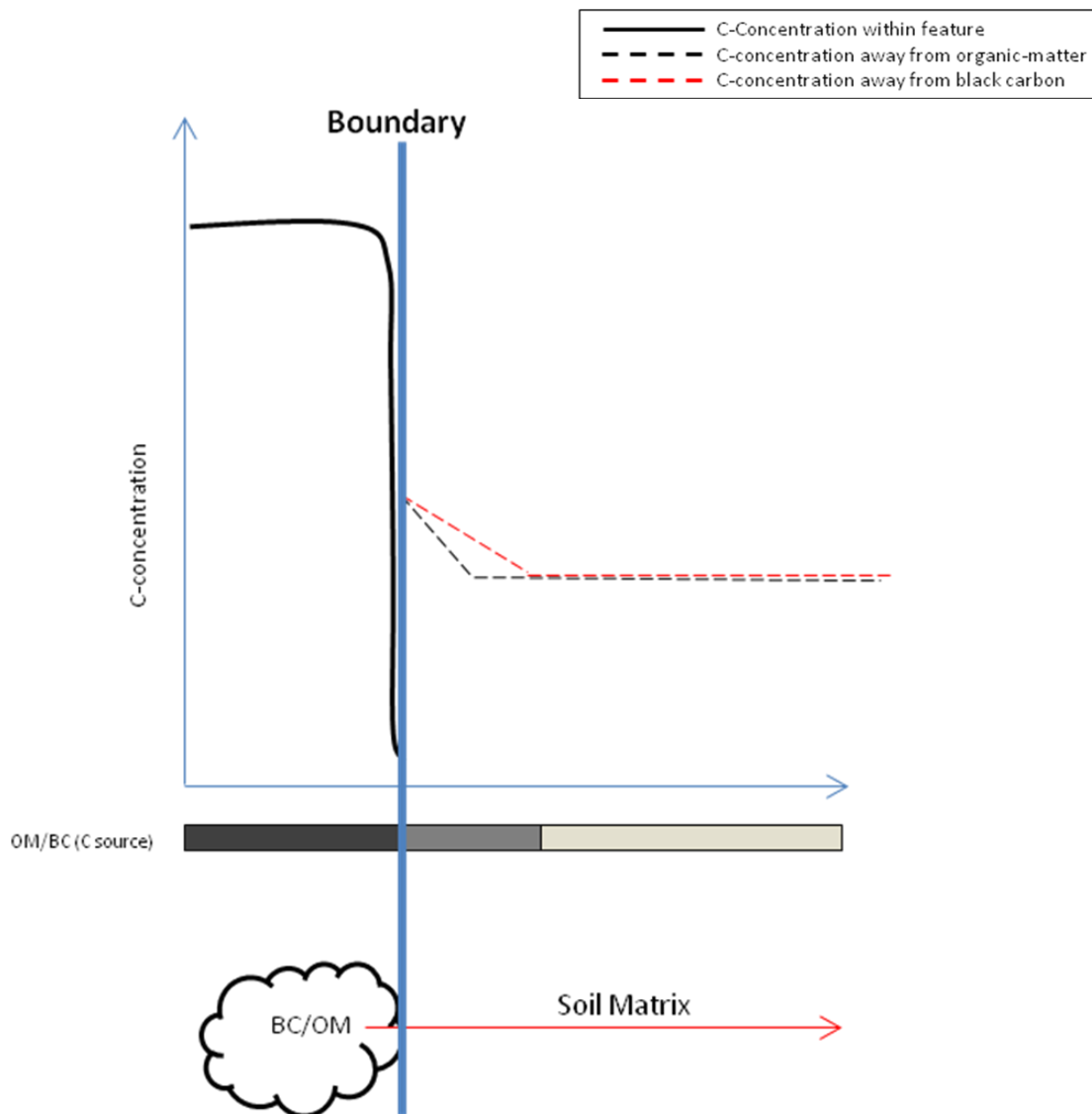


Figure 6.5: Revised theoretical C-distributions with distance away from organic matter and black carbon particles located within an intact soil structure, based on preliminary data. Transects will begin 30 μm within the feature of interest. Each transect will cross from the feature of interest into the soil matrix, presented schematically in the lower diagram. The Blue line represents the boundary between feature and soil matrix, dark black line represents C-concentration with features, due to topological effects there will be a drop in x-ray detection. Beyond the boundary differences in C-concentration will be detected due to the nature of C-containing features and the total C-contents of the soil. Within the graph, black dotted lines represent BC and red represents OM features that act as a source of carbon. The bars below the graph summarise the nature of the C-signal. Black represents where C is stored, dark grey where carbon is leaking into the soil matrix, and light grey represents background levels C within the soil matrix carbon.

Chapter 7: The Processes Controlling OC-Storage and the Wider Significance of the Research Findings.

Macro-scale analysis revealed that there are differences in the structural characteristics between soils contrasting in total SOC. In summary loose soil (or macro-scale) analysis revealed differences in the following characteristics, which can be explained by the nature or amounts of OC:

- a) Total SOM (determined by LOI)
- b) Bulk density
- c) Aggregate stability
- d) Water release characteristics

However soil structure observed and measured within thin-sections is highly variable. For instance, there is no difference in the total volume of OM, total porosity or total porosity by shape. However within thin-sections it is possible to detect some differences in soil structure, by comparing pore size distributions or the occurrence of excremental pedofeatures. Although there are no differences in the total amount of OM quantified within thin-sections the location and nature of OM in relation to soil structural features gives some indication about the process of OM decomposition and it's feedback into soil structure development and stability. The following section will discuss this in more detail.

7.1 Exploring the processes controlling OC-storage

Due to the reciprocal relationship between soil structure and OC-storage many studies report that water aggregate stability is correlated to total SOC. The relative aggregate stability between Broadbalk soils differs following different wetting treatments (**discussed in Section 6.2**). This suggests that aggregate stability is related not to the total amount of OC but also to the nature of the OC binding agents. As previously discussed studies have concluded that more labile forms of OC are largely responsible for the stability of aggregates, this is in accordance with AWS testing the stability of macroaggregates and is in accordance with Tisdall and Oades (1982) that labile forms of OC-binding agents are responsible for binding macroaggregates. This is further supported by studies investigating the impact of changes in land-use upon aggregate stability; in summary conversion of CT soils to pasture sees an increase in aggregate stability which is not proportionate to increases in OC-storage; indicating that the initial inputs of labile carbon are responsible for macro aggregate stability (Jastrow, 1996). However, within the grassland soil the occurrence of less decomposed (and therefore more labile) forms is not greater compared to agricultural treatments. In addition the location of less decomposed organ/tissue forms is consistent across all treatments, therefore it is concluded that the location of OM is not creating the difference in the stability of aggregates between

Broadbalk soils. One explanation could be that more labile forms of OC are not fully quantified within thin-sections, for instance up to 10% of the photosynthetic C fixed by plants is deposited into the soil via rhizodeposition (Hutsch, 2002). However this source of OC is water-soluble, therefore it is possible it has been lost during the impregnation of soil with resin. Nevertheless, practical constraints mean that it would only be possible to quantify rhizodeposition using pulse labelling techniques.

Within thin-sections evidence of aggregation is highly variable and difficult to interpret. Furthermore, the identification of aggregates within thin-sections differs with soil texture. For instance, in soils with high clay contents, aggregates are surrounded by voids, while in sandy soils compactness and sharpness of boundaries are diagnostic (Bullock *et al.*, 1985). Aggregation is largely evident in the form of excremental pedofeatures, which are associated with less decomposed forms of organic matter. In turn organ and tissue forms of OM are largely located in pores, as discussed previously this indicates that in-situ decomposition is occurring. SEM-EDS results, analysing Organ and Tissue fragments which have some contact with the soil matrix, revealed the potential of individual OM fragments to influence the structural stability of soil. The analysis showed that elevated C-concentrations are found within the soil matrix 40 μm away from OM inclusions; this demonstrates the diffusion capability of C and the potential for C to be available in the soil matrix. It also highlights a potential pathway of C into the lower horizons (**discussed below**).

Nunan *et al.*, (2003) demonstrated that within thin-sections of cropped top-soil, microbial abundance is greatest up to 50 μm away from soil pores and decreases thereafter. Several sources of C intimately associated within the soil matrix have been detected. Micromorphology results indicate that more decomposed forms of OM are located throughout the soil matrix, while the analysis of SEM-EDS indicate that less decomposed OM can act as a source of C with elevated C-concentrations up to 40 μm away from OM fragments. It is likely the more decomposed amorphous forms of OM are physically and chemically protected, for instance, ultra thin-sections of resin stable aggregates have shown amorphous OM stabilised with Al and Fe (Bartoli *et al.*, 1988b). Therefore amorphous OM may not represent a readily available source of C. During the decomposition of OM, microbial by-products are generated, which will further enhance soil structural stability. The results here suggest that by using SEM-EDS the distribution of C originating from OM can be measured at micrometer scales, i.e. relevant to microbes. Further analysis is required to determine if amorphous OM is functioning as a source of OC.

It is acknowledged that OM can enter the sub-soil through preferential flow paths or via plant roots, this creates a vertical stratification of horizons through the soil profile. Chabbi *et al.*, (2009) concluded that SOM located within sub-soils has a modern radiocarbon age, while SOM located in the bulk soil matrix has a radiocarbon age of several thousand years. Interestingly the SOM situated in

the regions of preferential flow and bulk soil matrix have similar lignin (i.e. similar recalcitrance), but it was found that SOM within the soil matrix is more chemically stabilised. The results from this study demonstrate that, across all treatments, less decomposed OM (i.e. organ and tissue) are consistently located within soil pores. The results from SEM-EDS analysis demonstrate that less decomposed organ and tissue particles act as a source of C, therefore it is reasonable to expect that if they are located within a preferential flow path, they function as a source of subsoil C.

7.2 The redistribution of OM and Soil Structural Development.

Models of aggregate formation and turnover suggest that “macroaggregates are formed around fresh organic residue which then becomes coarse intra-particulate organic matter” (Six *et al.*, 2000). There is little evidence from this study to support this, as organ and tissue residue was largely located within soil pores. However, as mentioned previously, there is substantial evidence for the incorporation of amorphous forms of OM within the soil matrix and previous studies have shown amorphous OM to be stabilised with Al and Fe (Bartoli *et al.*, 1988b). Particulate organic matter by definition means that cellular plant structure is evident. However, the capability to identify cellular structure is dependent upon the scale of investigation. For instance, Pulleman *et al.*, (2005) presented evidence for fine intra particulate organic matter within microaggregates, however under the SEM cellular structure was only evident at magnifications in excess of 2000x. As decomposition proceeds SOM loses cellular structure and becomes smaller in size (Guggenberger *et al.*, 1994) (Six *et al.*, 1998), it maybe possible that some OM identified as being amorphous in nature under the light microscope, will exhibit cellular structure at high magnifications under the SEM. In summary, the classification of amorphous OM is scale dependent and as with the identification of BC additional analysis using SEM is required. The absence of clear aggregation within the thin-sections makes it difficult to make extensive hypothesis regarding the role of particulate OM in aiding the formation of aggregates. However, the results suggest that the incorporation of organic matter into the soil matrix occurs when OM has undergone considerable decomposition and does not represent a fresh form of OM as has previously been suggested by Six *et al.*, (2000). **Figure 7.1** summarises the process of OM decomposition as observed within the soil thin-sections, in doing so it highlights the redistribution of OM and its impact upon soil structure.

a) Particulate OM located within soil pores.

b) Particulate OM is increasingly exploited and gradually incorporation into the soil matrix.

c) Within the soil matrix small amorphous OM is located away from pores.

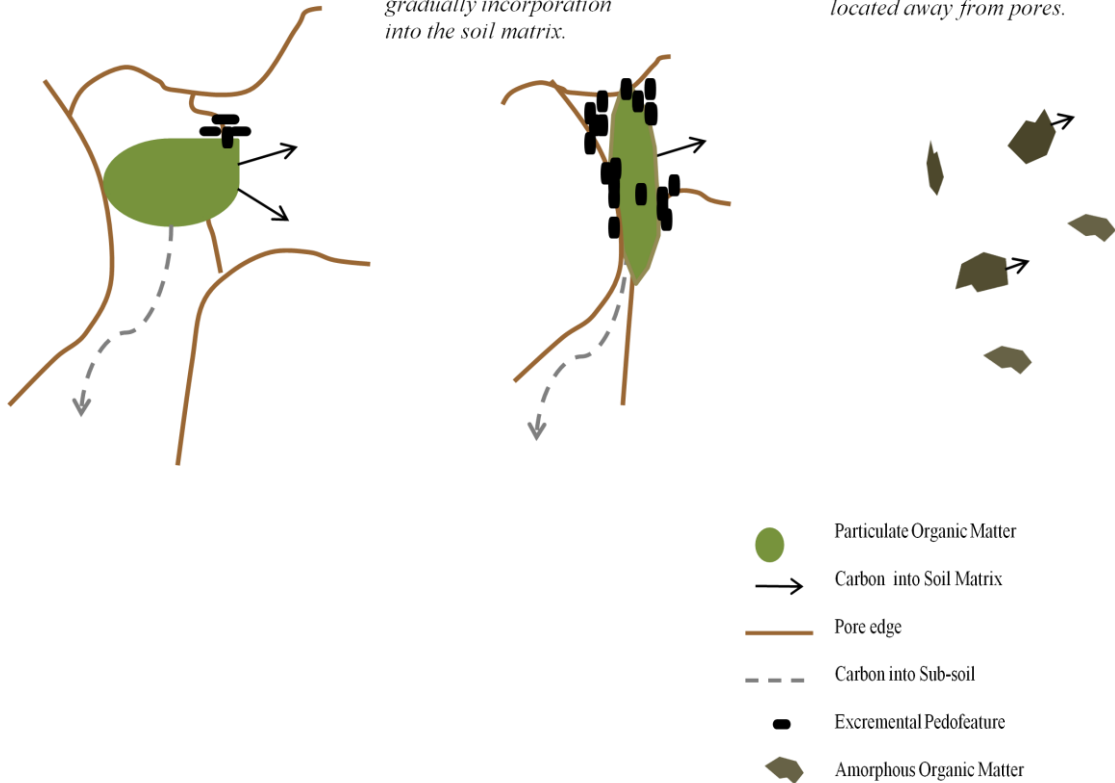


Figure 7.1: A summary of the process of OM decomposition and its impact upon soil structure, as evident within soil thin-sections. **a)** The decomposition of particulate organic matter will lead to the formation of a pore. **b)** As decomposition proceeds OM becomes fragmented and increasingly incorporated into the soil matrix and microaggregates in the form of excremental pedofeatures are more abundant. **c)** Towards the later stages of decomposition, under the light microscope OM appears amorphous in form and is incorporated into the soil matrix away from soil pores. Amorphous OM is likely to stabilise soil structure by organo-mineral interactions and therefore itself be more chemically and physically protected from decomposition. As evident by SEM-EDS analysis there is a movement of C into the soil matrix, this may further enhance soil structural stability, for particulate OM the extent that C enters the soil matrix is greater ($>40 \mu\text{m}$) compared to more recalcitrant black carbon ($20 \mu\text{m}$). Further analysis is required to investigate the extent to which amorphous OM acts as a source or store of OC. It is hypothesised that particulate OM located within soil pores may act as a source of labile carbon for sub-soil horizons. For instance, Chabbi *et al.*, (2009) reported that recent OC is located within preferential flow paths of sub-soils.

7.3 The Role of Black Carbon within the Soil Structure.

As discussed in **Chapter 1** BC represents a longer-term store of C due to its chemical recalcitrance. Studies have suggested that the resistance of BC to decomposition is largely due to its chemical recalcitrance since compared to SOM, BC is mainly located within the light soil fraction and is not bound to mineral particles (Glaser *et al.*, 2000). However, the ability of BC to interact with the soil mineral component is dependent upon the temperature used to form BC. Gundale and Deunca (2006) found that BC produced from pine at 300 °C had a higher nutrient status but lower sorptive abilities compared to BC formed at 800 °C. Furthermore, the presence of macropores within BC particles will also enhance the sorptive capacity of BC particles (Keech *et al.*, 2005). Therefore, the ability of BC to directly interact with the soil matrix will depend on the temperatures and source plant material used to produce BC. The indirect impact of BC upon soil structure is also being debated with studies reporting that biochar additions increase (Ishii & Kadoye, 1994) or decrease (Gaur & Adholeya, 2000) the association of mycorrhizal fungi with plant roots. If biochar was found to increase the population of mycorrhizal fungi, biochar could be described as being indirectly beneficial to soil structure, as it is well accepted that mycorrhizal fungi act as temporary stabilising agents of macroaggregates (Blanco-Canqui and Lal 2004). However, as discussed in Lehmann *et al.*, (2007) it has not yet being possible to separate the effects of biochar; e.g. is the increase in mycorrhizal fungi due to the unique properties of biochar or is it simply related to the input of C, if so can the same effects be observed with the addition of OM.

The ability of BC to interact with the soil mineral component has lead to questions about the temperature sensitivity of BC. As highlighted in **Chapter 1** chemical recalcitrant C forms are more temperature sensitive than labile SOM (Davidson *et al.*, 2006). Black carbon varies in its chemical, physical and structural properties, for instance in this study the structural characteristics of BC have ranged from amorphous, to forms exhibiting cellular structure. These attributes of BC are determined by biomass type and the temperatures used to create BC. More recently, research has focused upon determining the nature of BC formed by various pyrolysis and biomass sources in order to more accurately determine the effects that BC has on C-storage. Binh *et al.*, (2010), in a study comparing the temperature sensitivity of different BC particles, reported that more stable BC (oak sourced biomass) is more temperature sensitive than less stable BC (corn sourced biomass) when produced at both 350 °C and 600 °C. Interestingly Binh *et al.*, (2010), reported that corn sourced BC is more porous and has greater amounts of N, K, Ca associated with it compared to Oak derived BC; which in turn could affect the ability of BC to interact with the soil matrix and thereby the temperature sensitivity of BC.

In this study, evidence for the association of elements in addition to C and O with BC was sporadic, when present mainly Si and S were associated. Studies have demonstrated that the surface of BC particles is important for nutrient storage by having greater sorptive capabilities (Chun *et al.*, 2004). In this study there was just one clear example of the association of Ca with cracks at the edges of BC (Figure 7.2), since this is the only occurrence, it is difficult to explain the process by which it was formed.

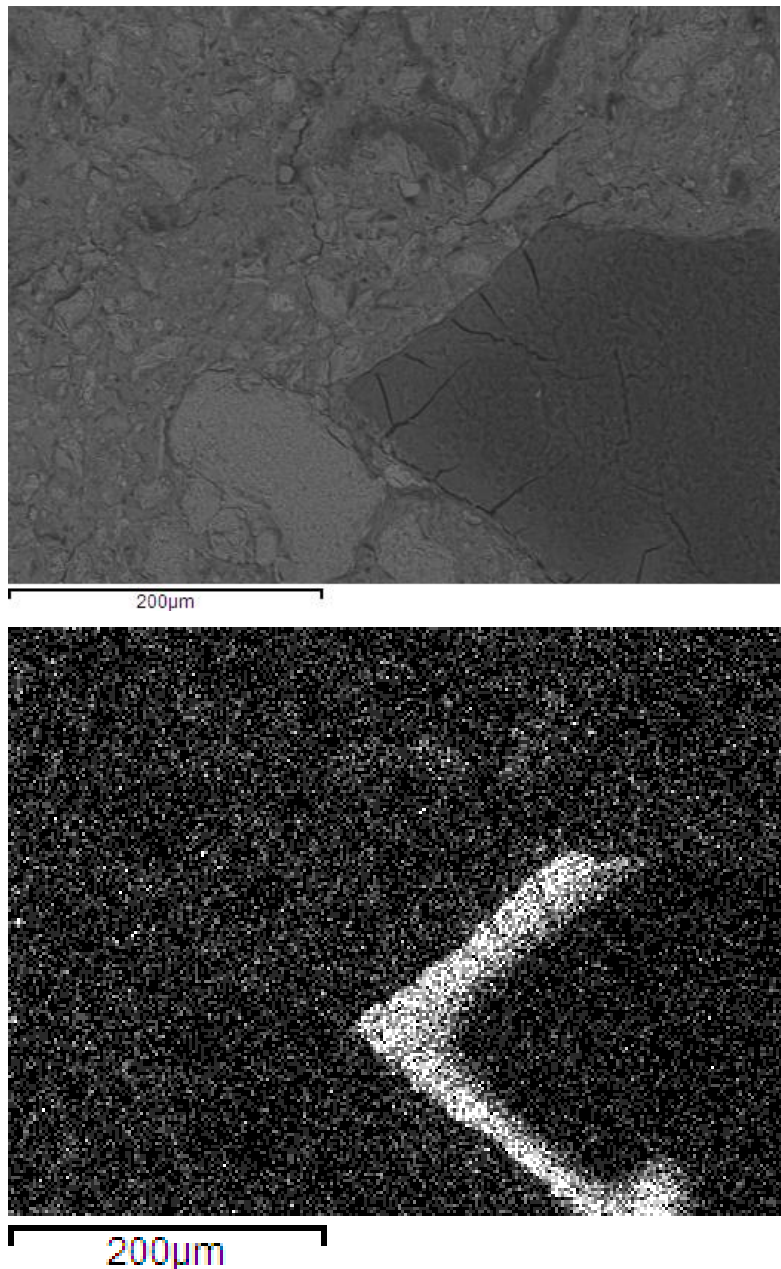


Figure 7.2: Back-scattered image of a black carbon particle within a soil thin-section (top) taken from Broadbalk Inorganic treated soil. Elemental distribution of Ca (bottom) determined by SEM-EDS analysis. Calcium appears to be largely associated with cracks around the edge of the black carbon particle.

7.4 Organic Matter and Soil Structure as an Indication of Soil Quality

The need to define the economic and social value of ecosystem function is receiving increasing focus, however it has been hampered by difficulties in assessing soil quality. The definition of soil quality should encompass the ability to perform all the functions required of the soil (Bone *et al.*, 2010). The complexity of this definition is demonstrated by considering the range of soil functions, for instance, the protection of archaeological remnants, carbon storage (e.g. peat) or food production, the ability buffer soil pollutants. In order to allow the routine monitoring of soil quality there is argument for a set of basic soil indicators and there is a census that indicators should monitor the biological, chemical and physical soil characteristics (Bone *et al.*, 2010) and where possible act as “cross functional-indicators”. Bone *et al.*, (2010) propose that the basic set of soil indicators should include “pH, soil texture, organic carbon, infiltration rate, root presence, plant cover, soil odour, soil organism presence and diversity, soil colour, evidence of anthropogenic disruption (i.e. presence of construction material, coal/soot) and penetrability”. Consistent with most basic lists, Bone *et al.*, (2010) propose that total OC is to be monitored; in addition soil structure is measured indirectly by penetrability and water infiltration rate. Measurements of total organic content and soil structure are to be expected given that (as highlighted in **Chapter 1**) they determine much of a soils physical, chemical and biological functioning. It seems likely that future determinates of soil quality will focus more upon soil structure, however to fully explain its impact upon soil functioning first the interactions between soil structure and carbon storage will need to be unravelled.

7.5 Recommendations for the Identification and Mapping of Features within Thin-sections.

It is concluded due to the nature of x-ray collection when identifying features based upon the O:C ratio this should be performed by point x-ray collection. This further supports the need for prior micromorphological analysis and the production of OM-pore maps. Previous studies have been successful in identifying BC within resin impregnated thin-sections (Davidson, 2006) using O:C ratios alone; however this analysis was restricted to point identification of features. To perform extensive mapping of areas prior micromorphological analysis and the production of OM-pore maps will be required. Analysis of a blank resin standard revealed that aside from O and C, other elements are not present. Therefore the presence or absence of elements in addition to O and C will confirm the location of resin, however, it may not be possible to phase resin located in micro-pores (e.g <10 µm) due to edge effects. **Table 7.1** presents a summary on how to identify features based upon chemical data; however the identification of features should be performed in conjunction with micromorphological analysis.

When mapping C, elemental analysis is best performed at 15 keV, this is still within the optimal range recommended by Goldstein (2003), but the higher accelerating voltage excites heavier elements, therefore phase analysis is more effective. In addition, it was found that the best results for mapping and subsequent phase analysis was achieved by collecting high resolution data, therefore reducing any edge effects (**Section 6.6.2**).

Table 7.1: Summary of EDS Analysis of Features Identified using Micromorphology Techniques.

Feature	Chemical signature	O:C ratio	Phase Analysis*
Resin	O & C	0.21-0.22	O:C:Si
Black carbon	O, C and trace amounts of S, Si or Ca	0.02-0.15	O:C:Si
Organic matter	Suite of elements	0.30-0.42	O:C:Si
Silicate features	Suite of elements	1.21-1.52	O:Si:Fe
Matrix	Suite of elements	0.72-1.01	O:Si:Fe

*Best combination of elements to phase features; at an accelerating voltage of 15 KeV

7.6 Reviewing the Classification of Organic Matter

Organic matter was classified according to its form and extend of decomposition by combining the recommended guidelines of Babel (1975) and Fitzpatrick (2003) (**Section 3.4.6**). This approach was chosen due to the difficulties in identifying OM down to tissue or organ type as recommended by many guidelines (e.g. Stoops 2001), because during later stages of decomposition the appearance of organ or tissue converges meaning that identification is open to misinterpretation (Babel 1975). Since no difference was found in the area cover or elemental signature of the same OM forms at different decomposition stages it is recommended that future analysis of OM to be simplified and remain at the form level (i.e. whether OM occurs as cells, tissue, organ or amorphous). The finding of no difference in the chemical signature of OM-classes is reasonable, because OM decomposition represents a continuum and within the same OM fragment several stages of decomposition can be evident. In short, OM in the early stages of decomposition will occur as fragments (typically > 20 µm) with a chemical structure similar to the source material, in the later stages OM will become amorphous in nature and more concentrated in chemically recalcitrant C-structures [Baldock and Skjemstad, 2000].

The ability to identify OM structures will vary between systems, for instance Dijkstra (1998) sampled a forest soil supporting *Pinus sylvestris* and *Deschampsia flexuosa*, OM was placed into one of 4 categories: needle, wood, root or tissue (when the degree of cellular preservation was poor). This simple classification is effective at describing the nature and form of OM. Dijkstra (1998) place OM for which the origin can not be identified into the tissue category, this class is considered to be more decomposed than OM which can be identified, this interpretation may be flawed. For instance, it is not known what form OM enters the soil, for example the sloughing of cells due to cell division at root tips (Campbell & Reece, 2002), is one mode by which fresh tissue/cell residue can enter the soil.

In conclusion, while broad differences in the extent of decomposition can be inferred between amorphous and organ or tissue forms of OM, attempts to classify the extent of decomposition of organ and tissue forms based on appearance must be done with caution.

7.7 Recommendations for Further Study.

1. One of the key points to come out of the literature review was the absence of a method by which both microbial and OM distributions can be investigated at scales relevant to microbes, to ascertain whether microbial distribution is related to substrate availability. It is proposed that the method presented within this thesis can be used in conjunction with existing methods to investigate the distribution of microbes and organic matter in relation each other and to soil structural features. Nunan *et al.*, propose a method by which image analysis and geostatistical tools can be used to quantify microbes within soil thin-sections. Alternatively, Eickhorst (2008) uses Fluorescence in Situ Hybridization (FISH), RNA markers, to map the distribution of active micro-organisms within soil thin-sections.
2. The results of this study disagree with models of aggregate turnover which suggest that aggregates are formed around fresh OM (Six *et al.*, 2000); micromorphological analysis indicates that OM which acts as a core for aggregation may be more decomposed than previously suggested. Therefore micromorphological and SEM analysis of fractionated aggregates may provide useful information about the form of OM that's been sampled by studies routinely performing fractionation.
3. One simple adjustment to the current project would be to sample subsoil horizons. Studies have shown that the location of OM within the subsoil is less random, as OC is restricted to entering deeper horizons via plant roots or regions of preferential flow (Lutzow *et al.*, 2006). Furthermore estimates of C-stocks are more focused upon the contribution made by the

subsoil. This mode of sampling would also compliment methods to investigate microbial and OM distribution within intact soil samples.

4. Much research is currently focused upon the role of BC in soils, in order to investigate whether it represents the “missing C sink”. The results are highly variable, with some reporting that BC can be exploited (Kaal & Van Mourik, 2008) and others that BC represents a chemically recalcitrant store of C (Krull *et al.*, 2003), but is highly sensitive to increases in temperature (Binh *et al.*, 2010). The variability in these results is partly due to differences in the temperature and source material used to generate BC. No research has been conducted on the impacts of BC upon soil structure within intact samples. The results here suggest that BC is acting as a source of C with C being elevated up to 20 µm away from BC particles. However more extensive studies where the method of pyrolysis is fully accounted for are required.
5. Although the approach for investigating the natural abundance of C¹³ within soil thin-sections was unsuccessful (**Appendix 3**) the method still has further applications. By using pulse labelling the location of recent photosynthates within an intact soil structure can be investigated. The investigation of pulse labelling has previously been conducted by Bruneau *et al.*, (2002) within soil thin-sections. The most useful approach would be to use a field impregnation (Mooney *et al.*, 2006), rather than artificially creating a plant growth median, therefore the complete root system and rhizosphere zone can be sampled whilst remaining intact.
6. The investigation of the 3D soil structure is the current focus of many studies. Research is already underway to integrate the information gathered from SEM-EDS with the 3D analysis of soil structure, to gather information about the redistribution within the soil structure as OM decomposes (Otten *et al.*, 2009.).
7. A simplified micromorphology classification of OM should also be applied (**Section 7.6**). Further investigation into the chemical and micromorphological characteristics of black carbon and black OM formed by lignification and melanisation is required.

7.8 Summary

In agricultural soils, which are the same in all aspects except total-OC content, differences were found in total OM, WRC, aggregate stability and PSD; therefore these differences could be attributed to the relationship between OC and soil structure. Differences in the WRC, aggregate stability and PSD were also observed between soils with similar OC-contents but from different land-uses.

No differences were found in the area of OM between treatments, calculated by image analysis, this is expected to be a methodological problem, which as discussed can easily be resolved for future studies. However, the analysis of OM within intact soil samples provided evidence for the redistribution of OM as it is decomposed within the soil structure. Since the same pattern of redistribution was observed in both agricultural and grassland soil this is likely to be directed by soil macro and micro fauna. The lack of aggregation within thin-sections makes it difficult to predict the mode of aggregate turnover. Nevertheless, the results contradict theories of aggregation, which state that aggregates are formed around “fresh” OM and it is argued that OM will undergo substantial decomposition before it acts as core for aggregation.

The results for the first time investigate the impact that the decomposition of OM and its associated OC has on soil structure within intact samples. Through SEM-EDS, it was shown that in the soil matrix adjacent to OM (plant/organ) fragments, occasionally there is a heightened concentration of C, indicating that these fragments maybe acting as a source of OC. Interestingly the results demonstrates that BC is not acting as a source of C, this is consistent with BC being recalcitrant in nature. Further analysis is required to validate these preliminary results.

A new integrated method for the analysis of OM and OC within soil thin-sections has been established. As with studies investigating the distribution of BC within soil thin-sections, this study has demonstrated the effectiveness of analysing OM and its associated OC using SEM-EDS. By adhering to hardware set-up as recommended by this study, identifying resin and phasing when mapping, should become more routine and easily accomplished. The results have signified the vast potential for the application of this method in future research (**Section 7.7**). It is anticipated that the best application of this method will be to integrate it with the analyses of the soil microbial population and the chemical nature of OM.

References

- Abid M. & Lal, M. 2008. Tillage and Drainage impact on Soil quality 1. Aggregate Stability, carbon and Nitrogen Pools. *Soil and Tillage Research*, 100 89-98.
- Adderley, W.P., Simpson, I.A. & Davidson, D.A. 2002. Colour description and quantification in mosaic images of soil thin sections. *Geoderma*, **108**, 181-195.
- Angers, D.A., Recous, S. & Aita, C. 1997. Fate of carbon and nitrogen in water-stable aggregates during decomposition of (CN)-C-13-N-15-labelled wheat straw in situ. *European Journal of Soil Science*, 48, 295-300.
- Angers, D.A. & C.C. 1998. Dynamics of Soil Aggregation and C Sequestration. In: *Soil Processes and Carbon Cycle* (ed R.Lal), pp. 199-206. CRC Press, Boca Raton, Florida.
- Arrouays, D., Saby, N., Walter, C., Lemerrier, B. & Schwartz, C. 2006. Relationships between particle-size distribution and organic carbon in French arable topsoils. *Soil Use and Management*, **22**, 48-51.
- Avery, B. W. and Catt J. A. The Soil at Rothamsted.
<http://www.rothamsted.ac.uk/eRA/pix.php?folder=home&page=imagemap> . 1985. 1-5-2009.
- Babel, U. 1975. Micromorphology of Soil Organic Matter. In: *Soil Components* (ed J.E.Gieseking), Springer, New York.
- Batjes N.H. 1996. Total Carbon and Nitrogen in the Soils of the World. *European Journal of Soil Science*, 47, 151-163
- Baldock, J.A. & Skjemstad, J.O. 2000. Role of the soil matrix and minerals in protecting natural organic materials against biological attack. *Organic Geochemistry*, **31**, 697-710.
- Baldock, J.A., Oades, J.M., Waters, A.G., Peng, X., Vassallo, A.M. & Wilson, M.A. 1992. Aspects of the Chemical-Structure of Soil Organic Materials As Revealed by Solid-State C-13 Nmr-Spectroscopy. *Biogeochemistry*, **16**, 1-42.
- Ball, D.F. 1964. Loss-On-Ignition As Estimate of Organic Matter + Organic Carbon in Non-Calcareous Soils. *Journal of Soil Science*, **15**, 84-&.
- Barrios, E. 2007. Soil biota, ecosystem services and land productivity. *Ecological Economics*, **64**, 269-285.
- Bartoli, F., Genevois-Gomendy, V., Royer, J.J., Niquet, S., Vivier, H. & Grayson, R. 2005. A multiscale study of silty soil structure. *European Journal of Soil Science*, **56**, 207-223.
- Bartoli, F., Philipp, R., Burtin, G.. 1988a. Aggregation in Soils with Small Amounts of Swelling Clays .1. Aggregate stability. *Journal of Soil Science*, **39**, 617-628.
- Bartoli, F., Paterson, E., Philipp, R., Demai, J.J. & Doirisse, M. 1988b. Aggregation in Soils with Small Amounts of Swelling Clays .2. Chemistry and Surface-Properties of Na Resin Stable Soil Aggregates. *Journal of Soil Science*, **39**, 617-628.
- Batey T. 1988. *Soil husbandry: a practical guide to the use and management of soils*. Soil and Land Use Consultants Ltd, Aberdeen.
- Bear, M.H. & Bruce, R.R. 1993. A Comparison of Methods for Measuring Water-Stable Aggregates - Implications for Determining Environmental-Effects on Soil Structure. *Geoderma*, 56, 87-104.

- Beare, M.H., Hus, S., Coleman, D.C. & Hendrix, P.F. 1997. Influences of mycelial fungi on soil aggregation and organic matter storage in conventional and no-tillage soils. *Applied Soil Ecology*, 5, 211-219.
- Bellamy, P.H., Loveland, P.J., Bradley, R.I., Lark, R.M. & Kirk, G.J.D. 2005. Carbon losses from all soils across England and Wales 1978-2003. *Nature*, 437, 245-248.
- Besnard, E., Chenu, C., Balesdent, J., Puget, P. & Arrouays, D. 1996. Fate of particulate organic matter in soil aggregates during cultivation. *European Journal of Soil Science*, 47, 495-503.
- Bhogal A., Nicholson F. A., Chambers B.J. 2009. Organic carbon additions: effects on soil bio-physical and physico-chemical properties *European Journal of Soil Science*, 60, 276-286
- Bickle, M.J. 1994. The role of metamorphic decarbonation reactions in returning strontium to the silicate sediment mass. *Nature*, 367, 699-704.
- Binh, T.N., Lehmann, J., Hockaday, W.C., Joseph, S. & Masiello, C.A. 2010. Temperature Sensitivity of Black Carbon Decomposition and Oxidation. *Environmental Science & Technology*, 44, 3324-3331.
- Blair, N., Faulkner, R.D., Till, A.R., Korschens, M. & Schulz, E. 2006. Long-term management impacts on soil C, N and physical fertility - Part II: Bad Lauchstadt static and extreme FYM experiments. *Soil & Tillage Research*, 91, 39-47.
- Blanco-Canqui, H. & Lai, R. 2004. Mechanisms of Carbon sequestration in Soil Aggregates. *Critical Reviews in Plant Sciences*, 23, 481-504.
- Blanco-Canqui, H., Lal, R., Sartori, F. & Miller, R.O. 2007. Changes in organic carbon and physical properties of soil aggregates under fiber farming. *Soil Science*, 172, 553-564.
- Blank, R.R. & Fosberg, M.A. 1989. Cultivated and Adjacent Virgin Soils in Northcentral South Dakota .2. Mineralogical and Micromorphological Comparisons. *Soil Science Society of America Journal*, 53, 1490-1499.
- Bolin, B. 2000. Global Perspective. In: In: IPCC, Land Use, Land-Use Change, and Forestry. A Special Report of the IPCC (ed. J.D. Watson), pp. 23-51. Cambridge University Press, Cambridge, UK.
- Bone, J., Head, M., Barraclough, D., Archer, M., Scheib, C., Flight, D. & Voulvoulis, N. 2010. Soil quality assessment under emerging regulatory requirements. *Environment International*, 36, 609-622.
- Bongiovanni, M.D. & Lobartini, J.C. 2006. Particulate organic matter, carbohydrate, humic acid contents in soil macro- and microaggregates as affected by cultivation. *Geoderma*, 136, 660-665.
- Bossuyt, H., Deneff, K., Six, J., Frey, S.D., Merckx, R. & Paustian, K. 2001. Influence of microbial populations and residue quality on aggregate stability. *Applied Soil Ecology*, 16, 195-208.
- Bottinelli, N., Hallaire, V., Menasseri-Aubry, S., Le Guillou, C. & Cluzeau, D. 2010. Abundance and stability of belowground earthworm casts influenced by tillage intensity and depth. *Soil & Tillage Research*, 106, 263-267.
- Boutton, T.W. 1996. *Mass Spectrometry of Soils*. CRC publishers.

- Boutton, T.W., Archer, S.R., Midwood, A.J., Zitzer, S.F. & Bol, R. 1998. δ C-13 values of soil organic carbon and their use in documenting vegetation change in a subtropical savanna ecosystem. *Geoderma*, **82**, 5-41.
- Brewer, R. 1964. *Fabric and Mineral Analysis of Soils*. John Wiley & Sons, New York.
- Brodowski, S., Amelung, W., Haumaier, L., Abetz, C. & Zech, W. 2005. Morphological and chemical properties of black carbon in physical soil fractions as revealed by scanning electron microscopy and energy-dispersive X-ray spectroscopy. *Geoderma*, **128**, 116-129.
- Brodowski, S., John, B., Flessa, H. & Amelung, W. 2006. Aggregate-occluded black carbon in soil. *European Journal of Soil Science*, **57**, 539-546.
- Brown, G.G., Barois, I. & Lavelle, P. 2000. Regulation of soil organic matter dynamics and microbial activity in the drilosphere and the role of interactions with other edaphic functional domains. *European Journal of Soil Biology*, **36**, 177-198.
- Bruneau, P.M.C., Davidson, D.A., Grieve, I.C., Young, I.M. & Nunan, N. 2005. The effects of soil horizons and faunal excrement on bacterial distribution in an upland grassland soil. *Fems Microbiology Ecology*, **52**, 139-144.
- Bruneau, P.M.C., Ostle, N., Davidson, D.A., Grieve, I.C. & Fallick, A.E. 2002. Determination of rhizosphere C-13 pulse signals in soil thin sections by laser ablation isotope ratio mass spectrometry. *Rapid Communications in Mass Spectrometry*, **16**, 2190-2194.
- Bruun, S., Agren, G.I., Christensen, B.T. & Jensen, L.S. 2010. Measuring and modeling continuous quality distributions of soil organic matter. *Biogeosciences*, **7**, 27-41.
- Bullock, P. & etc. 1985. *Handbook for Soil Thin Section Description*. Waine Research Publication, Woverhampton.
- Bundt, M., Widmer, F., Pesaro, M., Zeyer, J. & Blaser, P. 2001. Preferential flow paths: biological 'hot spots' in soils. *Soil Biology & Biochemistry*, **33**, 729-738.
- Campbell, N.A. & Reece J.B. 2002. *Biology*. Pearson Education, New Jersey.
- Capowiez, Y. 2000. Differences in burrowing behaviour and spatial interaction between the two earthworm species *Aporrectodea nocturna* and *Allolobophora chlorotica*. *Biology and Fertility of Soils*, **30**, 341-346.
- Carter, M.R. 2004. Researching structural complexity in agricultural soils. *Soil & Tillage Research*, **79**, 1-6.
- Cass A, C.B.T.J. 2010. New Approaches to Vineyard and Orchard Preparation and Management. In: *Vineyard Development and Revelopment* (ed P.F.Hayes), pp. 18-24. Australian Society of Viticulture and Oenology, Adelaide.
- Chabbi, A., Kogel-Knabner, I. & Rumpel, C. 2009. Stabilised carbon in subsoil horizons is located in spatially distinct parts of the soil profile. *Soil Biology & Biochemistry*, **41**, 256-261.
- Chan, K.Y. 2001. An overview of some tillage impacts on earthworm population abundance and diversity - implications for functioning in soils. *Soil & Tillage Research*, **57**, 179-191.
- Christensen, B.T. 2001. Physical fractionation of soil and structural and functional complexity in organic matter turnover. *European Journal of Soil Science*, **52**, 345-353.

- Chun,H.C., Gimenez,D. & Yoon,S.W. 2008. Morphology, lacunarity and entropy of intra-aggregate pores: Aggregate size and soil management effects. *Geoderma*, **146**, 83-93.
- Chun,Y., Sheng,G.Y., Chiou,C.T. & Xing,B.S. 2004. Compositions and sorptive properties of crop residue-derived chars. *Environmental Science & Technology*, **38**, 4649-4655.
- Ciais, P. A. S. Denning P. P. Tans J. A. Berry D. A. Randall G. J. Collatz P. J. Sellers J. W. C. White M. Trolier H. A. J. Meijer R. J. Francey P. Monfray and M. Heimann 1997. A three-dimensional synthesis study of ¹⁸O in atmospheric CO₂. 1. Surface Fluxes. *Journal of Geophysical Research - Atmosphere* **102**, 5857-5872. 1997.
- Cole,L., Buckland,S.M. & Bardgett,R.D. 2008. Influence of disturbance and nitrogen addition on plant and soil animal diversity in grassland. *Soil Biology & Biochemistry*, **40**, 505-514.
- Coleman,K., Jenkinson,D.S., Crocker,G.J., Grace,P.R., Klir,J., Korschens,M., Poulton,P.R. & Richter,D.D. 1997. Simulating trends in soil organic carbon in long-term experiments using RothC-26.3. *Geoderma*, **81**, 29-44.
- Crawford,J.W., Matsui,N. & Young,I.M. 1995. The Relation Between the Moisture-Release Curve and the Structure of Soil. *European Journal of Soil Science*, **46**, 369-375.
- Czimczik,C.I.& Masiello,C.A. 2007. Controls on black carbon storage in soils. *Global Biogeochemical Cycles*, **21**.
- Davidson,D.A.& Grieve,I.C. 2006. Relationships between biodiversity and soil structure and function: Evidence from laboratory and field experiments. *Applied Soil Ecology*, **33**, 176-185.
- Davidson,D.A., Bruneau,P.M.C., Grieve,I.C. & Wilson,C.A. 2004. Micromorphological assessment of the effect of liming on faunal excrement in an upland grassland soil. *Applied Soil Ecology*, **26**, 169-177.
- Davidson,D.A.& Carter,S.P. 1998. Micromorphological evidence of past agricultural practices in cultivated soils: The impact of a traditional agricultural system on soils in Papa Stour, Shetland. *Journal of Archaeological Science*, **25**, 827-838.
- Davidson,D.A., Dercon,G., Stewart,M. & Watson,F. 2006. The legacy of past urban waste disposal on local soils. *Journal of Archaeological Science*, **33**, 778-783.
- Davidson,D.A., Wilson,C.A., Meharg,A.A., Deacon,C. & Edwards,K.J. 2007. The legacy of past manuring practices on soil contamination in remote rural areas. *Environment International*, **33**, 78-83.
- Davidson,E.A.& Janssens,I.A. 2006. Temperature sensitivity of soil carbon decomposition and feedbacks to climate change. *Nature*, **440**, 165-173.
- De Gryze,S., Jassogne,L., Six,J., Bossuyt,H., Wevers,M. & Merckx,R. 2006. Pore structure changes during decomposition of fresh residue: X-ray tomography analyses. *Geoderma*, **134**, 82-96.
- Del Galdo,I., Six,J., Peressotti,A. & Cotrufo,M.F. 2003. Assessing the impact of land-use change on soil C sequestration in agricultural soils by means of organic matter fractionation and stable C isotopes. *Global Change Biology*, **9**, 1204-1213.
- Denef,K., Six,J., Merckx,R. & Paustian,K. 2004. Carbon sequestration in microaggregates of no-tillage soils with different clay mineralogy. *Soil Science Society of America Journal*, **68**, 1935-1944.

Denef,K., Six,J., Paustian,K. & Merckx,R. 2001. Importance of macroaggregate dynamics in controlling soil carbon stabilization: short-term effects of physical disturbance induced by dry-wet cycles. *Soil Biology & Biochemistry*, 33, 2145-2153.

Diaz,J.F.& Balkus,K.J. 1996. Enzyme immobilization in MCM-41 molecular sieve. *Journal of Molecular Catalysis B-Enzymatic*, 2, 115-126.

Dijkstra,E.F. 1998. A micromorphological study on the development of humus profiles in heavy metal polluted and non-polluted forest soils under Scots pine. *Geoderma*, **82**, 341-358

Don,A., Schumacher,J., Scherer-Lorenzen,M., Scholten,T. & Schulze,E.D. 2007. Spatial and vertical variation of soil carbon at two grassland sites - Implications for measuring soil carbon stocks. *Geoderma*, **141**, 272-282.

Drees,L.R., Karathanasis,A.D., Wilding,L.P. & Blevins,R.L. 1994. Micromorphological Characteristics of Long-Term No-Till and Conventionally Tilled Soils. *Soil Science Society of America Journal*, **58**, 508-517.

Edwards,A.P.& Bremner,J.M. 1967. Microaggregates in Soils. *Journal of Soil Science*, 18, 64-&.

Eickhorst,T.& Tippkotter,R. 2008. Improved detection of soil microorganisms using fluorescence in situ hybridization (FISH) and catalyzed reporter deposition (CARD-FISH). *Soil Biology & Biochemistry*, **40**, 1883-1891.

Elliott,E.T. 1986. Aggregate Structure and Carbon, Nitrogen, and Phosphorus in Native and Cultivated Soils. *Soil Science Society of America Journal*, 50, 627-633.

Emerson,W.W.& McGarry,D. 2003. Organic carbon and soil porosity. *Australian Journal of Soil Research*, **41**, 107-118.

Eswaran H., Reich P.F., Kimble J.M. 1997. Global Carbon Stocks. *Global Climate Change and Pedogenic Carbonates*, 15-25.

Ettema,C.H.& Wardle,D.A. 2002. Spatial soil ecology. *Trends in Ecology & Evolution*, 17, 177-183.

European Climate Change Programme. Working Group Sinks Related to Agricultural Soils, Final Report. http://ec.europa.eu/environment/climat/pdf/finalreport_agricsoils.pdf . 2001. 1-4-2007. Ref Type: Electronic Citation

FitzPatrick,E.A. 1993. *Soil Microscopy and Micromorphology*. J Wiley & Sons, Chichester.

Fogel,R.& Cromack,K. 1977. Effect of Habitat and Substrate Quality on Douglas-Fir Litter Decomposition in Western Oregon. *Canadian Journal of Botany-Revue Canadienne de Botanique*, 55, 1632-1640.

Francis,G.S.& Fraser,P.M. 1998. The effects of three earthworm species on soil macroporosity and hydraulic conductivity. *Applied Soil Ecology*, **10**, 11-19.

Fromm,H., Winter,K., Filser,J., Hantschel,R. & Beese,F. 1993. The Influence of Soil Type and Cultivation System on the Spatial Distributions of the Soil Fauna and Microorganisms and Their Interactions. *Geoderma*, 60, 109-118.

- Gaillard, V., Chenu, C. & Recous, S. 2003. Carbon mineralisation in soil adjacent to plant residues of contrasting biochemical quality. *Soil Biology & Biochemistry*, **35**, 93-99.
- Gaillard, V., Chenu, C., Recous, S. & Richard, G. 1999. Carbon, nitrogen and microbial gradients induced by plant residues decomposing in soil. *European Journal of Soil Science*, **50**, 567-578.
- Gale, W.J., Cambardella, C.A. & Bailey, T.B. 2000. Root-derived carbon and the formation and stabilization of aggregates. *Soil Science Society of America Journal*, **64**, 201-207.
- Garnier, P., Ezzine, N., De Gryze, S. & Richard, G. 2004. Hydraulic properties of soil-straw mixtures. *Vadose Zone Journal*, **3**, 714-721.
- Gaur, A. & Adholeya, A. 2000. Effects of the particle size of soil-less substrates upon AM fungus inoculum production. *Mycorrhiza*, **10**, 43-48.
- Giardina, C.P. & Ryan, M.G. 2000. Evidence that decomposition rates of organic carbon in mineral soil do not vary with temperature. *Nature*, **404**, 858-861.
- Glaser, B., Balashov, E., Haumaier, L., Guggenberger, G. & Zech, W. 2000. Black carbon in density fractions of anthropogenic soils of the Brazilian Amazon region. *Organic Geochemistry*, **31**, 669-678.
- Golchin, A., Oades, J.M., Skjemstad, J.O. & Clarke, P. 1994a. Soil-Structure and Carbon Cycling. *Australian Journal of Soil Research*, **32**, 1043-1068.
- Golchin, A., Oades, J.M., Skjemstad, J.O. & Clarke, P. 1994b. Study of Free and Occluded Particulate Organic-Matter in Soils by Solid-State C-13 Cp/Mas Nmr-Spectroscopy and Scanning Electron-Microscopy. *Australian Journal of Soil Research*, **32**, 285-309.
- Goldberg, E.D. 1985. *BLACK CARBON IN THE ENVIRONMENT*. Wiley, New York.
- Goldstein J, Dale E, Newbury D.C., Patrick J., Echlin C., Lyman E & Lifshin E. 2003. *Scanning Electron Microscopy and X-ray Microanalysis*. Springer, New York.
- Gonod, L.V., Chenu, C. & Soulas, G. 2003. Spatial variability of 2,4-dichlorophenoxyacetic acid (2,4-D) mineralisation potential at a millimetre scale in soil. *Soil Biology & Biochemistry*, **35**, 373-382.
- Gonzalez-Perez, J.A., Gonzalez-Vila, F.J., Almendros, G. & Knicker, H. 2004. The effect of fire on soil organic matter - a review. *Environment International*, **30**, 855-870.
- Greenland, D.J. 1979. Soil Management and Soil Degradation. *Journal of Soil Science*, **32**, 301-322.
- Gregory, A.S., Bird, N.R.A., Whalley, W.R., Matthews, G.P. & Young, I.M. 2010. Deformation and Shrinkage Effects on the Soil Water Release Characteristic. *Soil Science Society of America Journal*, **74**, 1104-1112.
- Grieve, I.C., Davidson, D.A. & Bruneau, P.M.C. 2005. Effects of liming on void space and aggregation in an upland grassland soil. *Geoderma*, **125**, 39-48.

- Grieve, I.C., Davidson, D.A., Ostle, N.J., Bruneau, P.M.C. & Fallick, A.E. 2006. Spatial heterogeneity in the relocation of added C-13 within the structure of an upland grassland soil. *Soil Biology & Biochemistry*, 38, 229-234.
- Griffith, S.M. & Schnitzer, M. 1975. Analytical Characteristics of Humic and Fulvic Acids Extracted from Tropical Volcanic Soils. *Soil Science Society of America Journal*, 39, 861-867.
- Guggenberger, G., Christensen, B.T. & Zech, W. 1994. Land-Use Effects on the Composition of Organic-Matter in Particle-Size Separates of Soil .1. Lignin and Carbohydrate Signature. *European Journal of Soil Science*, 45, 449-458.
- Guggenberger, G., Elliott, E.T., Frey, S.D., Six, J. & Paustian, K. 1999. Microbial contributions to the aggregation of a cultivated grassland soil amended with starch. *Soil Biology & Biochemistry*, 31, 407-419.
- Gundale, M.J. & Deluca, T.H. 2006. Temperature and source material influence ecological attributes of ponderosa pine and Douglas-fir charcoal. *Forest Ecology and Management*, 231, 86-93.
- Gundula Azeez. Soil Carbon and Organic Farming A Review of the Evidence of Agriculture's Potential to Combate Climate Change. 2009. Bristol, Soil Association. 11-3-2010. Reference type report
- Hallett, P.D., Nunan, N., Douglas, J.T. & Young, I.M. 2004. Millimeter-scale spatial variability in soil water sorptivity: Scale, surface elevation, and subcritical repellency effects. *Soil Science Society of America Journal*, 68, 352-358.
- Hassink, J., Whitmore, A.P. & Kubat, J. 1997. Size and density fractionation of soil organic matter and the physical capacity of soils to protect organic matter. *European Journal of Agronomy*, 7, 189-199.
- Hedges, J.I. & Oades, J.M. 1997. Comparative organic geochemistries of soils and marine sediments. *Organic Geochemistry*, 27, 319-361.
- Hillel D. 1982. *Introduction to Soil Physics*. Elsevier Science & Technology.
- Horgan, G.W. 1998. Mathematical morphology for analysing soil structure from images. *European Journal of Soil Science*, 49, 161-173.
- Houghton, R.A. 1999. The annual net flux of carbon to the atmosphere from changes in land use 1850-1990. *Tellus Series B-Chemical and Physical Meteorology*, 51, 298-313.
- Houghton, R.A. 2003. Revised estimates of the annual net flux of carbon to the atmosphere from changes in land use and land management 1850-2000. *Tellus Series B-Chemical and Physical Meteorology*, 55, 378-390.
- Hubert, F., Hallaire, V., Sardini, P., Caner, L. & Heddadj, D. 2007. Pore morphology changes under tillage and no-tillage practices. *Geoderma*, 142, 226-236.
- Hutsch, B.W., Augustin, J. & Merbach, W. 2002. Plant rhizodeposition - an important source for carbon turnover in soils. *Journal of Plant Nutrition and Soil Science-Zeitschrift für Pflanzenernährung und Bodenkunde*, 165, 397-407.
- Ibraim, C., Guilherme S. P., Wadt S., Alves s. Decrease in carbon stocks in an oxisol due to land use and cover change in southwestern Amazon. *An Interdisciplinary Journal of Applied Science*, 4, 1603-1611

Ingham,R.E., Trofymow,J.A., Ingham,E.R. & Coleman,D.C. 1985. Interactions of Bacteria, Fungi, and Their Nematode Grazers - Effects on Nutrient Cycling and Plant-Growth. *Ecological Monographs*, **55**, 119-140.

IPCC. IPCC Third Assessment Report - Climate Change 2001. IPCC 2001 . 2001. 10-4-2007. Ref Type: Internet Communication

Ishii,T.& Kadoya,K. 1994. Effects of Charcoal As A Soil Conditioner on Citrus Growth and Vesicular-Arbuscular Mycorrhizal Development. *Journal of the Japanese Society for Horticultural Science*, **63**, 529-535.

Jastrow,J.D. 1996. Soil aggregate formation and the accrual of particulate and mineral-associated organic matter. *Soil Biology & Biochemistry*, **28**, 665-676.

Jenkinson,D.S. 1977. Studies on Decomposition of Plant Material in Soil .4. Effect of Rate of Addition. *Journal of Soil Science*, **28**, 417-423.

Jenkinson,D.S. 1990. The Turnover of Organic-Carbon and Nitrogen in Soil. *Philosophical Transactions of the Royal Society of London Series B-Biological Sciences*, **329**, 361-368.

Jongmans,A.G., Pulleman,M.M., Balabane,M., van Oort,F. & Marinissen,J.C.Y. 2003. Soil structure and characteristics of organic matter in two orchards differing in earthworm activity. *Applied Soil Ecology*, **24**, 219-232.

Kaal,J.& Van Mourik,J.M. 2008. Micromorphological evidence of black carbon in colluvial soils from NW Spain. *European Journal of Soil Science*, **59**, 1133-1140.

Kay,B.D. 1990. Rates of Change of Soil Structure Under Different Cropping Systems. *Advances in Soil Science*, **12**, 1-52.

Keech,O., Carcaillet,C. & Nilsson,M.C. 2005. Adsorption of allelopathic compounds by wood-derived charcoal: the role of wood porosity. *Plant and Soil*, **272**, 291-300.

Kelley,S.P., Fallick,A.E., Mcconville,P. & Boyce,A.J. 1992. High-Precision, High Spatial-Resolution Analysis of Sulfur Isotopes by Laser Combustion of Natural Sulfide Minerals. *Scanning Microscopy*, **6**, 129-138.

Knorr,W., Prentice,I.C., House,J.I. & Holland,E.A. 2005. Long-term sensitivity of soil carbon turnover to warming. *Nature*, **433**, 298-301.

Kogel-Knabner,I. 2002. The macromolecular organic composition of plant and microbial residues as inputs to soil organic matter. *Soil Biology & Biochemistry*, **34**, 139-162.

Krull,E.S., Baldock,J.A. & Skjemstad,J.O. 2003. Importance of mechanisms and processes of the stabilisation of soil organic matter for modelling carbon turnover. *Functional Plant Biology*, **30**, 207-222.

Ladd,J.N., Foster,R.C. & Skjemstad,J.O. 1993. Soil Structure - Carbon and Nitrogen-Metabolism. *Geoderma*, **56**, 401-434.

Lai,R., Kimble,J.M., Follett,R.F. & Stewart,B.A. 2001. *Assessment Methods For Soil Carbon*. Lewis Publishers, Florida.

Laird,D.A., Chappell,M.A., Martens,D.A., Wershaw,R.L. & Thompson,M. 2008. Distinguishing black carbon from biogenic humic substances in soil clay fractions. *Geoderma*, **143**, 115-122.

- Lavelle, P., Bignell, D., Lepage, M., Wolters, V., Roger, P., Ineson, P., Heal, O.W. & Dhillon, S. 1997. Soil function in a changing world: the role of invertebrate ecosystem engineers. *European Journal of Soil Biology*, 33, 159-193.
- LeBissonnais, Y. 1996. Aggregate stability and assessment of soil crustability and erodibility .1. Theory and methodology. *European Journal of Soil Science*, 47, 425-437.
- Lehmann, J., Kinyangi, J. & Solomon, D. 2007. Organic matter stabilization in soil microaggregates: implications from spatial heterogeneity of organic carbon contents and carbon forms. *Biogeochemistry*, 85, 45-57.
- Li, D.C., Velde, B. & Zhang, T.L. 2004. Observations of pores and aggregates during aggregation in some clay-rich agricultural soils as seen in 2D image analysis. *Geoderma*, 118, 191-207.
- Lloyd, J. 1996. The CO₂ dependence of photosynthesis, plant growth responses to elevated atmospheric CO₂ concentrations, and their interaction with soil nutrient status. I. General principles and forest ecosystems. *Functional Ecology*, 10, 4-32.
- Luo, Y.Q., Reynolds, J., Wang, Y.P. & Wolfe, D. 1999. A search for predictive understanding of plant responses to elevated [CO₂]. *Global Change Biology*, 5, 143-156.
- Lützow, M.V., Kögel-Knabner, I., Ekschmitt, K., Matzner, E., Guggenberger, G., Marschner, B. & Flessa, H. 2006. Stabilization of Organic Matter in Temperate soils: mechanisms and their relevance under different soil conditions-a review. *European Journal of Soil Science*, 57, 426-445.
- MacCarthy P., Malcolm, C.E. & Bloom, P.R. 1990. *Humic Substances in Soil and Crop Sciences*. American Society of Agronomy & Soil Science of America.
- Marinissen, J.C.Y. & Dexter, A.R. 1990. Mechanisms of Stabilization of Earthworm Casts and Artificial Casts. *Biology and Fertility of Soils*, 9, 163-167.
- Marinissen, J.C.Y., Nijhuis, E. & van Breemen, N. 1996. Clay dispersability in moist earthworm casts of different soils. *Applied Soil Ecology*, 4, 83-92.
- Marshall, T.J., Holmes, J.W. & Rose, C.W. 1979. *Soil Physics*. Cambridge University Press, Cambridge.
- Martens, D.A. 2000a. Management and crop residue influence soil aggregate stability. *Journal of Environmental Quality*, 29, 723-727.
- Martens, D.A. 2000b. Plant residue biochemistry regulates soil carbon cycling and carbon sequestration. *Soil Biology & Biochemistry*, 32, 361-369.
- Martin, J.P. & Haider, K. 1971. Microbial Activity in Relation to Soil Humus Formation. *Soil Science*, 111, 54-&.
- Mayer, L.M., Schick, L.L., Hardy, K.R., Wagal, R. & McCarthy, J. 2004. Organic matter in small mesopores in sediments and soils. *Geochimica et Cosmochimica Acta*, 68, 3863-3872.
- McConkey, B.G., Liang, B.C., Campbell, C.A., Curtin, D., Moulin, A., Brandt, S.A. & Lafond, G.P. 2003. Crop rotation and tillage impact on carbon sequestration in Canadian prairie soils. *Soil & Tillage Research*, 74, 81-90.
- McDonald, S., Bishop, A.G., Prenzler, P.D. & Robards, K. 2004. Analytical chemistry of freshwater humic substances. *Analytica Chimica Acta*, 527, 105-124.

- Mcghie,D.A.& Posner,A.M. 1980. Water Repellence of A Heavy-Textured Western-Australian Surface Soil. *Australian Journal of Soil Research*, **18**, 309-323.
- Melillo,J.M., Aber,J.D. & Muratore,J.F. 1982. Nitrogen and Lignin Control of Hardwood Leaf Litter Decomposition Dynamics. *Ecology*, **63**, 621-626.
- Milcu,A., Partsch,S., Langel,R. & Scheu,S. 2006. The response of decomposers (earthworms, springtails and microorganisms) to variations in species and functional group diversity of plants. *Oikos*, **112**, 513-524.
- Mooney,S.J., Tams,A.R. & Berry,P.M. 2006. A reliable method for preserving soil structure in the field for subsequent morphological examinations. *Geoderma*, **133**, 338-344.
- Murphy,C.P., Mckeague,J.A., Bresson,L.M., Bullock,P., Kooistra,M.J., Miedema,R. & Stoops,G. 1985. Description of Soil Thin-Sections - An International Comparison. *Geoderma*, **35**, 15-37.
- Nannipieri,P., Ascher,J., Ceccherini,M.T., Landi,L., Pietramellara,G. & Renella,G. 2003. Microbial diversity and soil functions. *European Journal of Soil Science*, **54**, 655-670.
- Norby,R.J. 1994. Issues and Perspectives for Investigating Root Responses to Elevated Atmospheric Carbon-Dioxide. *Plant and Soil*, **165**, 9-20.
- Nunan,N., Wu,K.J., Young,I.M., Crawford,J.W. & Ritz,K. 2003. Spatial distribution of bacterial communities and their relationships with the micro-architecture of soil. *Fems Microbiology Ecology*, **44**, 203-215.
- Oades,J.M. 1984. Soil Organic-Matter and Structural Stability - Mechanisms and Implications for Management. *Plant and Soil*, **76**, 319-337.
- Oades,J.M. 1988. The Retention of Organic-Matter in Soils. *Biogeochemistry*, **5**, 35-70.
- Oades,J.M.& Waters,A.G. 1991. Aggregate Hierarchy in Soils. *Australian Journal of Soil Research*, **29**, 815-828.
- Oleary,M.H. 1988. Carbon Isotopes in Photosynthesis. *Bioscience*, **38**, 328-336.
- Oorts,K., Bossuyt,H., Labreuche,J., Merckx,R. & Nicolardot,B. 2007. Carbon and nitrogen stocks in relation to organic matter fractions, aggregation and pore size distribution in no-tillage and conventional tillage in northern France. *European Journal of Soil Science*, **58**, 248-259.
- Oren,R., Ellsworth,D.S., Johnsen,K.H., Phillips,N., Ewers,B.E., Maier,C., Schafer,K.V.R., McCarthy,H., Hendrey,G., McNulty,S.G. & Katul,G.G. 2001. Soil fertility limits carbon sequestration by forest ecosystems in a CO₂-enriched atmosphere. *Nature*, **411**, 469-472.
- Otten, W. Grinev D. and Wilson C. Visualizing chemical phases in 3-D heterogeneous soil environments: combining X-ray microtomography with SEM-EDX. Geophysical Research Abstracts, EGU General Assembly 11. 2009.
- Pachepsky,Y., Yakovchenko,V., Rabenhorst,M.C., Pooley,C. & Sikora,L.J. 1996. Fractal parameters of pore surfaces as derived from micromorphological data: Effect of long-term management practices. *Geoderma* , **74**, 305-319.

- Pagliai, M., Guidi, G., Lamarca, M., Giachetti, M. & Lucamante, G. 1981. Effects of Sewage Sludges and Composts on Soil Porosity and Aggregation. *Journal of Environmental Quality*, **10**, 556-561.
- Pagliai, M., Vignozzi, N. & Pellegrini, S. 2004. Soil structure and the effect of management practices. *Soil & Tillage Research*, **79**, 131-143.
- Parton, W.J., Schimel, D.S., Cole, C.V. & Ojima, D.S. 1987. Analysis of Factors Controlling Soil Organic-Matter Levels in Great-Plains Grasslands. *Soil Science Society of America Journal*, **51**, 1173-1179.
- Patra, D.D., Brookes, P.C., Coleman, K. & Jenkinson, D.S. 1990. Seasonal-Changes of Soil Microbial Biomass in An Arable and A Grassland Soil Which Have Been Under Uniform Management for Many Years. *Soil Biology & Biochemistry*, **22**, 739-742.
- Peech, M., Deen, L. A., Reas, J. 1947. Methods of Soil Analysis for Soil Fertility Investigation. US Dept. Agri.
- Piccolo, A. 2002. *The supramolecular structure of humic substances: A novel understanding of humus chemistry and implications in soil science*. ACADEMIC PRESS INC, SAN DIEGO.
- Poulton, P.R. 1996. The Rothamsted long-term experiments: Are they still relevant? *Canadian Journal of Plant Science*, **76**, 559-571.
- Puget, P., Chenu, C. & Balesdent, J. 2000. Dynamics of soil organic matter associated with particle-size fractions of water-stable aggregates. *European Journal of Soil Science*, **51**, 595-605.
- Pulleman, M.M., Six, J., Uyl, A., Marinissen, J.C.Y. & Jongmans, A.G. 2005a. Earthworms and management affect organic matter incorporation and microaggregate formation in agricultural soils. *Applied Soil Ecology*, **29**, 1-15.
- Pulleman, M.M., Six, J., van Breemen, N. & Jongmans, A.G. 2005. Soil organic matter distribution and microaggregate characteristics as affected by agricultural management and earthworm activity. *European Journal of Soil Science*, **56**, 453-467.
- Raich, J.W.a.W.H.S. 1992. The global carbon-dioxide flux in soil respiration and its relationship to vegetation and climate. *Tellus Series B-Chemical and Physical Meteorology*, **44**, 81-89.
- Read, D.B. & Gregory, P.J. 1997. Surface tension and viscosity of axenic maize and lupin root mucilages. *New Phytologist*, **137**, 623-628.
- Read, D.B., Bengough, A.G., Gregory, P.J., Crawford, J.W., Robinson, D., Scrimgeour, C.M., Young, I.M., Zhang, K. & Zhang, X. 2003. Plant roots release phospholipid surfactants that modify the physical and chemical properties of soil. *New Phytologist*, **157**, 315-326.
- Ringrosevoase, A.J. 1996. Measurement of soil macropore geometry by image analysis of sections through impregnated soil. *Plant and Soil*, **183**, 27-47.
- Robertson, G.P. & Freckman, D.W. 1995. The Spatial-Distribution of Nematode Trophic Groups Across A Cultivated Ecosystem. *Ecology*, **76**, 1425-1432.
- Ronn, R., Griffiths, B.S., Ekelund, F. & Christensen, S. 1996. Spatial distribution and successional pattern of microbial activity and micro-faunal populations on decomposing barley roots. *Journal of Applied Ecology*, **33**, 662-672.

Rossi,J.P., Lavelle,P. & Albrecht,A. 1997. Relationships between spatial pattern of the endogeic earthworm *Polypheretima elongata* and soil heterogeneity. *Soil Biology & Biochemistry*, 29, 485-488.

Rowell,D.L. 1994. *Soil Science Methods and Applications*. Pretice Hall, Essex.

Russell,E.W. 1988. *Soil conditions and plant growth*. Longman, London.

Schlesinger,W.H. 2000. Carbon sequestration in Soils. *Science*, **284**, 2095.

Schmidt,M.W.I., Skjemstad,J.O. & Jager,C. 2002. Carbon isotope geochemistry and nanomorphology of soil black carbon: Black chernozemic soils in central Europe originate from ancient biomass burning. *Global Biogeochemical Cycles*, **16**.

Schmidt,M.W.I., Skjemstad,J.O., Gehrt,E. & Kogel-Knabner,I. 1999. Charred organic carbon in German chernozemic soils. *European Journal of Soil Science*, 50, 351-365.

Schnitzer,M. 1991. Soil Organic-Matter - the Next 75 Years. *Soil Science*, 151, 41-58.

Shaw,M.R., Zavaleta,E.S., Chiariello,N.R., Cleland,E.E., Mooney,H.A. & Field,C.B. 2002. Grassland responses to global environmental changes suppressed by elevated CO₂. *Science*, 298, 1987-1990.

Shipitalo,M.J.& Protz,R. 1988. Factors Influencing the Dispersibility of Clay in Worm Casts. *Soil Science Society of America Journal*, 52, 764-769.

Six,J., Bossuyt,H., Degryze,S. & Deneff,K. 2004. A history of research on the link between (micro)aggregates, soil biota, and soil organic matter dynamics. *Soil & Tillage Research*, 79, 7-31.

Six,J., Elliott,E.T. & Paustian,K. 2000a. Soil structure and soil organic matter: II. A normalized stability index and the effect of mineralogy. *Soil Science Society of America Journal*, **64**, 1042-1049.

Six,J., Elliott,E.T. & Paustian,K. 2000b. Soil macroaggregate turnover and microaggregate formation: a mechanism for C sequestration under no tillage agriculture. *Soil Biology & Biochemistry*, 32, 2099-2103.

Six,J., Elliott,E.T., Paustian,K. & Doran,J.W. 1998. Aggregation and soil organic matter accumulation in cultivated and native grassland soils. *Soil Science Society of America Journal*, 62, 1367-1377.

Six,J., Paustian,K., Elliott,E.T. & Combrink,C. 2000c. Soil structure and organic matter: I. Distribution of aggregate-size classes and aggregate-associated carbon. *Soil Science Society of America Journal*, 64, 681-689.

Stevenson,F.J. 1994. *Humus Chemistry, Genesis, Composition, Reactions*. Wiley, New york.

StoffynEgli,P., Potter,T.M., Leonard,J.D. & Pocklington,R. 1997. The identification of black carbon particles with the analytical scanning electron microscope: Methods and initial results. *Science of the Total Environment*, 198, 211-223.

Stoops G 2003. *Guidelines for Analysis and Description of Soil Regolith Thin-Sections*. Soil Science Society of America, Madison.

- Sullivan,L.A. 1990. Soil Organic-Matter, Air Encapsulation and Water-Stable Aggregation. *Journal of Soil Science*, **41**, 529-534.
- Tan,Z., Lal,R., Owens,L. & Izaurrealde,R.C. 2007. Distribution of light and heavy fractions of soil organic carbon as related to land use and tillage practice. *Soil & Tillage Research*, **92**, 53-59.
- Tate,K.R. 1987. *soil organic matter*. John Wiley & Sons, Chirchester.
- Tejada,M.& Gonzalez,J.L. 2007. Influence of organic amendments on soil structure and soil loss under simulated rain. *Soil & Tillage Research*, **93**, 197-205.
- Tisdall,J.M.& Oades,J.M. 1982. Organic-Matter and Water-Stable Aggregates in Soils. *Journal of Soil Science*, **33**, 141-163.
- Van Mourik,J.M. 1985. *Pollen Profiles of Slope Deposits in the Galician Area (N.W. Spain)*. Universiteit van Amsterdam, Amsterdam.
- VandenBygaart,A.J.& Protz,R. 1999. The representative elementary area (REA) in studies of quantitative soil micromorphology. *Geoderma*, **89**, 333-346.
- VandenBygaart,A.J., Fox,C.A., Fallow,D.J. & Protz,R. 2000. Estimating earthworm-influenced soil structure by morphometric image analysis. *Soil Science Society of America Journal*, **64**, 982-988.
- Vanvliet,P.C.J., West,L.T., Hendrix,P.F. & Coleman,D.C. 1993. The Influence of Enchytraeidae (Oligochaeta) on the Soil Porosity of Small Microcosms. *Geoderma*, **56**, 287-299.
- Verma, S. & Sharma P.S. 2007. Effect of long-term manuring and fertilizers on carbon pools, soil structure, and sustainability under different cropping systems in wet-temperate zone of northwest Himalayas. *Biological fertility of Soils*. **44**, 235–240
- Wachinger,G., Fiedler,S., Zepp,K., Gattinger,A., Sommer,M. & Roth,K. 2000. Variability of soil methane production on the micro-scale: spatial association with hot spots of organic material and Archaeal populations. *Soil Biology & Biochemistry*, **32**, 1121-1130.
- Watts,C.W., Clark,L.J., Poulton,P.R., Powlson,D.S. & Whitmore,A.P. 2006. The role of clay, organic carbon and long-term management on mouldboard plough draught measured on the Broadbalk wheat experiment at Rothamsted. *Soil Use and Management*, **22**, 334-341.
- Watts,C.W., Whalley,W.R., Longstaff,D., White,R.P., Brooke,P.C. & Whitmore,A.P. 2001. Aggregation of a soil with different cropping histories following the addition of organic materials. *Soil Use and Management*, **17**, 263-268.
- Whalen,J.K., Sampedro,L. & Waheed,T. 2004. Quantifying surface and subsurface cast production by earthworms under controlled laboratory conditions. *Biology and Fertility of Soils*, **39**, 287-291.
- Whalley,W.R., Riseley,B., Leeds-Harrison,P.B., Bird,N.R.A., Leech,P.K. & Adderley,W.P. 2005. Structural differences between bulk and rhizosphere soil
- White R E 2006. *Principles and Practise of Soil Science, The Soil as a Natural Resource*. Blackwell Publishing.
- Williams,S.N.S.J.S.M.L.C.a.D.L. 1992. Global carbon dioxide emission to the atmosphere by volcanoes. *Geochimica et Cosmochimica Acta*, **56**, 1765-1770.

Wilson,C.A., Davidson D.A., Cresser, M.S. 2005. An evaluation of multi-element analysis of soil contamination to differentiate space use and former function in and around abandoned farms. *The Holocene*, **15**, 1094-1099.

Winsome,T.& Mccoll,J.G. 1998. Changes in chemistry and aggregation of a California forest soil worked by the earthworm *Argilophilus papillifer* Eisen (Megascolecidae). *Soil Biology & Biochemistry*, **30**, 1677-1687.

Yamashita,T., Flessa,H., John,B., Helfrich,M. & Ludwig,B. 2006. Organic matter in density fractions of water-stable aggregates in silty soils: Effect of land use. *Soil Biology & Biochemistry*, **38**, 3222-3234.

Yoo,G., Spomer,L.A. & Wander,M.M. 2006. Regulation of Carbon mineralization rates by Soil Structure and water in an Agricultural field and Prairie-like soil. *Geoderma*, **135**, 16-25.

Young,I.M., Crawford,J.W. & Rappoldt,C. 2001. New methods and models for characterising structural heterogeneity of soil. *Soil & Tillage Research*, **61**, 33-45.

Zar J.H. 1998. *Biostatistical Analysis*. Prentice Hall, New Jersey.

Zhang,H.Q. 1994. Organic-Matter Incorporation Affects Mechanical-Properties of Soil Aggregates. *Soil & Tillage Research*, **31**, 263-275.

Appendix 1: Area of interest description @ 40x mag Broadbalk and Wilderness.

Sample	AOI	Field	Treatment	Coarse Mineral (> 10µm)			Micromass (<10 µm)	Organ residue			Tissue (> 5 cells)	Fine organic matter (< 5 cells)				Pedofeatures						Voids					C:F related distribution (10µm)									
				Calcite	Quartz	Calcite biospheres		living/ fresh	Moderately decomposed	Strongly decomposed	living/ fresh	Moderately decomposed	Strongly decomposed	Cells/ cell residue	Very strongly decomposed (Amorphous red)	Very strongly decomposed (Amorphous yellow)	Very strongly decomposed (Amorphous Black)	Punctuations	Organic pigment monomorphic	Coatings	Hypocoatings	Quasicoatings	Excrements (mammilate)	Excrements (cylindrical)	Excrements (spheroid)	Infillings excrements	Infillings crystals	Mg/Fe nodules	Vughis	Channels	Chambers	Planar	Complex Packing			
1	1	Broadbalk	FYM	○	●		Brown stipple speckled								●	○	+																		double-spaced porphyric	
1	2	Broadbalk	FYM	○	+		Brown stipple speckled								●	○	+																		single-spaced porphric	
1	3	Broadbalk	FYM	○	●		Brown stipple speckled								●	○	○	○	○																open porphyric	
2	1	Broadbalk	FYM	○	●		Brown stipple speckled								●	○	○	○	○																single-spaced porphric	
2	2	Broadbalk	FYM	○	●		Brown stipple speckled								○	○	○	○	○																open porphyric	
2	3	Broadbalk	FYM	○	●		Brown stipple speckled								○	○	○	○	○																open porphyric	
3	1	Broadbalk	FYM	●	●		Brown stipple speckled								○	○	○	○	○																double-spaced porphyric	
3	2	Broadbalk	FYM	●	●		Brown stipple speckled								○	○	○	○	○																single-spaced porphric	
3	3	Broadbalk	FYM	●	○		Brown stipple speckled								○	○	○	○	○																single-spaced porphric	
4	1	Broadbalk	FYM	○	●		Brown stipple speckled								○	○	○	○	○																single-spaced porphric	
4	2	Broadbalk	FYM	○	●		Brown stipple speckled								○	○	○	○	○																open porphyric	
4	3	Broadbalk	FYM	○	●	○	Brown stipple speckled								○	○	○	○	○																single-spaced porphric	
6	1	Broadbalk	FYM	○	●	○	Drk brown stipple speckled								○	○	○	○	○																open porphyric	
6	2	Broadbalk	FYM	○	○		Drk brown stipple speckled								○	○	○	○	○																open porphyric	
6	3	Broadbalk	FYM	○	○		Brown stipple speckled								○	○	○	○	○																double-spaced porphyric	
1	1	Broadbalk	NIL	○	●	○	Brown stipple speckled								○	○	○	○	○																double-spaced porphyric	
1	2	Broadbalk	NIL	○	+		Brown stipple speckled								○	○	○	○	○																double-spaced porphyric	
1	3	Broadbalk	NIL	○	+		Brown stipple speckled								○	○	○	○	○																	double-spaced porphyric
2	1	Broadbalk	NIL	○	+		Brown stipple speckled								○	○	○	○	○																	open porphyric
2	2	Broadbalk	NIL	○	+		Brown stipple speckled								○	○	○	○	○																	double-spaced porphyric
2	3	Broadbalk	NIL	○	+		Brown stipple speckled								○	○	○	○	○																	single-spaced porphric
3	1	Broadbalk	NIL	○	+		Brown stipple speckled								○	○	○	○	○																	double-spaced porphyric
3	2	Broadbalk	NIL	○	+		Brown stipple speckled								○	○	○	○	○																	double-spaced porphyric
3	3	Broadbalk	NIL	○	+		Brown stipple speckled								○	○	○	○	○																	double-spaced porphyric
4	1	Broadbalk	NIL	○	+		Brown stipple speckled								○	○	○	○	○																	double-spaced porphyric
4	2	Broadbalk	NIL	○	+		Brown stipple speckled								○	○	○	○	○																	double-spaced porphyric
4	3	Broadbalk	NIL	○	●	○	Brown stipple speckled								○	○	○	○	○																	single-spaced porphric
4	3	Broadbalk	NIL	○	●		Brown stipple speckled								○	○	○	○	○																	open porphyric
5	1	Broadbalk	NIL	○	○		Brown stipple speckled								○	○	±	○	○																	open porphyric
5	2	Broadbalk	NIL	○	○	+	Drk brown stipple speckled								○	○	○	○	○																	double-spaced porphyric
5	3	Broadbalk	NIL	○	○	+	Brown stipple speckled								○	○	○	○	○																	open porphyric
1	1	Broadbalk	INORGANIC	○	+		Brown stipple speckled								○	○	○	○	○																	double-spaced porphyric
1	2	Broadbalk	INORGANIC	○	+		Brown stipple speckled								○	○	○	○	○																	double-spaced porphyric
1	3	Broadbalk	INORGANIC	○	+		Brown stipple speckled								○	○	○	○	○																	open porphyric
2	1	Broadbalk	INORGANIC	○	+		Brown stipple speckled								○	○	○	○	○																	open porphyric
2	2	Broadbalk	INORGANIC	○	+		Brown stipple speckled								○	○	○	○	○																	double-spaced porphyric
2	3	Broadbalk	INORGANIC	○	+		Brown stipple speckled								○	○	○	○	○																	open porphyric
3	1	Broadbalk	INORGANIC	○	+		Brown stipple speckled								○	○	○	○	○																	open porphyric
3	2	Broadbalk	INORGANIC	○	○		Brown stipple speckled								○	○	○	○	○																	open porphyric
3	3	Broadbalk	INORGANIC	○	○		Brown stipple speckled								○	○	○	○	○																	double-spaced porphyric
4	1	Broadbalk	INORGANIC	○	+		Brown stipple speckled								○	○	○	○	○																	double-spaced porphyric
4	2	Broadbalk	INORGANIC	○	+		Brown stipple speckled								○	○	○	○	○																	open porphyric
4	3	Broadbalk	INORGANIC	○	+		Brown stipple speckled								○	○	○	○	○																	open porphyric
1	1	Broadbalk	wild	○	○		Brown stipple speckled								○	○	○	○	○																	open porphyric
1	2	Broadbalk	wild	○	+		Brown stipple speckled								○	○	○	○	○																	open porphyric
1	3	Broadbalk	wild	○	+		Brown stipple speckled								○	○	○	○	○																	open porphyric
2	1	Broadbalk	wild	○	+		Brown stipple speckled								○	○	+	○	○																	open porphyric
2	2	Broadbalk	wild	○	+		Brown stipple speckled								○	○	○	○	○																	double-spaced porphyric
2	3	Broadbalk	wild	○	+		Brown stipple speckled								○	○	○	○	○																	double-spaced porphyric
3	1	Broadbalk	wild	○	+		Brown stipple speckled								○	○	○	○	○																	double-spaced porphyric
3	2	Broadbalk	wild	○	+		Brown stipple speckled								○	○	○	○	○																	double-spaced porphyric
3	3	Broadbalk	wild	○	+		Brown stipple speckled								○	○	○	○	○																	double-spaced porphyric
4	1	Broadbalk	wild	○	○		Brown stipple speckled								○	○	○	○	○																	single-spaced porphric
4	2	Broadbalk	wild	○	+		Brown stipple speckled								○	○	○	○	○																	single-spaced porphric
4	3	Broadbalk	wild	○	+		Brown stipple speckled								○	○	○	○	○																	single-spaced porphric
5	1	Broadbalk	wild	○	+		Brown stipple speckled								○	○	○	○	○																	single-spaced porphric
5	2	Broadbalk	wild	○	+		Brown stipple speckled								○	○	○	○	○																	single-spaced porphric
5	3	Broadbalk	wild	○	+		Brown stipple speckled								○	○	○	○	○																	single-spaced porphric
6	1	Broadbalk	wild	○	+		Brown stipple speckled								○	○	○	○	○																	single-spaced porphric
6	2	Broadbalk	wild	○	+		Brown stipple speckled								○	○	○	○	○																	double-spaced porphyric
6	3	Broadbalk	wild	○	+		Brown stipple speckled								○	○	○	○	○																	double-spaced porphyric
7	1	Broadbalk	wild	○	+		Brown stipple speckled								○	○	○	○	○																	double-spaced porphyric
7	2	Broadbalk	wild	○	+		Brown stipple speckled																													

Appendix 3: The Redistribution of Organic Carbon as it is Retained within the Soil Structure.

Due to numerous methodological problems the data collected from the short-term pot experiment and Hoosfield Continuous Maize will not be discussed and therefore are not presented in the main body of the thesis. In this section the methodological set backs are outlined and it is reasoned that the findings are not a reflection of any real effect.

Appendix 3.1: Aims and Objectives

Aim 3: To examine the redistribution of OC as it is retained within the soil structure.

Objective 3.1: To investigate the distribution of recent and older carbon in relation to soil structural features.

Objective 3.2: To compare the $\delta^{13}\text{C}$ of macroaggregates and microaggregates as identified by micromorphology and the surface volume calculated by image analysis.

Objective 3.3: To investigate the location of organic-carbon newly deposited by plant roots (10 weeks of growth) (**Appendix 3.4**).

***Hypothesis 3.1:** In contrast to recent inputs older carbon will be incorporated into the soil matrix away from soil pores.*

***Hypothesis 3.2:** The highest concentration of new carbon inputs by root deposition (after 10-weeks of growth) will be located within the rhizosphere soil and closely associated with soil-pore interface (**Appendix 3.4**).*

Appendix 3.2: Slide Quality and Micromorphology

The approach used to analyse Hoosfield slides differs to the method used to analyse samples removed from Broadbalk (**Chapter 5**) due to the differences in the manufacture process (**Section 3.4.3**). To recap, samples from Hoosfield were grounded to 30 μ m using a bench sander. However, the manufacture of thin-sections created artefacts including, loss of soil material, variable slide thickness and surface abrasions. To control for this variability areas of the thin-section were selected for analysis. Due to the limited regions within thin-section suitable for analysis, micromorphology was performed at 20x and restricted to identifying and describing features of interest, the area of features was calculated using image analysis (**Figure 1a-c**)

Appendix 3.3: Results from Hoosfield Continuous Maize

A number of methodological problems mean that it is not possible to analyse the results from the δ - ^{13}C short term experiment (**Section 3.1.4**) or Hoosfield Continuous Maize (**Section 3.1.3**). The LA-IRMS and closed tube combustion followed by IRMS methods are outlined in **Section 3.2.3**. In summary all the δ ^{13}C PDB results for LA-IRMS and closed-tube combustion fall within the δ ^{13}C values for C_3 plants (-32 to -20 ‰), this section will present a summary of the results combined with an explanation of why the data collected is not reflecting any real effect.

To obtain a standard value of δ ^{13}C PDB for PEG-resin, a sample of pure PEG was analysed by closed tube combustion giving a mean value of -27.76 (SD \pm 0.06), this falls well within the δ ^{13}C PDB range of C_3 plants, while previous analysis showed that PEG resin has a δ ^{13}C value of -30.4 ‰ \pm 0.5 (Bruneau et al., 2002). All features identified using micromorphology have a δ ^{13}C value falling within the range of C_3 plants (**Fig. 2**). Further practical constraints should also be considered; multiple burns from the same class of features are required to capture enough CO_2 (15 μmol) for subsequent IRMS analysis, however the set-up of the microscope-laser system meant it was difficult to locate features previously identified with a petrological microscope. Since results from IRMS consistently fall within the δ ^{13}C PDB range of C_3 plants, suggests that samples obtained by the analysis of features (within thin-sections) using LA-IRMS are swamped with CO_2 originating from PEG-resin.

The results from closed-tube combustion of bulk samples are consistent with LA-IRMS, in that all soils have a δ ^{13}C value that falls within the range of C_3 plants (**Fig. 3**), this is either due to C_4 plants not having a strong enough signal in either the pot experiment or Hoosfield soil and is hence diluted by the C_3 carbon. Alternatively, it is a result of a practical constraint, specifically that the amount of soil analysed (5mg) was insufficient to permit detection of carbon originating from C_4 plants. Since it was not possible to obtain conclusive results from the LA-IRMS, it was deemed not necessary to repeat soil closed-tube analysis with a greater mass of soil.

In summary, due to imaging drawbacks and the relative low amount of CO_2 captured after laser ablation the CO_2 signal is dominated by carbon originating from either C_3 plants or more probably PEG-resin. Taking into consideration also the many slide artefacts created by the manufactory process (**Appendix 3.2**) the accuracy of the data produced by this method is questionable.

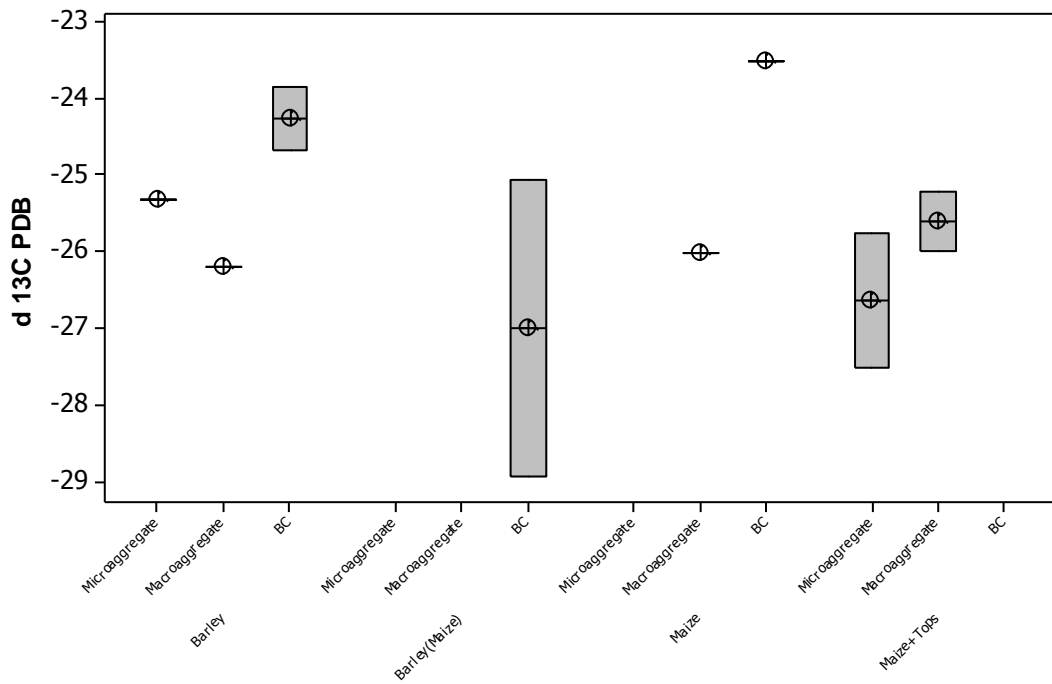


Figure 2: The $\delta^{13}\text{C}$ PDB values determined by LA-IRMS of microaggregates, macroaggregates or black carbon, identified using micromorphology, taken from Barley, Barley (Maize), Maize and Maize +tops treatments removed from Hoosfield Continuous Maize. Box represent the interquartile range, the line represents the median value while the symbol denotes the mean value.

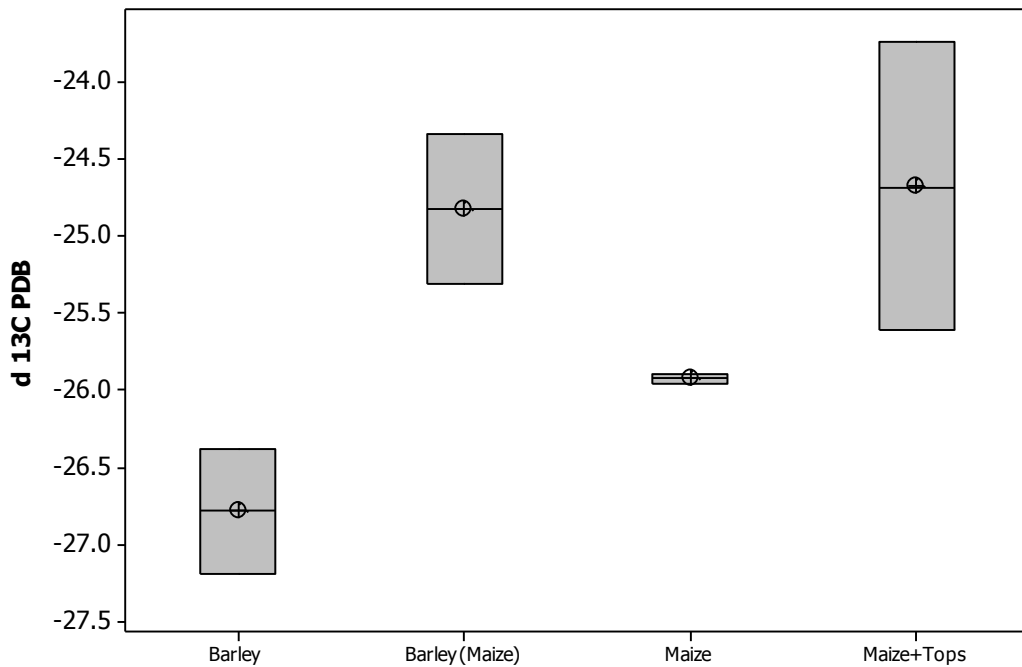


Figure 3: The $\delta^{13}\text{C}$ PDB values determined by closed tube combustion followed by IRMS taken from Barley, Barley (Maize), Maize and Maize +tops treatments removed from Hoosfield Continuous Maize. Box represent the interquartile range, the line represents the median value while the symbol denotes the mean value.

Appendix 3.4: Short Term δ -13C Experiment

In addition to the Hoosfield Continuous Maize experiment soil was collected from the Broadbalk buffer zone, which has not received any inputs from C_4 vegetation this was used in a pot-experiment. In summary individual *Zea mays* plants were grown in 500ml pots (**Fig. 4**), the whole pot was impregnated allowing the distribution of recent C-inputs to be investigated around the root system. Consistent with the Hoosfield results a C_4 signal was not detected. For reference the methodology is presented in this section, as it maybe possible to adapt the method to investigate the distribution of pulse labelled C within an intact soil structure surrounding plant root system.

Appendix 3.4.1 Design of Short Term δ -13C Experiment

Soil was collected from the buffer zone between Broadbalk Winter-Wheat and Broadbalk Wilderness in June 2007 and this soil was selected since it has a similar texture to the Hoosfield soil and is known not to have received C-inputs from C_4 vegetation. The upper surface of the soil horizon was removed to a depth of 20cm ensuring that the soil sampled would be removed from the same depth as at the other sites. The soil was wet sieved (16mm), air dried and then passed through a 2mm sieve before being packed into pots.

Zea mays and *H. vulgare* were grown in pots (**Fig. 4**) containing the soil collected from the buffer zone separating Broadbalk Winter-Wheat and Broadbalk Wilderness. The design of this experiment allowed recent carbon inputs from C_4 plants (with a stable isotope ratio δ -13C 13‰) to be distinguished from older OM contents from C_3 plants (with a ratio of δ -13C 27‰). This experiment complements the intact samples removed from the Hoosfield maize experiment (during its 11th year), with the aim of showing the redistribution of OC as it is retained within the soil structure. The two data sets also allow comparison of the occurrence and form of organic compounds from both recent and older carbon inputs through the use of light microscopy and laser ablation- isotope ratio mass spectrometry (LA-IRMS).

Seeds of both *Z. mays* (variety Hudson treated with Thiram; supplier Advanta seeds, sealford, Lincolnshire, UK) and *H. vulgare* (variety optic treated with raxil pro; supplier Dalgety, Morton, Essex, UK) were germinated on filter paper saturated with distilled water, which was stored in Petri dishes and kept at room temperature. Within 72 hours of germination uniform seedlings were selected and transplanted to polypropylene (autoclavable) laboratory 500 ml beakers, capacity, with 3 x 5mm drainage holes drilled into the bases. Initially 20 pots were prepared, the sieved soil was packed to a mean bulk density of $1.3 \text{ g}^{-1} \text{ cm}^{-3}$ corresponding to the treatments at Hoosfield. Moist soil was packed in increments of 100 ml and set to the

desired bulk density by shaking on an automatic bottle shaker for approximately 15 minutes. Pots were watered daily to maintain air-filled porosity between 10-15%, by weighing each pot and calculating the volumetric water content based on the bulk density (as determined at the initiation of the experiment) and on the particle density of quartz (2.65 g cm^{-3}). Soil was left to equilibrate within laboratory beakers for 2 weeks before either a single *Z. mays* or *H. vulgare* seedling was planted into each pot.

Sources of error include organic inputs and penetration by plant roots that can each alter the bulk density of soil which may cause errors when calculating air-filled porosity. It is essential that soil bulk density does not hinder root penetration since high soil bulk densities tend to increase root exudation as plants attempt to loosen the surrounding soil {Barber & Gunn, 1974} {Swennen, et al., 1995}. Unrealistically high bulk densities within pot experiments will therefore falsify rates of rhizodeposition. Plants were stored in growth-chambers with a photoperiod of 8 hours and 16-hour darkness at a temperature of 20°C and a relative humidity of 65% {Whalley et al., 2005}. Pots are rotated daily to ensure that uniform conditions were experienced by each plant.

Plants were grown for 10 weeks in accordance with other pot experiments growing maize measuring the ^{13}C concentration within plant tissue {Dercon, 2006}. The proportion of carbon contributing to rhizodeposition decreases during plant growth development with the absolute amount being dependent upon species and environmental conditions. Since the plants were grown in small pots it's probable that pot size limited plant growth into the growing season and consequently any appreciable increases in rhizodeposition. Upon completion twelve plants were selected for analysis. Three replicates of each *Z. mays* and *H. vulgare* were impregnated with polyethylene glycol (PEG) to produce slides for laser-ablation isotope ratio mass spectrometry (LA-IRMS), while 3 replicates of each treatment were utilised for bulk analysis.

Soil water content is a major control of the water stresses status of a plant, with pot size having a negligible impact {Ray & Sinclair, 1998}. Ensuring that plants are not water stressed is essential since the rate of photosynthesis decreases due to a lower rate of stomatal conductance as the plant attempts to maintain water-use-efficacy. More significantly under water-stressed conditions the proportion of ^{13}C fixed by C_4 plants decreases as ^{13}C leaks from the bundle sheath leading to a reduction in $\delta^{13}\text{C}$ within plant tissue {Dercon, 2006}. Delta ^{13}C values between -12.42‰ to -11.20‰ have been recorded for water-stressed *Z. mays* grown in pots for 60 days {Dercon, 2006}. The reduction in $\delta^{13}\text{C}$ is well recognised and it is hoped that

this will be developed as a diagnostic tool for both C₃ and C₄ plants experiencing water-stressed-conditions {Dercon, 2006}.

3.4.2 Modification to the Resin Impregnation Method

To ensure a complete impregnation of the pots used to grow maize and barley the following approach was applied. Pots used to grow maize and barley for IA-IRMS analysis were impregnated with PEG to retain an intact soil structure. For a full impregnation of 500 ml pots, the following amendments made to the impregnation method: the soil containing pots were placed into larger 600ml pots to ensure a total submersion of the soil with resin, to ensure a complete impregnation of these larger pots they were retained in an oven at 60 °C for 2 months. Thin-sections were produced by making a vertical cut through the centre of the pot allowing thin-sections to be made of the root and surrounding soil.



Figure 4: *Zea mays* after 10 weeks of growth. Plants in laboratory beakers are intended for PEG impregnation while plants grown in standard growth containers will be used for bulk analysis.